

# **EXPERIMENTAL ANALYSIS OF STRUCTURAL ELEMENT CONNECTIONS, MADE OF HIGH STRENGTH STEEL COMPONENTS, MONOTONE AND CYCLIC LOADED.**

Teză destinată obținerii  
titlului științific de doctor inginer  
la  
Universitatea "Politehnica" din Timișoara  
în domeniul INGINERIE CIVILĂ  
de către

**Ing. Nicolae MUNTEAN**

Conducător științific:

Prof.Dr.Ing. Dr.H.C. Dan DUBINĂ,  
Universitatea "Politehnica" din Timișoara

Referenți științifici:

Prof.Ph.D.Eng. Darko BEG  
University of Ljubljana

Prof.Dr.Ing. Cristina CÂMPIAN  
Universitatea Tehnică din Cluj-Napoca

Prof.Dr.Ing. Daniel GRECEA  
Universitatea "Politehnica" din Timișoara

Ziua susținerii tezei: 26 Septembrie 2011

Seriile Teze de doctorat ale UPT sunt:

- |                        |   |
|------------------------|---|
| 1. Automatică          | 7. Inginerie Electronică și Telecomunicații |
| 2. Chimie              | 8. Inginerie Industrială                    |
| 3. Energetică          | 9. Inginerie Mecanică                       |
| 4. Ingineria Chimică   | 10. Știința Calculatoarelor                 |
| 5. Inginerie Civilă    | 11. Știința și Ingineria Materialelor       |
| 6. Inginerie Electrică |   |

Universitatea „Politehnica” din Timișoara a inițiat seriile de mai sus în scopul diseminării expertizei, cunoștințelor și rezultatelor cercetărilor întreprinse în cadrul școlii doctorale a universității. Seriile conțin, potrivit H.B.Ex.S Nr. 14 / 14.07.2006, tezele de doctorat susținute în universitate începând cu 1 octombrie 2006.

Copyright © Editura Politehnica – Timișoara, 2006

Această publicație este supusă prevederilor legii dreptului de autor. Multiplicarea acestei publicații, în mod integral sau în parte, traducerea, tipărirea, reutilizarea ilustrațiilor, expunerea, radiodifuzarea, reproducerea pe microfilme sau în orice altă formă este permisă numai cu respectarea prevederilor Legii române a dreptului de autor în vigoare și permisiunea pentru utilizare obținută în scris din partea Universității „Politehnica” din Timișoara. Toate încălcările acestor drepturi vor fi penalizate potrivit Legii române a drepturilor de autor.

România, 300159 Timișoara, Bd. Republicii 9,  
tel. 0256 403823, fax. 0256 403221  
e-mail: editura@edipol.upt.ro

## Acknowledgements

The thesis was developed during my activity (2006 – 2011) within the Department of Steel Structures and Structural Mechanics (CMMC), the Center of Excellence in the Mechanics of Materials and Safety of Structures (CEMSIG), from the "Politehnica" University of Timișoara.

First of all I would like to express my gratitude to my advisor, Prof. Ph.D. Eng. Dr. H.C. Dan Dubină, C.M. of Romanian Academy for his generosity, support and guidance throughout my research activity. His advices and comments along these years made it possible for me to conclude my work.

I would like to thank him for the chance that he has been given me, in year 2002 to be a part of his team and to become an engineer first of all and a researcher after. Thanks to him I had the chance to meet and work with wonderful people that each contribute to my professional carrier. I wish I were wiser in all those years and see how lucky I was.

I would like to thank my scientific references, Prof. Darko Beg, Prof. Cristina Câmpian and Prof. Daniel Grecea for their constructive feedback and comments that pushed the thesis one step further and for their acceptance to be a member in my PhD jury, which honours me.

Special thanks to Assoc. Prof. Aurel Stratan and Senior Lecturer Adrian Dogariu for their support and assistance. Their valuable advices helped me with the development of the experimental program and numerical simulations.

My sincere thanks to Assoc.Prof.Florea Dinu, Assoc.Prof. Viorel Ungureanu, Assoc.Prof. Raul Zaharia, Assoc.Prof.Adrian Ciutină, Assoc.Prof.Mircea Cristutiu, PhD.Eng. Iosif Szabo and PhD.Eng Ludovic Fulop for all their friendship, support and guidance through all these years. Also thanks to them I learned everything I know today.

My thanks to my friends and colleagues Ph.D. eng. Filip Vacarescu Norin, Ph.D. eng. Danku Gelu, Ph.D. eng. Neagu Calin, Ph.D. Andrei Crisan, Ph.D Sorin Bordea and Dan Scarlat for their help with the laboratory work.

And last, but not least, I am grateful to my wife, to my friend Adrian Dogariu, to my parents and my brother for all the unconditional support, for encouraging me and for allways being there in difficult moments.

As a final remark, looking back through all these years I must say that it wasn't easy....but they were the best years of my life. And for this, I will never forget.

Thank you.

Timișoara, September,2011

Nicolae Muntean

To my wife.

Muntean, Nicolae

**Experimental analysis of structural element connections, made of high strength steel components, monotone and cyclic loaded.**

Teze de doctorat ale UPT, Seria 5, Nr. 83, Editura Politehnica, 2011, 218 pagini, 129 figuri, 62 tabele.

Key words,: high strength steels, strength, ductility, dual steels structures, bolted T-stub, Macro-component, Monotonic and Cyclic loading, seismic resisting structure.

.....  
Abstract,

Seismic resistant building frames designed as dissipative structures must allow for plastic deformations to develop in specific members, whose behavior has to be predicted by proper design. Members designed to remain predominantly elastic during earthquake, such as columns, are responsible for robustness of the structure and prevention the collapse, being characterized by high strength demands. Consequently a framing solution obtained by combining High Strength Steel - HSS in non-dissipative members (e.g. columns) provided with adequate overstrength, and Mild Carbon Steel - MCS in dissipative members, working as fuses (e.g. beams, links or braces) seems to be logical. The robustness of structures to severe seismic action is ensured by their global performance, in terms of ductility, stiffness and strength, e.g. the "plastic" members of MCS (S235 to S355) will dissipate the seismic energy, while the "elastic" members (HSS - S460 to S690) by higher resistance of material and appropriate size of sections, will have the capacity to carry the supplementary stresses, following the redistribution of forces, after appearance of plastic hinges. Such a structure is termed Dual-Steels Structure. DS concept is extended to connections, too, on the same philosophy related to ductile and brittle components, in order to achieve both ductility and robustness criteria. In fact, when connecting MCS beams to HSS columns it will result a DS beam-to-column joint.

Starting from the above considerations, a large experimental research program was carried out in order to study the performance of dual-steel configuration for beam-to-column joints under monotonic and cyclic loading.



<b>LIST OF TABLES .....</b>	<b>24</b>
<b>LIST OF FIGURES .....</b>	<b>26</b>
<b>1 INTRODUCTION .....</b>	<b>30</b>
<b>1.1 Motivation.....</b>	<b>30</b>
<b>1.2 Thesis objectives .....</b>	<b>32</b>
<b>1.3 Research framework.....</b>	<b>33</b>
<b>1.4 Thesis outline .....</b>	<b>33</b>
<b>2 STRUCTURAL STEELS.....</b>	<b>35</b>
<b>2.1 Introduction .....</b>	<b>35</b>
<b>2.2 Common steels for constructions.....</b>	<b>35</b>
2.2.1 Standard structural steels in Europe.....	37
2.2.2 Standard structural steels in USA .....	38
2.2.3 Weathering steel "W" .....	39
2.2.4 Fine grain steel - "N" or "NL" .....	40
2.2.5 Steel for Cryogenic and Low-Temperature Service .....	40
<b>2.3 High strength steel .....</b>	<b>40</b>
2.3.1 High strength steel production.....	44
2.3.2 Mechanical characteristics of HSS steels .....	47
2.3.3 Chemical composition.....	50
2.3.4 Welding technology.....	51
2.3.5 Design of elements made of high strength steel .....	52
<b>2.4 Summary review on previous research of HSS Connections.....</b>	<b>58</b>
<b>2.5 Requirements and criteria for choosing steel in structural applications .....</b>	<b>60</b>
<b>2.6 Conclusions.....</b>	<b>63</b>
<b>3 OPPORTUNITIES OF USING HSS STEEL IN SEISMIC RESISTANT BUILDING FRAMES .....</b>	<b>64</b>
<b>3.1 Introduction .....</b>	<b>64</b>

<b>3.2 Seismic performance on Dual-Steel frames .....</b>	<b>65</b>
3.2.1 DS frames modelling and design.....	65
3.2.2 Performance based evaluation.....	67
<b>3.3 Conclusions.....</b>	<b>73</b>
<b>4 PERFORMANCE CRITERIA AND DETAILING FOR BEAM TO COLUMN JOINTS OF MULTI-STOREY STRUCTURES .....</b>	<b>76</b>
<b>4.1 Introduction .....</b>	<b>76</b>
<b>4.2 Stiffness and Strength classification of joints (EN 1993-1-8) ...</b>	<b>76</b>
4.2.1 Classification by stiffness .....	77
4.2.2 Classification by strength.....	78
<b>4.3 Provisions and performance criteria for beam to column joints</b>	<b>79</b>
4.3.1 USA Provisions .....	79
4.3.2 European Provisions.....	85
<b>4.4 Constructional detailing for Beam-to-Column Joints .....</b>	<b>89</b>
4.4.1 USA practice .....	89
4.4.2 European Practice.....	93
<b>4.5 Prequalification criteria for MR beam to column joints .....</b>	<b>95</b>
<b>4.6 Conclusions.....</b>	<b>97</b>
<b>5 HSS EXPERIMENTAL PROGRAM .....</b>	<b>98</b>
<b>5.1 Introduction .....</b>	<b>98</b>
<b>5.2 DESIGN OF THE EXPERIMENTAL PROGRAM.....</b>	<b>99</b>
<b>5.3 Experimental platform .....</b>	<b>101</b>
<b>5.4 METHODOLOGY OF EXPERIMENTAL WORK.....</b>	<b>103</b>
5.4.1 Tensile tests on material.....	103
5.4.2 Charpy V-notch toughness tests .....	106
5.4.3 Welded specimen tests.....	108
5.4.4 Tests on T-stub specimens.....	126
5.4.5 Beam-to-Column Joints Experimental Program .....	159
<b>6 NUMERICAL MODELLING PROGRAM .....</b>	<b>179</b>
<b>6.1 Introduction .....</b>	<b>179</b>
<b>6.2 NUMERICAL ANALYSIS .....</b>	<b>182</b>

<b>6.3 Conclusions.....</b>	<b>192</b>
<b>7 SUMMARY, CONCLUSIONS AND PERSONAL CONTRIBUTIONS</b> <b>.....</b>	<b>193</b>
<b>7.1 Summary .....</b>	<b>193</b>
<b>7.2 Concluding remarks .....</b>	<b>194</b>
<b>7.3 Personal contributions.....</b>	<b>195</b>
<b>BIBLIOGRAPHY .....</b>	<b>197</b>
<b>APPENDIX A .....</b>	<b>203</b>
<b>APPENDIX B .....</b>	<b>209</b>

## LIST OF TABLES

Table 2.1 - Steels for resistance structures in constructions .....	37
Table 2.2 - Comparison table of typical steel grades .....	39
Table 2.3 - COR-TEN Chemical composition .....	40
Table 2.4 - Strength requirements for structural steel .....	42
Table 2.5 - Minimal material properties of some high strength steels[15].....	48
Table 2.6 - High performance steels for seismic applications .....	50
Table 2.7 - Chemical composition of S235, S460, S690 .....	51
Table 2.8 - Carbon equivalence for S235, S460, S690.....	51
Table 3.1 - First mode periods and multiplicative factors for the structures[31] ....	67
Table 3.2 - Target displacement, $D_t$ , for the MDOF systems for ULS .....	68
Table 3.3 - Interstorey drift demands for SLS.....	70
Table 3.4 - Plastic deformation demands in members at SLS ( $\lambda = 0.5$ ), ULS ( $\lambda = 1.0$ ) and CPLS ( $\lambda = 1.5$ ) .....	74
Table 4.1 - Performance structural levels for un-braced frame structures.....	84
Table 4.2 - Description of the structural performance levels .....	85
Table 4.3 - Acceptance criteria for the non-linear analysis.....	85
Table 4.4 - Prequalified moment connections – AISC 358-05 .....	95
Table 4.5 - Parametric limitations on prequalification[5].....	96
Table 5.1 - Summary of testing program.....	100
Table 5.2 - Average material characteristics .....	103
Table 5.3 - Charpy V notch test .....	107
Table 5.4 - welded connections – type of material .....	108
Table 5.5 - Welded specimen legend.....	109
Table 5.6 - Welded specimen 235FW – nominal geometry .....	113
Table 5.7 - Welded specimen 235KW – nominal geometry .....	114
Table 5.8 - Welded specimen 235VW – nominal geometry .....	114
Table 5.9 - Welded specimen 235VRW – nominal geometry .....	115
Table 5.10 - Welded specimen 460FW – nominal geometry .....	115
Table 5.11 - Welded specimen 460KW – nominal geometry .....	116
Table 5.12 - Welded specimen 460VW – nominal geometry .....	116
Table 5.13 - Welded specimen 690FW – nominal geometry .....	117
Table 5.14 - Welded specimen 690KW – nominal geometry .....	117
Table 5.15 - Welded specimen 690VW – nominal geometry .....	118
Table 5.16 - Welded specimen 690VRW – nominal geometry .....	118
Table 5.17 - T-stub specimen legend .....	130
Table 5.18 - T-stub characteristics.....	131
Table 5.19 - Measured properties T-stub specimen (Monotone Loading) .....	133
Table 5.20 - Measured properties T-stub specimen (Cyclic Loading) .....	134
Table 5.21 - Experimental (monotonic) and analytical T-stub characteristics .....	147
Table 5.22 - Interpretation of cyclic tests in term of energy .....	155
Table 5.23 - Plastic rotation demands (in rad) at ULS and CPLS for the eccentrically and concentrically braced frames, average and maximum of all records.....	160
Table 5.24 - Nominal characteristics of joint specimens .....	161
Table 5.25 - Beam-to-Column legend.....	162
Table 5.26 - Material properties – flat steel (end-plates, stiffeners) – UnionOcel .	165
Table 5.27 - Material properties – sections, ARCELOR-MITTAL .....	165

Table 5.28 - Properties of joints: nominal / actual material characteristics .....	165
Table 5.29 - C355WC Test results .....	169
Table 5.30 - C460WC Test results .....	169
Table 5.31 - C355EP12 Test results .....	170
Table 5.32 - C460EP12 Test results .....	170
Table 5.33 - C355EP16 Test results .....	171
Table 5.34 - C460EP16 Test results .....	171
Table 5.35 - C355EP20 Test results .....	172
Table 5.36 - C460EP20 Test results .....	172
Table 5.37 - Characteristics of joints under monotonic loading.....	173
Table 5.38 - Characteristics of joints under cyclic loading.....	173
Table 5.39 - Brief description of failure modes of joint specimens .....	177
Tabel 6.1 -T-stub FEM specimens .....	179
Table 6.2 -Beam-to-Column FEM specimens (BUC & BV) .....	180
Table 6.3 -Beam-to-Column FEM specimens .....	181
Table 6.4 - Classification of joints according to T-stub failure mode.....	185
Table 6.5 - Bucharest & Brasov joints configuration .....	186
Table 6.6 - Bucharest(BUC) & Brasov (BV) Joint properties and classification.....	186
Tabel 6.7 - Joint rotation capacity under numerical analysis .....	190
Table 6.8 - Experimental plastic rotation capacity of joints.....	191

## LIST OF FIGURES

Fig. 2.1 – Regular steel cross sections .....	36
Fig. 2.2 – Non-alloy structural steel according to European Standard – Mechanical properties.....	37
Fig. 2.3 - Non-alloy structural steel according to European Standard – Chemical composition .....	38
Fig. 2.4 - Historical development of production processes for rolled steel products [73] .....	41
Fig. 2.5 – Relative costs in % for S355 and DILIMAX 550, 690, 890, 965, 1100 regarding base material, weld, welding and plate thickness.....	42
Fig. 2.6 - Weight and material cost comparison for a column made of S235, S355 and S460 dimensioned at compression 4000kN (left) and 22500kN (right).....	43
Fig. 2.7 - Weight and material cost comparison for a column made of S355 and S460 dimensioned at compression 42600kN.....	43
Fig. 2.8 - Weight and material cost comparison for a beam made of S235, S355 and S460 loaded with 1250kN .....	43
Fig. 2.9 Recyclability degree of different materials .....	44
Fig. 2.10 - Manufacturing technology of normalized steel profiles [8] .....	45
Fig. 2.11 - Comparison between the rolling processes [8] .....	45
Fig. 2.12 - Intervals of the heating temperatures for quenching and reheating of the carbon steel .....	46
Fig. 2.13 - HISTAR[8] manufacturing procedure .....	47
Fig. 2.14 - Characteristic curve unit stress – specific deformation for steel grade 690 subjected to the thermal treatment of quenching and reheating [72] .....	49
Fig. 2.15 - The influence of preheating temperature on weldability of elements made of different types of steel [8].....	51
Fig. 2.16 – Local buckling resistance curves for slabs-stiffened elements [72] .....	52
Fig. 2.17 - Local buckling resistance curves for slabs-un-stiffened elements [72] ..	53
Fig. 2.18 - Local buckling resistance curves for box columns, steel 690MPa, Australian norm [72].....	54
Fig. 2.19 - Local buckling resistance curves for double T columns, steel 690MPa, Australian norm [72].....	55
Fig. 2.20 – Local buckling resistance curves for long columns, box sections, steel grade 690MPa [72] .....	56
Fig. 2.21 - Local buckling resistance curves for slender columns, double T sections, steel grade 690MPa [72].....	57
Fig. 2.22 – Comparison of toughness requirements according to EN 10025 and actual toughness properties from European deliveries for rolled sections[37] .....	61
Fig. 2.23 – Reduction in weight of columns through use of Histar 460 (MAPFRE Tower) .....	62
Fig. 3.1 - Frame systems: (a) plan view and elevation of EBF8, CBF8, BRB8 and SW8 structures; (b) plan view and elevation of EBF16, CBF16, BRB16 and SW16 structures .....	66
Fig. 3.2 - Determination of the structures performance (MRF5) .....	68
Fig. 3.3 - Pushover curves (normalized base shear vs. normalized top displacement) for eight story buildings a) and plastic hinges at ULS for EBF8, CBF8, BRB8 and SW8 structures b) .....	69

Fig. 3.4 - Pushover curves (normalized base shear vs. normalized top displacement) for sixteen story buildings a) and plastic hinges at ULS for EBF16, CBF16, BRB16 and SW16 structures b) .....	70
Fig. 3.5 - Elastic response spectrum of the semi-artificial accelerograms comparable to .....	the design spectrum (P100-1/2006, $a_g=0.24g$ , $T_c=1.6s$ )
Fig. 3.6 - Ground acceleration according to the recurrence period [44] .....	72
Fig. 3.7 - Acceleration - Interstorey drift curves, for EBF8 .....	72
Fig. 3.8 - Acceleration - Interstorey drift curves, for (EBF16) .....	72
Fig. 3.9 - Acceleration - Interstorey drift curves, for CBF8 .....	73
Fig. 3.10 - Acceleration - Interstorey drift curves, for CBF16.....	73
Fig. 3.11 - Ductility Demand Ratios for the buckling restrained braces.....	74
Fig. 4.1 - Boundaries for stiffness classification of joints .....	77
Fig. 4.2 - Boundaries for strength classification of joints .....	78
Fig. 4.3 - Full-strength resistance .....	79
Fig. 4.4 - Inelastic Behaviour of Frames with Hinges in Beam Span[38] .....	81
Fig. 4.5 - Plastic hinges position on beam[38].....	81
Fig. 4.6- Defining performance levels function the frequency of the earthquake ....	83
Fig. 4.7 - Response spectrum according to FEMA-273, for a 5% damping .....	84
Fig. 4.8 - Design principle of non-dissipative joints .....	86
Fig. 4.9 - Plastic rotation capacity.....	87
Fig. 4.10 - Joint classification based on ductility .....	87
Fig. 4.11 - Joint Moment - Rotation .....	88
Fig. 4.12 - Beam deflection for the calculation of $\theta_p$ [34].....	89
Fig. 4.13 - Beam to column joints - American practice.....	91
Fig. 4.14 - Recommended Weld Access Hole Detail[4] .....	92
Fig. 4.15 - Beam to column joints - European practice .....	94
Fig. 4.16 - Reduced beam section connection [5] .....	95
Fig. 5.1 - Structures Laboratory in the CMMC Department - building A. ....	101
Fig. 5.2 - Universal trial device UTS/ZWICK with a capacity of 250 KN and hydraulic fixing.....	101
Fig. 5.3 - Experimental stand for connection tests.....	102
Fig. 5.4 - Digital Image Correlation system - LIMESS Vic 3D .....	102
Fig. 5.5 - Stress-strain diagrams of standard tensile tests.....	104
Fig. 5.6 - Tensile test on materials .....	104
Fig. 5.7 - Load vs. Tensile Strength on M20 bolts .....	105
Fig. 5.8 - Load vs. Tensile Strength on M22 bolts .....	105
Fig. 5.9 - Failure mode for M20 bolts .....	105
Fig. 5.10 - Failure mode for M22 bolts.....	105
Fig. 5.11 - Metal Charpy Pendulum Impact Tester .....	106
Fig. 5.12 - Welded specimen.....	108
Fig. 5.13 - Welded connections - experimental platform.....	110
Fig. 5.14 - Welded specimen equipped with measuring devices .....	110
Fig. 5.15 - Welding technology for $\frac{1}{2}$ V bevel weld .....	112
Fig. 5.16 - Welded specimens - nominal geometry.....	113
Fig. 5.17 - Experimental characteristics of welded specimens.....	119
Fig. 5.18 - Load - displacement curves for FW and KW specimens.....	119
Fig. 5.19 - Load - displacement curves for VW specimens.....	120
Fig. 5.20 - Load - displacement curves for S235 and S460 specimens(FW,KW,VW,VRW).....	120
Fig. 5.21 - Load - displacement curves for S690(FW,KW,VW,VRW) specimens...	120
Fig. 5.22 - Load - displacement curves for S690KW_M1,M2,M3 specimens.....	121

---

Fig. 5.23 – Load – displacement curves for S235 and S460 specimens(FW Monoton/Cyclic).....	121
Fig. 5.24 – Load – displacement curves for S690 specimens(FW Monotone/Cyclic).....	122
Fig. 5.25 – Load – displacement curves for S235 specimens(KW Monotone/Cyclic).....	122
Fig. 5.26 – Load – displacement curves for S460 specimens(KW Monotone/Cyclic).....	123
Fig. 5.27 – State of strain in welded specimens at yield and failure using digital image correlation technique .....	123
Fig. 5.28 – Load – displacement curves for S235 specimens(VW Monotone/Cyclic).....	124
Fig. 5.29 – Load – displacement curves for S460 specimens(VW Monotone/Cyclic).....	124
Fig. 5.30 – Load – displacement curves for S690 specimens(VW Monotone/Cyclic).....	124
Fig. 5.31 – Load – displacement curves for S235 specimens(VRW Monotone/Cyclic).....	125
Fig. 5.32 – Load – displacement curves for S690 specimens(VRW Monotone/Cyclic).....	125
Fig. 5.33 - Welding details fractography.....	125
Fig. 5.34 - Different types of bolted T-stub connection assemblies[49] .....	126
Fig. 5.35 – T-stub Type A .....	127
Fig. 5.36 – T-stub Type B .....	128
Fig. 5.37 – T-stub Type C .....	128
Fig. 5.38 – T-stub specimen .....	129
Fig. 5.39 – T-stub test set up. ....	130
Fig. 5.40 – T-stub TST_12B_S690 design characteristics .....	131
Fig. 5.41 – T-stub specimen – Experimental stand .....	134
Fig. 5.42 – Displacement transducers and Vic3D on T-stub specimen .....	135
Fig. 5.43 – Force-displacement TST type A –thin End Plate .....	136
Fig. 5.44 – Force-displacement TST type B –thin End Plate .....	136
Fig. 5.45 – Force-displacement TST type C –thin End Plate .....	137
Fig. 5.46 – Force-displacement TST type A –thick End Plate .....	137
Fig. 5.47 – Force-displacement TST type B –thick End Plate .....	137
Fig. 5.48 – Force-displacement TST type C –thick End Plate .....	138
Fig. 5.49 – Experimental characteristics of TST-8A-S690-M1 T-stub specimen....	138
Fig. 5.50 - Experimental characteristics of T-stub specimens.....	144
Fig. 5.51 - Ultimate displacement of T-stub specimens: monotonic vs. cyclic loading .....	146
Fig. 5.52 - Yield Force - experimental (monotonic) vs. analytical values.....	147
Fig. 5.53 – Force –Displacement relationship for T-stubs with “thin” end plate....	150
Fig. 5.54 - Force –Displacement relationship for T-stubs with “thick” end plate... ..	152
Fig. 5.55 - Fatigue strength curves for normal stress ranges .....	154
Fig. 5.56 - Cumulated energy .....	157
Fig. 5.57 – Welded beam-to-column joint. ....	161
Fig. 5.58 – Bolted extended end-plate beam-to-column joint.....	161
Fig. 5.59 – Beam-to-column joint specimen – test setup.....	162
Fig. 5.60 – Beam-to-column joint specimen 3D Model .....	163
Fig. 5.61 – Measurements devices on beam-to-column joint specimen .....	163
Fig. 5.62 - Bolts collapse mechanism.....	166



---

Fig. 5.63 - Force –Displacement relationship for Beam-To-Column specimens loaded Monotonic.....	167
Fig. 5.64 – Experimental characteristics of C355EP12_M1 specimen.....	168
Fig. 5.65 - State of strain in the column web at yield and failure using digital image correlation technique.....	174
Fig. 5.66 - Joint tested specimens.....	176
Fig. 6.1 - Continuum solid element – 8 node element.....	180
Fig. 6.2 - Elastic perfectly plastic steel material curve.....	181
Fig. 6.3 – T-stubs numerical vs. Experimental results.....	183
Fig. 6.4 – C460EP16S460 Numerical versus experimental results.....	184
Fig. 6.5 – C460EP12S690 Numerical versus experimental results.....	185
Fig. 6.6 - Brasov joint configuration .....	186
Fig. 6.7 - Detail of stiffener on the upper flange.....	186
Fig. 6.8 - T-stub behavior and failure mode according to numerical analysis.....	188
Fig. 6.9 - -Bucharest T-stub behaviour according to numerical analysis .....	189
Fig. 6.10 – Brasov T-stub behaviour according to numerical analysis.....	189
Fig. 6.11 – Bucharest Joint behaviour.....	189
Fig. 6.12 - Joint rotation capacity with components (web panel and end-plate)...	190
Fig. 6.13 - Joint rotation capacity under numerical analysis.....	191
Fig. 0.1 - Joint configurations tested within the COPERNICUS "RECOS" project. ..	204

# 1 INTRODUCTION

## 1.1 Motivation

The deciding factors for the choice of the structural material are usually the economic aspects; therefore the overall economy has a great significance. The material cost, production economy and maintenance costs during the design lifetime of the product are the biggest influencing factors of overall economy.

If the governing factor is strength then HSS is more likely to be used and thus an important advantage being the lower self weight of the final product. The lower self weight generates secondary benefits such as a lower transportation, handling costs, smaller weld metal volumes due to thinner steel plates and therefore increased production speed. The welding process can be automated due to smaller and simpler welds.

Quenching hardens steel by introducing brittle martensite, which becomes ductile after tempering. Hence, there is always a trade-off between ductility and brittleness. Ductility is a qualitative, subjective property of a material [21]. It is generally defined as the ability of a material to accommodate inelastic deformation without breaking. Ductile material tolerates the designer errors in stress calculation or the prediction of severe loads [19]. The maximum allowable stress should be less than yield stress therefore this definition is no longer of any use as it refers to elastic design. The difference between yield and ultimate tensile strength is comprised the "additional" strength. From the tension tests several engineering measures of ductility can be obtained.

The ultimate-to-yield strength ratio  $f_u/f_y$  is the most commonly presented material ductility parameter. Offset yield strength  $R_p$  0,2, which is stress corresponding to the intersection of the stress-strain curve and a line parallel to the elastic part of the curve offset by the strain of 0,002, determines the yield strength  $f_y$ . In order to obtain the engineering fracture strain  $\epsilon_{fr}$  the length at fracture  $L_u$  of the gage section with original length  $L_0$  is required. Engineering fracture strain  $\epsilon_{fr}$  is expressed as percentage and is called percentage total elongation after fracture  $A_c$ . In the necked region of the test specimen an appreciable fraction of the plastic deformation will be concentrated therefore the value of  $A_c$  will depend on the original gage length  $L_0$  over which the measurement was taken. Thus geometrically proportional tension test specimens should be machined according to appropriate standard or the gage length should always be given when reporting the percentage total elongation at fracture. The percent reduction in area  $Z$  is another measure of ductility. By comparing the cross sectional area after fracture  $S_u$  with the original gage area  $S_0$  gives the percent reduction in area  $Z$ . After failure by putting the specimen back together and taking the required measurements using marks placed a known distance apart prior to the tests both quantities are obtained.

$$A_t = 100\epsilon_{fr} = \frac{L_u - L_0}{L_0} \quad (1.1)$$

$$Z = 100 \frac{S_0 - S_u}{S_0} \quad (1.2)$$

Standard for HSS EN 1993-1-12 recommends lower limits for ductility requirements than EN 1993-1-1. The recommended values for ultimate-to-yield ratio is lowered from  $f_u/f_y \geq 1,10$  to  $f_u/f_y \geq 1,05$ , elongation at failure is lowered from  $\epsilon_{fr} \geq 15\%$  to  $\epsilon_{fr} \geq 10\%$  while the requirement for ultimate strain remains unchanged  $\epsilon_u \geq 15f_y/E$ , where E is the Young's modulus. The latter requirement is stricter for higher steel grades ( $\epsilon_u \geq 1,68\%$  – for S235,  $\epsilon_u \geq 4,93\%$  – for S690,  $\epsilon_u \geq 9,29\%$  – for S1300). Very typical steel S690 has relative fracture elongation  $\epsilon_{fr}$  more than 14% (required by EN 10025-6), uniform strain  $\epsilon_u$  that corresponds to tensile strength  $f_u$  around 5% and ultimate-to-yield ratio around  $f_u/f_y = 1,05$  [9]

Samples of steel made by different producers all around the world were used in determining the material parameters. Without a doubt they prove that high strength steels have lower ductility than mild steels in terms of engineering measures of ductility. An essential role at the constitution of stress state in an element is given by the strain hardening and the capability of large deformations. In order to transfer the load between all fasteners and to reduce stress concentrations at connections ductility is of great importance. If the material does not have the ability of local plastic deformations, fractures open due to stress peaks. Only the elastic global analysis for sections classified as Class 2 or higher is allowed in EN 1993-1-12.

The use of HSS is favourable in members in tension where the strength governs. In case of compressive loading, various buckling phenomena may occur (lateral buckling, local buckling and lateral torsional buckling). The buckling is mainly governed by elastic modulus E, which is the same for all steel grades. Hence, the use of HSSs may seem unwise. However, weight savings can still be obtained if slenderness is low  $\lambda < 60-80$  [55]. Moreover, better buckling curve can be applied to HSS than to mild steels due to relatively lower residual stresses [72][9][16][54]. An economic solution regarding the problem of local buckling are hybrid steel girders, where the flanges are made of higher steel grade than the web. A limitation that strength of the flanges should not exceed twice that of the web for serviceability reasons is suggested [79]. It was also observed that significant improvements in rotational capacity can be achieved in hybrid girders [54]. The deflections are important criteria in serviceability limit state. The moment of inertia and Young's modulus, which are the parameters for the deflection function, are independent of steel grade, thus the stiffness needs relatively more attention for the structures in HSS.

When material weldability is discussed, it is essential that steel has a chemical composition that promotes the fusion of the base material and the filler metal, without the formation of cracks and other imperfection [10]. In the last ten years the use of HSS has increased enormously, mainly due to contemporary welding methods [56]. The costs of these steels are greatly reduced if preheating is omitted. With the correct choice of steel quality, welding consumables and welding process, the preheating is in many cases unnecessary [55]. It can be necessary for thicker plates to avoid cold cracking. The scope of studies was also aimed at undermatched welds, which can be successfully used in HSS structures [59][17].

The fatigue resistance is mainly governed by stress range  $\Delta\sigma$  and notch effect. The strength of steel has only a minor effect on the fatigue resistance. The use of HSS in fatigue loaded structures will result in higher stress ranges than in

structures of mild steel. The important key to the fatigue resistance is the notch effect and micro cracks that usually form where large amount of energy is added (flame cutting, welding, punching, and drilling). Stress concentration leads to crack propagation, resulting in macro crack and finally in a brittle fracture. The solution at HSSs can be [56][63] new or modified detailing, shifting of details in less stressed sections, improved welding procedures, better workmanship and post-weld improvement methods (such as grinding, Tungsten Inert Gas dressing, needle or hammer penning...). The investigations showed positive fatigue behaviour for HSS in the high load cycle  $\geq 2 \times 10^6$ , especially on special notch cases from mobile crane structures [12], as well.

Seismic resistant building frames designed as dissipative structures must allow for plastic deformations to develop in specific members, whose behaviour has to be predicted by proper design. Members designed to remain predominantly elastic during earthquake, such as columns, are responsible for robustness of the structure and prevention the collapse, being characterized by high strength demands. Consequently a framing solution obtained by combining High Strength Steel - HSS in non-dissipative members (e.g. columns) provided with adequate over strength, and Mild Carbon Steel – MCS in dissipative members, working as fuses (e.g. beams, links or braces) seems to be logical. The robustness of structures to severe seismic action is ensured by their global performance, in terms of ductility, stiffness and strength, e.g. the "plastic" members of MCS – (S235 to S355) will dissipate the seismic energy, while the "elastic" members (HSS - S460 to S690) by higher resistance of material and appropriate size of sections, will have the capacity to carry the supplementary stresses, following the redistribution of forces, after appearance of plastic hinges. Such a structure is termed Dual-Steels Structure - DS. DS concept is extended to connections, too, on the same philosophy related to ductile and brittle components, in order to achieve both ductility and robustness criteria. In fact, when connecting MCS beams to HSS columns it will result a DS beam-to-column joint. When HSS is used in members designed to remain predominantly elastic, as columns or in end-plates of bolted joints, DS T-stub macro-components made of two steel grades are obtained.

Starting from the above considerations, a large experimental research program (e.g. STOPRISC) was carried out at the "Politehnica" University of Timisoara, CEMSIG Re-search Centre (<http://cemsig.ct.upt.ro>) in order to study the performance of dual-steel configuration for beam-to-column joints under monotonic and cyclic loading. Joint specimens, T- stub and weld detail specimens have been tested. Present thesis in mainly is based on this research.

## **1.2 Thesis objectives**

The main objective of the thesis was to evaluate the opportunity of using HSS in DS buildings frames located in seismic areas and, on this basis, to investigate and evaluate the performance of DS beam-to-column connections. Particularly, bolted extended-end-plate beam-to-column joints have been examined in an attempt to control their overall behaviour mainly by the DS T-stub macro components.

On this purpose an extensive experimental program involving all the components a structural joint has, was carried out – e.g. materials, weld details, T-stubs, beam-to-column joints. A companion numerical simulation program extends the area of experimental investigation.

### **1.3 Research framework**

The results of the studies, analyses and of the experimental part represented a point of interest within the framework of national research projects: CEEEX – MATNANTECH (2005-2008), contract 29/2005, “STOPRISC - Sisteme constructive si tehnologii avansate pentru structuri din oteluri cu performante ridicate destinate cladirilor amplasate in zone cu risc seismic”. The involvement in this project was performed through CEMSIG, from the CMMC department of the Civil Engineering Faculty of Timisoara. Also, all results were disseminated by the participation of the author at national/international conferences and meetings. The results of the research presented in this thesis were also presented in European research projects, RFCS-CT-00024 HSS-SERF (2009-2012).

### **1.4 Thesis outline**

The thesis lineout is closely related to above mentioned objectives:

#### **Chapter 1**

In the first chapter the subject of the thesis is presented. Motivation, objectives, scope and justification in the current context and in the context of the national and international research programs in which the author of the thesis and the research centre CEMSIG is involved are also presented.

#### **Chapter 2**

The second chapter presents a wide range of steels for construction structural elements. The steels used for constructions are described while high performance steels are highlighted. Still in this chapter are described requirements and election criteria for steels in structural applications.

#### **Chapter 3**

In the third chapter a parametric study is performed on multi storey steel frame structures for buildings placed in seismic areas with components of high strength steel. The numerical simulation program that represents the basis of the study is presented, together with the results and conclusions.

#### **Chapter 4**

The fourth chapter analyses constructive solutions and performance criteria for beam to column connections of multi storey frame structures placed in seismic zones. There are described constructive solutions from European and American practice as well as requirements and design criteria of the European and American norm.

#### **Chapter 5**

In the fifth chapter is presented the experimental program investigating the behaviour of beam to column connections with components made of high strength steel. Aspects of the experimental program regarding welding detailing are presented on elements of type T-stub as well as on beam-column joints. The tests protocols are described as well as the equipment used and the experimental stand. In this chapter are also analysed the experimental tests and are presented the results and the conclusions of the tests.

**Chapter 6**

The sixth chapter presents the numerical simulation program on components of type T-stub and on joint made of different types of steel. The methodology of the numerical simulation is described; the numerical studied models together with the results as well as the conclusions are presented.

**Chapter 7**

The last chapter, presents a summary review of the thesis, the conclusions and the personal contributions of the author as well as the capitalizing of the studied results.

## **2 STRUCTURAL STEELS**

### **2.1 Introduction**

Structural steel has been used in constructions for more than 100 years. The material and its many products have undergone significant changes since through time some of these prompted by demand for higher strength and improved economies of construction, and many caused by developments in joining techniques and fabrication.

The primary characteristics of structural steel include mechanical and chemical properties, metallurgical structures and weldability. In the past structural engineers have tended to focus only on tensile properties. Since the modulus of elasticity  $E$  is constant for all grades of steel, it has rarely been a consideration other than for serviceability issues. Weldability, deformability and ductility were assumed to be adequate for all steels because the design specifications have offered limited specific requirements.

In addition, the performance of the material in recent earthquakes raised a number of questions related to the design and fabrication of steel structures. Historically accepted criteria especially connection geometries were questioned. The suitability of the properties as determined by the common uniaxial tension specimen was called into question since several failure modes seemed to demand higher and better defined orthogonal strength characteristics [10].

On this background, significant research and design projects were undertaken to determine the necessary properties of the steels that would satisfy the requirements for acceptable service under all conditions. These materials, defined by good performance in tensile stress, toughness, weldability, cold forming and corrosion were identified as High Performance Steels (HPS).

The efficiency of steel structural members and connections can in many cases be enhanced by using steels with high values of yield stress and/ or tensile strength. These steels named High Strength Steels (HSS) are already used on machine, automotive and aeronautical industries and their use for building industry represents one of the main development directions in the field, and represents a challenge for metallurgic industry, steel fabricators, researchers and designers. Their need in building industry it is motivated by strong casualties (earthquakes, hurricanes, low temperatures, fire and blast actions) inducing high strain rates.

In this chapter it will be presented a summary review on previous research of HSS connections, a review on common used steel for resistance structures focusing on mainly high strength steels, steels that represent the subject of this thesis. There will be presented also requirements and criteria for choosing steel in structural applications.

### **2.2 Common steels for constructions**

In most developed countries, the shapes available are set out in published standards, although a number of custom and proprietary cross sections are also available.



Fig. 2.1 – Regular steel cross sections

- I-beam (I-shaped cross-section) - in Europe it includes the IPE, HE, HL, HD and other sections; in Great Britain these include Universal Beams (UB) and Universal Columns (UC); in the USA it includes Wide Flange (WF) and H sections
- RHS-Shape (Rolled Hollow section also known as SHS (structural hollow section) and including square, rectangular, circular (pipe) and elliptical cross sections)
- Z-Shape (half a flange in opposite directions)
- Angle (L-shaped cross-section)
- Channel ( [ -shaped cross-section)
- Tee (T-shaped cross-section)
- Plate
- Bar
- Rod

Commonly used steels in constructions are carbon steels or low alloyed steels delivered in the form of hot rolled profiles. Steel grade is defined by the yielding limit and ultimate strength. The mechanical characteristics especially the yielding limit are differentiated function the thickness of the elements.

Steels up to S235 are Mild Carbon Steels. These possess remarkable plastic characteristic.

Steels of type S275 and S355 are low alloyed steels that have as alloyed elements, besides carbon, manganese, silica and aluminium, sometimes elements such as vanadium, niobium or titanium in small percentages. Low alloyed steels also possess good plastic properties.

Chemical composition is rigorously dosed and controlled with the means of avoiding fragile structures in different situation of mounting and exploitation. The maximum carbon concentration varies between 0.17 and 0.25%. The maximum manganese concentration varies between 0.85...1.55%, silica is found in insignificant percentages in rimmed steels and in percentages of 0.40...0.50% in dead-melted steels or low alloyed steels. Aluminium is found in higher percentages in low alloyed steels of superior quality. Sulphur and phosphorus are found in reduced quantities. Vanadium and titanium have the role of creating a structure with a fine granulation and are found in reduced quantities imposed by weld-ability conditions.

The differentiation of steels in different quality grades is made by chemical composition and toughness. Toughness, the ability of a material to absorb energy and plastically deform without fracturing, depends on chemical composition and the manufacturing process of the steel.

Function of the using conditions, respectively the guaranteed characteristics of the finite product steels for metallic structures can be classified as follows:

- Standard structural steel
- Weathering steel
- Fine grain steel



- Steel for Cryogenic and Low-Temperature Service  
High strength steel

**2.2.1 Standard structural steels in Europe**

Most steels used throughout Europe are specified to comply with the European standard EN 10025. However, many national standards also remain in force.

Typical grades are described as 'S275J2' or 'S355K2W'. In these examples, 'S' denotes structural rather than engineering steel; 275 or 355 denotes the yield strength in newtons per square millimetre or the equivalent megapascals; J2 or K2 denotes the materials toughness by reference to Charpy impact test values; and the 'W' denotes weathering steel. Further letters can be used to designate fine grain steel ('N' or 'NL'); quenched and tempered steel ('Q' or 'QL'); and thermo-mechanically rolled steel ('M' or 'ML').

The normal yield strength grades available are 195, 235, 275, 355, 420, and 460, although some grades are more commonly used than others e.g. in Europe, almost all structural steel is grades S275 and S355. Higher grades are available in quenched and tempered material (500, 550, 620, 690, 890 and 960 - although grades above 690 receive little if any use in construction at present).

Steels for resisting structures in constructions		
Common steels in constructions	High performance steels	Special steels
Carbon steel or low alloyed steels delivered as rolled profiles	Low alloyed steels Thermal treatments	Steels characterised by good Resistance, ductility and weldability
S235; S275; S355	HISTAR 460, 690 DILLIMAX 550,690,890,965,1100	S235,S275,S355 (M, ML) S235,S275,S355 (W)

Table 2.1 - Steels for resistance structures in constructions

Standard	Grades	Minimum yield strength $R_{eH}$						Tensile strength $R_m$		Minimum elongation $L_0 = 5,65 \sqrt{S_0}$ %				Notch impact test	
		MPa						MPa						Temperature	Min. absorbed energy
		Nominal thickness (mm)						Nominal thickness (mm)		Nominal thickness (mm)				°C	J
		≤16	>16 ≤40	>40 ≤63	>63 ≤80	>80 ≤100	>100 ≤125	≥3 ≤100	>100 ≤125	≥3 ≤40	>40 ≤63	>63 ≤100	>100 ≤125	°C	J
EN 10025:1990 + A1: 1993	S 235 JR G2													+20	27
	S 235 J0	235	225			215	195		340-470	26	25	24	22	0	27
	S 235 J263/G4*													-20	27
	S 275 JR													+20	27
	S 275 J0	275	265	255	245	235	225	410-560	400-540	22	21	20	18	0	27
	S 275 J263/G4*													-20	27
	S 355 JR													+20	27
	S 355 J0	355	345	335	325	315	295	490-630	470-630	22	21	20	18	0	27
	S 355 J263/G4													-20	27
S 355 K263/G4													-20	40	

Fig. 2.2 – Non-alloy structural steel according to European Standard – Mechanical properties

Standard	Grades	Ladle analysis									
		C max. %			Mn max. %	Si max. %	P max. %	S max. %	N max. %	CEV max. %	
		Nominal thickness (mm)								Nominal thickness (mm)	
		≤16	>16 ≤40	>40 <sup>a</sup>	≤40	>40 ≤125					
EN 10025:1990 + A1:1993	\$ 235 JRG2	0,17	0,17	0,20	1,40	-	0,045	0,045	0,009	0,35	0,38
	\$ 235 J0	0,17	0,17	0,17	1,40	-	0,040	0,040	0,009	0,35	0,38
	\$ 235 J263/G4	0,17	0,17	0,17	1,40	-	0,035	0,035	-	0,35	0,38
	\$ 275 JR	0,21	0,21	0,22	1,50	-	0,045	0,045	0,009	0,40	0,42
	\$ 275 J0	0,18	0,18	0,18	1,50	-	0,040	0,040	0,009	0,40	0,42
	\$ 275 J263/G4	0,18	0,18	0,18	1,50	-	0,035	0,035	-	0,40	0,42
	\$ 355 JR	0,24	0,24	0,24	1,60	0,55	0,045	0,045	0,009	0,45	0,47
	\$ 355 J0	0,20	0,20	0,22	1,60	0,55	0,040	0,040	0,009	0,45	0,47
	\$ 355 J263/G4	0,20	0,20	0,22	1,60	0,55	0,035	0,035	-	0,45	0,47
	\$ 355 K263/G4	0,20	0,20	0,22	1,60	0,55	0,035	0,035	-	0,45	0,47

Fig. 2.3 - Non-alloy structural steel according to European Standard – Chemical composition

## 2.2.2 Standard structural steels in USA

Steels used for building construction in the US use standard alloys identified and specified by ASTM International (American Society for Testing and Materials). These steels have an alloy identification beginning with A and then two, three, or four numbers. The four-number AISI steel grades commonly used for mechanical engineering, machines, and vehicles are a completely different specification series.

The standard commonly used structural steels are:

- **Carbon steels**
  - A36 - structural shapes and plate
  - A53 - structural pipe and tubing
  - A500 - structural pipe and tubing
  - A501 - structural pipe and tubing
  - A529 - structural shapes and plate
- **High strength low alloy steels**
  - A441 - structural shapes and plates
  - A572 - structural shapes and plates
  - A618 - structural pipe and tubing
  - A992 - W shapes beams only
  - A270 - structural shapes and plates
- **Corrosion resistant high strength low alloy steels**
  - A242 - structural shapes and plates
  - A588 - structural shapes and plates
- **Quenched and tempered alloy steels**
  - A514 - structural shapes and plates
  - A517 - boilers and pressure vessels

A comparison between structural steels according EN 10025:1993, American Standards and Japanese standards is shown in Table 2.2.

Aciers de construction / Structural steels / Baustähle											
EN 10025: 1993	Normes antérieures / Previous standards / Frühere Normen								ASTM	CSA G 40-21	JIS G 3101 JIS G 3106
	NF A 35-501	DIN 17100	BS 4360	NBN A21-101 UNE 36 080	UNI 7070	SS 14	NS 12 101	ÖNORM M1316			
S 235 JRG2 S 235 JO	E 24-3	RSr 37-2 St 37-3 U	40 B 40 C	AE 235B-FN AE 235-C	Fe 360 B-FN Fe 360 C	13 12-00	NS 12 123 NS 12 124	RSr 360 B St 360 C	A 36	260 W	SS 400 SM 400 A/B/C
S 275 JR S 275 JO	E 28-2 E 28-3	St 44-2 St 44-3 U	43 B 43 C	AE 255-B AE 255-C	Fe 430 B Fe 430 C	14 12-00	NS 12 142 NS 12 143	St 430 B St 430 C			SS 400
S 355 JR	E 36-2		50 B	AE 355-B	Fe 510 B				A 572 Gr 50 A 992 Gr 50	300 W 350 W	SS 490
S 355 JO	E 36-3	St 52-3 U	50 C	AE 355-C	Fe 510 C	21 32-01	NS 12 153	St 510 C			
S 355 J2G3		St 52-3 N	50 D	AE 355-D	Fe 510 D	21 34-01	NS 12 153	St 510 D			
S 355 J2G4			50 D	AE 355-D	Fe 510 D						
S 355 K2G3	E 36-4			AE 355-DD							
S 355 K2G4	E 36-4			AE 355-DD							

Table 2.2 – Comparison table of typical steel grades

### 2.2.3 Weathering steel "W"

Weathering steel, best-known under the trademark COR-TEN steel and sometimes written without the hyphen as "Corten steel", is a group of steel alloys which were developed to eliminate the need for painting, and form a stable rust-like appearance if exposed to the weather for several years.

Weathering means that due to their chemical compositions COR-TEN steels, when utilised unprotected, exhibits increased resistance to atmospheric corrosion compared to unalloyed steels. This is because it forms a protective layer on its surface under the influence of the weather. The corrosion retarding effect of the protective layer is produced by the nature of its structure components and the particular distribution and concentration of alloying elements in it. The layer protecting the surface develops and regenerates continuously when subjected to the influence of the weather. Formation, duration of development and protective effect of the covering layer on weathering steels depend largely upon the corrosive character of the atmosphere. Its influence varies and depends mainly upon general weather condition (e.g. continental) macroclimate (e.g. industrial, urban, maritime or countryside climate) and the orientation of the structure components (e.g. exposed to or shaded from the weather, vertical or horizontal position). The amount of aggressive agents in the air has to be taken into account. In general the covering layer offers protection against atmospheric corrosion in industrial, urban and countryside climate. When utilising this steel in unprotected condition it is up to the designer to take into account the expected loss of thickness due to corrosion and as far as necessary, compensate for it by increasing the thickness of the material. In cases of particular air pollution by aggressive agents conventional surface protection is recommended. Coating is absolutely necessary in cases of contact with water for long periods, when permanently exposed to moisture, or if it is to be used in the vicinity of the sea. The susceptibility of paint coats to undercreepage by rust is less in the case of weathering steel than in the case of comparable non-weathering steel [7].

Grade	C	Si	Mn	P	S	Cr	Cu	V	Ni
COR-TEN A	0.12	0.25-0.75	0.20-0.50	0.07-0.15	0.030	0.50-1.25	0.25-0.55		0.65
COR-TEN B	0.16	0.30-0.35	0.80-1.25	0.030	0.030	0.40-0.65	0.25-0.40	0.02-0.10	0.40

Table 2.3 – COR-TEN Chemical composition

### 2.2.4 Fine grain steel - “N” or “NL”

These steels are low alloyed steels with a fine granulation. In their composition is included aluminium, niobium, vanadium, zirconium and titanium. After the process of normalizing the values of the yield limit are obtained between 285 and 1100 MPa. By their chemical composition and manufacturing technology they contain nitrous precipitates and finely distributed carbides that impede the increase of the granulation in the austenitic domain and determine the formation of a fine granulation.

Having high mechanical characteristics, plastic properties and a good behaviour in welding, remarkable resistance in brittle failure and toughness in low temperatures, these steels are recommended for welded metallic structures heavily loaded in hard exploitation conditions.

### 2.2.5 Steel for Cryogenic and Low-Temperature Service

Carbon and alloy grades for low-temperature service are required to provide the high strength, ductility, and toughness in vehicles, vessels, and structures that must serve at  $-45^{\circ}\text{C}$  and lower.

The only alloy steel recommended for cryogenic service is 9% nickel steel. It is satisfactory for service down to  $-195^{\circ}\text{C}$  and is used for transport and storage of cryogenics because of its low cost and ease of fabrication. Other alloy steels are suitable for service in the low-temperature range. The steels A201 and T-1 can suffice to  $-45^{\circ}\text{C}$ , nickel steels with 2.25% Ni can suffice to  $-59^{\circ}\text{C}$ , and nickel steels with 3.5% Ni to  $-101^{\circ}\text{C}$ .

## 2.3 High strength steel

The development of new high strength steels has been driven by the following reasons [73]:

- **Economy:** By increasing the strength of steel, the structural section can be reduced. This may reduce the weight of the structure, and subsequently the volume of weld metal ( $\sim t^2$ ) and hence fabrication and erection costs.
- **Architecture:** The size of structural elements can be reduced enabling special aesthetic and elegant structures, which embed in the environment in an outstanding manner.
- **Environment:** Construction with less steel means also a reduced consumption of our world’s rare resources.
- **Safety:** Modern high strength steel grades do not only show high strength values. Special grades combine this strength with excellent toughness

properties so that a high safety both in fabrication and application of the structures is applied.

In the 1960's the application of the quenching and tempering process for structural steel grades began. Beside the special heat treatment the good balance between strength and toughness is based on the fact, that these steels are alloyed by adding micro alloying elements (niobium, vanadium, titanium) precipitating as finely distributed carbon nitrides.

Today this process enables steel grades with yield strength up to 1100 Mpa, although only grades up to 960 MPa yield stress are standardized (EN 10025-6). The crane industry uses these "ultra-high" strength steels because of the extraordinary role of light weight for performance. For European classical steel construction, e.g. for buildings and bridges, the strength is mostly limited to steel grades up to S690.

In the 1970's the thermo mechanical (TM) rolling process was developed and first applied for pipeline plates, but then fast found the way into the fields of ship building and construction of offshore platforms both for plates and rolled sections. TM rolling is a process, in which final deformation is carried out in a certain temperature range leading to material properties, which cannot be achieved by heat treatment alone. The resulting steel grade has high strength as well as high toughness and at the same time a minimum alloying content resulting in best weldability. Plates with guaranteed minimum yield strength up to 500 Mpa are available in thickness up to 80 mm used in shipbuilding and offshore construction. For construction steel work even plates of 120 mm have been produced in particular for bridges.[43]

Fig. 2.4 demonstrates the historical development of production processes for rolled steel products in Europe

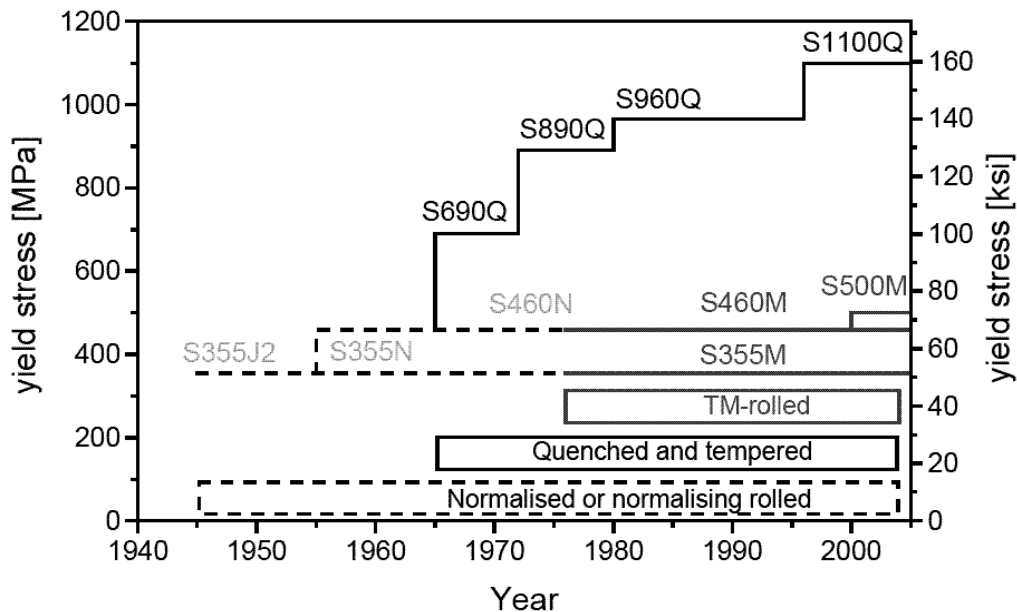


Fig. 2.4 - Historical development of production processes for rolled steel products [73]

In Table 2.4 are presented strength requirements for high strength steel (HSS) from Europe, United States and Japan.

	Grade	Min.yield strength [MPa]	Ultimate tensile Strength[MPa]
<b>Europe</b>	S420M	370-420	470-680
	S460M, Q	400-460	500-720
	S550Q	490-550	590-820
	S690Q	630-690	710-940
	S890Q	830-890	880-1100
	S960Q	960	980-1150
<b>United States</b>	HPS50W	345	485
	HPS70W	485	586-760
	HPS100W	690	760-895
<b>Japan</b>	SM570,570W	420-460	570-720
	HPS485W	485	585-760
	BHS500,500W	500	570
	BHS700W	700	780

Table 2.4 – Strength requirements for structural steel

The efficiency of structures for buildings designed as steel frames can be improved in certain situations by using steels with higher values of the yielding limit and/or ultimate strength. By using steels with higher resistance/weight ratio material savings can be obtained especially in the case of heavy constructions. Compared to common steels, that have a yielding limit that does not cross over 355 N/mm<sup>2</sup>, high strength steels present higher levels in general between 420N/mm<sup>2</sup> and 690N/mm<sup>2</sup>. By increasing the strength of steel the dimension of the cross section can be reduced. This leads to a reduction in the weight of the structure, the welding volume, meaning implicitly lower manufacturing and assembling costs (Fig. 2.5).

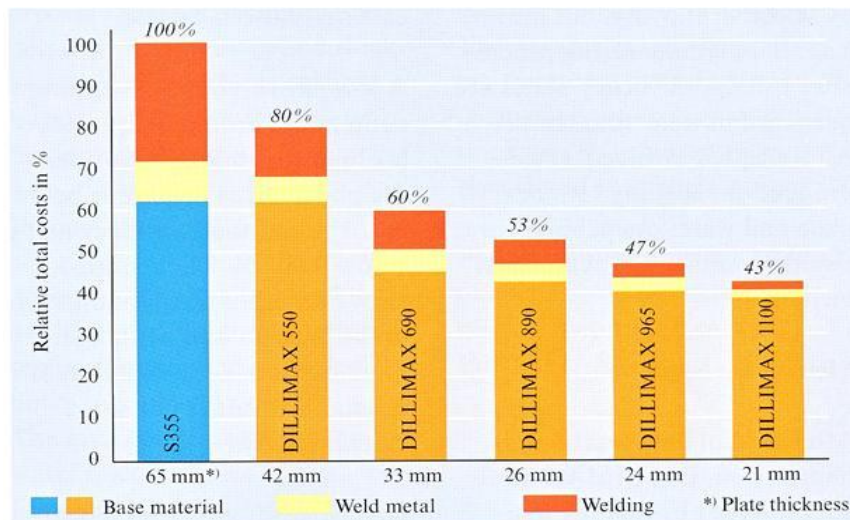


Fig. 2.5 – Relative costs in % for S355 and DILLIMAX 550, 690, 890, 965, 1100 regarding base material, weld, welding and plate thickness



In Fig. 2.6 it is shown weight and material cost comparison for a section made of S235, S355 and S460 dimensioned on compression at 4000kN (left) and 22500kN (right).

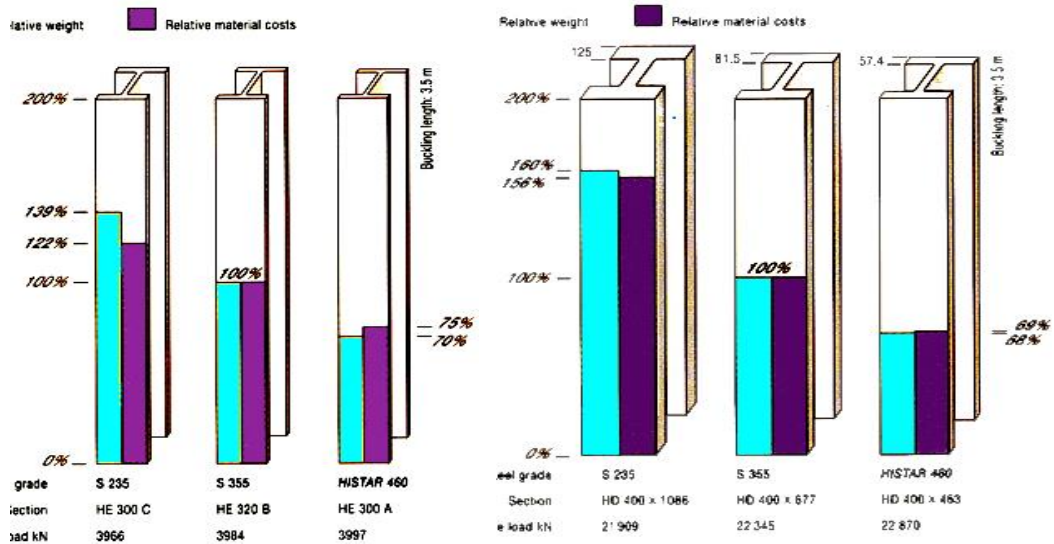


Fig. 2.6 - Weight and material cost comparison for a column made of S235, S355 and S460 dimensioned at compression 4000kN (left) and 22500kN (right).

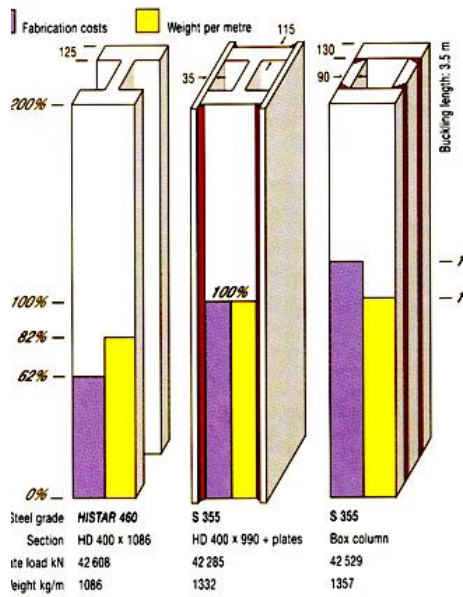


Fig. 2.7 - Weight and material cost comparison for a column made of S355 and S460 dimensioned at compression 42600kN

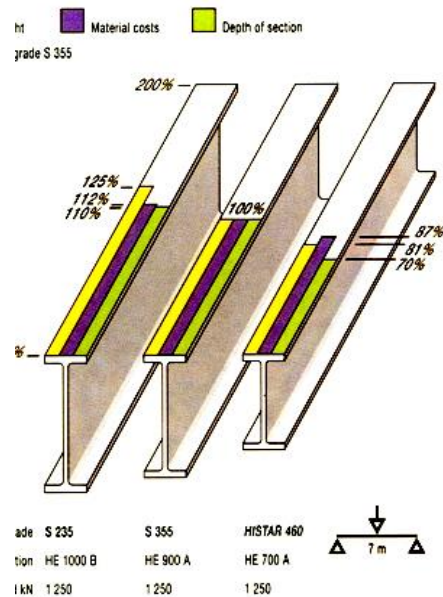


Fig. 2.8 - Weight and material cost comparison for a beam made of S235, S355 and S460 loaded with 1250kN

Using HSS in structural design mainly for their strength capacity means, at the end, to reduce the quantity of the raw material. Also it means less welding. So HSS instead of MCS could be a decision of sustainability.

Achieving sustainability will enable the Earth to continue supporting human life as we know it. Less steel consumption means the reduction of the consumption of raw material, gas emissions reduction and energy consumption reduction. As it can be seen in Fig. 2.9 steel is the material with the higher degree of recyclability.

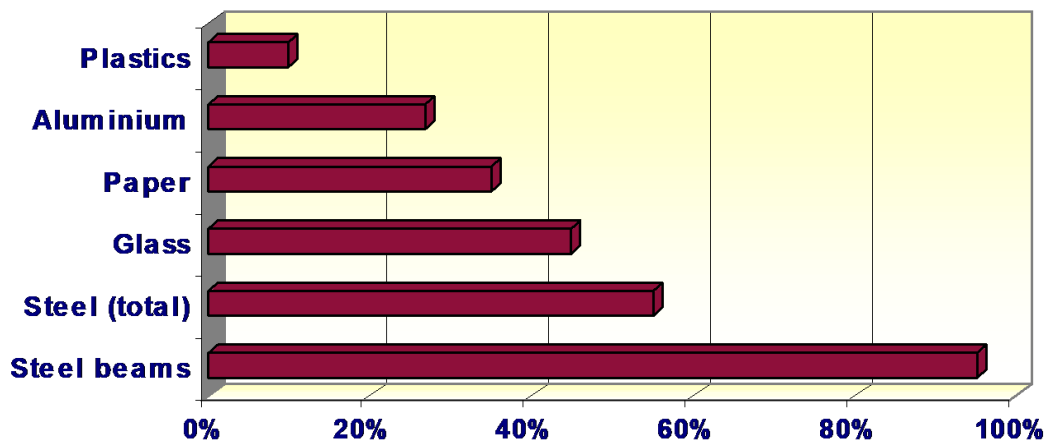


Fig. 2.9 Recyclability degree of different materials

### 2.3.1 High strength steel production.

The mechanical properties of steel, such as resistance and ductility, depend on its chemical composition and its microstructure, meaning the displaying pattern and the chemical composition of the micro crystals that compose the steel. This micro structure depends mainly on:

- Chemical composition
- Thermal treatment

By increasing the content of alloy elements, an increase in the resistance of steel is produced, but also a reduction of weld ability and ductility. That is why, if a weldable steel is necessary, the content of alloy elements must be situated between relatively restricted boundaries.

Another possibility to increase the resistance without affecting the ductility and weld ability represents the thermal treatment and the temperature control during rolling.

In the present day a number of procedures are used for improving the resistance of the steel elements, of which the last two on a larger scale:

**Steel normalizing (N):** The strength of normalized steel is mainly given by the alloy elements and not by the microstructure. If an adequate control of the temperature is ensured during rolling, further normalization is not necessary. In the classic manufacturing procedure, the steel is normalized (heated until 920-9300C and then slowly cooled) in order to improve its mechanical characteristics, especially ductility



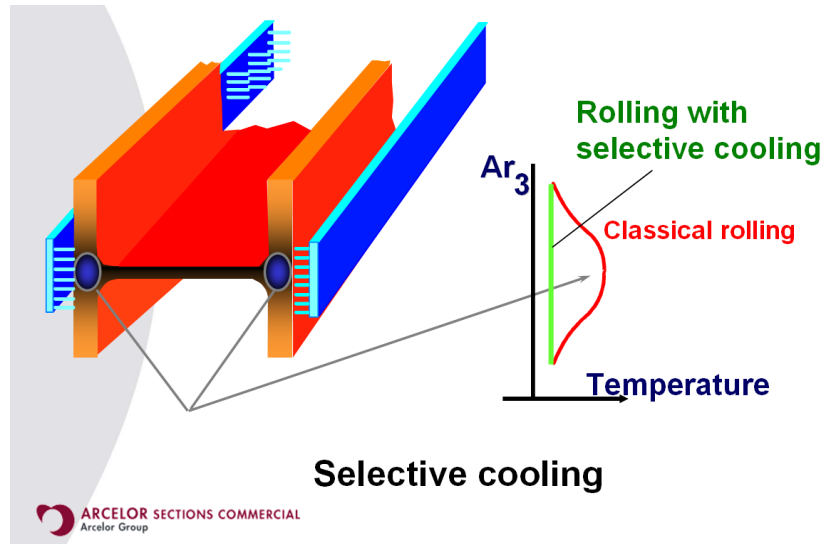


Fig. 2.10 - Manufacturing technology of normalized steel profiles [8]

**Thermo-mechanical steels (TM):** The resistance of thermo-mechanical steels is mainly given by the microstructure. The alloy content is less than in the case of normalized steels.

**Hardening thermal treatment followed by regression to high temperature (QST):** this is a thermal process in which the steel, after being heated, is rapidly cooled in water (quenching) in order to achieve an increase in strength and then it is heated in order to obtain a finer granulation and a better ductility and weld ability. The improvement treatment is applied in most cases to steels with the yielding limit between 420N/mm<sup>2</sup> and 690N/mm<sup>2</sup>

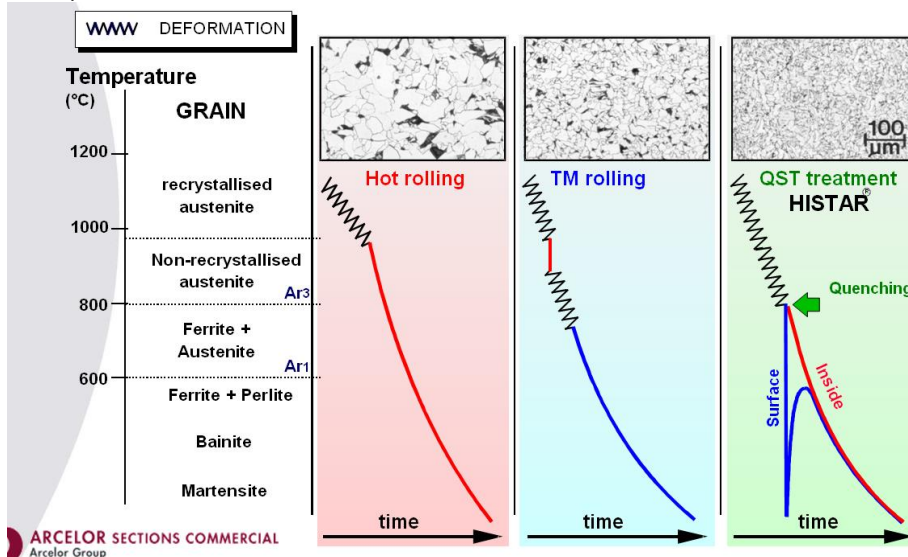


Fig. 2.11 - Comparison between the rolling processes [8]

### Quenching and the reheating to high temperature of high strength steels

Improvement consists of two opposite thermal treatments quenching and the return to high temperature.

In the case of steels that have a carbon content of at least 0.3%, quenching consist of heating the metal at a temperature with 30...500C above curve A (Fig. 2.12) at which it is maintained until the piece is heated in all its width.

After this, a quick cooling in water (in the case of carbon steels) or oil (in the case of alloy steels) is done, obtaining a fragile martensite structure with a very high hardness.

The property of forming this martensitic tough structure, respectively to quench, is function of the carbon content and other alloy elements; the critical cooling speed is in an inverse relation with the percent of these elements. When the carbon or the alloy elements are found in to smaller quantities, quenching cannot be done.

Due to the lack of plastic properties, quenched steel cannot be used in steel structures. That is why it is subjected to a supplementary thermal treatment called reheating.

Reheating consist in the heating of the metal at a temperature under the A1 curve that follows a quick cooling in water or oil. By reheating a finer granulation is obtained and also a more uniform distribution of the structural components. The carbon from the martensite diffuses in the ferrite mass and forms iron carbides. The intervals of the heating temperatures for quenching and reheating are given in Fig. 2.12. By reheating the quenched steel has a lower toughness and tensile strength but the elongation increases. The mechanical properties of quenched and reheated steel are superior to the metal that is not thermally treated.

The lower the reheating temperature the higher the mechanical resistances and the elongation smaller. There are: reheating to high temperature (550...700°C), when big elongations are obtained and the tensile strength is higher with 20...50% than the untreated material (in rolled form); comeback to the low temperature (350...500°C) when there are obtained tensile strengths with 70...100% bigger than the untreated material, but with smaller elongations.

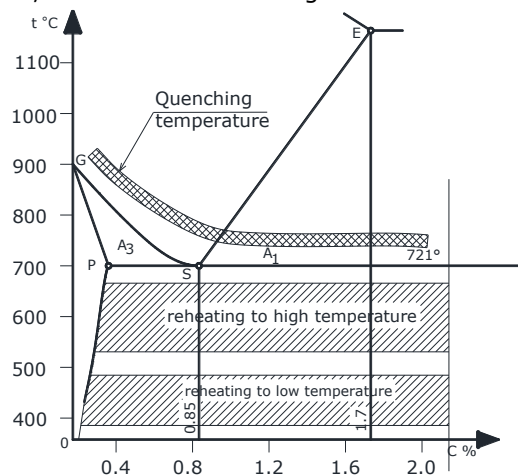


Fig. 2.12 - Intervals of the heating temperatures for quenching and reheating of the carbon steel

The enhancement thermal treatment consist of, as it was shown previously, quenching followed by reheating at high temperature; it is applied in general to steels with a higher content of carbon ( $C > 0.3\%$ ) and to alloy steels used in the building of machine pieces.

In steels that have been subjected to quenching and reheating, the value of the yielding limit and of the tensile strength is closer together. If for the steels that have not been thermally treated the ratio  $\sigma_c / \sigma_r$  has values between 0.65 and 0.7, for improved steels this ratio rises to values between 0.8 and 0.9 (sometimes even higher). The ratio is even closer to unit value as the reheating temperature is lower and decreases as these increases.

Lately, the thermal improvement treatment has been extended to rolled sheets of low alloy steels. By improving with the reheating to high temperature are obtained steels with a yielding limit with 30...50% higher than of a steel that is not thermally treated. In this case due to the low concentration of carbon, by quenching is actually obtained a bainite structure and in a more reduced manner a martensite structure.

Due to the fine crystalline and uniform structure, obtained by improvement, low alloy improved steels present superior toughness properties then of low alloy normalized steels, especially in the domain of low temperatures; the elements of low alloy improved steels can be welded considering come special conditions.

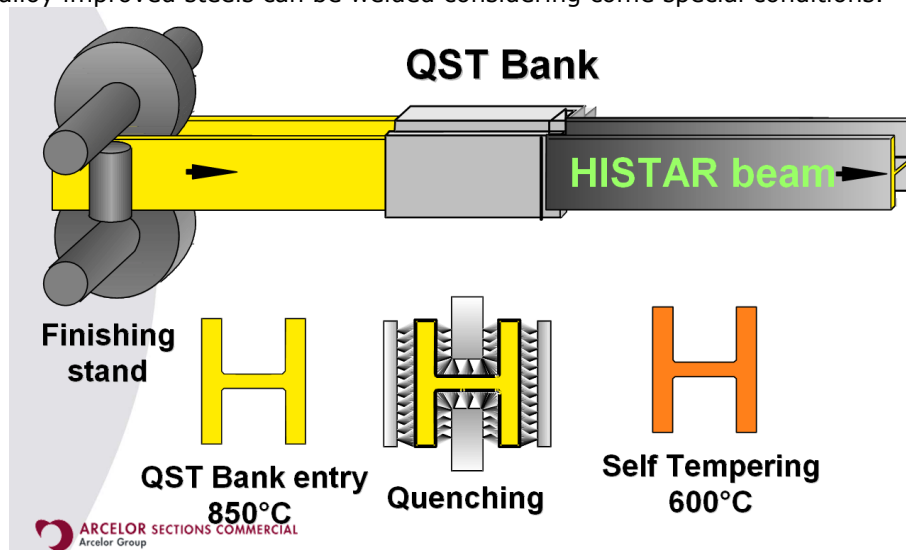


Fig. 2.13 - HISTAR[8] manufacturing procedure

### 2.3.2 Mechanical characteristics of HSS steels

High strength steels, with properties of weld ability and ductility that satisfy the corresponding requirements applied to structures in constructions, have the yielding limit ( $f_y$ ) between the values of 460-690 N/mm<sup>2</sup>, with elongations of 15-20%. These thermally treated steels, are usually low alloy steels with a carbon content ranging between 0.06% and 0.1%, without exceeding 0.2%, having  $CE \leq 0.48\%$ .

The chrome content is limited to 0.7%. There are also used as alloy elements, in small percentages, magnesium, molybdenum, vanadium, columbium, copper, nickel. In these steels the content of sulphur and phosphorus do not exceed 0.01% and 0.015%. The Charpy toughness at 5°C must be minimum 27J [10]

Grade		Source	Yielding limit $f_y$ , N/mm <sup>2</sup>	Tensile strength, $f_u$ , N/mm <sup>2</sup>	Elongation
Bisplate	60	Australia	500	590-730	20%
	70		600	690-830	20%
	80		690	790-930	18%
HT690	70	Japonia	590	690	----
HT780	80		685	780	----
ROT	601	UK (CORUS)	620	690-850	----
	701		690	790-930	----
HPS	485W	USA	485	-	----
A514		USA	620-690	690-895	16-18%
S460		Europe (Arcelor)	430-460	530-720	17%
HISTAR 460			450-460	550-720	17%

Table 2.5 - Minimal material properties of some high strength steels[15]

In Fig. 2.14 is presented the characteristic curve stress – strain specific for a steel grade 690 subjected to the thermal treatment of quenching and reheating [72]. By analysing the characteristic curve, several conclusions can be drawn, that can be applied in the general case of quenched and reheated steels:

- Stress strain characteristic curve – the specific deformation does not present the inferior and superior yielding limit, so as usual steels used in constructions (S235, S275, S355)
- Yielding is produced gradually, near the yielding plateau, the yielding limit being usually defined by the value corresponding to a residual elongation of 0.2%.
- - Specific elongation corresponding to the ultimate tensile strength is of the order 8%.
- The ratio between the ultimate tensile strength and the yielding limit is of order 1,1.

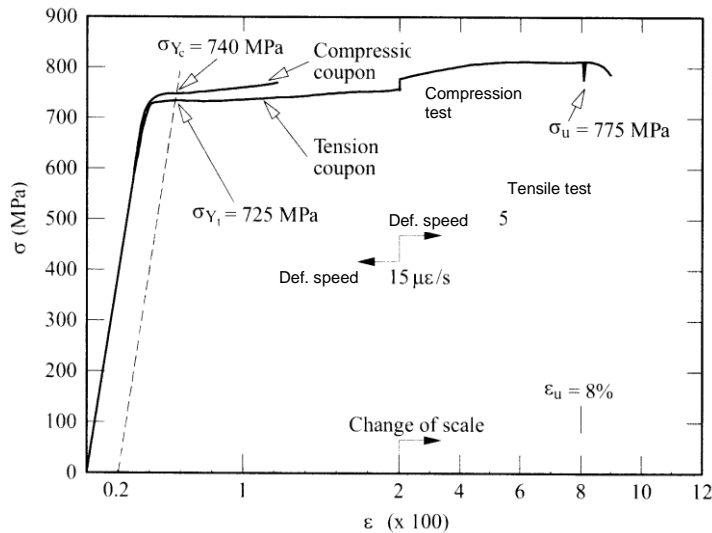


Fig. 2.14 - Characteristic curve unit stress – specific deformation for steel grade 690 subjected to the thermal treatment of quenching and reheating [72]

So it can be observed that the ratio between the ultimate tensile strength and yielding limit is of the order of 1,1, much smaller than in the case of common steels, where it has a value of approximately 1,4. Moreover, ductility is even more reduced than the one of common steels that is of the order of 30%. These ductility and cold-straining reductions lead to in the end to modification in the calculus and the forming of the elements made of steel subjected to quenching and reheating.

High strength steels can be also the ones with a reduced yielding limit and a high plastic deformation capacity. In Japan there are ongoing studies and incipient explanations regarding the combination in the same structure of high strength steels, in the structural elements that are mainly designed to work in the elastic domain, with steels with reduced yielding limit in the dissipative structural elements [80] In Table 2.6 are presented high strength steels from both categories, produced by JFE Steel Corporation in Japan (<http://www.jfe-steel.co.jp/en/>).

Grade	Characteristics	Product description
HBL 325 HBL 355 HBL 385	High yielding limit and a reduced yielding ratio (ratio between the yielding limit and the tensile strength) made by TMCP	HBL325,355 has a higher yielding limit than JIS Standard for thicknesses between 40 and 100mm, is authorized by the Land, Infrastructure and Transport Ministry, a high plastic deformation capacity due to a low yielding ratio. JFE Steel has developed steel with an even higher yielding limit: HBL385.
SA440 SA440U	High resistance, with a tensile strength of min.	SA440U is the steel with the yielding limit of

	590N/mm <sup>2</sup> , a reduced yielding ratio, high toughness and weldability	590N/mm <sup>2</sup> that allows the drastic reduction of pre-heating before welding in comparison to the conventional SA440.
HBL 325FR HBL 355FR	Steel with improved fire resistance; guaranteed resistance to high temperatures.	In accordance to JIS G3106 and G3136 with regards to ambient temperature and it guarantees a yielding limit at 6000C higher by 2/3 from the characteristic one
JFE-LY 100 JFE-LY 160 JFE-LY 225	Reduced yielding limit with an excellent deformation capacity for applications in dissipative elements.	Possesses an extremely low yielding limit, for the use in dissipative elements with a high capacity of energy dissipation. Three levels of the yielding limit can be selected.

Table 2.6 - High performance steels for seismic applications

In the present in the USA have been developed the so called Advanced High Strength Steels (AHSS) and Ultra High Strength High Toughness Steels, having a tensile strength of  $f_u > 1000\text{N/mm}^2$ , designed for the automobile industry, having the form of thin sheets. From here to the cold formed thin wall profiles for constructions is not a long way. Furthermore, in Australia is currently used the G550 steel ( $f_y = 550\text{N/mm}^2$ ) to produce profiles with sections C and U, with widths of 0.4-0.9mm, that are used in building houses with a steel structure.

In Europe are produced hot rolled profiles, IPE, HEA, HEB and HEM form S460. HISTAR 460 manufacture by ARBED is characterized besides the properties in Table 2.5 by a very good resilience to very low temperatures ( $K_v = 45\text{J}$  at  $00\text{C}$  and  $40\text{J}$  at  $-200\text{C}$ ). There are also produced pipes for constructions from S420 and S460. Romania does not produce high performance steels. Although there are produced steels with a high strength for other types of applications (automobile industry, pressure tanks, etc.). The profiles and pipes from S420 and S460 can be supplied on the Romanian market, as well as the sheets made from S690.

### 2.3.3 Chemical composition

In Table 2.7 it is illustrated the comparison between chemical composition of S235JO, S460QL and S690QL while in Table 2.8 it is presented a comparison between carbon equivalence at the same steel grades.

Steel grade	Chemical composition [%], max.														
	C	Si	Mn	P	S	Al	Cr	Ni	Mo	Cu	V	Nb	Ti	N	B
S235JO	0,17	-	1,40	0,030	0,030	-	-	-	-	0,55	-	-	-	0,012	-

S460QL	0,22	0,86	1,8	0,025	0,012	0,01	1,6	2,1	0,74	0,55	0,14	2,1	0,07	0,016	0,006
S690QL	0,22	0,86	1,8	0,025	0,012	0,01	1,6	2,1	0,74	0,55	0,14	2,1	0,07	0,016	0,006

Table 2.7 – Chemical composition of S235, S460, S690

Steel grade	Equivalent carbon	
	C <sub>e</sub> [%]	
S235JO	0,35	
S460QL	0,42	
S690QL	0,46	

Table 2.8 – Carbon equivalence for S235, S460, S690

### 2.3.4 Welding technology

Weldability of high-strength steels (HSS) can be a problem, especially at low-temperatures and cyclic loading. From the point of view of chemical composition, it is important the limitation of the CE factor. In USA, for example, CE is limited to 0.43 (ASTM A992), while the trend is to limit this value to around 0.3 ([10]). HISTAR 460 steel, produced by ARCELOR in Europe, has CE between 0.41 and 0.43, depending on plate thickness.

In order to prevent brittle fracture, a particular attention is paid to welding technology, including both weld metal and welding operation. Welding procedure (EN ISO 15609-1 and 2; EN 287-2004) is qualified experimentally, this operation being more complex than in the case of standard steels.

In Fig. 2.15 it is illustrated the influence of preheating temperature on weldability of elements made of different types of steel.

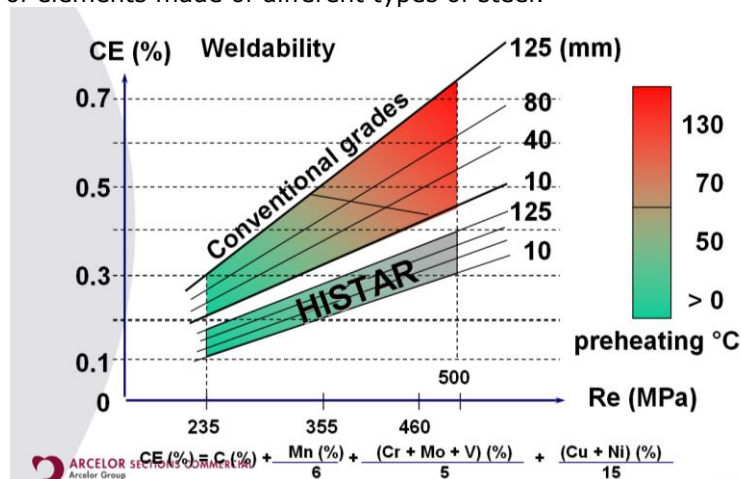


Fig. 2.15 - The influence of preheating temperature on weldability of elements made of different types of steel [8]

## 2.3.5 Design of elements made of high strength steel

### 2.3.5.1. HSS in tensioned elements

If the tensile strength of the element is the one leading the calculus, choosing a high strength steel, for example S460, instead of a regular one S355, can achieve a material saving up to 30%. If the S460 steel is 20% more expensive, then its use leads to in the end to a drop in the final price of about 10%.

### 2.3.5.2. Section strength calculus (local deflection calculus)

In the case of the reduced slenderness value domain, where the elements reach yielding point without losing stability, resistance is influenced by the cold strain hardening capacity. It is well known that in the case of short slabs, ultimate stress reached is with about 30% higher than the yielding limit. That is why in the case of high strength steels, it is expected that this increase to be much reduced. The influence of residual stresses from the weld is most commonly smaller than in the case of regular steels. The magnitude of the residual compression stresses measured in the welded sections of the high strength steels don not differ as much from the ones measure in the case of regular steel, so the ratio between the residual compression stresses and the yielding limit are smaller for high strength steels then for regular ones.

A number of tests were done in order to establish the local buckling resistance curves for slabs made of high strength steels (Fukumoto si Itoh 1984). Some of these tests (Usami si Fukumoto 1982) and some of a more recent date [72] were done on stiffened and un-stiffened elements are presented in Figure 7.a and Figure 7.b.

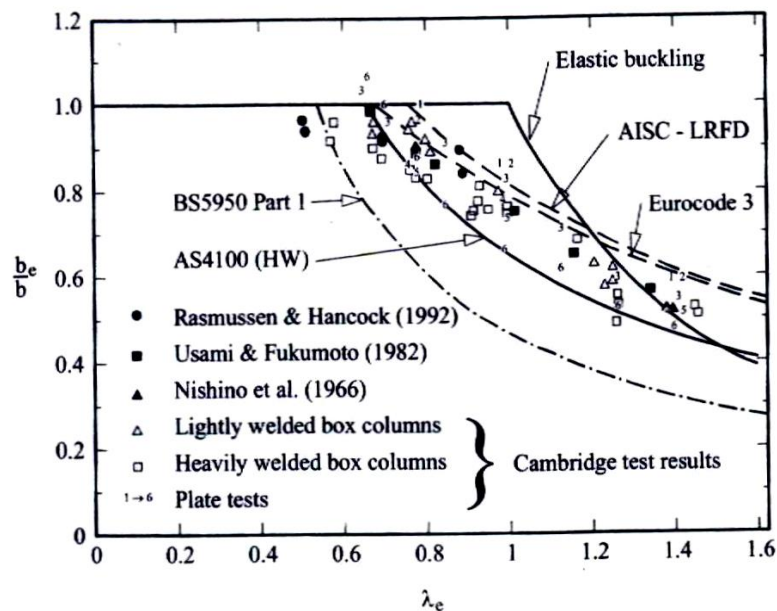


Fig. 2.16 – Local buckling resistance curves for slabs-stiffened elements [72]



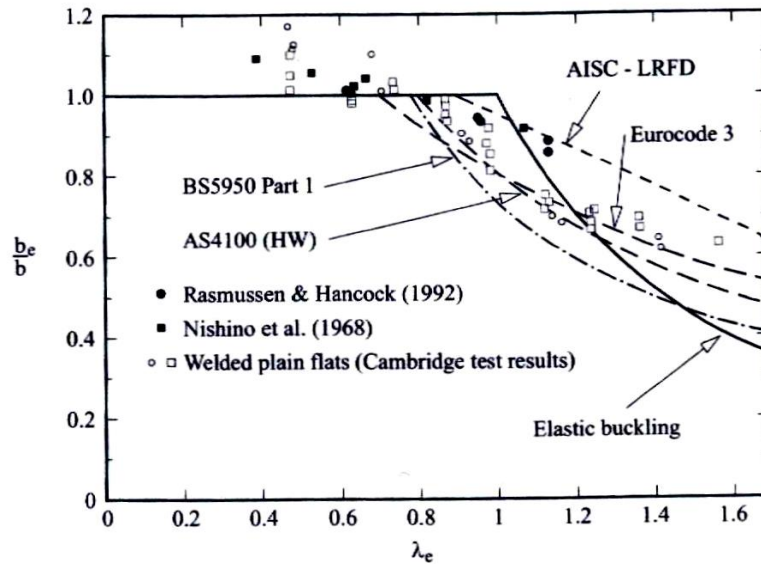


Fig. 2.17 - Local buckling resistance curves for slabs-un-stiffened elements [72]

### 2.3.5.3. The effect of residual stresses on HSS

As it was previously mentioned, high strength steels are less affected by residual stresses than regular steels because the ratio between the residual stresses and the yielding limit is smaller. The residual stresses affect the strength of the elements, especially for columns and unbraced beams. In the case of columns, the slenderness  $\lambda = \sqrt{\sigma_y / \sigma_E}$  is function of the yielding limit and the critic unit elastic

stress,  $\sigma_E = \frac{\pi^2 E}{(L_e/r)^2}$  where:  $L_e$  is the effective length, which depends on the

boundary conditions and  $r$  is the gyration ratio,  $r = \sqrt{\frac{I}{A}}$ .

The critic unit elastic stress does not depend on the yielding limit, that is why a regular steel column and a high strength one having the same cross section and the same boundary conditions will have the same critic unit elastic stress. That is why, if there are considered two columns with the same geometrical characteristics, one made of regular steel and the other of high strength steel, then the ratio between the residual stresses and the yielding limit will be significantly smaller for the high strength steel column, consequently the dimensionless resistance being higher.

### 2.3.5.4. Member buckling (flexural bending)

In order to investigate the resistance of high strength steel columns, Nishino si Tall (1970) made experimental tests on columns made from hot rolled profiles and also from welded sheeting, made from steel ASTM-514, having the yielding limit

equal to 690MPa. In the same period of time in Europe were made numerical tests on the same type of elements. Both studies have shown that these columns can be computed based on a superior buckling curve in comparison to regular steel columns. It must be mentioned though that in the experimental tests done by Nishino si Tall in USA the loadings were introduced centrally, the influence of the imperfections not being taken into account.

Further testing was done by Rasmussen and Hancock [72] in order to determine the strength of the columns made from high strength steel with initial imperfections(initial curvature). The tests were done on double T welded columns and also on welded box columns with the yielding limit of 690MPa. The sections were designed in such a manner that they would reach the yielding limit before losing local stability. For the long columns there were considered hinges at the ends and for the short ones fixed ends. The tests were made with and without initial imperfections, in order to determine the deflection curves for these columns. The result are presented in Fig. 2.18 si Fig. 2.19. the resistances of the columns are dimensionless by reference to the compression force  $A\sigma$  and the slenderness  $\lambda$  will be defined as follows:

$$\lambda = \sqrt{\frac{\sigma_y}{\sigma_E}} \quad (2.1)$$

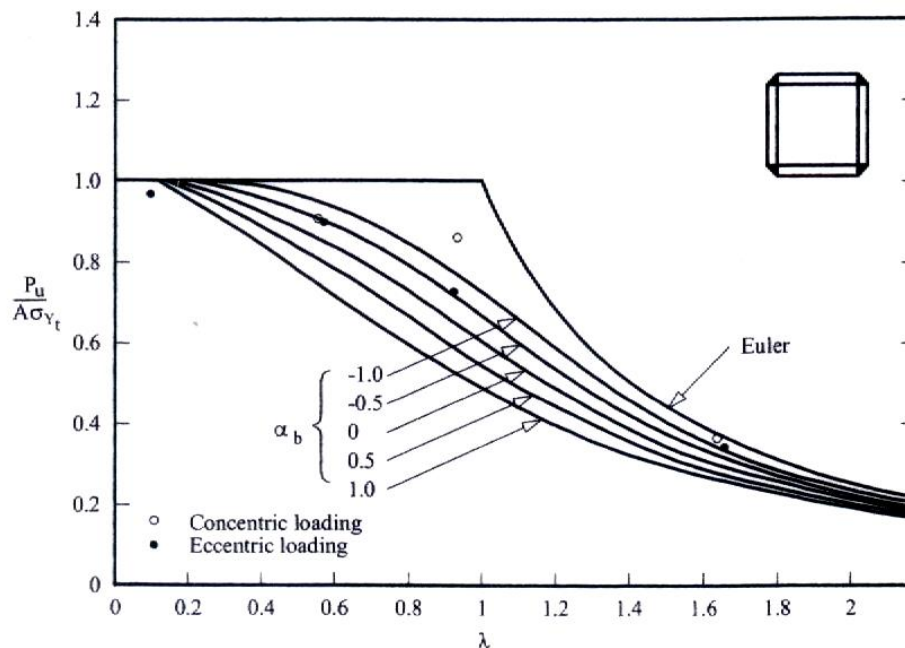


Fig. 2.18 - Local buckling resistance curves for box columns, steel 690MPa, Australian norm [72]

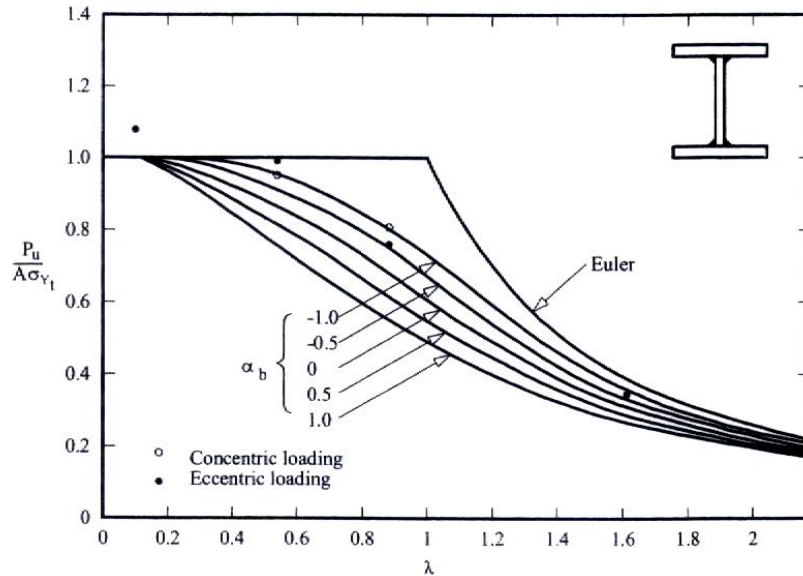


Fig. 2.19 - Local buckling resistance curves for double T columns, steel 690MPa, Australian norm [72]

The curves from Eurocode are based on the provisions from Section 5.1. Appendix D from Eurocode 3 allows the use in calculus of some superior curves for double T rolled profiles made from steels with the yielding limit of 420MPa and 460MPa compared to the same profiles made from regular steels, having the yielding limits equal to 235MPa, 275MPa and 355MPa.

Still, the curves presented in Appendix D for welded double T sections and the box sections made from steels with a yielding limit of 420MPa and 460MPa are identical to the ones in Section 5.5.1 from Part 1.1 for regular steels. As a reference in order to fit the sections in one of the buckling curves, the relation from Eurocode 3 is used, based on the proposal of Rondal Maquoi (Rondal si Maquoi 1979). According to this proposal, the ECCS buckling curves (European) a, b and c are approximated with enough accuracy by the reducing factor due to slenderness:

$$\chi = \frac{1}{\varphi + \sqrt{\varphi^2 - \lambda^2}} \leq 1 \quad (2.2)$$

where: 
$$\varphi = \frac{1}{2}(1 + \eta + \lambda^2) \quad (2.3)$$

$$\lambda = \sqrt{\frac{\sigma_y}{\sigma_E}} \quad (2.4)$$

$$\sigma_E = \frac{\pi^2 E}{(L_e/r)^2} \quad (2.5)$$

$$\eta = \alpha(\lambda - 0.2) \quad (2.6)$$

$$\alpha = \begin{cases} 0.21 & \text{curve } a \\ 0.34 & \text{curve } b \\ 0.49 & \text{curve } c \end{cases} \quad (2.7)$$

In Fig. 2.20 and Fig. 2.21 are presented the results of the experimental tests compared to the buckling curves from a number of norms. It can be observed that the experimental results are very well approximated by buckling curve "a" provided by ECCS. Although, the buckling curves mentioned in Eurocode 3 for welded box sections and double T sections are b and c. Analyzing the results presented in previous mentioned figures the following general conclusions can be drawn:

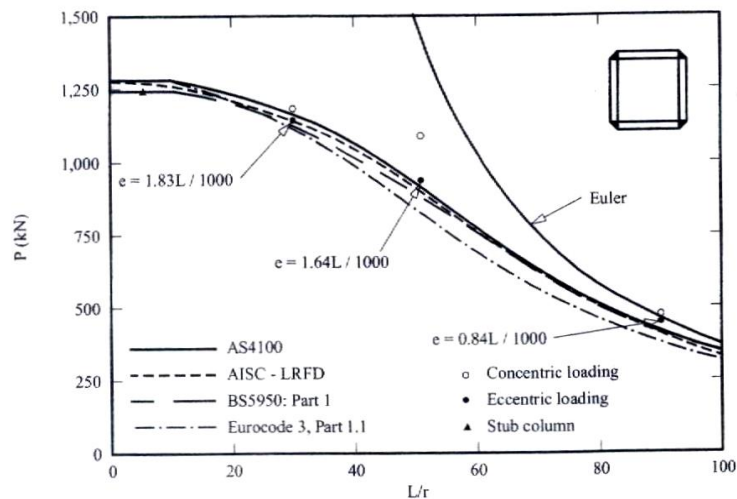


Fig. 2.20 – Local buckling resistance curves for long columns, box sections, steel grade 690MPa [72]

- The buckling curves provided by the Australian, USA and UK norm are almost identical in the case of the columns of high strength steels, with a box cross section and double T, bent after the minimum inertia axis and are in accordance with the experimental values.
- Eurocode 3 uses buckling curve b for the welded box columns, meanwhile in the Australian, USA and UK norms is presented a curve much more similar to curve a in the ECCS. The curve in the British norms almost similar to curve a, mainly because the imperfections parameter is function of this norm is function the yielding limit. For welded double T sections bent after the minimum axis, the buckling curve in Eurocode is conservative because it was based on curve c, meanwhile he prescriptions in the other three norm are based on similar curves with curve a. By comparison the buckling curves in Eurocode have been obtained based on the prescriptions in Section 5.1.

Appendix D of Eurocode 3 allows the use in calculus of the buckling curve a for rolled double T profiles made of steels with yielding limit of 460MPa. The experimental results have shown that this curve can be used for double T welded profiles bent after the minimum inertia axis.

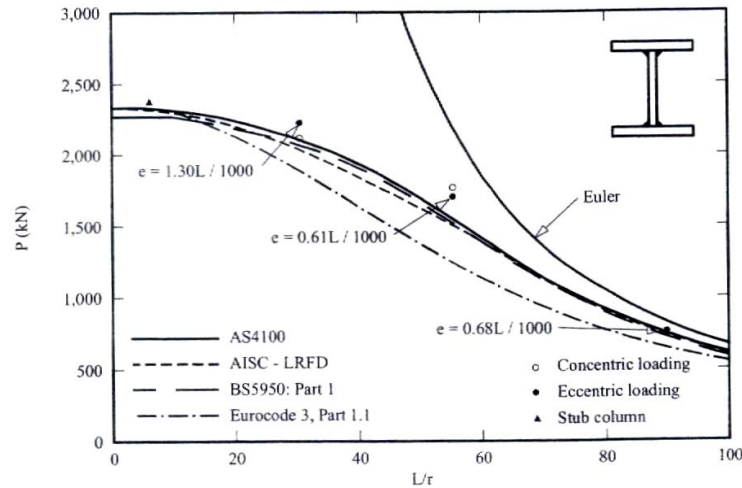


Fig. 2.21 - Local buckling resistance curves for slender columns, double T sections, steel grade 690MPa [72]

#### 2.3.5.5. Fatigue resistance

Using high strength steels for structure loaded at fatigue will lead to bigger values of the values interval for tension compared to the ones made of regular steel [55]. That is why for structures made of high strength steel, fatigue becomes a more common design parameter than when regular steels are used. In many norms it is stated that the interval of the values of tension must be in the limit of the elastic domain of the material. For example, in the provisions of Eurocode 3 and the International Institute of Welding, IIW, it is stated that the interval of the tensions values must not exceed  $1,5f_y$  for normal tensions and  $1,5f_y/\sqrt{3}$  for shearing tensions. As it has been said before, using high strength steels leads to an increase of the influence of fatigue. Although using them can prove advantageous in many applications. For example, HSS can be used in the structures parts where the tension level produced by the static component of loading is big. The explication of this phenomenon is given by the fact that in the fatigue prescriptions, the loading parameter depends on interval values of tension  $\Delta\sigma$  and not on the maximum tension  $\sigma_{max}$ . Also by choosing adequate welding details or by later performed thermal treatment the effect of fatigue can be reduced.

#### 2.3.5.6. Limits when using steels subjected to the thermal treatment of quenching and reheating for structures

The Australian standard ASA100(1998) limits the yielding limit to 450MPa. This does not exclude the use of some steels subjected to the thermal treatment of quenching and reheating but it requires that for steels that have a higher yielding limit, to be considered in calculus a value equal to 450MPa.

The British standard BS5950 part 1 (BSI 2001) contains provisions for steels with yielding limit smaller than 460MPa. This provision is compatible with Appendix D from Eurocode 3, part 1.1, that allows the calculus of steels subjected to the

thermal treatment of quenching and reheating having yielding limits equal to 420MPa and 460MPa. However, according to section 3.2.2.2 from Eurocode 3 using plastic analysis requires that  $\sigma_u/\sigma_y \geq 1,2$  ( $\sigma_u$  ultimate tensile strength),  $\varepsilon_t \geq 15\%$  (total elongation at failure) and  $\varepsilon_u \geq 20\varepsilon_y$  ( $\varepsilon_u$  and  $\varepsilon_y$  are the specific deformations corresponding to the ultimate strength and respectively yielding limit). Some of the steel grade 460 included in Appendix D do not fulfil the before mentioned requirements.

The provisions from AISC-LRFD (1999) allow the use of steels subjected to the thermal treatment of quenching and reheating, including here steel from ASTM A852 (2001) having a yielding limit of 485MPa to steel ASTM A14 (2000) having the yielding limit 690MPa. In any case the use of these for structures in seismic zones is not allowed (AISC 1997). Furthermore, section 5.1 from the same norm does not allow plastic calculus for steels with the yielding limit higher than 448MPa. This restriction was imposed by the lack of information regarding the behaviour in moment – rotation of steels subjected to the thermal treatment of quenching and reheating. The test conducted by McDermott (1969) on steel beams with yielding limit of 690MPa (ASTM A514) have proven reduced values of the rotation capacity.

## **2.4 Summary review on previous research of HSS Connections**

The performances of DS bolted T-stub specimens, un-stiffened one and one or both-sides stiffened are analyzed in present paper. Similar tests on MCS and DS bolted T-stubs, un-stiffened and one-side stiffened were realized by (Girao Coelho et al. 2004) [1], under monotonic loading and stiffener on the end-plate, and by (Piluso & Rizzano 2007)[69], which applied cyclic loading on MCS un-stiffened T-stubs.

An extensive experimental research of plates with holes and tension splices made of steel grade S690 was performed during 2007/2008 at University of Ljubljana, Faculty of Civil Engineering and Geodesy by Prof. Darko Beg and team. The purpose of the research was to establish whether local ductility of bolted connections made of high strength steel can assure sufficient ductility for the transfer of loading between all bolts. In a bolted shear connection the loading is transmitted by bolt bearing. This connection type transfers loading from one steel plate to another by the contact between the bolt and the plates. The contact is characterized by high stresses that enforce transverse shear in the bolts and high local compression stress to the plate. Concentrations of stresses are therefore unavoidable. Another characteristic of bearing type connections is initial slip due to bolthole clearance. In general, contacts between bolts and plates are not established simultaneously. A single contact may be established sooner. In such case the whole loading is transferred through this single contact. For that reason, the local ductility of the connection in terms of plastic deformations has to be sufficient in order to assure bolthole elongation, so that the remaining contacts will be established and the loading will be transferred through all bolts. If local ductility it is not sufficient, the stress concentration would cause rupture of the steel plate or shear fracture of the bolt. In either case the maximum connection resistance would be equal to the resistance of a single bolt connection. Results of experimental tests proved that local ductility of bolted shear connections is sufficient to distribute the loading between all

bolts evenly in four-bolt connection with the most unfavourable initial position of the bolts.

The characterization of the ductility of bolted end plate beam-to-column steel connections was done by [48][49][50][51][52]. The steel grade used for the connections was S355 and S690. The rotational response of a joint based on the component method was characterized by a methodology that was implemented and calibrated against experimental results. The behaviour of joints was governed by the end plate modelled as equivalent T-stubs in tension. A basis for the proposal of some criteria for the verification of sufficient rotation capacity was given by the results of this study as well as the conclusions drawn from the analysis of individual T-stubs. The proposal was made in terms of a non-dimensional parameter, the joint ductility index [48]. The research on block shear tear-out failure in gusset-plate welded connections in structural hollow sections and steel S1300 showed that design rules for block tearing resistance according to Eurocode, as well as American standard are inadequate [64]. There were also proposed a modification of the definitions of the effective net area and failure stress.

Test results of multi-bolt shear connections were presented by Kouhi and Kortasma (1990)[62]. For the test the steel used had a nominal yield strength of 640 MPa and nominal ultimate strength of 700 MPa. The thickness of the plates for which actual material strength was given is 3, 4, 6 and 8 mm. Considering the failure mechanism; the specimens were divided in four series. The connections used for this study included connections with two bolts positioned in the direction of loading and a connection with four bolts in 2×2 configuration. The cover plates were the ones sustaining the main deformation and failure, for test series H which failed in net cross-section. The test results were compared to bearing, net area and block tearing resistances according to various standards. Aalberg and Larsen [2] prepared a report on a comparative research of bolted connections in HSS and mild steel was prepared. Tension splices with three bolts in double shear, block tear tests and tension tear-out test were performed. The net cross-section was the one to fail in all tension splices. The resistance test was compared to, according to Eurocode and AINSI standard to block tearing resistance. It was concluded that ultimate-to-yield ratio  $f_u/f_y = 1.05$  did not significantly affect the ductility.

Another investigation regarding shear connections with one or two bolts placed parallel to the loading was done by Kim and Yura (1999)[61]. In the testing the steel used was mild steel and also steel with yield strength of  $f_y = 483 \text{ N/mm}^2$  and ultimate tensile strength of 545 MPa. For the bolts to be in single shear the specimens were connected to rigid plate. The experimental resistance was compared to bearing resistance according to American AISC standard and to Eurocode standard in which conservatism was found.

Duplicating Kim and Yura tests, using steel grades S690 and S1100 was done by Aalberg and Larsen (2001, 2002)[2][3]. In EN 1993-1-12 the steel grade S1100 is not considered. For both steel grades the value of ultimate tensile to yield ratio was equal to  $f_u/f_y = 1,05$ . Because of low  $f_u/f_y$  ratio local ductility of connections was not decreased. 1330 MPa is the actual yield strength of steel S1100. The ultimate strain was reached at  $\epsilon_u = 0,03$ , while percentage total elongation after fracture was equal to  $A_c = 10 \%$ . This steel did not satisfy the ductility requirements set by EN 1993-1-12 having  $\epsilon_u = 0,03 \geq 15 f_y/E = 15 \times 1330/210000 = 0,095$ . Large hole elongations and ductile failures were observed.

Shear connections made of steel grade S460 ( $f_u/f_y = 1,23$ ) with two bolts placed perpendicular to loading was the focus of Puthli and Fleisher (2001)[71].



They also experienced block tear failure. They compared experimental resistances to resistance according to EN 1993-1-8. They were focused in minimum end and edge distances, resulting the suggestion to reduce minimum distances and to modify bearing resistance formula.

Rex and Easterling (2003)[72] researched the behaviour of a bolt bearing on a single plate, this being part of larger investigation of the behaviour of partially restrained steel and composite connections. The plate of different high steel grades (ultimate strength from 665 to 752 MPa) and thick of 6,5 mm was tested against bearing resistance. Several curling failures were observed due to small plate thickness and large end distance  $e_1$ . The Delft University of Technology [16] realized a research on single bolt shear connection. Ductile behaviour of the connections and the conservatism of Eurocode bearing resistance formula were reported.

## **2.5 Requirements and criteria for choosing steel in structural applications**

High strength steels are required for the following applications in the domain of resistance structures in constructions with high dimensions and loads, multi-storey buildings, bridges, marine platforms, etc. – subjected to severe loads – high intensity earthquakes, powerful winds, explosions, great live loads, impact forces, etc. As it was presented in the above paragraphs, steel must possess high mechanical resistances, a good toughness, strength to fatigue, resistance to corrosion and weldability. These steels are known as “thermo-mechanical steels”. In what concerns the required properties in the applications for multi-storey building and bridges, these can be synthesized as follows[40]:

- High resistances and a reduced ratio between the yielding limit and tensile strength (LYR: Low Yield to tensile strength ratio), associated with big elongations at failure(>15%), in order to allow post elastic deformations in the case of structures subjected to seismic action.
- The reduced variation of the yielding limit in order to ensure the consecutive appearance of plastic hinges foreseen in the analysis, respectively a relatively constant level of the yielding limit ( $\sigma = f_y$ ) in structural element with medium to high thicknesses.
- Steels with reduced yielding limit, smaller than common carbon steels, respectively smaller than high strength steels, with which it can be combined in structures with hybrid elements or in structures with dual composition, can ensure that like a “cartridge-use” focusing the inelastic deformations and dissipating the seismic energy, meanwhile the rest of the structure remains in the elastic domain or with low degrees of deterioration.
- A higher elasticity modulus than for normal steels (experimentally proven) meant to lead to an increase in rigidity and deformation reduction – high resistances to losing stability and limiting the second order effects.

When building bridges, the hybrid beams, with flanges of high strength steel and web made of steel with lower resistance have already proven their efficiency, both in the terms of technical performances as well as economical[60]. These beams can be used with success not only for bridges, but also for other structures with big spans. Also, there can be made pipe lattice beams or profiles with flanges from HSS and diagonals and posts from regular carbon steel. In the structures for multi-storey buildings several options arise based on the use of HPS and/or HSS:



- For big heights (>P+10E), dual frames that combine unbraced spans with braced spans with dissipative braces or with panels made of steel with reduced yielding limit; there are incipient applications in Japan [80]
- For medium heights (<P+10E), unbraced frames, with columns with mixed section steel (HSS) and concrete, partially imbedded in concrete, with controlled dissipation through beams with reduced cross-section (RBS) and/or web panels of columns.
- Braced frame structures, unbraced, dual, homogenous with regard to material (HSS) or with columns from HSS and beam from normal steel.

Recent studies have been performed by [37] in order to throw light on the definition of the upper-shelf toughness requirements in terms of J or in terms of Charpy energy  $|KV|_{US}$  and their extension  $T_{US}$  both for monotonic loading corresponding to plastic design according to EN 1993-1-1 and to cyclic loading corresponding to the design of seismic resistant structures according to EN 1998 for sufficient energy dissipation by hysteretic behaviour.[37] The project was carried out with test specimens made of rolled beams from ordinary European deliveries, which have toughness properties as indicated in Fig. 2.22.

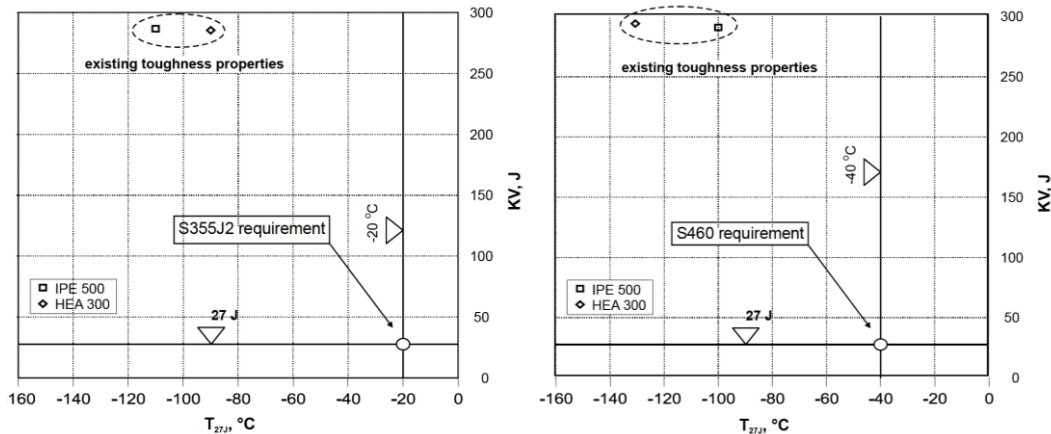


Fig. 2.22 – Comparison of toughness requirements according to EN 10025 and actual toughness properties from European deliveries for rolled sections[37]

In terms of material properties from steel deliveries the steels from rolled sections fulfil the EricksonKirk correlation, so that for example for steel structures in buildings the material choice S355J2 is sufficient to apply full plastic design. For plates for built up sections the EricksonKirk correlation is not automatically fulfilled; additional quality specifications are necessary.[37], conclusion that applies for earthquake resistant structures subjected to energy dissipation by plastic hysteretic behaviour. It is evident from Fig. 2.22 that to fulfil the conclusions for the Erickson Kirk correlation ordering steels S355J2 simply to EN 10025 is not sufficient and could lead to safety problems when full plastic design is applied. The ordering should refer to the quality level of the steels needed to comply with the EricksonKirk correlation. For quality below there would be possibly additional requirements for more sophisticated structural detailing and fabrication quality that should be assessed for the specific case.

In terms of minimum toughness to avoid crack initiation in case of local (notch effects) or global (plastic design with plastic rotations in hinges) ductility demands it has been proven both by fracture mechanics and by damage mechanics that for steels qualities as given in Fig. 2.22 the magnitude of upper shelf Charpy impact energy and the maximum strain resistance are sufficient to allow full plastic design with local notch effects and global plastic rotations. For steels not belonging to the group shown in Fig. 2.22 the damage curves could be lower; this would suggest to perform assessments for the specific case to find out under which conditions a full or partial plastic design could be performed.[37].

In terms of material properties for seismic design it has been shown that for the given steel qualities indicated in Fig. 2.22 ultra-low-cycle fatigue is not a problem that could limit the use of the behaviour factor  $q$  provided that a useful limitation of the inter-storey drift (e.g.3.5%) has been used to define the numerical value of the  $q$  factor. In case the steel qualities are inferior to those given in Fig. 2.22, studies should be carried out to determine the associated damage curves or  $\Delta\Phi_{pl} - N$  - resistances in order to see what further reduction of the  $q$  factor is necessary.[37].

The key to a safe application of plastic design for monotonic or seismic loading is the toughness quality of the steel, that according to usual practice should by far be higher than the minimum requirement specified in EN 10025, see Fig. 2.22. To guarantee the properties as given in Fig. 2.22 steel producers should market these steels with a specific brand-name (e.g. seismic resistant steels) or an option should be included in EN 10025 that specifies the minimum properties complying with the EricksonKirk correlation as given in Fig. 2.22. [37].

AFPC/OTUA (1997) presents, in the year 1997, a remarkable number of applications in Europe for bridges and marine platforms, where it was used steel grade S420, S450 and S460. The applications in buildings are more reduced:

- MAPFRE tower from Barcelona, having 42 floors and 150m, H columns were used made of S460M, resulting a reduction in weight of 24% compared to the solution with S355.
- Europe Tower in Madrid, that had a 14° inclination, all its structural elements made of S460M.
- Pleiades Tower in Brussels, columns made of S460N, with a 20% economy compared to S355J0.

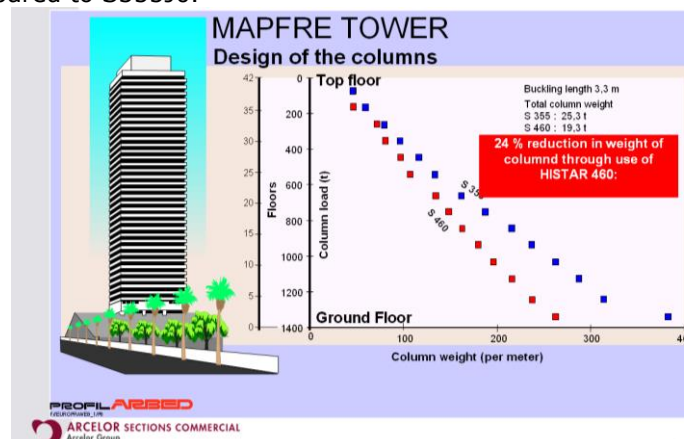


Fig. 2.23 – Reduction in weight of columns through use of Histar 460 (MAPFRE Tower)

## 2.6 Conclusions

A wide range of High Strength Steels are available at this moment. HSS steels with yield strengths above 355MPa up to 690MPa can be found in forms of plates and in forms of laminates. Also, tubes with yield range up to 700 MPa are fabricated. This opens horizons for using them on steel construction purposes. There are a lot of applications of HSS in bridge construction but only a few in buildings.

High strength steel fabrication properties are similar to those of ordinary steels. Thermo mechanically rolled sections are characterised by high toughness. Quenched and tempered steels have higher strengths that can be exploited.

With all these opportunities some new interests are raised regarding:

- Behaviour of HSS elements under repeated actions: high-cycle and low-cycle fatigue produced under earthquake loading.
- Behaviour of HSS elements in plastic domain if they are cyclic loaded.

## 3 OPPORTUNITIES OF USING HSS STEEL IN SEISMIC RESISTANT BUILDING FRAMES

### 3.1 Introduction

As previously stated use of HSS for building structures represents one of the main development directions in the field of steel construction. Problems of practical application of such materials are related, on one hand, to properties of base materials – strength, stiffness, ductility – and, on the other hand, to connections, especially to weldability. A particular problem is behaviour of HSS elements under repeated actions: high-cycle and low-cycle fatigue produced under earthquake loading.

Multi-storey steel buildings are assigned to one of the following structural types, depending to the behaviour of their lateral force resisting systems[34]:

- moment resisting frames (MRF), in which the horizontal forces are mainly resisted by members acting essentially in flexural mode; for such structures the performance of MR joints is crucial;
- frames with concentric bracings (CBF), in which the horizontal forces are mainly resisted by members subjected to axial forces;
- frames with eccentric bracings (EBF), in which the horizontal forces are mainly resisted by axially loaded members, but where the eccentricity of the layout is such that energy can be dissipated in seismic links by means of either cyclic bending or cyclic shear;
- moment resisting frames combined with dissipative shear walls (SW), which resist lateral forces by shear.

Combining a MRF with one of the lateral resisting systems, e.g. MRF + CBF, MRF + EBF, MRF + SW results a current building frame called Dual Structure (DS).

Each of these Dual-Structures dissipates a part of the seismic energy through plastic deformations in the dissipative zones of ductile members (i.e. beams in MRF, links in EBF or braces in CBF). The other members (columns) should remain in linear range of response. In order to avoid the development of plastic hinges in non-dissipative members, they must be provided with sufficient overstrength. To ensure this overstrength, European seismic design code EN1998, amplifies the design forces and moments by a multiplier equal to  $1,1\gamma_{ov}$ , where 1.1 takes into account for stress hardening,  $\gamma_{ov}$  is the overstrength factor and  $\Omega$  is the ratio between the plastic resistance and the design value of the force in the dissipative member. In case of HSS structures, the values of factors composing this multiplier need to be very care-fully analyzed. For some structural configurations (i.e. CBFs), the  $\Omega$  factor may result considerably high, due to the fact that other non-seismic combinations (e.g. wind load) could be critical. A similar approach is also used in the AISC 2005 [4], where this factor may reach a value of 3 for some structural types. Even though, the verification of the non-dissipative members using such amplified forces do not guarantee they will behave entirely in the elastic range.[31].

In order to get an economic design of the structure is necessary to keep the stresses quite low in the “dissipative” members using lower yield steel, and therefore to reduce the demand in the “non-dissipative” members, made by higher yield strength steel but still current. Such a solution has been recently applied to the

design of a 26 story steel building frame in Bucharest, where lower yield strength steel S235 was used for the dissipative braces in the CBFs, while the other members were of S355 [23]. If this option is not possible, the alternative is to increase the strength of the non-dissipative members by using heavier sections or by using higher yield strength steel. For MRF structures, first option is recommended, as this will lead to an increase of the stiffness, which in many cases is critical in the seismic design, but for braced structures or for dual structures, this will lead to a stress concentration in the non-dissipative members (i.e. columns). For these structures, the adoption of high strength steel in the non-dissipative members (e.g. to remain in elastic range during the earthquake) seems to be more likely. However, previous results obtained by [24] have shown that for MRF structures, strengthening of columns by using HSS may be effective to avoid column failure in case of “near-collapse” state. This may also improve robustness of structure in case of other extreme loads (e.g. impact, blast). In case of such Dual Steel Frames, particular care is needed for the proper location and sizing of member sections of different materials, as well as for their connections.

The design target is to obtain a dissipative structure, composed by “plastic” and “elastic” members, able to form a full global plastic mechanism at the failure, in which the history of occurrence of plastic hinges in ductile members can be reliable controlled by design procedures. To sustain these assumptions, a numerical study developed on DS of conventional CBF and EBF and on non-conventional braced systems, e.g. EBF of bolted removable links, CBF of Buckling Restrained Braces (BRB) and MRF of Steel Plate Shear Walls (SPSW), is presented in this chapter. These so called “non-conventional” systems use dissipative components made by Mild Carbon Steel (MCS), which act as “seismic fuses” and are sacrificial member, which after a strong earthquake can be replaced.

## 3.2 Seismic performance on Dual-Steel frames

### 3.2.1 DS frames modelling and design

Four building frame typologies of eight and sixteen story, respectively, are considered [20]. The four lateral load resisting systems are:

- Eccentrically Braced Frames (EBF),
- Centrally V Braced Frames (CBF),
- Buckling Restrained Braced Frames (BRB)
- Shear Walls (SW)

They are made by European H-shaped profiles. EBF, CBF and BRB systems have three bays of 6m. SW system has exterior moment frames bays of 5.0m, interior moment frame bay of 3.0m and shear wall bays of 2.5m. All structures have equal storey heights of 3.5m. Each building structure use different combinations of Mild Carbon Steel S235 and High Strength Steel S460. The design was carried out according to EN1993-1 [6], EN1998-1 and P100-1/2006 (Romanian seismic design code, aligned to EN1998-1) [7]. A 4 kN/m<sup>2</sup> dead load on the typical floor and 3.5kN/m<sup>2</sup> for the roof were considered, while the live load amounts 2.0kN/m<sup>2</sup>. The buildings are located in a moderate to high risk seismic area (i.e. the Romanian capital, Bucharest), which is characterized by a design peak ground acceleration for a returning period of 100 years equal to 0.24g and soft soil conditions, with T<sub>c</sub>=1.6sec. It is noteworthy the long corner period of the soil, which in this case may affect flexible structures. In such a case, there is a large demand in terms of

plastic deformation capacity for dissipative designed components, while it is very difficult to keep elastic the non-dissipative ones. For serviceability check, the returning period is 30 years (peak ground acceleration equal to 0.12g), while for collapse prevention it is 475 years (peak ground acceleration equal to 0.36g) (P100-1, 2006). Interstorey drift limitation of 0.008 of the storey height was considered for the serviceability verifications.

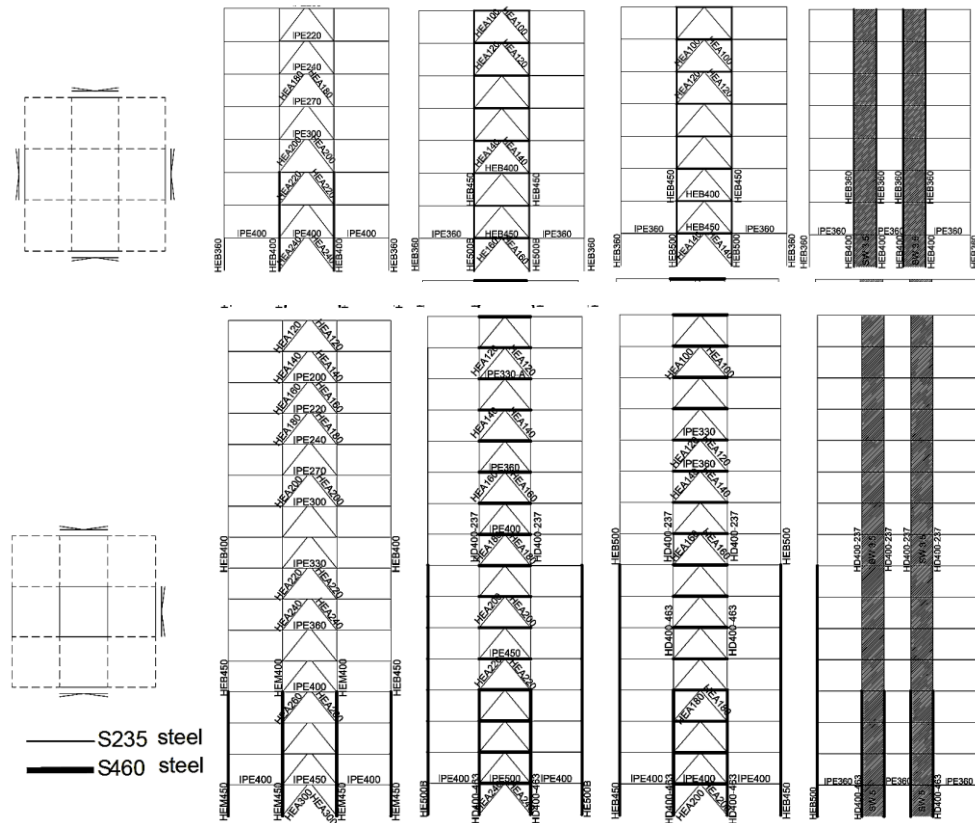


Fig. 3.1 - Frame systems: (a) plan view and elevation of EBF8, CBF8, BRB8 and SW8 structures; (b) plan view and elevation of EBF16, CBF16, BRB16 and SW16 structures

According to EN1998-1, the maximum value of the reduction factor  $q$  for dual frame systems of moment frames and eccentrically braced frames (MRF+EBF) is equal to 6. For dual frame systems made from moment frames and centrally braced frames (MRF+CBF),  $q$  factor amounts 4.8. For dual frame systems of moment frames and buckling restrained braces (MRF+BRB) and moment frames and shear walls (MRF+SW), EN1998-1 does not provide any recommendations regarding the  $q$  factor. For these structural systems, AISC 2005 provisions were taken as guidance. According to the later code, the reduction factor for MRF+BRB systems and MRF+SW is similar to that of special moment frames. Concluding, the design was based on a  $q$  factor equal to 6, excepting the MRF+CBF, which was designed for  $q$  equal to 4.8. For designing the non-dissipative members, EN1998-1 and P100-1/2006 amplifies the design seismic action by a multiplicative factor  $1.1g_{ov}$ , where  $g_{ov}$  is equal to 1.25. Unlike EN1998-1, which considers  $\Omega$  as the minimum value of

$\Omega$ ; among all dissipative members, Romanian code P100-1/2006 suggests the use of maximum value. A similar approach is also employed in AISC 2005, where the multiplicative factor  $1.1g_{ov}$   $\Omega$  is replaced by a unique factor  $\Omega_0$ , called the overstrength factor. AISC 2005 and P100-1/2006 also contain values of multiplicative factors to be used in design, which ranges between 2.0 and 2.5. Table 3.1 presents the multiplicative factors for each structural system obtained by calculation. The overstrength factors  $\Omega$  range between 1.90 and 2.90 for eight story structures and between 1.70 and 2.90 for sixteen story structures. For the eight-story building, two exterior bays of braces or shear walls on each exterior frames were necessary. For sixteen story building, the larger demand in lateral resisting capacity leads to braces or shear walls in all for bays.

The four structural systems were designed for similar base shear force capacities, with the exception of EBF, which were designed for lower capacities. The first mode periods for eight and sixteen story structures are presented in Table 1. It may be seen the four structural systems amount almost identical the first-mode periods.

Structure	EBF8	CBF8	BRB8	SW8
$1.1g_{ov} \Omega$	2.2	2.2	1.9	2.9
Period, [sec]	0.92	0.97	0.97	1.00
Structure	EBF16	CBF16	BRB16	SW16
$1.1g_{ov} \Omega$	2.9	1.7	2.1	2.5
Period, [sec]	1.79	1.53	1.61	1.61

Table 3.1 - First mode periods and multiplicative factors for the structures[31]

### 3.2.2 Performance based evaluation

In order to evaluate the structures response in the inelastic domain, a static non-linear calculus was made, using the N2 method as well as dynamic non-linear calculus, using recorded accelerograms.

The N2 method was developed at the University of Ljubljana by Fajfar [36] it can be used to verify the seismic performances of buildings designed by current methods (ex. Spectral analysis). The method combines the non-linear static analysis (push-over) of a system with multiple degrees of freedom MDOF with an analysis based on the response spectrum of a system with one degree of freedom SDOF and it is enclosed in the new P100-1/2006.

For the static non-linear analysis the program SAP2000 was used.

In the design a vertical distribution of the lateral forces was used resulted from the modal analysis for the predominant vibration mode, normalized so that the value of the peak loading to be equal to unity. The displacement requests of the SDOF equivalent system, for the ultimate limit state (ULS), are obtained from the calculus spectrum from norm P100/2006 for Bucharest(ground acceleration is equal to 0.24g).

According to N2 method, the displacement requirement is expressed by the displacement spectrum of the seismic response, determined for the equivalent system with one degree of freedom and the structures response by a force-displacement curve determined for the real system MDOF. This curve established for the real structure is converted into a force-displacement formula for the equivalent system with one degree of freedom in order for its parameters to be in a direct relation with the seismic response spectrum, built for SDOF systems. The

performance of the equivalent system SDOF is marked by the intersection between the displacement spectrum and the force-displacement curve,  $S_d$ . after determining the displacement requirements of the SDOF system they are converted into displacement requirements  $D_t$  for the real structures.

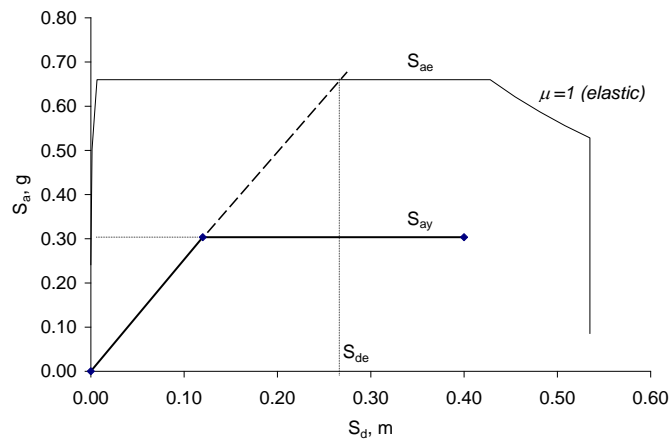


Fig. 3.2 - Determination of the structures performance (MRF5)

The elastic acceleration response spectrum was determined according to Romanian seismic code P100-1/2006, for a peak ground acceleration of 0.24g. The lateral force, used in the push-over analysis, has a "uniform" pattern and is proportional to mass, regardless of elevation (uniform response acceleration). Table 2 shows the values of target displacement,  $D_t$ , for the studied frames, calculated using N2 method.

Structure	EBF8	CBF8	BRB8	SW8
$D_t$ , [m]	0.34	0.29	0.31	0.32
Structure	EBF16	CBF16	BRB16	SW16
$D_t$ , [m]	0.64	0.49	0.53	0.62

Table 3.2 - Target displacement,  $D_t$ , for the MDOF systems for ULS

Three performance levels were considered:

- serviceability limit state (SLS),
- ultimate limit state (ULS)
- collapse prevention limit state (CPLS).

Intensity of earthquake action at the ULS is equal to the design one (intensity factor  $\lambda = 1.0$ ). Ground motion intensity at the SLS is reduced to  $\lambda = 0.5$  (similar to  $v = 0.5$  in EN 1998-1), while for the CPLS limit state was increased to  $\lambda = 1.5$  [39]. Based on [39], the following acceptance criteria were considered in the study:

- link deformations at SLS, ULS and CPLS are  $\gamma_u=0.005\text{rad}$ ,  $\gamma_u=0.11\text{rad}$  and  $\gamma_u=0.14\text{rad}$ .
- for conventional braces in compression (except EBF braces), plastic deformations at SLS, ULS and CPLS are  $0.25\Delta_c$ ,  $5\Delta_c$  and  $7\Delta_c$ , where  $\Delta_c$  is the axial deformation at expected buckling load.



- for conventional braces in tension (except EBF braces), plastic deformations at SLS, ULS and CPLS are  $0.25\Delta_t$ ,  $7\Delta_t$  and  $9\Delta_t$ , where  $\Delta_t$  is the axial deformation at expected tensile yielding load.
- for beams in flexure, the plastic rotation at ULS and CPLS are  $6\theta_y$  and  $8\theta_y$ , where  $\theta_y$  is the yield rotation
- for columns in flexure, the plastic rotation at ULS and CPLS are  $5\theta_y$  and  $6.5\theta_y$ , where  $\theta_y$  is the yield rotation.

The performance is assessed by comparing the capacity of the structure, obtained from the push-over analysis, with the seismic demand expressed by the target displacement. Pushover curves for the EBF, CBF, BRB and SW structures and the occurrence of plastic hinges up to the target point are shown in Fig. 3.3 and Fig. 3.4. Table 3.3 presents the interstorey drift demands for SLS and Tabel 3.4 presents the plastic deformations demand in members for the SLS, ULS and CPLS.

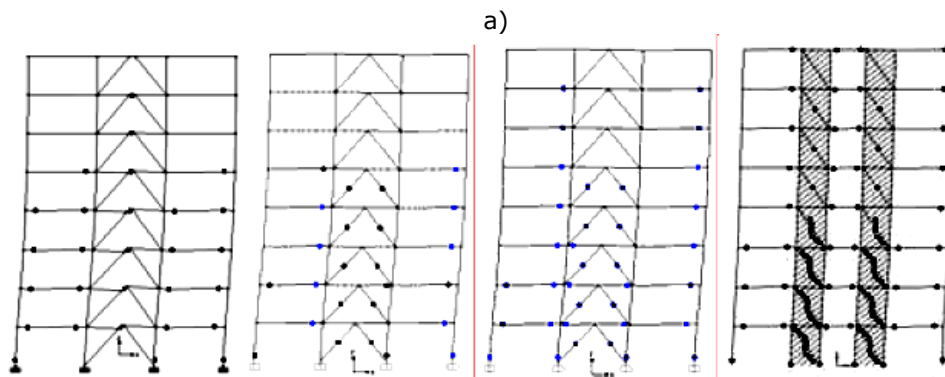
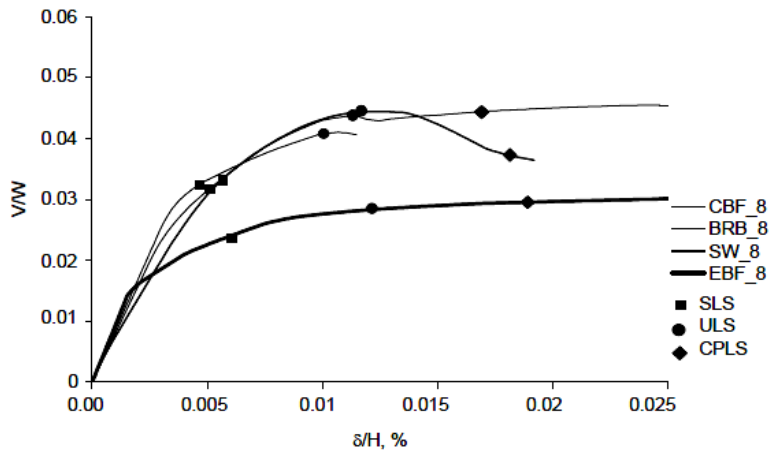


Fig. 3.3 - Pushover curves (normalized base shear vs. normalized top displacement) for eight story buildings a) and plastic hinges at ULS for EBF8, CBF8, BRB8 and SW8 structures b)

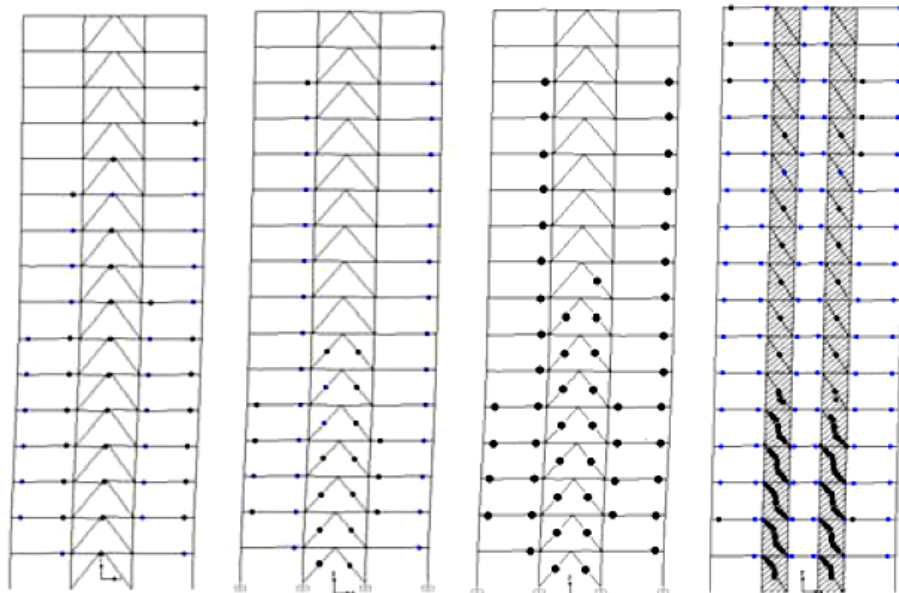
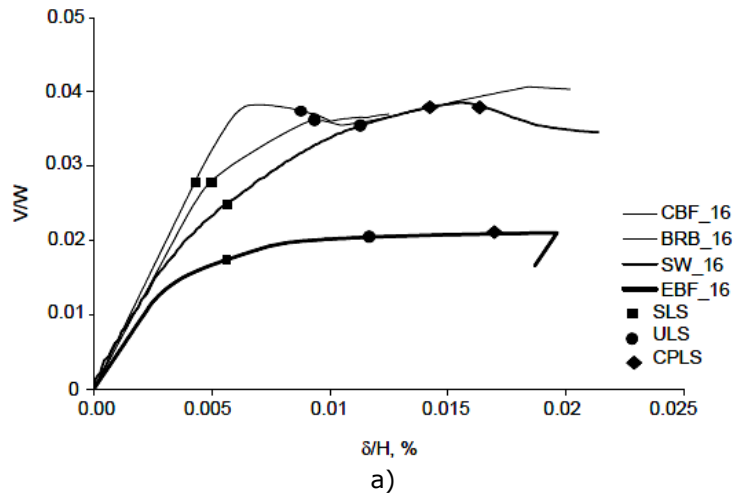


Fig. 3.4 - Pushover curves (normalized base shear vs. normalized top displacement) for sixteen story buildings a) and plastic hinges at ULS for EBF16, CBF16, BRB16 and SW16 structures b)

Structure	EBF8	CBF8	BRB8	SW8
$\delta/H_s$ , %	0.008	0.007	0.008	0.007
Structure	EBF16	CBF16	BRB16	SW16
$\delta/H_s$ , %	0.008	0.005	0.006	0.007

Table 3.3 - Interstorey drift demands for SLS

In the second step of the study, incremental non-linear dynamic (IDA) tests were conducted for CBF and EBF structures. The dynamic non-linear calculus

eliminates a part of the simplifications done in the static non-linear calculus, especially regarding the influence of the superior vibration modes.

Seven seismic recording were used. The spectral characteristics of the movements were modified by scaling the Fourier amplitudes to the values in the design spectrum from P100-1/2006. This way were obtained a series of semi-artificial accelerograms representative for the seismic source. The procedure was done with the program SIMQKE-1.

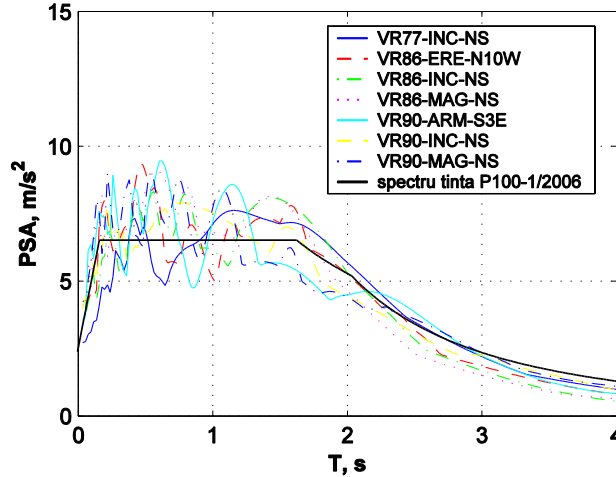


Fig. 3.5 - Elastic response spectrum of the semi-artificial accelerograms comparable to the design spectrum (P100-1/2006,  $a_g=0.24g$ ,  $T_c=1.6s$ )

In the case of performance based design, the performance levels are associated to the levels of seismic intensity (recurrence periods). If for the reference acceleration of the ground is considered the acceleration corresponding to failure limit state (SLD) –  $a_d$ , for the other limit states the corresponding accelerations are determined with the help of the equation proposed by [44].

$$\frac{a}{a_d} = \left( \frac{p_r}{p_{rd}} \right)^{0.28} \tag{3.1}$$

With the values for the recurrence periods previously stated, the following values for the acceleration to SLS and SLU result:

$$a_s = 0.412a_d \tag{3.2}$$

$$a_u = 1.22a_d \tag{3.3}$$

In Fig. 3.5 is represented the variation of the ratio between the acceleration corresponding to a specific limit state and the base acceleration (corresponding to SLD)  $a/a_d$ , with the recurrence period of the seismic motion.

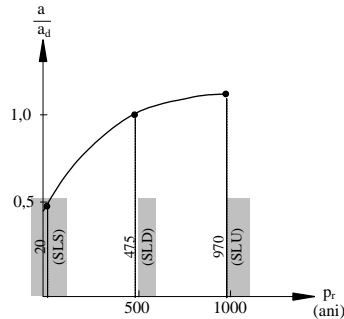


Fig. 3.6 - Ground acceleration according to the recurrence period [44]

The results obtained confirm the conclusions drawn from the static non-linear analysis. The EBF structures have a corresponding behaviour at the level of life support ( $\lambda=1$ ) but at the level of collapse prevention ( $\lambda=1.22$ ) the structure EBF8 has a not satisfying behaviour. In the case of modified centric braced structures, similar results are obtained, the structures having a corresponding behaviour at all 3 levels of performance.

This shows that the requirements from the seismic norm cover adequately ultimate limit state but not in all the cases and the one of collapse prevention.

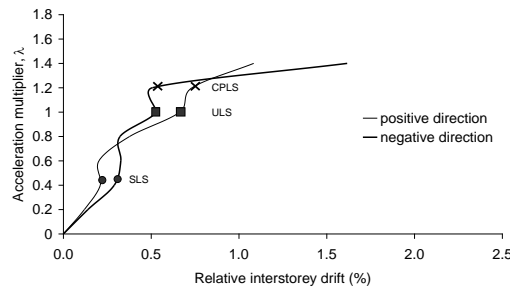


Fig. 3.7 - Acceleration - Interstorey drift curves, for EBF8

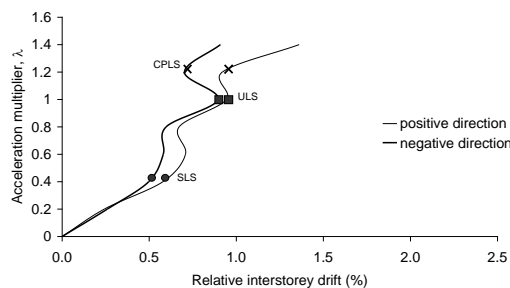


Fig. 3.8 - Acceleration - Interstorey drift curves, for (EBF16)

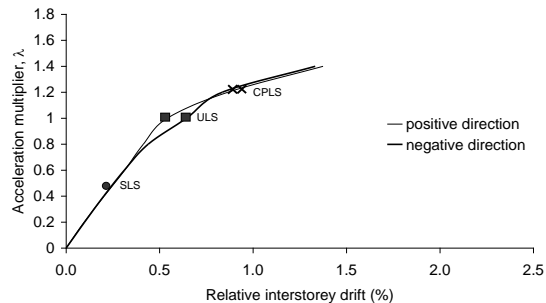


Fig. 3.9 - Acceleration - Interstorey drift curves, for CBF8

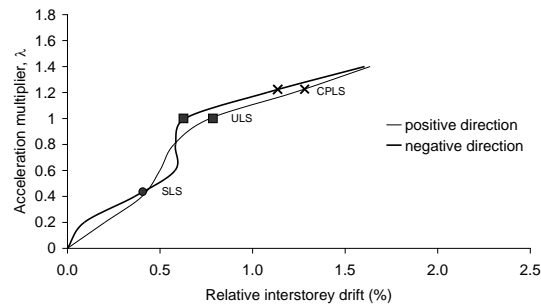


Fig. 3.10 - Acceleration - Interstorey drift curves, for CBF16

### 3.3 Conclusions

First of all, before detailing the comparative analysis of studied frames, it is important to observe that no plastic hinges occur in columns for 16 story frames, even for CPLS, excepting conventional CBF system. For 8 story frames, practically no plastic hinges appear in columns up to ULS (the values of plastic hinge deformation demands in Tabel 3.4 are very low), which is for sure that, with plastic deformation recor4ded for CPLS stage, the frames are safely standing up, but again, excepting CBF system.

In comparison with the centrally braced structures (using conventional braces CBF and buckling restrained braces BRB), the ones using eccentrically braces (EBF) and shear walls (SW) are characterized by lower stiffness. Base shear force capacity is very similar for CBF, BRB and SW structures, implying similar design strength under seismic action. Lower base shear force capacities are recorded for EBF structures. Displacements demands for SLS are lower than the interstorey drift limitation of  $0.008H_s$  used in design (Table 3.3). Structures designed using the dissipative approach, may experience structural damage even under moderate (SLS) earthquake. This is clearly seen in Tabel 3.4, where plastic deformation demands in members are presented. Plastic deformations in dissipative members indicate a moderate damage to the structure at SLS.

All structures satisfy the criteria for ULS. Plastic deformation demands in beams are more severe for EBF and SW compared to CBF and BRB, and plastic mechanisms develop almost on entire height of the structures. Shear wall frames show a very good ductility, comparable to eccentrically braced ones, but also providing a higher stiffness. For sixteen story buildings, no plastic hinges are recorded in the columns, while for eight story buildings plastic hinges are recorded at the bottom part of the first story columns. This shows that in case of higher buildings, when the contribution of the gravity loads (i.e. dead loads, live loads) is lower, the  $\Omega$  factor is more effective in design of non-dissipative members. Dissipation capacity shown by the structures confirms the reduction factors  $q$  used in design. Ductility of EBF, BRB and SW structures is similar to that of MRF, while CBF proved to be less ductile.

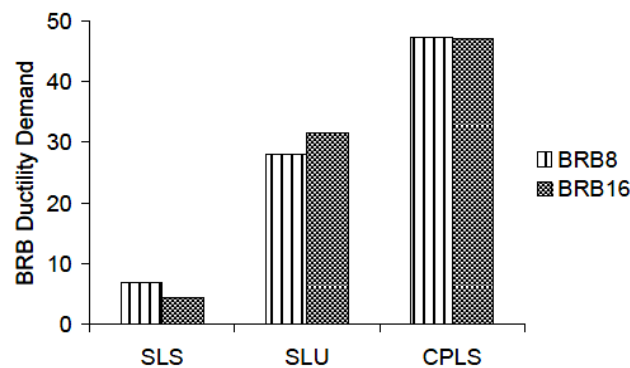


Fig. 3.11 - Ductility Demand Ratios for the buckling restrained braces

	beams				columns				links	braces	
	[rad]				[rad]				[rad]	[rad]	
	EBF 8	CBF 8	BRB 8	SW 8	EBF 8	CBF 8	BRB 8	SW 8	EBF 8	CBF 8	BRB 8
SLS	0.004	0.0013	0.0012	0.005	-	-	-	-	0.04	0.001	0.003
ULS	0.018	0.016	0.016	0.016	0.006	0.002	0.002	0.004	0.1	0.043	0.0034
CPLS	0.027	PF*	0.035	0.038	0.01	PF*	0.03	0.033	0.15	PF*	0.094
	EBF 15	CBF 15	BRB 15	SW 15	EBF 15	CBF 15	BRB 15	SW 15	EBF 15	CBF 15	BRB 15
SLS	0.007	0.0004	0.007	0.007	-	-	-	-	0.037	-	0.0038
ULS	0.021	0.013	0.015	0.017	-	-	-	-	0.11	0.044	0.028
CPLS	0.033	PF*	0.028	0.027	-	PF*	-	-	0.165	PF*	0.067

\* PF – premature failure following the buckling of braces

Tabel 3.4 - Plastic deformation demands in members at SLS ( $\lambda = 0.5$ ), ULS ( $\lambda = 1.0$ ) and CPLS ( $\lambda = 1.5$ )

Structures perform well till the attainment of the target displacement at CPLS, excepting CBF systems, which fail prematurely, mainly due to the failure of the braces in compression. When conventional braces are replaced by BRBs, the performance is improved and the performance level of collapse prevention is reached.

In case of EBF structures, plastic rotation demands in links exceed the rotation capacity. However, experimental tests on such elements have shown that in

case of very short links, plastic rotation capacity may reach 0.17-0.20 rad [75]. The ductility demands in the buckling restrained braces are plotted in Fig. 3.11. Experimental investigation on such type of members has shown the ductility demand of braces may exceed 25-30, depending on the material properties [11]

## **4 PERFORMANCE CRITERIA AND DETAILING FOR BEAM TO COLUMN JOINTS OF MULTI-STOREY STRUCTURES**

### **4.1 Introduction**

In the last years the interest of specialists in the domain of seismic engineering has significantly grown and also of the national authorities in elaborating norms for seismic design. This fact is due to first of all to the major seismic events that have marked the last years (Mexico City 1985, Northridge 1994, Kobe 1995, Turkey 1999, Taiwan 1999), events that had a great number of human life losses and also significant material damages. The concept that is the basis of the actual norms was conceived over 70 years ago. It is based on the design of structures so that they satisfy one criteria meaning avoiding collapse of the structure and protecting human life in the case of a very big seismic event. The earlier mentioned earthquakes, that have affected highly populated zones or with a high degree of economic development, have shown that the design based on one criterion is not enough anymore. Besides satisfying the condition to avoid collapse, a modern design should ensure the continuance of the activities of institutions with a role in first aid in case of a catastrophe (hospitals, fire stations, communications buildings, etc.), limiting the risk for buildings with a great risk factor (nuclear centres, multi-storey buildings, buildings with human agglomerations, chemical material deposits, etc.) and last but not least, limiting generalized damages, damages that can have a great impact on a region's or country's economy. In this context it has appeared on a worldwide plan a new concept that introduces several levels of performance or limit states. This way in the last years have been developed, especially in the USA, methods that serve the evaluation of the performances of existing buildings (ATC-40, 1996, FEMA 273, 1997) as well as for designing new structures (SEAOC Vision 2000, 1995, SAC-FEMA 356, 2001).

From previous chapter it can be concluded that for a DS structure to fulfil performance criteria to ULS, SLS and CFS there is also necessary that beam-to-column connections satisfy specific strength and ductility demands. In present chapter, it will be enounced beam-to-column performance demands in terms of strength and ductility requested by American and European standards. Constructive solutions for beam-to-column joints from American and European practice are illustrated too.

### **4.2 Stiffness and Strength classification of joints (EN 1993-1-8)**

The joints can be classified according to the values of their main structural properties, i.e. rotational stiffness, strength in bending and rotational capacity (or ductility). The structural properties of all the joints need to correspond to the assumptions made in the structural frame analysis and in the design of the



members. In particular, as far as simple joints are concerned, the available rotation capacity of the joints should be sufficient to accept the rotations evaluated in the analysis process. In Eurocode 3 Part 1-8, joints are classified by stiffness and by strength. Ductility aspects are also to be considered.

### 4.2.1 Classification by stiffness

This classification is only applicable to beam-to-column joint configurations. Through the comparison of its actual rotational stiffness  $S_{j,ini}$  with classification boundaries (Fig. 4.1), a joint may be considered as:

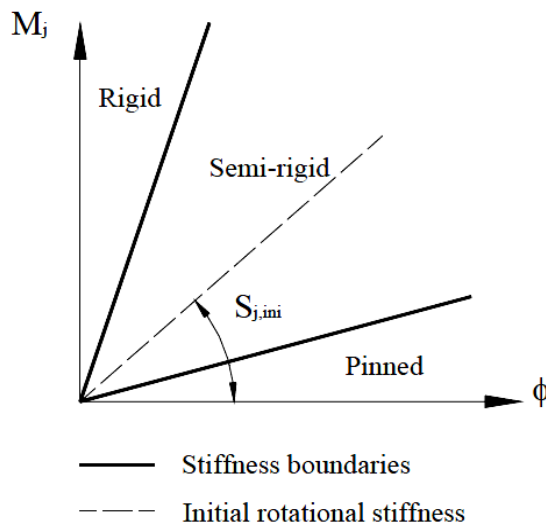


Fig. 4.1 - Boundaries for stiffness classification of joints

*Nominally pinned connection* - The joint shall be capable of transmitting the internal forces, without developing significant moments which might adversely affect the structural members. It shall be also capable of accepting the resulting rotations under the design loads.

$$S_{j,ini} \leq 0,5 EI_b / L_b \tag{4.1}$$

*Rigid connection*: The joint shall be capable of transmitting the internal forces, without developing significant moments which might adversely affect the structural members. It shall be also capable of accepting the resulting rotations under the design loads.

$$S_{j,ini} \geq k_b EI_b / L_b \tag{4.2}$$

where  $k_b = 8$  for frames where the bracing system reduces the horizontal displacement by at least 80%;  
 $k_b = 25$  for other frames.

*Semi-rigid*: The joint provides a predictable degree of interaction between members, based on the design moment-rotation characteristics of the joint. It should be able to transmit internal forces and moments.

Boundaries: A joint which doesn't meet the criteria for a rigid or a nominally pinned joint shall be classified as a semi-rigid joint.

Where: E is the elastic modulus of the beam material;

$I_b$  is the second moment area of the beam;

$L_b$  is the beam span (distance between the axis of the supporting columns).

#### 4.2.2 Classification by strength

Through the comparison of its actual design moment resistance  $M_{j,Rd}$  with the design moment resistances of the members that it connects ( Fig. 4.2), a joint may be classified as:

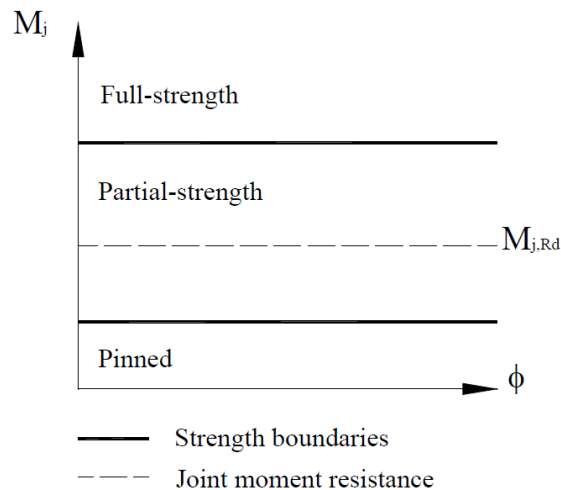


Fig. 4.2 - Boundaries for strength classification of joints

*Nominally pinned connection:* The joint shall be capable of transmitting the internal forces, without developing significant moments which might adversely affect the members of the structure. It shall also be capable of accepting the resulting rotations under the design loads.

- Boundary:  $M_{j,Rd} \leq 0,25 M$  full-strength (see Fig. 4.2)

*Full-strength connection* - The design resistance of a full strength joint shall be not less than that of the connected members.

- Boundary:  $M_{j,Rd} \geq M$  full-strength (see Fig. 4.3)

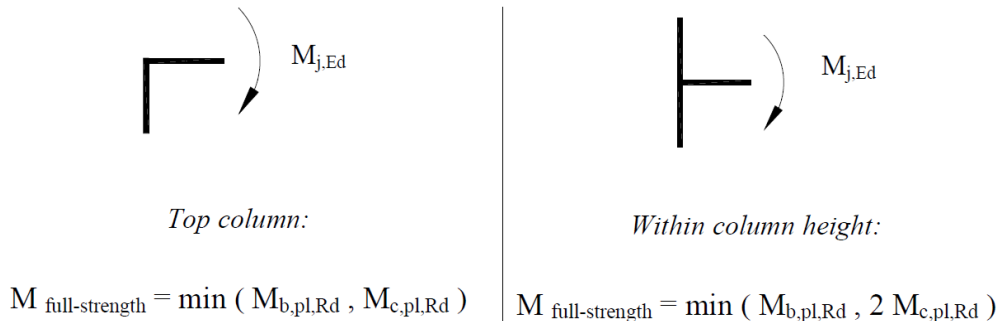


Fig. 4.3 - Full-strength resistance

*Partial-strength connection:* joint which doesn't meet the criteria for full-strength or nominally pinned joints should be considered to have a partial-strength resistance.

## 4.3 Provisions and performance criteria for beam to column joints

### 4.3.1 USA Provisions

The researches that followed the earthquakes in the 90's have tried to establish improved constructive solutions for the types of joints commonly used in the north-American practice. These solutions lead to the formation of a data base with prequalified joints used in seismic zones. All these results were included in the seismic norm AISC 2005. This way, in conformity to this norm[4], the joints used in special steel frames must satisfy specific requirements. These requirements depends on the type of Moment Frame used.

According to [4] there are 3 types of Moment Frames:

- Special Moment Frames (**SMF**) which are expected to withstand significant inelastic deformations when subjected to the forces resulting from the motions of the design earthquake.
- Intermediate moment frames (**IMF**) which are expected to withstand limited inelastic deformations in their members and connections when subjected to the forces resulting from the motions of the design earthquake.
- Ordinary moment frames (**OMF**) which are expected to withstand minimal inelastic deformations in their members and connections when subjected to the forces resulting from the motions of the design earthquake.

**SMF** Beam-to-Column Connections requirements[4]:

- The connection shall be capable of sustaining an interstory drift angle of at least 0.04 radians.
- The measured flexural resistance of the connection, determined at the column face shall equal at least  $0.80M_p$  of the connected beam at an interstory drift angle of 0.04 radians.
- The required shear strength of the connection shall be determined using the following quantity for the earthquake load effect E:

$$E = 2[1.1R_y M_p] / L_h \quad (4.3)$$

Where:

$R_y$  = ratio of the expected yield stress to the specific minimum  
yield stress  $F_y$   
 $M_p$  = nominal plastic flexural strength  
 $L_h$  = distance between plastic hinge locations.

**IMF** Beam-to-Column Connections requirements[4]:

- The required interstory drift angle shall be a minimum of 0.02 radian
- The required shear strength of the connection shall be determined using (4.3).

**OMF** Beam-to-Column Connections requirements[4]:

Beam-to-Column Connections shall be made with welds and/or high-strength bolts. Connections are permitted to be fully restrained (FR) or partially restrained (PR) moment connections as follows:

Fully restrained (FR) moment connections that are part of the seismic load resisting system shall be designed for a required flexural strength that is equal to  $1.1R_yM_p$ , as appropriate, of the beam, or the maximum moment that can be developed by the system, whichever is less.

FR connections shall meet the following requirements:

Where steel backing is used in connections with complete-joint-penetration (CJP) beam flange groove welds, steel backing and tabs shall be removed, except that top-flange backing attached to the column by a continuous fillet weld on the edge below the CJP groove weld need not be removed. Removal of steel backing and tabs shall be as follows:

- Following the removal of backing, the root pass shall be backgouged to sound weld metal and backwelded with a reinforcing fillet. The reinforcing fillet shall have a minimum leg size of 8 mm.
- Weld tab removal shall extend to within 3 mm of the base metal surface, except at continuity plates where removal to within 6 mm of the plate edge is acceptable. Edges of the weld tab shall be finished to a surface roughness value of  $13 \mu\text{m}$  or better. Grinding to a flush condition is not required. Gouges and notches are not permitted. The transitional slope of any area where gouges and notches have been removed shall not exceed 1:5. Material removed by grinding that extends more than 2 mm below the surface of the base metal shall be filled with weld metal. The contour of the weld at the ends shall provide a smooth transition, free of notches and sharp corners.

where weld access holes are provided, they shall be as shown in Fig. 4.14. The Weld access hole shall have a surface roughness value not to exceed  $13 \mu\text{m}$ , and shall be free of notches and gouges. Notches and gouges shall be repaired as required by the engineer of record. Weld access holes are prohibited in the beam web adjacent to the end-plate in bolted moment end-plate connections.

The required strength of double-sided partial-joint-penetration groove welds and double-sided fillet welds that resist tensile forces in connections shall be  $1.1R_yF_yA_g$ , as appropriate, of the connected element or part. Single-sided partial-joint-penetration groove welds and single-sided fillet welds shall not be used to resist tensile forces in the connections.

For the joints to be considered prequalified several demands regarding detailing and general arrangement of the structures elements must be met. The frames must be built and detailed so that the relative level displacement can be developed as a combination between the elastic deformation and a plasticisation in certain areas of the frame (Fig. 4.4).

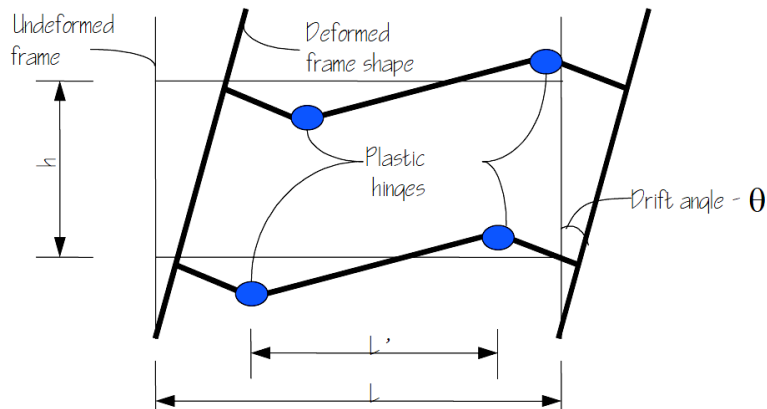


Fig. 4.4 – Inelastic Behaviour of Frames with Hinges in Beam Span[38]

In the frame illustrated above the inelastic relative level displacement is developed by plastic rotation of the formed hinges. Total relative level displacement is obtained by adding this deformation to the elastic relative level-displacement resulted in bending of the structural elements. Shortening or elongations of the columns due to axial forces are not included. The development of the plastic hinges in beams leads to energy dissipation thru plastic deformation. In case plastic hinges are formed in columns the dissipation capacity is reduced due to the smaller number of plasticized elements.

For the calculus of the maximum efforts in the critical sections, the position of the plastic hinges must be determined previously. If for a structure, efforts in elements from gravitational loads add up to max. 30% of the bearing capacity of element the determination of the position of plastic hinges is done according to Fig. 4.5.

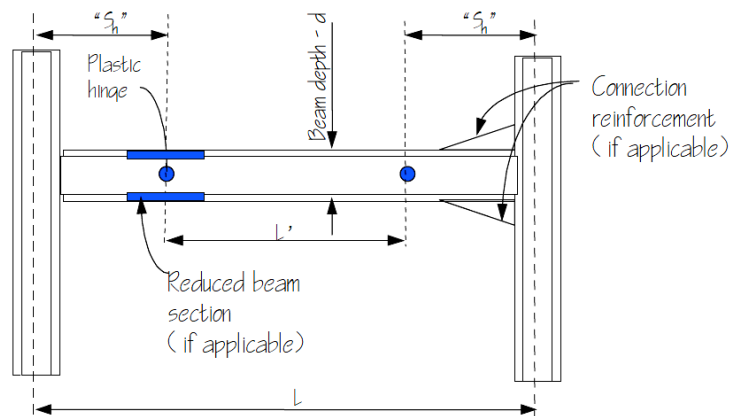


Fig. 4.5 – Plastic hinges position on beam[38]

Max. plastic bending moment in plastic hinges, can be determined with following relation:

$$M_{pr} = C_{pr} \cdot R_y \cdot Z_e \cdot F_y \quad (4.4)$$

Where:

$M_{pr}$  – Max. bending moment in plastic hinge.

$C_{pr}$  - factor depending on max. resistance of the joint, material hardening, local hardenings usually,  $C_{pr}$  is determined with relation:

$$C_{pr} = \frac{F_y + F_u}{2 \cdot F_y} \quad (4.5)$$

$R_y$  – coefficient depending on steel grade

$Z_e$  – plastic resistance modulus for the section(or joint)

$F_y$  – material yielding limit

$F_u$  – material ultimate strength.

#### Panel Zone Strength

Moment-resisting connections should be proportioned either so that shear yielding of the panel zone initiates at the same time as flexural yielding of the beam elements or so that all yielding occurs in the beam. For panel zone strength the following procedure is recommended:

**Step 1:** Calculate  $t$ , the thickness of the panel zone that results in simultaneous yielding of the panel zone and beam from the following relationship:

$$t = \frac{C_y M_c \times \frac{h-d_b}{h}}{(0.9) \times 0,6 \times F_{yc} \times R_{yc} \times d_c \times (d_b - t_{fb})} \quad (4.6)$$

Where:

$h$  = the average story height of the stories above and below the panel zone.

$R_{yc}$  = the ratio of the expected yield strength of the column material to the minimum specified yield strength.

**Step 2:** If  $t$ , as calculated, is greater than the thickness of the column web, provide doubler plates, or increase the column size to a section with adequate web thickness.

In the USA, the most important provisions refer to the design based on performance given by FEMA (Federal Emergency Management Agency), ATC (Applied Technology Council) and SEAOC (Structural Engineers Associations of California). In the proposed methodology by SEAOC Vision 2000 (1995), the structures are designed such that they satisfy the four levels of performance, function of the destination of the construction and the frequency of the earthquakes (Fig. 23). The performance objectives increase (less damages are admitted) as the frequency of the earthquake increases (seismic actions of low intensity that can occur several times in the life time of a building) or with the increase in the importance degree of the construction. In Fig. 23 it can be observed that under the action of a frequent earthquake, the structure will not suffer any kind of damage but under the action of a rare or very rare earthquake the level of the damages will be extended but protecting life and preventing collapse will be ensured.

The damage corresponding to each level of performance depend on the type of the structure and on the type of the materials used. Even though it's an important step in seismic design, the methodology proposed by Vision 2000 has some shortcomings and limitations:

- it does not offer calculus methods or analytical procedures to ensure the safety of the building;
- it is difficult to define the intermediary levels of performance;

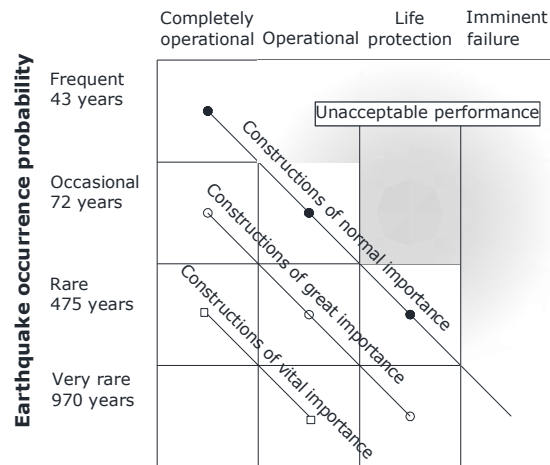


Fig. 4.6- Defining performance levels function the frequency of the earthquake

An important progress in this way was brought by FEMA-237 (1997). The performance objectives are defined analytically. Every performance objective consists of defining a degradation limit state, called performance level and a associated seismic intensity, for which the performance level mentioned must be reached. This guarantees that, in the case the seismic motion so defined loads the structure, the level of damages, will not be greater than the one foreseen in the performance objective. In the methodology given by FEMA 273, as opposed to Vision 2000, the performance levels of the building are obtained by combining the performance levels of the structure with the ones of the non-structural elements. In Table 3 are defined the three levels of performance of the structure, for which are supplied also the limit level displacements.

- Performance level	- Damage state description	Maximum drift [%]	Residual maximum drift [%]
- Continuous occupancy S-1	- Negligible damages of structural elements - Local buckling and residual distortions in some elements - Local deformation of some sections	- 0,7	- negligible
- Life protection S-3	- Plastic hinges in some elements - Local buckling in some elements - Severe distortions and failure in some connections	2,5	1,0

	- Local breakage on some elements		
- Imminent collapse	- Severe distortions in columns as well as in beams	5,0	5,0
- S-5	- Numerous connections failure		

Table 4.1 - Performance structural levels for un-braced frame structures

For earthquakes of reduced intensity, lateral displacements will be reduced and the supporting structure will be in the elastic stage. In the elastic stage in the structure damages do not occur. For seismic actions of greater intensity, the lateral displacements will be big and some structural elements will be plasticised. Besides the three performance levels FEMA 273 provide two performance domains:

- performance domain characterized by the degradation level, it is confined by the performance levels of continuous occupation and life protection (S-2);
- performance domain described by a limited life safety, it is confined by the life safety performance level and imminent collapse (S-4);

Unlike Vision 2000, FEMA 273 defines for each of the previously presented earthquakes their seismic response spectra (Fig. 24), where:

- SS : spectral response acceleration for short periods;
- S1 : spectral response acceleration a period of 1 sec;
- BS, B1 : coefficients function of damping.

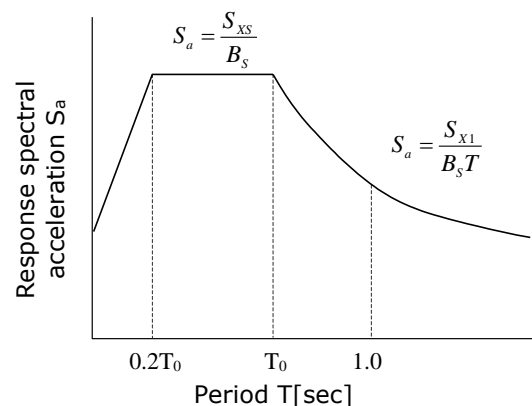


Fig. 4.7 - Response spectrum according to FEMA-273, for a 5% damping

The performance levels of the nodes represent discrete levels of degradation selected from all possible degradation states that a node can withstand, as a consequence of the seismic response. For example, FEMA350[38] provides 3 levels of performance, namely:

- Immediate Occupancy (IO)
- Life Safety (LS)
- Collapse Prevention (CP)

For each of these performance levels, a description of the degradation state of the elements and connections is provided (see Table 4.2). For the performance level Immediate Occupancy (IO), usually is considered that the structure is in the elastic domain that is why no damages are allowed.



Elements	Levels of structural performance	
	CP	IO
Beam-column joint	A lot of cracked connections where the bearing capacity is almost worn-out	Less than 10% of the cracked connections at any level. Incipient local plastic zones in other connections.
Web panel of column	Extended deformations	Minor deformations
Continuity joint to column	No cracks	No plastic zones
Base plate column	Extended plasticised zones in anchorage bolts and base plate	No degradations or visible deformations

Table 4.2 - Description of the structural performance levels

FEMA356[39] provided also quantity acceptance criteria for each level of performance, function of the type of structural analysis (Table 7.6).

Type of node	Plastic rotation, rad		
	IO	LS	CP
Welded nodes	0.128- 0.0003 <i>d</i>	0.0284- 0.0009 <i>d</i>	0.0337- 0.0004 <i>d</i>
Welded nodes, gusset plates on flanges	0.0140- 0.0003 <i>d</i>	0.0319- 0.0006 <i>d</i>	0.0426- 0.0008 <i>d</i>
Reduced beam section	0.0125- 0.0001 <i>d</i>	0.0380- 0.0002 <i>d</i>	0.0500- 0.0003 <i>d</i>
Node with bolts, with a weak component in:	End plate	0.010	0.028
	Bolts	0.008	0.010
	Weld	0.003	0.008

Note: *d* – beam height

Table 4.3 - Acceptance criteria for the non-linear analysis

### 4.3.2 European Provisions

Dissipative joints, among the stiffness and strength must fulfil ductility demands (experimentally validated) imposed by the seismic norms (e.g. EN 1998-1, P100-1/2006(Romania)) considering the type of the structure and ductility class.

Joints are one of the most sensitive points regarding seismic resistance of a structure. A special attention should be given to the components of the joints where dissipative zones are formed.

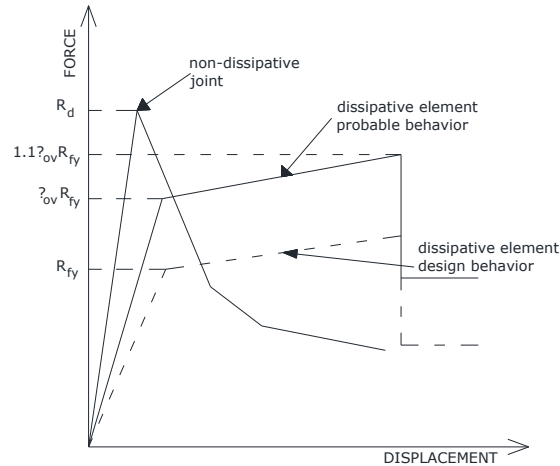


Fig. 4.8 – Design principle of non-dissipative joints

Joints can be designed as dissipative (i.e. plastic deformations take place in the joint) or non-dissipative ones (plastic deformations occur in the connected elements). Due to the complex behaviour of connections under seismic loads, geometry and calculus must be validated by experimental tests.

Design principle of non-dissipative joints that connect dissipative structural elements is presented in Fig. 4.8.

Non-dissipative joints must be designed in the elastic domain ensuring that the plastic deformations will form in dissipative zones of elements connected in joint. The design of the non-dissipative joints is not based on the efforts resulted from structural analysis but on efforts corresponding to dissipative plasticised and consolidated zones.

Checking formula can be expressed as[34]:

$$R_d \geq 1.1 \cdot \gamma_{ov} \cdot R_{fy} \quad (4.7)$$

Where :

- $R_d$  joint resistance
- $R_{fy}$  plastic resistance of element based on calculus yielding limit
- 1,1 factor that takes into account hardening of the dissipative zone
- $\gamma_{ov}$  overstrength factor

Dissipative semi-rigid and/or partial strength connections are permitted, provided that all of the following requirements are verified:

- a) the connections have a rotation capacity consistent with the global deformations
- b) members framing into the connections are demonstrated to be stable at the ultimate limit state (ULS);
- c) the effect of connection deformation on global drift is taken into account using nonlinear static (pushover) global analysis or non-linear time history analysis.

A classification based on the plastic rotation capacity of the joints  $\Phi_{pl}$  corresponding to design value of the resistance to plastic bending moment  $M_{j,Rd}$  (Fig. 4.9) was recently introduced in connections literature.

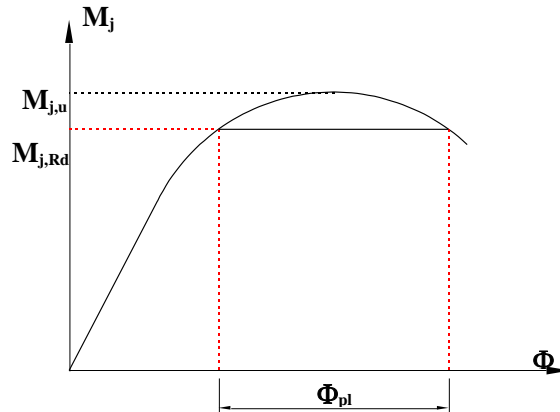


Fig. 4.9 – Plastic rotation capacity

There are 3 classes of joints based on ductility.

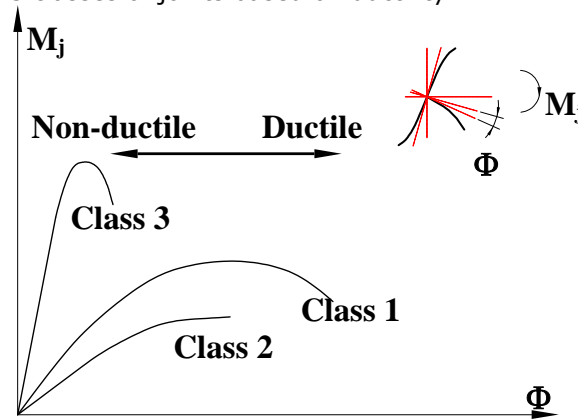


Fig. 4.10 – Joint classification based on ductility

Class 1 – Ductile Joints – A joint it is considered to be ductile if when reaching for the resisting plastic moment develops a high rotation capacity.

Class 2 - Intermediate ductility joints - A joint it is considered to be intermediate ductile if when reaching for the resisting plastic moment develops a limited rotation capacity.

Class 3 – Non-ductile Joints - A joint it is considered to be non-ductile if when before reaching the resisting plastic moment a premature failure to one of the joints components occurs.

Rotation capacity of a joint  $\Phi_{CD}$  is given by the maximum recorded rotation on the Moment –Rotation chart (Fig. 4.11).

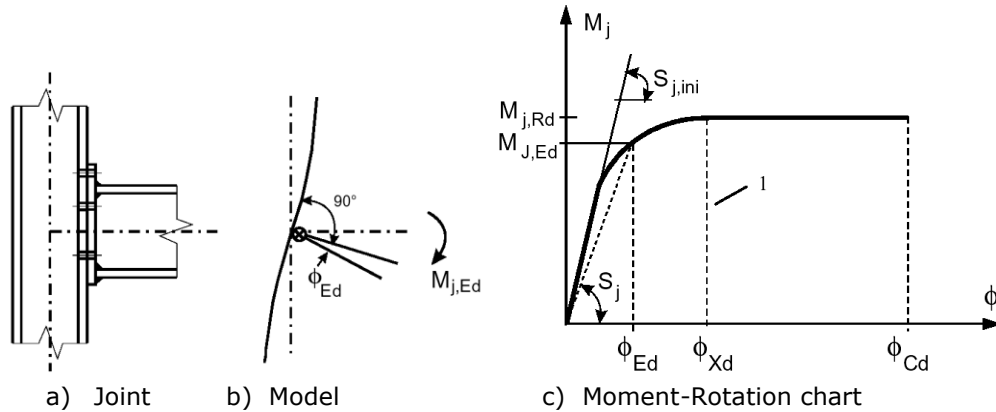


Fig. 4.11 – Joint Moment - Rotation

A bolted beam-to-column joint for which  $M_{j,Rd}$  it is determined from column web in shear it is assumed to have enough rotation capacity for a plastic global analysis if

$$d/t_w \leq 69 \cdot \varepsilon \quad (4.8)$$

A bolted beam-to-column joint it is assumed to have enough rotation capacity for a plastic global analysis if the following are fulfilled:

- $M_{j,Rd}$  is determined by one of the next components:
  - Flange of the column in bending
  - End plate tensioned in bending
- Thickness  $t$  of column flange or beam end-plate satisfy the condition:

$$t \leq 0.36d \sqrt{\frac{f_{ub}}{f_y}} \quad (4.9)$$

Where  $f_y$  it is yielding limit of the base component.

A joint for which  $M_{j,Rd}$  is determined by resistance of bolts in shear cannot be considered as having enough rotation capacity for a global plastic analysis.

Rotation capacity  $\Phi_{CD}$  of a welded beam-to-column joint can be considered at least equal to the following value:

$$\Phi_{CD} = 0.025 \frac{h_c}{h_b} \quad (4.10)$$

only if:

- The web of the column is stiffened in compression and unstiffened in tension
- $M_{j,Rd}$  is not determined by the resistance of the columns web.

A welded beam-to-column joint, unstiffened, can be considered as having a rotation capacity of min. 0.015 rad if previous conditions are met.

A beam-to-column joint doesn't require rotation capacity check if  $M_{j,Rd}$  is at least with 20% bigger than  $M_{pl,Rd}$  of the weakest element in the joint.

The connection design should be such that the rotation capacity of the plastic hinge region  $\theta_p$  is not less than 35 mrad for structures of ductility class DCH

and 25 mrad for structures of ductility class DCM with  $q > 2$ . The rotation  $\theta_p$  is defined as [34]

$$\theta_p = \delta / 0.5L \quad (4.11)$$

Where (see Fig. 4.12):

$\delta$  is the beam deflection at midspan;  
 $L$  is the beam span

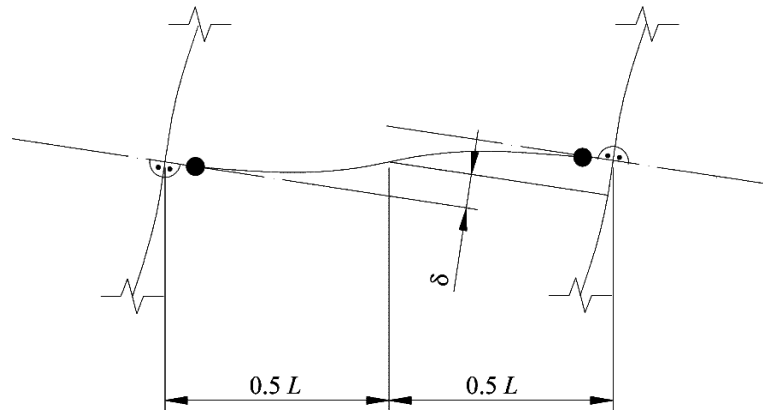


Fig. 4.12 - Beam deflection for the calculation of  $\theta_p$  [34]

The rotation capacity of the plastic hinge region  $\theta_p$  should be ensured under cyclic loading without degradation of strength and stiffness greater than 20%. This requirement is valid independently of the intended location of the dissipative zones.

In experiments made to assess  $\theta_p$  the column web panel shear deformation should not contribute for more than 30% of the plastic rotation capability  $\theta_p$ [34].

The column elastic deformation should not be included in the evaluation of  $\theta_p$ .

When partial strength connections are used, the column capacity design should be derived from the plastic capacity of the connections[34].

## 4.4 Constructional detailing for Beam-to-Column Joints

Usually beam-to-column joints designed for bending moment form plastic hinges in the beam or in the connection, in this way avoiding the formation of the plastic zone in the column. Although there are several technical solutions for joints designed to bending moment the most used are types that combine beams to the columns both structural elements having I and or H profile sections:

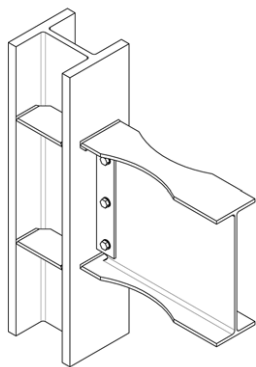
- Connections with end plate and bolts
- Welded connections
- Connections with L shape profiles

### 4.4.1 USA practice

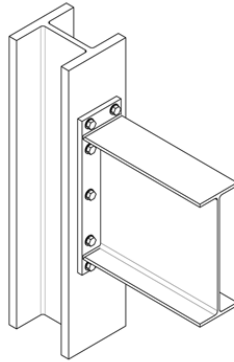
Fig. 4.13 presents commonly used beam-to-column joints in USA. The extended end plate connection with bolts (Fig. 4.13c), is used when it is an extended resistance to bending moment is required. For joint resistance to be

comparable with beam resistance it is necessary that the end plate and the bolts to be properly dimensioned. In most cases when HD profile sections are used there is no need to stiffen the column web in order to increase its resistance. For strengthening the connections in case of column sections with thin web (and not only) horizontal stiffeners (Fig. 4.13 a, c, d, e, g) can be used. These stiffeners overtake the tension forces from the upper part of the connection as well as the compression efforts from the inferior part.

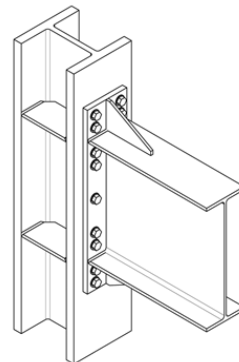
Beam to Column joint with reduced section (Fig. 4.13a) are prequalified connections in USA. Reducing the beam section is done by removing a small part of the beams' flange this way the formation of the plastic hinge being imposed.



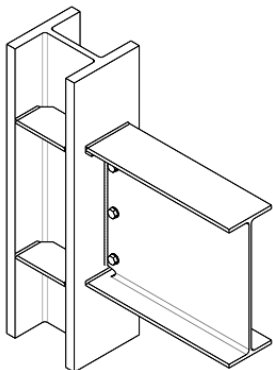
a) Beam with reduced section.



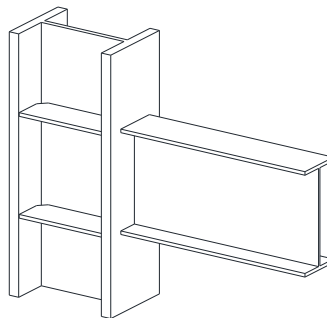
b) Extended end plate connection, with bolts not stiffened.



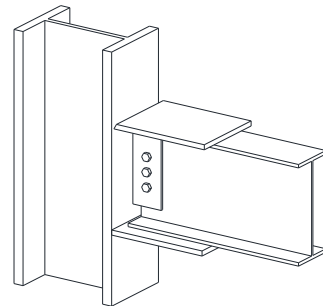
c) Extended end plate connection, with bolts, stiffened.



d) Stiffened Welded connection on the flanges of the beam.



e) Welded connection



f) Unstiffened Welded connection on the flanges of the beam.

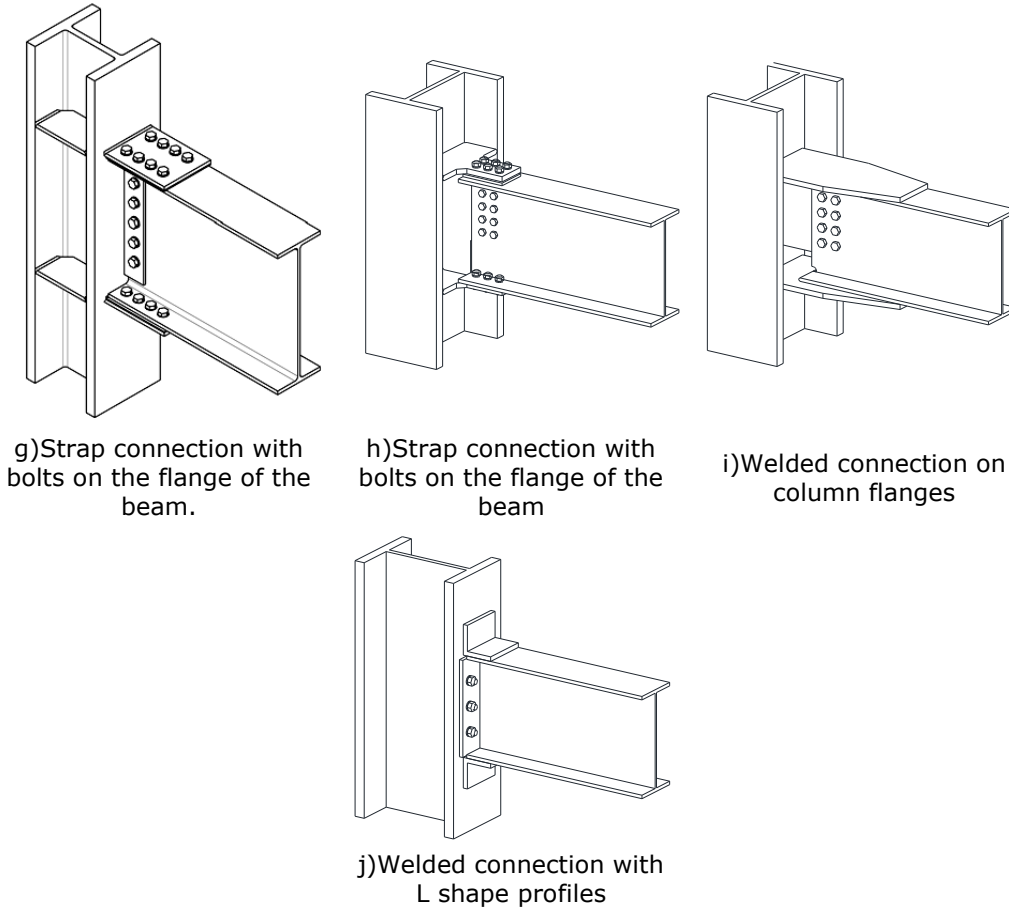


Fig. 4.13 – Beam to column joints – American practice

L shape sections from Fig. 4.13j that can be fixed with welds or bolts, overtake the tension, compression and shear forces of the joint. The main disadvantages of this type of connection are related to sliding of the bolts in flange holes and bending of the L shape section.

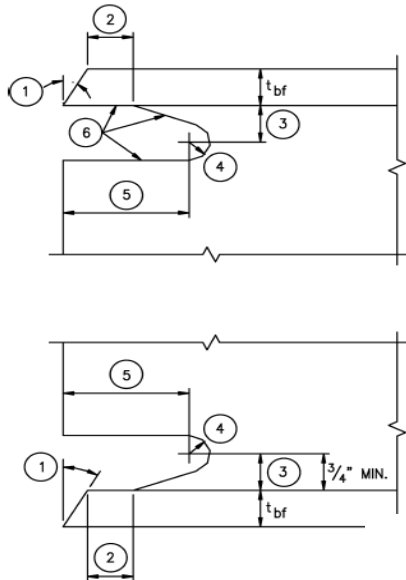
In USA welded connections like the one presented in Fig. 4.13e, are very often used even though this requires site welding.

**General conditions for Beams**

These conditions refers to flanges and webs max. admitted slenderness.

- $b_f/2t_f \leq 52/\sqrt{F_y}$  limit slenderness for flanges
- $h_c/t_w \leq 520/\sqrt{F_y}$  limit slenderness for webs

For **welded connections** following conditions must be satisfied:



1. Bevel as required by AWS D1.1 for selected groove weld procedure.
2. Larger of  $t_{bf}$  or  $\frac{1}{2}$  inch. (plus  $\frac{1}{2} t_{bf}$ , or minus  $\frac{1}{4} t_{bf}$ )
3.  $\frac{3}{4} t_{bf}$  to  $t_{bf}$ ,  $\frac{3}{4}$ " minimum ( $-\frac{1}{4}$  inch).
4.  $\frac{3}{8}$ " minimum radius (plus not limited, or minus 0).
5.  $3 t_{bf}$ . ( $-\frac{1}{2}$  inch)

Fig. 4.14 - Recommended Weld Access Hole Detail[4]

### Continuity Plates

Unless project-specific connection qualification testing is performed to demonstrate that beam flange continuity plates are not required, moment-resisting connections should be provided with beam flange continuity plates across the column web when the thickness of the column flange is less than the value given either by next formula:

$$t_{cf} < 0,4 \sqrt{1,8 b_f t_f \frac{F_{yb} \cdot R_{yb}}{F_{yc} \cdot R_{yc}}} \quad (4.12)$$

where:

$t_{cf}$  = minimum required thickness of column flange when no continuity plates are provided

$b_f$  = beam flange width

$t_f$  = beam flange thickness

$F_{yb}$  ( $F_{yc}$ ) = Minimum specified yield stress of the beam (column) flange,

$R_{yb}$  ( $R_{yc}$ ) = the ratio of the expected yield strength of the beam (column) material to the minimum specified yield strength

Prequalified connection details are permitted to be used for moment frame connections for the types of moment frames and ranges of the various design parameters indicated in the limits accompanying each prequalification. Project-specific testing should be performed to demonstrate the adequacy of connection details that are not listed in American norms as prequalified, or are used outside the range of parameters indicated in the prequalification. The following criteria were applied to connections listed as prequalified[38]:



1. There is sufficient experimental and analytical data on the connection performance to establish the likely yield mechanisms and failure modes for the connection.
2. Rational models for predicting the resistance associated with each mechanism and failure mode have been developed.
3. Given the material properties and geometry of the connection, a rational procedure can be used to estimate which mode and mechanism controls the behaviour and the deformation capacity (that is, interstorey drift angle) that can be attained from the controlling conditions.
4. Given the models and procedures, the existing data base is adequate to permit assessment of the statistical reliability of the connection.

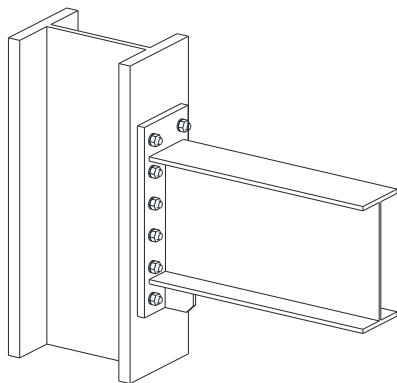
#### 4.4.2 European Practice

In Europe regularly used sections for columns are HEB, HEM sections, while for beams are IPE and HEA sections. The most commonly used type of fixed beam-to column joint is the extended end plate one. These can have unstiffened or stiffened extended end plates (Fig. 4.15a,b), horizontal stiffeners (Fig. 4.15b,c,d,f), supplementary column web plates (Fig. 4.15d) or haunches (Fig. 4.15e,f). Eurocode 1993-1-8 does not provide yet design formulas for stiffened extended end plate.

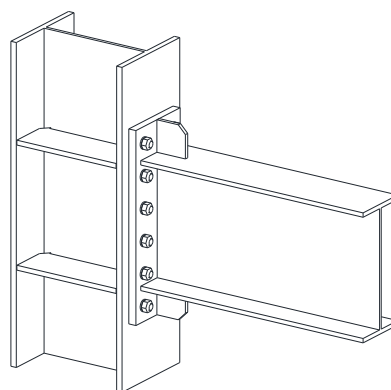
In any of the possible beam-to-column joint types (bolted or welded) column web can be the weakest component. Due to the fact that the rotation of the column web is limited by EN 1998 to 30% of total rotation of the joint this can be strengthened by welding supplementary panels on it (see Fig. 4.15d). Research made at "POLITEHNICA" University of Timisoara proves that the increase in strength is direct proportional with the area of the supplementary plates while the joint ductility remains high during monotone as well as cyclic loading.

Joints with reduced section of the beam (see Fig. 4.15c) are not included yet in Eurocode 1993-1-8, even though these types of joints are prequalified connections on USA. In the nearest future these types of joints will be included in European norms.

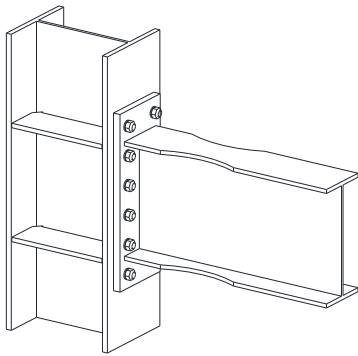
Starting from welded connection type regularly used in USA, in Europe it was developed and frequently used the splice connection presented in Fig. 4.15g.



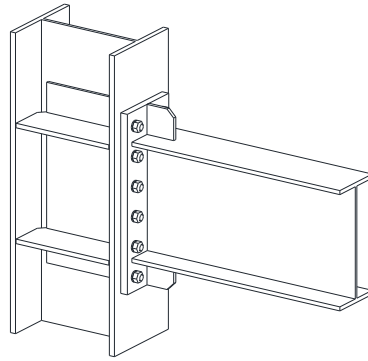
a) Extended end plate connection, with bolts, unstiffened at the upper part



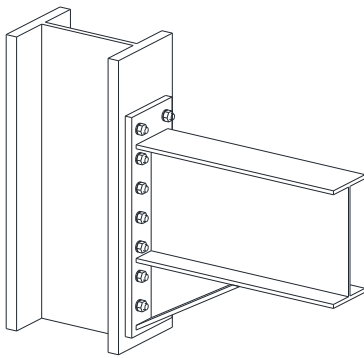
b) Extended end plate connection, with bolts, stiffened.



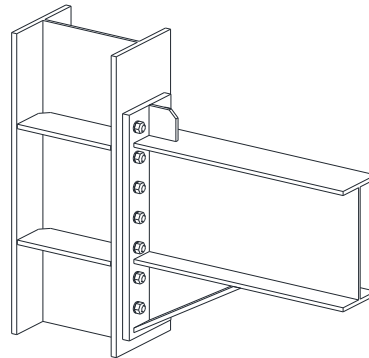
c) Beam with reduced section  
Extended end plate connection,  
stiffened



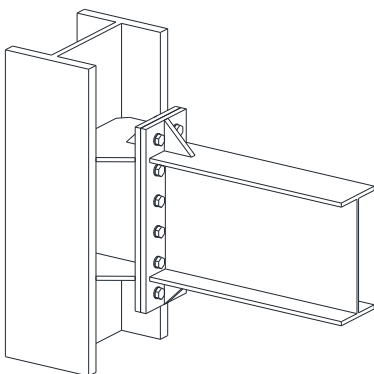
d) Extended end plate connection, with bolts,  
stiffened with supplementary column web  
plates.



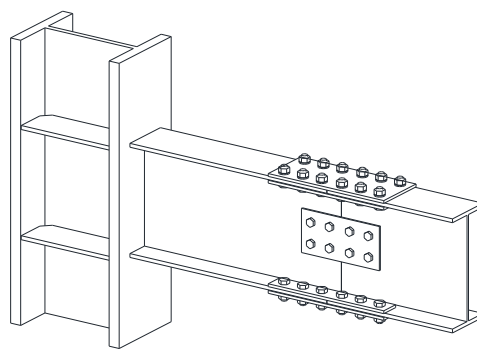
e) Extended end plate haunched  
connection, with bolts, unstiffened



f) Extended end plate haunched connection,  
with bolts, stiffened



h) Extended end plate connection,  
with bolts, stiffened.



g) Splice connection

Fig. 4.15 - Beam to column joints – European practice

## 4.5 Prequalification criteria for MR beam to column joints

The connection types listed in Tabel 4.4 are prequalified for use in connecting beams to columns flanges in special moment frames (SMF) and intermediate moment frames (IMF). All listed connections are considered fully restrained for the purpose of seismic analysis.

Prequalified Moment Connections [5]		
Connection type	Connection abbreviation	Moment Frame system
Reduced beam section	RBS	SMF, IMF
Bolted unstiffened extended end plate	BUEEP	SMF, IMF
Bolted stiffened extended end plate	BSEEP	SMF, IMF

Tabel 4.4 – Prequalified moment connections – AISC 358-05

In a reduced beam section (**RBS**) moment connection (Fig. 4.16) portions of the beam flanges are selectively trimmed in the region adjacent to the beam to column connection. Yielding and hinge formation are intended to occur primarily within the reduced section of the beam. RBS connections are prequalified for use in special moment frames (SMF) and intermediate moment frames (IMF) systems.

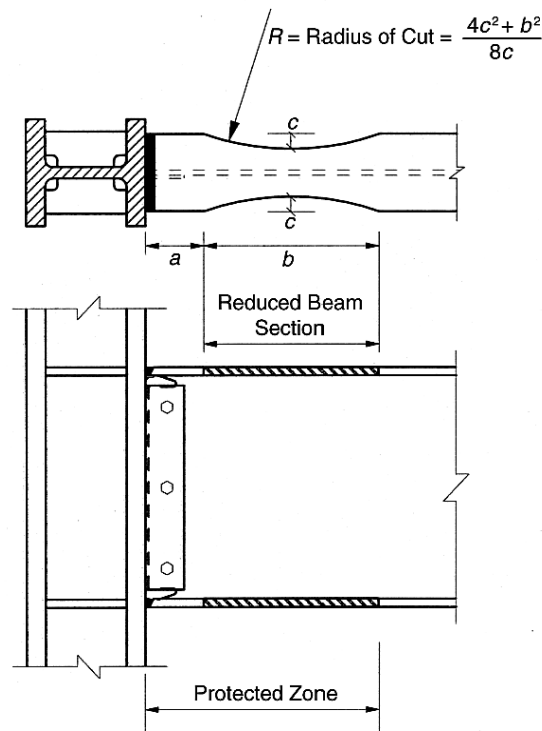


Fig. 4.16 – Reduced beam section connection [5]

A reduced beam section moment connection to be prequalified must satisfy, beside radius of cut and length of protected zone limitations, specific beam

limitations, specific column limitations, specific beam-column limitations, specific beam flange to column flange weld limitations, beam web to column connection limitations and to enrol in specific fabrication of flange cuts provisions.

Bolted-end plate connections are made by welding the beam to an end-plate and bolting the end-plate to a column flange. The three end-plate configurations shown in Fig. 4.13a,b,c are prequalified under the AISC seismic provisions.

The behaviour of the this type of connection can be controlled by a number of different limit states including flexural yielding of the beam section, flexural yielding of the end-plates, yielding of the column panel zone, tension failure of the end plate bolts, shear failure of the end plate bolts, or failure of various welded connections. The intent is to provide sufficient strength in the elements of the connections to ensure that the inelastic deformation of the connection is achieved by beam yielding. Extended end-plate connections are prequalified for use in special moment frame (SMF) and intermediate moment frame(IMF) systems.

Table 4.5 is a summary of the range of parameters that have been satisfactorily tested. All connection elements should be within the range shown.

Parameter	Four-Bolt Unstiffened (4E)		Four-Bolt Stiffened (4ES)		Eight-Bolt Stiffened (8ES)	
	Maximum in. (mm)	Minimum in. (mm)	Maximum in. (mm)	Minimum in. (mm)	Maximum in. (mm)	Minimum in. (mm)
$t_p$	2 <sup>1</sup> / <sub>4</sub> (57)	1/2 (13)	1 <sup>1</sup> / <sub>2</sub> (38)	1/2 (13)	2 <sup>1</sup> / <sub>2</sub> (64)	3/4 (19)
$b_p$	10 <sup>3</sup> / <sub>4</sub> (273)	7 (178)	10 <sup>3</sup> / <sub>4</sub> (273)	10 <sup>3</sup> / <sub>4</sub> (273)	15 (381)	9 (229)
$g$	6 (152)	4 (102)	6 (152)	3 <sup>1</sup> / <sub>4</sub> (83)	6 (152)	5 (127)
$p_{fi}, p_{fo}$	4 <sup>1</sup> / <sub>2</sub> (114)	1 <sup>1</sup> / <sub>2</sub> (38)	5 <sup>1</sup> / <sub>2</sub> (140)	1 <sup>3</sup> / <sub>4</sub> (44)	2 (51)	1 <sup>3</sup> / <sub>4</sub> (44)
$p_b$	—	—	—	—	3 <sup>3</sup> / <sub>4</sub> (95)	3 <sup>1</sup> / <sub>2</sub> (89)
$d$	55 (1400)	25 (635)	24 (610)	13 <sup>3</sup> / <sub>4</sub> (349)	36 (914)	18 <sup>1</sup> / <sub>2</sub> (470)
$t_{bf}$	3/4 (19)	3/8 (10)	3/4 (19)	3/8 (10)	1 (25)	19/32 (16)
$b_{bf}$	9 <sup>1</sup> / <sub>4</sub> (235)	6 (152)	9 (229)	6 (152)	12 <sup>1</sup> / <sub>4</sub> (311)	7 <sup>3</sup> / <sub>4</sub> (197)

Table 4.5 – Parametric limitations on prequalification[5]

Where:

$t_p$  = thickness of the end-plate, in. (mm)

$b_p$  = width of the end-plate, in. (mm)

$g$  = horizontal distance between bolts, in. (mm)

$p_{fi}$  = vertical distance between beam flange and the nearest inner row of bolts, in. (mm)

$p_{fo}$  = vertical distance between beam flange and the nearest outer row of bolts, in. (mm)

$p_b$  = distance between the inner and outer row of bolts in an eight-bolt connection, in. (mm)

$d$  = depth of the connecting beam, in. (mm)

$t_{bf}$  = thickness of beam flange, in. (mm)

$b_{bf}$  = width of beam flange, in. (mm)

A bolted stiffened or unstiffened extended end-plate moment connection to be prequalified must satisfy, beside Parametric limitations, specific beam limitations, specific column limitations, specific continuity plates limitations, specific bolts limitations and to enrol in specific connection detailing provisions.

## 4.6 Conclusions

All beam-to-column joints typologies presented in this thesis chapter are moment resisting joints. They could be dimensioned to be either full strength or partial strength joints rigid or semi-rigid. In principle a rigid joint is usually also full strength.

In case when beam-to-column joints solution is a full strength rigid one, the plastic rotation is expected to develop in plastic hinge formed at the end of the beam. However, in practice if the yielding limit of the steel used in beam is characterised by a larger value than the one accepted as overstrength (25%) related to the nominal value of  $F_y$  (it can happen for mild carbon steels S235, S275, S355). Components of the beam to column connection could be in the situation to undergo plastic deformations (this could be mostly the situation of extended end plate bolted joints). For this reason it is useful even for full strength rigid joints to control if they poses enough plastic rotation capacity.

Since the code EN 1998-1 limit the contribution of column web panel regarding the plastic rotation capacity of the joint at most 30% and also in case when HSS is used in columns, on the purpose to maintain the column predominantly elastic during earthquake, for the extended end plate bolted connection the most important contribution for plastic rotation could be concentrated in the end plate. In Chapter 6 we will try demonstrate that.

## 5 HSS EXPERIMENTAL PROGRAM

### 5.1 Introduction

Previous studies realized by [25][26] showed the advantages of using High Strength Steel (HSS) in combination with Mild Carbon Steel (MCS) in Dual-Steel Structures (DSS), to enhance robustness and better control of the response of seismic resistant building frames.

Reducing the demand on non-dissipative members by approaching dissipative elements to their plastic capacity under design forces can lead to an advanced design of a seismic resistant structure, both economic and safe point of view. The best way to accomplish this is to realise them of MCS(mild carbon steel) and HSS(high strength steel) correspondingly and not by changing size of section elements in dissipative and non-dissipative members because it also changes their stiffness. A well balanced design of a DSS system in terms of stiffness, strength and ductility of members and connections enables the achievement of three critical tasks of a seismically robust structure:

- secure plastic deformations in structural members targeted as dissipative
- multiple routes for transfer of forces and ensure their redistribution through yielding of other members
- sufficient overstrength to structural members that are not allowed to yield.

In a DSS system, MCS members have to behave like fuses, dissipating the seismic energy through plastic deformation, while HSS members have to remain predominantly elastic, or with limited damage, being responsible for robustness of the structure. This principle applies both, for members and joint components. In case of moment resisting frames designed according to the strong column - weak beam philosophy, the columns are usually designed to remain predominantly elastic during earthquakes, while the beams have to be ductile. For welded beam-to-column joints, the main contributors for ductility are column web in shear and the beam end, while for extended end-plate bolted connection, beside the beam end and the column web, the end-plate in bending becomes very important.

Starting from the above considerations a large experimental research program was designed and carried out in order to study the performance of dual-steel configuration for beam-to-column joints under monotonic and cyclic loading. When HSS is used in members designed to remain predominantly elastic, as columns, for instance, or in end-plates of bolted joints, T-stub components made of two steel grades are obtained. The aim of the testing program which is summarized hereafter was to investigate experimentally the performance of welded connections and bolted T-stub components realized from two different steel grades. Similar tests on T-stubs were realized by [49] but without cyclic loading and stiffener on the end-plate, and by [69] which applied cyclic loading but no HSS components and stiffener on end-plate.

## **5.2 DESIGN OF THE EXPERIMENTAL PROGRAM**

The experimental program is synthesized in Table 5.1 The program took 24 months.

Toughness tests, non-destructive control, chemical and metallographic analysis, including the interpretation of the failure mechanisms based on the theories in the failure mechanics have been realised at ISIM Timisoara (National R&D Institute for welding and Material Testing) which owns all the necessary equipment and qualification necessary for material and sub-assemblies investigations.

The tensile tests on materials, on weld connections, on T-stubs and on nodes were developed at UPT-CEMSIG. The Research Centre for Mechanics of Materials and Structural Safety - CEMSIG is a RTD (Research and Technical Development) unit of the "Politehnica" University of Timisoara, at the Faculty of Civil Engineering, Department of Steel Structures and Structural Mechanics. The research centre was established in 1999. In 2001 CEMSIG was qualified as Research Centre of Excellence by the National University Research Council (CNCSIS). In 2006 CEMSIG was again qualified as Research Centre of Excellence.

CEMSIG has earned its name on a national and international plan by participating in various research projects, where tests of a similitude to the ones made for this thesis were performed, on samples and similar models, only made from common steels: S235 and S355.

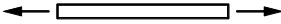
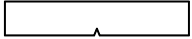

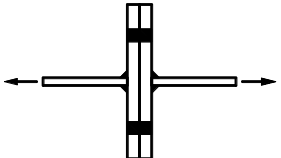
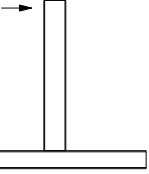
Test type	Scheme and steel grades	Test characteristics	No. of specimens	
			Per type	Total
<b>Materials (MAT): Base and weld</b>	 S235 S460 S690	monoton quasi-static tensile tests	3	42
	 S235 S460 S690	Charpy V-notch toughness tests (-20°C)	3	42
<b>Welded connections (SUD)</b>	 web and stiffeners: S235, t = 15 mm  end-plate: S235, t = 20 mm S460, t = 15 mm S690, t = 12 mm	<b>weld type:</b> - fillet weld - 1/2V bevel weld without root rewelding - 1/2V bevel weld with root rewelding - K bevel weld  <b>type of loading:</b> - monotone quasi-static loading - cyclic quasi-static loading	3	72
<b>T-stub specimens (STUB)</b>	 web and stiffeners: S235, t = 15 mm  end-plate: S235, t = 12, 20 mm S460, t = 10, 15 mm S690, t = 8, 12 mm	<b>* type of welding:</b> - from welded plates with K bevel weld  <b>* type of loading:</b> - monotonic quasi-static loading - cyclic quasi-static loading  <b>* type of end plate thickness of end plate corresponding to:</b> - end-plate failure - mixed failure mode  <b>* type of T-stub stiffening:</b> - T-stub with no stiffeners - T-stub with one stiffener - T-stub with two stiffeners	3	108
<b>Beam to Column specimens</b>		<b>* type of connection</b> - welded connection - bolted connection  <b>* type of loading</b> - monotone quasi-static loading - cyclic quasi-static loading	1	18

Table 5.1 – Summary of testing program



### 5.3 Experimental platform

Tensile testing on materials, welded connections, T-stub, and on nodes were made in the Structures Laboratory in the CMMC Department – building A (Fig. 5.1).



Fig. 5.1 - Structures Laboratory in the CMMC Department – building A.

For the tests on materials and welding detail in cyclic manner, the universal device UTS RSA 250, at CEMSIG, equipped with hydraulic fixing devices and a numerical command and acquisition system (Fig. 5.2).



Fig. 5.2 - Universal trial device UTS/ZWICK with a capacity of 250 kN and hydraulic fixing

For tests on welded connections, T-stub specimens and Beam to Column specimens the trial frame was used (Fig. 5.3) equipped with dynamic Quiri actuator of 1000kN and 500kN with numerical command, control and data, acquisition

system also existing. This is the only equipment of this type in Romania, having dynamic actuators, which can be manoeuvred in force and displacement control. For the cyclic tests there were taken into account the ECCS procedure (European Convention of Steel Structures), using two loading protocols (static and dynamic).

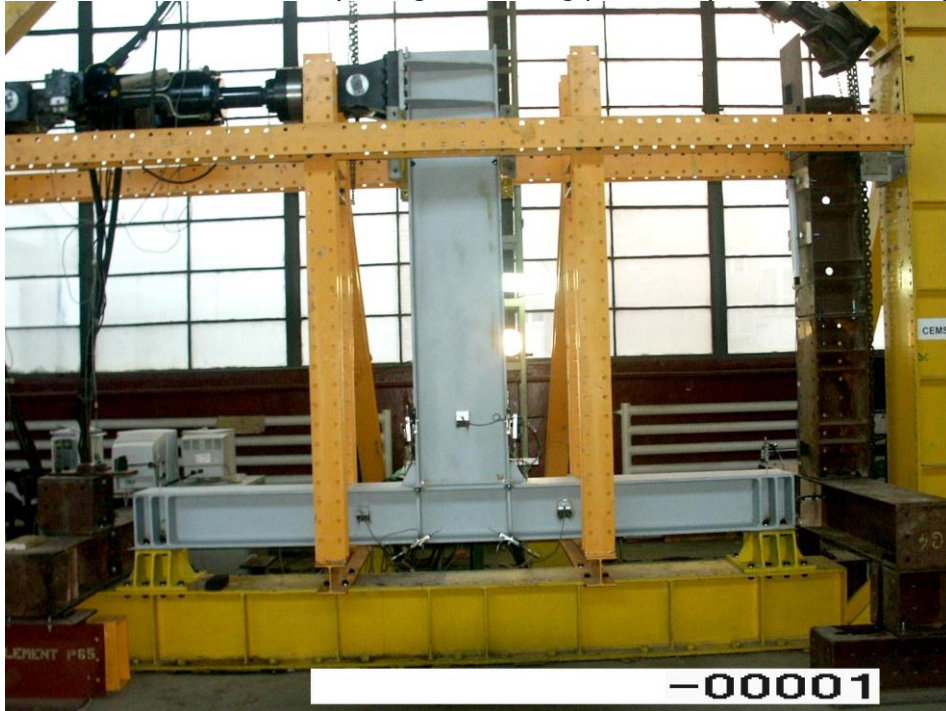


Fig. 5.3 - Experimental stand for connection tests

Special attention was given to the selection of measuring devices and techniques so that the results could be compared to numerical simulations.

In the laboratory tests three types of gauges:

- displacement transducers
- force gauges
- optical system Vic3D that can measure displacements as well as deformations (Fig. 5.4);



Fig. 5.4 - Digital Image Correlation system – LIMESS Vic 3D

All data have been recorded by an external HP3852A Data Acquisition and control unit system.

The experimental program contains:

- 2 sets of material tests (a tension monotone quasi-static trial and a toughness test);
- 1 set of tests for welded connections;
- 1 set of tests for T-stub specimens;
- 1 set of tests for sub-assemblies (frame node type);

The type of steel used:

- S235 ( $f_y = 235\text{N/mm}^2$ ,  $f_u = 360\text{N/mm}^2$ ),
- S460 ( $f_y = 460\text{N/mm}^2$ ,  $f_u = 550\text{N/mm}^2$ )
- S690 ( $f_y = 690\text{N/mm}^2$ ,  $f_u = 770\text{N/mm}^2$ ).

## 5.4 METHODOLOGY OF EXPERIMENTAL WORK

### 5.4.1 Tensile tests on material

The steel plates were made by Czech producer UNIOCEL. The marketing name of the used steel it is DOMEX 460 MC D respectively ALDUR 700 QL which fulfils requirements of S460QL, S690 QL according to EN 10025-6 (CEN, 2004b). The dimensions of the plates were  $b/l/t = 300/700/8,10,12,15,20$  mm.

**Tensile testing on materials** were done accordingly to SR EN 10002-1(1990) and they serve in determination of the physical and mechanical characteristics of the metals. The test consist of slowly, continuously and progressively applying a tensile force without shocks, until the break, on the longitudinal axis of the sample, in order to determine the following mechanical characteristics: yielding limit, tensile strength, elongation and necking. Proportional test pieces from each plate were extracted from the plates according to EN ISO377 (CEN, 1997b). During this phase was tested a number of 3 specimens for each type of steel grade (S235, S460, S690), a number of 3 specimens for each type of material thickness (8mm, 10mm, 12mm, 15mm, 20mm). Total number of specimens tested it was 42 pieces.

The standard tensile tests were performed in longitudinal direction of rolling, using testing machine UTS/ZWICK 250kN The displacements were measured on a defined original gauge length  $L_0$  by external sensor arm extensometers. The speed of the test was defined by the displacement of the extensometers. The prescribed displacement rate it was 1.5mm/min. Force and displacement was recorded every 0.01 seconds. Table 5.2 shows the measured average values of yield stress  $f_y$ , tensile strength  $f_u$  and elongation at rupture A. It has to be recognizes that the value of elongation for S460 is surprisingly large. The engineering stress-strain curves are shown in Fig. 5.5

Nominal steel grade	$f_y$ , N/mm <sup>2</sup>	$f_u$ , N/mm <sup>2</sup>	A, %	Actual steel grade
S235	266	414	38	S235
S460	458	545	25	S460
S690	831	859	13	S690

Table 5.2 – Average material characteristics

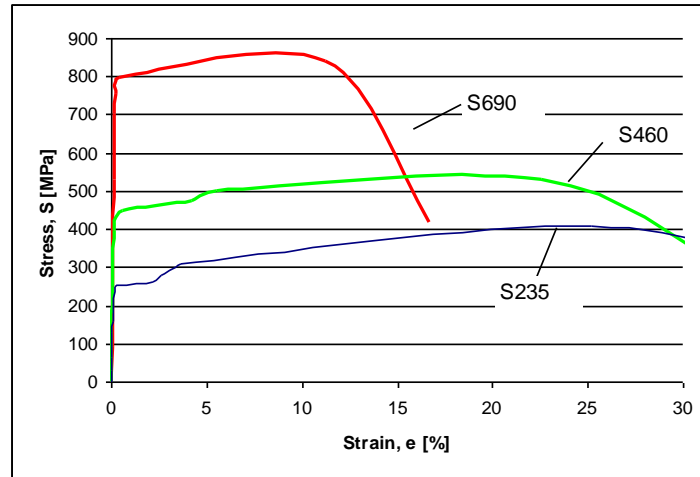


Fig. 5.5 - Stress-strain diagrams of standard tensile tests

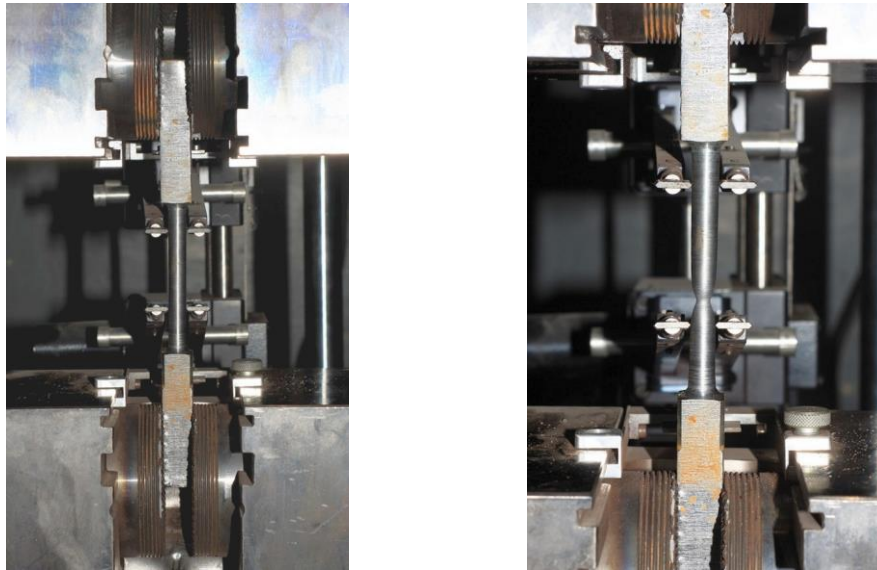


Fig. 5.6 - Tensile test on materials

Bolts were tested in tension as well, showing an average ultimate strength of 862.6 N/mm<sup>2</sup> for M20 bolts and an average ultimate strength of 1182.8 N/mm<sup>2</sup> for M22 bolts. The failure mode of the bolts was either by failure of the screw or failure of the nut filet, as it can be seen in Fig. 5.9 and Fig. 5.10.

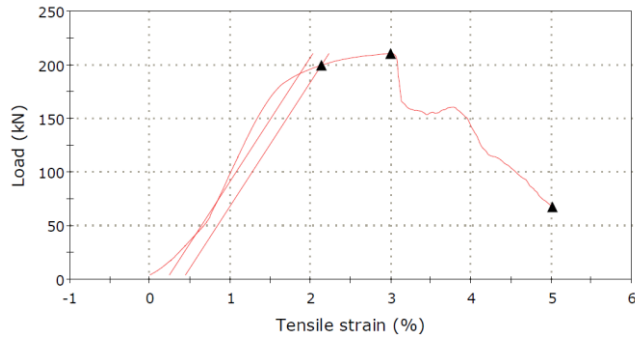


Fig. 5.7 – Load vs. Tensile Strength on M20 bolts

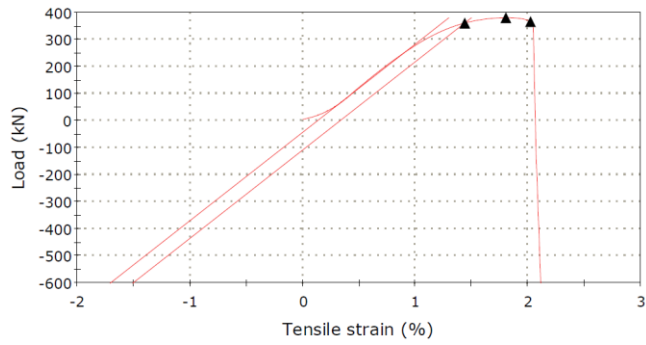


Fig. 5.8 – Load vs. Tensile Strength on M22 bolts



Fig. 5.9 – Failure mode for M20 bolts



Fig. 5.10 – Failure mode for M22 bolts



### 5.4.2 Charpy V-notch toughness tests

**Toughness test** has the purpose of determining toughness of metals, respectively the capacity of holding mechanical work. The tests were done at  $-20^{\circ}\text{C}$  (with the help of the equipment that has a temperature chamber), and it consist of failure due to a single blow with a pendulum hammer of a sample with a V notch in the middle, placed freely on two supports. For each type of steel and for every material thickness three tests were done, resulting a total number of 36 tests.

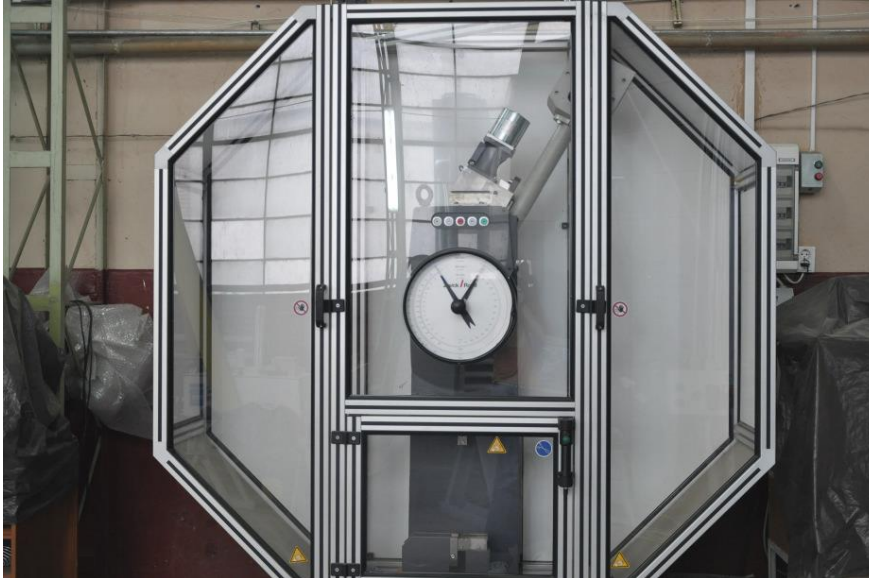


Fig. 5.11 – Metal Charpy Pendulum Impact Tester

In order to determine the real values of the mechanical characteristics of the samples tested, the principal of determination of the failure energy on two perpendicular directions was adopted.

For the checking of the influences of the thermal processes at welding on the base metal at intersection with the welding bending shock tests were done on KV samples with notch in the near area of the intersection (crossing zone).

The samples with welds were obtained from the same material samples, with a unique welding technology for a butt welding with V and X shaped joints. The sampling plans contain the marks of all samples and plates used for the welded connections. These are identified by the marks:

- mark 1 (200 x 300 x 10 mm) –steel S690QL;
- mark 2 (135 x 300 x 12 mm) – steel S460QL;
- mark 3 (135 x 165 x 15 mm) – steel S235JO.

The plate with mark 3 did not have enough size to do the Charpy V notch test on transversal direction and at ambient temperature. So, the obtained result will refer only to the testing temperature -  $-20^{\circ}\text{C}$  for steel S235JO.

The results for the Charpy V notch test made on the base material as well as on the thermally influence zone (ZIT) on two directions and at two temperatures ( $+20^{\circ}\text{C}$  and  $-20^{\circ}\text{C}$ ) are presented in Table 5.3.

Sample	Sample mark	Failure energy, KV [J]		
		MB Ia +20°C	MB Ia -20°C	ZIT Ia - 20°C
1	34		156	
	35		157	
	36		145	
	31	148		
	32	149		
	33	140		
	28		142	
	29		110	
	30		140	
	37	156		
	38	175		
	39	159		
	11			165
	12			159
13			158	
2	2	252		
	4	190		
	6	199		
	12	144		
	15	246		
	18	185		
	1		149	
	3		210	
	5		197	
	11		128	
	14		179	
	17		226	
	21			182
	22			90
23			184	
3	01		14	
	20		15	
	21		26	
	22		10	
	24		64	
	26		12	
	23	99		
	25	104		
	27	126		
	31			80
	32			121
	33			97

Table 5.3 - Charpy V notch test

The Charpy V notch test on the base material at a temperature of - 20°C has shown that differences between the two directions of assay meaning:

- For smaller values the rolling direction is identified;

- For bigger values the transversal direction of the plate is identified

The toughness of the steel grades quenched and reheated (S460QL, S690QL) is ensured at a temperature of - 20°C, meanwhile the steel S235JO was checked only at the temperature of 0°C, with a minimum accepted value of 27 J. Considering that in the thermally influenced zone when welding this steel with the experimental technological parameters has the toughness high at - 20°C (average of 99 J, minimum of 80 J), the compatibility at welding is ensure, even if the base material is checked only for temperatures until reaching 0°C.

This way we can consider that the experimental material has acceptable characteristics from the point of view of weldability.

### 5.4.3 Welded specimen tests

#### 5.4.3.1. Welded specimens test set-up

The tests on welded connections study the behaviour of the welds between the web of the beam and the end plate (or the flange of the column). The experimental specimen is the one presented in Fig. 5.12.

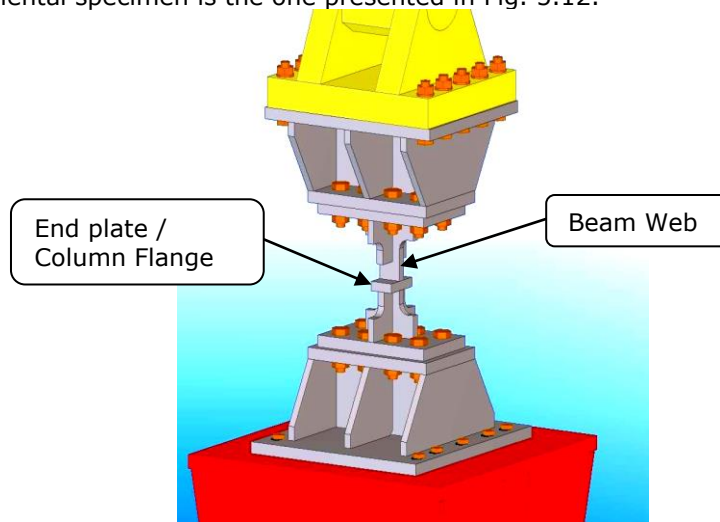


Fig. 5.12 – Welded specimen

The type of material used for the welded connections as well as its thickness is presented in Table 5.4.

Web of Beam & Stiffeners		End Plate or Column Flange	
Grade	Thickness [mm]	Grade	Thickness [mm]
S235	15	S235	20
		S460	15
		S690	12

Table 5.4 – welded connections – type of material

In preparing the specimens 4 types of welds were used as follows:



- **Fillet welds** – the type of weld most commonly used, it doesn't require special treatment of the elements, it can be done in the plants as well as on site, it's the fastest and cheapest type of weld. Fillet welds are difficult to realize in such a manner that they would possess an overstrength from the base material.
- **1/2V bevel weld without root rewelding** – this is the type of weld that requires a preparation on one side of the material that will be welded. It has an economical advantage as the preparation and weld is made on one side, but this reduces the resistance of the weld (example STAS 10108-0/78 reduces the strength of the weld with 0.7 due to possible cracks in the root of the weld). This is really easy to do on site due to the possibility of welding on one side.
- **1/2V bevel weld with root rewelding** this is the type of weld that require a preparation on one side of the material that will be welded. The weld will be executed on both sides, in this manner obtaining a weld with a resistance equal to the one of the base material. The disadvantage of this method consists of the execution of the weld on both sides.
- **K bevel weld** – this is a type of weld of very good quality, that requires the preparation of the element that will be welded, on both sides, the root is welded again. Due to these aspects the possible cracks are at the root of the weld are eliminated. It is possible to ensure an overstrength of the weld from the base material.

For each combination (beam web S235 – end plate S235, S460, S690) three specimens were made times four types of welds. In the end it resulted a number of 72 specimens.

Loading speed of the specimens was of two types, monotone quasi-static and cyclic quasi-static. The cyclic loading has as goal the study of the behaviour of the connections in case of a seismic loading. As a consequence, all the specimens will be tested monotone as well as cyclic.

The experimental assembling used for the testing on the welded specimens can be observed in Appendix B. In the laboratory tests for this type of testing 3 types of gauges were used:

- 3 displacement transducers (Fig. 5.14)
- force gauge
- optical system Vic3D that measures displacements as well as deformations (Fig. 5.4);

The label used for the welded specimens corresponds to the description from Table 5.5.

End Plate Grade	Weld Type	Loading type specimen no.
<b>460FW_M3</b>		
<b>S460</b>	<b>Fillet Weld</b>	<b>Monotone quasi-static specimen no.3</b>

Table 5.5 – Welded specimen legend

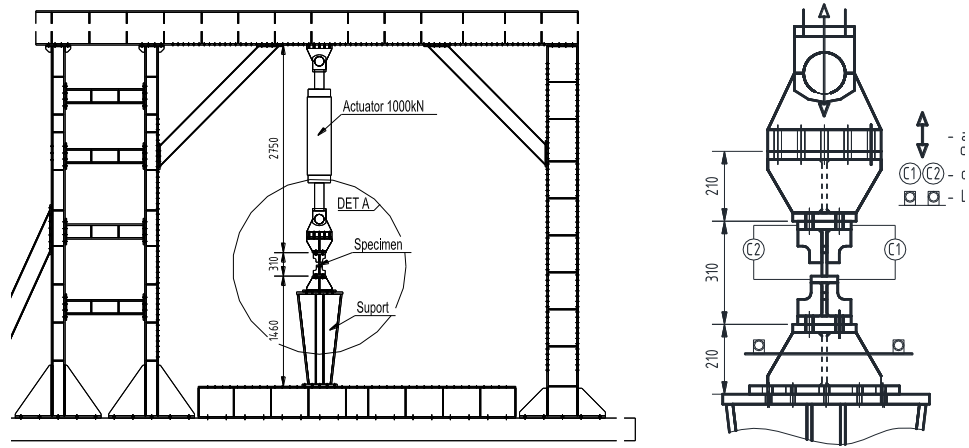


Fig. 5.13 – Welded connections – experimental platform

where :




 Actuator moving direction  
 Displacement transducers  
 Limess Vic-3D – optic measurement device



Fig. 5.14 – Welded specimen equipped with measuring devices

The welded specimens, named "460FW\_M3" were cut by mechanical saw from specimens type SBx.x according to drawings in Appendix B, in this way obtaining a total number of 72 welded specimens.

The specimens of type SB (from 1.1 to 1.4; from 2.1 to 2.4 and from 3.1 to 3.4) are composed of three elements: P183, P184 as webs and P125 as flange of the connection;

**Specimen SB.1.1** is characterized by the flange element P125 made of steel S690 and web element P183 and P184 made of steel S235JO. The flange elements P125 has the thickness of 12 mm, and the webs have the thickness of 15 mm. The welded connection is in cross, formed by four fillet welds, unpenetrated that have the thickness of  $a = 8$  mm.

The dimensions of the web are:

- P183 of 140 x 850 x 15 mm;
- P184 of 100 x 850 x 15 mm;

The dimensions of the flanges are:

- 81 x 850 x 12 mm.

**Specimen SB.1.2** is different from the SB.1.1 by the fact that the welded connection in cross if formed by four welds completely penetrated and the preparation of the elements to be connected (edges of the webs) is in  $\frac{1}{2}$  V, the welds being executed on one side, without root support, multi-layered (ss nb ml). (According to norm SREN 287-1, ss=weld on one side, nb = without root support, ml.= multi-layered).

**Specimen SB 1.3** is similar to the sample SB.1.2 with the difference that the welds are executed with the rewelding of the root (bs gg ml). (According to standard SREN 287-1, bs = welded on both sides, gg = polishing the root, ml = multi-layer).

**Specimen SB 1.4** is similar to sample SB 1.3 with the difference that the welds are executed on both sides with the preparations of the borders in K (bs ml). (According to Standard SREN 287-1, bs = welded on both sides, ml = multi-layer).

**Specimen SB.2.1** is characterized by the flange elements P126 of steel S460 and the web elements P183 and P184 of steel S235JO. The flange element P126 has the thickness of 15 mm, and the webs have the thickness of 15mm. The welded connection is in cross formed by four fillet welds unpenetrated with the thickness of  $a = 10$ mm.

The dimensions of the web are, for:

- P183 of 140 x 850 x 15 mm;
- P184 of 100 x 850 x 15 mm;

The dimensions of the flange are:

- 81 x 850 x 15 mm.

**Specimen SB.2.2** is different from the SB 2.1 by the fact that the welded connection in cross is formed by four welds completely penetrated, and the preparation of the connecting elements (web edges) is in  $\frac{1}{2}$  V, the welds being done from one side, without root support, multi-layer (ss nb ml). (According to norm SREN 287-1, ss=weld on one side, nb = without root support, ml.= multi-layered).

**Specimen SB 2.3** is similar to SB.2.2 with the difference that the welds are executed with the rewelding at the root (bs gg ml). (According to standard SREN 287-1, bs = welded on both sides, gg = polishing the root, ml = multi-layer).

**Specimen SB.2.4** is similar to specimen SB.2.3 with the difference that the welds are executed on both sides and the edges are prepared in K (bs ml). (According to Standard SREN 287-1, bs = welded on both sides, ml = multi-layer).

**Specimen SB.3.1** is characterized by the flange element P3 of steel S235JO and the web elements P183 and P184 of steel S235JO. The flange element P3 has a thickness of 20 mm, and the webs have a thickness of 15 mm. The welded connection is in cross, formed by four fillet welds unpenetrated that have the thickness of  $a = 10\text{mm}$ .

The dimensions of the web are, for:

- P183 of 140 x 850 x 15 mm;
- P184 of 100 x 850 x 15 mm;

The dimensions of the flange are:

- 81 x 850 x 20 mm.

**Specimen SB.3.2** is different from specimen SB.3.1 by the fact that the welded connection in cross is formed by four welds completely penetrated, and the preparation of the pieces to be connected (edges of webs) is in  $\frac{1}{2} V$ , the welds being executed on one side, without supporting the root, multi-layered (ss nb ml). ). (According to norm SREN 287-1, ss=weld on one side, nb = without root support, ml.= multi-layered).

**Sample SB.3.4** is similar to sample SB.33 with the difference that the welds are executed from both sides with the preparation of the edges in K (bs ml). According to Standard SREN 287-1, bs = welded on both sides, ml = multi-layer).

Referring to the welded specimens (F, V, VR and K) it is once more mentioned that these are subassemblies made from samples taken from the SB specimens, with dimensions presented in Appendix B. To these specimens plates and welded ribs are added in order to adapt them to the actuator in CMMC.

The plate elements P105, have the dimensions of 160 x 265 x 25 mm, are provided with 8 holes  $\varnothing 20$ , according to the drawings in the Appendix. These are welded to the ends of the samples with fillet welds, unpenetrated, with the thickness of  $a = 6\text{mm}$ . The ribs P44 and P45 with the thickness of 15 mm, and the dimensions presented in the drawings in the Appendix, are welded to the webs of the sample with fillet welds, unpenetrated with the thickness of  $a = 6\text{ mm}$ , and on the flange is welded only the rib P44, with welds on both sides in K completely penetrated.

MAG welding was used, with G3Si1 (EN 440) electrodes for S235 to S235 welds, and ER 100S-G/AWS A5.28 (LNM Moniva) for S235 to S460 and S690 welds.

Weld preparation and the technology for  $\frac{1}{2} V$  bevel weld, for instance, is shown in Fig. 5.15.

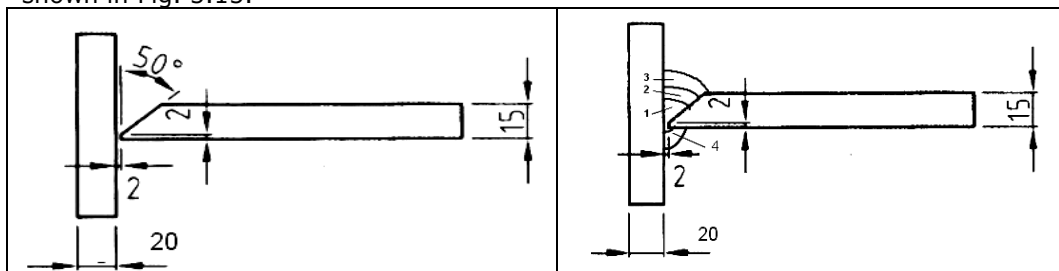


Fig. 5.15 – Welding technology for  $\frac{1}{2} V$  bevel weld

The actual and nominal geometry of specimens is presented in Table 5.6 to Table 5.16.

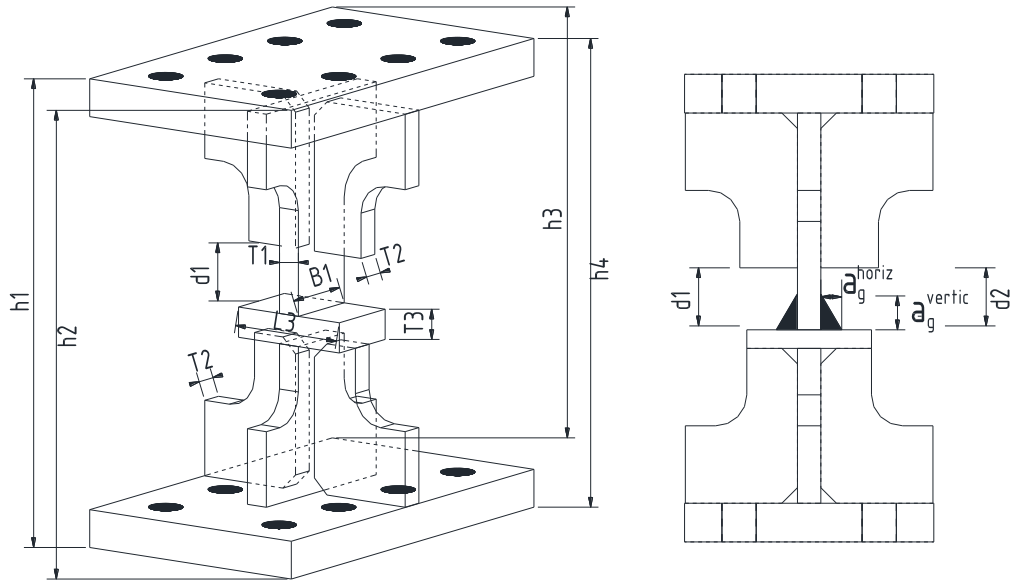


Fig. 5.16 – Welded specimens - nominal geometry

Specimen	235FW_M1	235FW_M2	235FW_M3	235FW_C1	235FW_C2	235FW_C3
T1	14.90	14.90	14.90	15.00	15.10	14.90
B1	50.10	50.10	50.10	50.10	50.00	49.80
T2	15.00	15.00	15.00	15.00	15.00	15.18
T3	20.70	20.70	20.70	20.00	20.00	20.30
L3	81.90	81.90	81.90	81.90	82.30	82.20
h1	303.60	304.20	304.80	299.00	306.60	299.40
h2	306.40	306.20	306.80	304.20	301.40	304.80
h3	300.10	300.70	301.40	301.70	306.00	305.00
h4	303.60	303.60	303.60	309.50	300.70	299.50
d1	37.80	37.80	37.80	36.70	39.20	34.50
d2	37.40	36.40	36.40	39.80	35.00	38.90
Agv	12.50	12.70	12.70	11.90	11.00	10.00
Agh	11.60	11.30	11.30	13.10	12.00	12.00
Agv	10.40	10.60	10.30	13.30	11.00	12.00
Agh	12.20	12.20	12.20	11.90	12.00	12.00
Agv	10.50	10.00	9.80	9.70	11.00	9.50
Agh	12.40	11.90	11.80	13.20	10.00	12.00
Agv	11.00	10.60	10.60	12.30	11.00	12.00
Agh	10.80	11.20	11.20	9.50	11.00	12.50

Table 5.6 – Welded specimen 235FW – nominal geometry

Specimen	235KW_M1	235KW_M2	235KW_M3	235KW_C1	235KW_C2	235KW_C3
T1	15.00	15.10	15.00	15.10	15.10	15.40
B1	50.00	49.95	49.70	50.10	49.80	49.90
T2	15.00	15.00	15.70	15.20	15.50	15.40
T3	20.00	20.20	20.50	20.50	20.50	20.70
L3	82.00	82.25	82.20	82.20	82.20	82.30
h1	311.40	310.60	302.80	307.40	311.20	305.90
h2	298.30	300.10	306.30	300.50	304.20	307.00
h3	313.70	310.60	305.20	311.10	309.60	303.70
h4	299.50	299.90	308.60	304.40	302.00	305.20
d1	42.10	39.60	36.90	39.10	40.60	38.60
d2	35.20	37.29	38.10	36.40	37.50	36.80
Agv	14.40	14.70	16.00	11.50	18.00	15.50
Agh	10.20	12.20	12.00	13.00	11.50	12.50
Agv	11.60	11.20	12.00	11.00	12.00	11.50
Agh	17.50	15.70	18.00	17.50	15.50	17.00
Agv	15.00	11.80	17.00	16.00	16.00	15.50
Agh	10.00	15.10	12.00	12.50	12.50	13.00
Agv	10.30	15.20	10.50	10.00	12.00	11.50
Agh	18.20	10.40	18.00	17.50	16.00	17.00

Table 5.7 – Welded specimen 235KW – nominal geometry

Specimen	235VW-M1	235VW-M2	236VW-M3	235VW-C1	235VW-C2	235VW-C3
T1	15.00	15.00	15.40	15.00	15.10	15.10
B1	50.00	50.00	49.60	50.50	50.00	56.40
T2	15.70	15.40	15.00	15.00	16.00	15.10
T3	20.60	20.40	20.50	20.90	20.00	20.00
L3	83.70	82.20	82.90	82.60	82.10	82.30
h1	308.20	313.50	311.50	313.50	309.20	307.70
h2	315.20	307.50	308.50	309.20	306.00	312.50
h3	309.60	313.60	313.40	312.00	310.00	3.8.5
h4	316.50	307.60	310.00	307.40	311.70	39.20
d1	41.00	40.50	40.00	40.40	42.00	40.00
d2	39.60	40.60	38.00	39.00	36.10	40.00
Agv	17.00	14.15	15.05	15.25	15.5	16.16
Agh	14.50	11.85	12.2	12.25	12.9	12.59
Agv	11.7	14.80	15.60	16.00	11.55	15.50
Agh	15.8	14.50	15.70	14.50	16.45	13.40
Agv	13.325	14.95	15.2	16.1	21.00	14.94
Agh	18.00	12.4	13.03	12.5	9.90	13.98
Agv	14.00	16.00	16.40	15.30	11.88	22.00
Agh		17.00	16.00	15.50	12.63	11.70

Table 5.8 – Welded specimen 235VW – nominal geometry

Specimen	235VRW_M 1	235VRW_M 2	235VRW_M 3	235VRW_C 1	235VRW_C 2	235VRW_C 3
T1	15.00	15.00	14.96	14.84	15.00	15.10
B1	50.30	50.60	49.14	51.30	49.90	49.80
T2	15.00	15.10	14.80	14.92	14.90	15.40
T3	19.90	19.50	20.00	20.20	19.90	19.90
L3	84.50	85.00	84.76	84.80	84.50	84.80
h1	305.20	308.50	311.40	308.80	311.20	311.40
h2	308.30	311.30	308.50	312.50	309.70	310.50
h3	308.30	307.70	311.00	306.80	312.00	310.50
h4	316.20	310.50	308.00	310.90	310.50	309.60
d1	39.60	37.80	42.90	37.80	44.00	43.90
d2	43.90	42.60	36.20	40.50	40.00	39.30
Agv	6.40	17.60	6.50	17.70	6.60	6.40
Agh	4.00	12.50	5.00	12.90	6.60	4.12
Agv	18.40	6.00	19.80	6.00	19.20	17.50
Agh	12.40	4.00	11.20	4.00	9.52	10.70
Agv	6.60	18.90	5.00	19.00	5.50	6.80
Agh	3.90	12.00	4.10	10.50	5.10	4.50
Agv	18.40	6.00	18.10	5.00	20.10	19.20
Agh	12.00	3.50	12.40	4.40	11.30	22.30

Table 5.9 – Welded specimen 235VRW – nominal geometry

Specimen	460FW_M1	460FW_M2	460FW_M3	460FW_C1	460FW_C2	460FW_C3
T1	15.00	15.00	14.80	14.90	15.00	15.10
B1	50.50	50.30	49.80	51.10	50.00	49.20
T2	15.00	15.00	14.80	15.00	15.10	15.10
T3	16.20	16.20	16.40	16.30	16.20	16.30
L3	79.30	79.60	79.20	79.10	79.10	79.20
h1	302.00	303.50	303.20	299.60	306.10	302.80
h2	301.00	306.40	299.90	305.30	307.60	305.00
h3	304.00	300.00	301.80	298.90	308.00	304.00
h4	302.50	303.00	302.00	305.20	306.80	301.40
d1	34.20	38.50	41.50	36.30	42.70	38.00
d2	41.40	40.80	36.50	41.50	43.70	40.60
Agv	12.00	12.30	10.10	12.90	15.70	13.30
Agh	13.00	11.50	12.40	10.90	11.20	14.30
Agv	11.30	11.20	11.00	11.90	13.30	12.80
Agh	11.20	12.40	9.40	11.10	8.10	12.80
Agv	12.50	12.60	10.50	12.00	15.30	13.40
Agh	13.00	13.30	11.60	11.90	10.00	12.20
Agv	11.20	12.40	11.50	9.20	12.70	9.80
Agh	11.10	12.70	10.40	11.30	10.50	12.50

Table 5.10 – Welded specimen 460FW – nominal geometry

Specimen	460KW_M1	460KW_M2	460KW_M3	460KW_C1	460KW_C2	460KW_C3
T1	14.90	15.00	15.0	15.50	15.1	15.1
B1	51.00	50.80	50.7	49.70	50.6	50.4
T2	15.00	15.00	15.0	15.00	15.0	15.0
T3	16.30	16.40	16.3	16.30	16.3	16.3
L3	79.50	79.30	79.5	79.70	79.5	79.5
h1	305.00	307.40	305.3	307.60	306.3	306.7
h2	308.30	308.70	307.8	308.60	308.4	308.4
h3	305.00	306.00	303.7	306.00	305.2	305.2
h4	309.00	308.50	306.8	307.50	308.0	307.7
d1	39.00	41.50	39.7	40.00	40.0	40.3
d2	44.50	42.70	42.7	44.00	43.5	43.2
Agv	14.20	13.80	13.4	13.00	13.6	13.5
Agh	9.50	9.60	10.2	11.40	10.2	10.3
Agv	14.80	14.90	13.6	13.50	14.2	14.1
Agh	10.10	8.50	10.3	9.20	9.5	9.4
Agv	13.80	13.40	13.3	13.10	13.4	13.3
Agh	10.30	11.60	11.7	11.50	11.3	11.5
Agv	15.00	13.00	13.5	12.00	13.4	13.0
Agh	9.50	8.40	10.2	7.70	9.0	8.8

Table 5.11 – Welded specimen 460KW – nominal geometry

Specimen	460VW-M1	460VW-M2	460VW-M3	460VW-C1	460VW-C2	460VW-C3
T1	15.40	15.40	15.3	15.40	15.50	15.4
B1	50.50	50.50	50.5	50.50	50.30	50.5
T2	15.00	15.50	15.1	15.00	15.00	15.2
T3	16.40	16.20	16.3	16.30	16.30	16.3
L3	79.60	80.00	79.6	79.80	80.00	79.8
h1	309.30	312.50	308.7	312.00	310.6	310.6
h2	314.50	309.00	310.1	309.50	310.8	310.8
h3	307.00	309.00	306.6	310.00	308.1	308.1
h4	312.50	306.00	308.5	307.50	308.6	308.6
d1	44.00	42.70	41.8	42.60	43.70	42.8
d2	44.50	41.00	43.0	43.50	42.70	43.0
Agv	17.00	16	15.0	16	15	16.0
Agh	6.00	7	8.4	8	4.00	7.3
Agv	13.7	14.2	14.0	14.0	14.0	14.0
Agh	10.6	10.0	9.9	10.0	10.1	10.1
Agv	15.00	16	14.4	16.5	14.00	15.5
Agh	17.00	8	12.0	9	6.00	11.5
Agv	12.0	13.3	12.9	12.8	12.8	12.8
Agh	10.1	9.5	9.3	9.4	9.6	9.6

Table 5.12 – Welded specimen 460VW – nominal geometry



Specimen	690FW-M1	690FW-M2	690FW-M3	690FW-C1	690FW-C2	690FW-C3
T1	15.00	15.10	15.10	14.90	15.10	15.20
B1	50.00	49.90	50.30	49.7	50.30	50.30
T2	15.00	15.10	15.60	15.10	15.00	14.90
T3	12.10	12.10	12.70	12.10	12.10	12.10
L3	79.70	79.60	80.80	79.80	79.80	79.80
h1	295.70	293.30	293.30	295.80	296.00	298.00
h2	295.30	296.30	296.20	296.50	291.80	297.00
h3	296.50	297.80	294.30	294.00	298.20	295.50
h4	295.50	300.60	296.00	295.00	2943.00	294.50
d1	36.30	37.50	37.30	39.00	36.40	38.20
d2	36.00	36.90	35.30	40.10	36.60	33.30
Agv	11.60	12.60	13.20	12.90	10.80	12.30
Agh	14.30	14.50	11.00	13.40	15.00	13.60
Agv	13.80		11.60	11.20	13.00	12.00
Agh	11.00		13.40	14.80	11.40	14.00
Agv	10.20	12.50	12.30	13.00	10.00	11.20
Agh	14.00	14.00	14.50	14.50	15.80	13.10
Agv	13.40	11.90	11.50	11.00	12.10	12.40
Agh	11.60	13.70	14.50	14.30	13.00	14.40

Table 5.13 – Welded specimen 690FW – nominal geometry

Specimen	690KW-M1	690KW-M2	690KW-M3	690KW-C1	690KW-C2	690KW-C3
T1	15.0	15.20	15.1	15.00	15.1	15.1
B1	50.0	50.90	50.1	50.20	50.3	50.3
T2	15.2	15.00	15.2	15.10	15.0	15.1
T3	12.2	12.20	12.2	12.20	12.2	12.2
L3	79.9	80.00	80.0	79.80	79.9	79.9
h1	294.8	298.50	295.6	300.50	296.6	297.5
h2	295.2	298.00	295.3	300.00	295.5	297.1
h3	296.2	298.00	295.6	299.50	296.7	297.0
h4	826.0	299.00	930.9	298.90	1058.7	529.9
d1	37.3	38.30	37.6	39.00	37.6	38.1
d2	37.0	36.00	36.5	37.50	35.9	36.0
Agv	12.2	11.70	12.3	9.40	11.9	11.6
Agh	13.6	11.50	13.3	15.00	13.4	13.4
Agv	9.9	9.70	11.5	12.30	11.2	11.1
Agh	10.1	16.00	12.7	12.80	12.9	13.1
Agv	11.6	12.20	11.6	9.40	11.3	11.2
Agh	14.6	13.50	14.5	16.40	14.3	14.4
Agv	12.0	10.30	11.8	12.80	11.7	11.9
Agh	13.4	13.30	13.9	12.10	13.6	13.4

Table 5.14 – Welded specimen 690KW – nominal geometry

Specimen	690VW-M1	690VW-M2	690VW-M3	690VW-C1	690VW-C2	690VW-C3
T1	15.10	15.20	15.30	15.30	15.60	15.00
B1	50.10	50.40	50.00	49.70	49.80	50.00
T2	15.30	15.40	15.10	14.80	15.20	15.00
T3	12.20	12.20	12.30	12.20	12.20	12.30
L3	80.70	80.00	80.20	80.50	81.00	80.60
h1	305.80	303.40	304.10	298.00	301.40	303.40
h2	303.40	298.50	304.10	304.80	300.40	299.50
h3	302.20	301.00	300.70	298.40	302.60	303.50
h4	300.50	306.00	300.30	304.50	302.00	299.60
d1	41.80	40.20	27.20	36.70	38.50	41.00
d2	36.90	63.30	39.30	41.00	38.80	38.00
Agv	17.80	20.30	-	-	-	19.60
Agh	9.60	12.50	-	-	-	11.10
Agv			22.10	20.30	19.80	-
Agh			11.20	11.90	11.80	-
Agv	18.00	20.60	-	-	-	18.50
Agh	11.20	10.10	-	-	-	13.70
Agv			13.80	21.20	18.70	-
Agh			19.00	13.10	9.50	-

Table 5.15 – Welded specimen 690VW – nominal geometry

Specimen	690VRW-M1	690VRW-M2	690VRW-M3	690VRW-C1	690VRW-C2	690VRW-C3
T1	15.20	15.00	15.20	15.10	15.00	15.00
B1	50.20	50.40	50.20	50.20	50.10	50.40
T2	15.00	15.00	15.00	15.20	15.00	15.10
T3	12.20	12.20	12.10	12.10	12.20	12.10
L3	81.20	80.90	81.00	80.80	81.40	81.10
h1	298.10	299.50	297.00	303.30	299.50	298.40
h2	299.00	297.30	300.50	299.80	296.80	298.00
h3	299.80	299.50	299.00	302.00	300.50	298.50
h4	300.50	296.80	302.00	298.50	298.20	297.50
d1	39.00	45.90	37.40	44.60	45.50	39.80
d2	44.00	38.30	44.00	40.10	36.20	41.80
Agv	19.60	7.50	21.90	6.20	6.70	20.60
Agh	6.80	6.10	7.30	5.90	5.50	7.80
Agv	5.00	19.40	6.10	18.30	20.50	7.00
Agh	5.70	7.60	5.20	9.20	8.50	6.10
Agv	19.50	8.10	21.20	9.10	6.30	20.30
Agh	8.50	6.50	8.50	7.00	5.20	7.00
Agv	7.20	22.00	6.20	21.10	21.40	6.00
Agh	5.50	6.80	5.80	9.50	6.10	6.00

Table 5.16 – Welded specimen 690VRW – nominal geometry

**5.4.3.2. Welded specimen tests results**

In the first phase was carried out monotone quasi-static tensile tests.

The speed of the test was defined by the displacement of the actuator. The prescribed displacement rate it was 1.5mm/min. Force and displacement was recorded every 0.01 seconds.

For the welded specimens, the following parameters were determined for each experimental test: initial stiffness  $K_{ini}$ , maximum force  $F_{max}$ , yield force  $F_y$ , and ultimate deformation,  $D_y$ . The initial stiffness was obtained by fitting a linear polynomial to the force-displacement curve between 0 and 25% of the maximum force. The yield force was determined at the intersection of the initial stiffness and tangent stiffness line, where the tangent stiffness was obtained by fitting a linear polynomial to force-displacement curve between 75% and 100% of the maximum force. The ultimate deformation was determined as the displacement corresponding to a 10% drop of the maximum force.

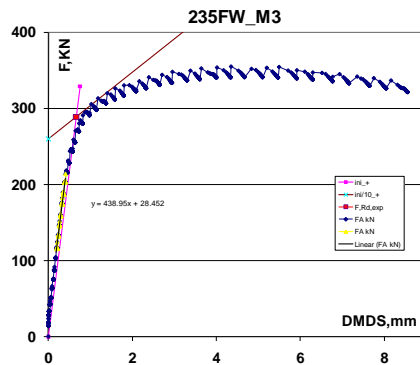


Fig. 5.17 – Experimental characteristics of welded specimens

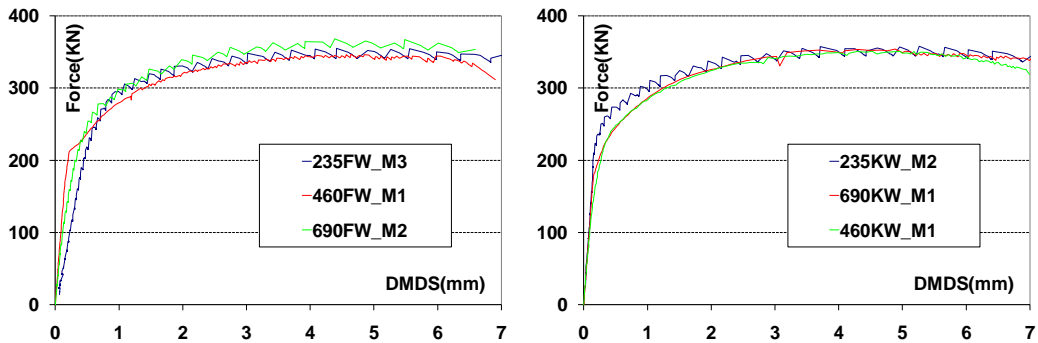


Fig. 5.18 – Load – displacement curves for FW and KW specimens

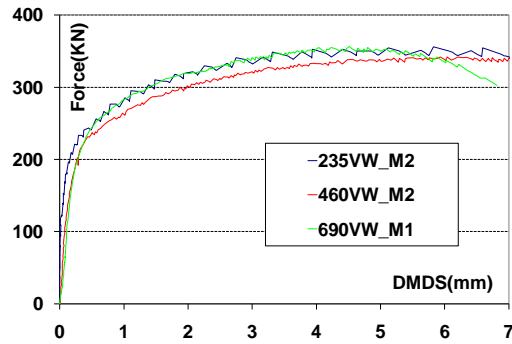


Fig. 5.19 - Load – displacement curves for VW specimens

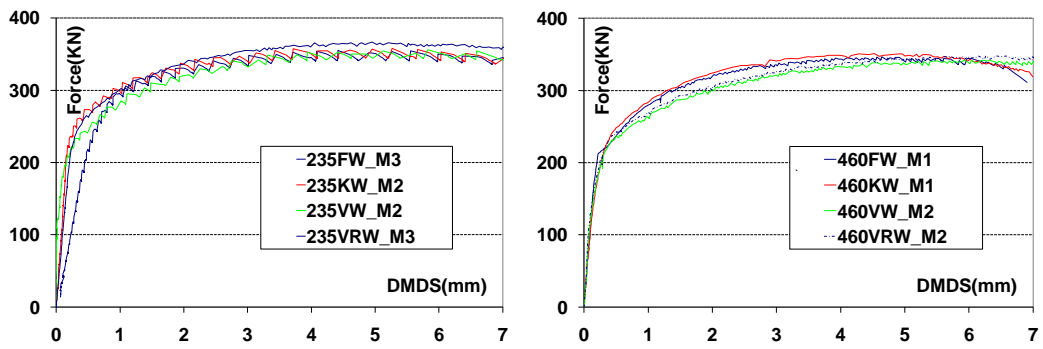


Fig. 5.20 – Load – displacement curves for S235 and S460 specimens(FW,KW,VW,VRW)

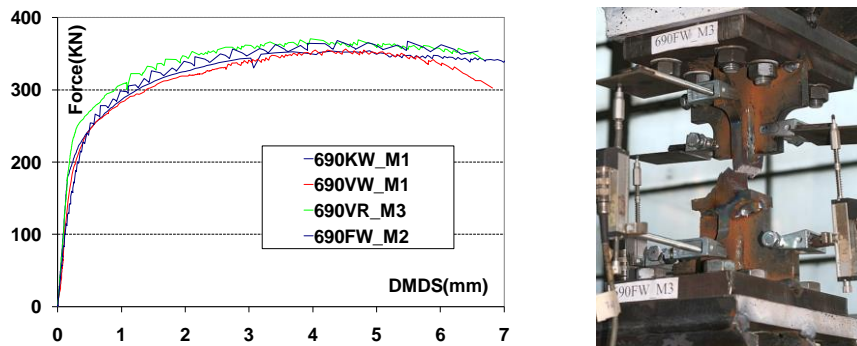


Fig. 5.21 – Load – displacement curves for S690(FW,KW,VW,VRW) specimens

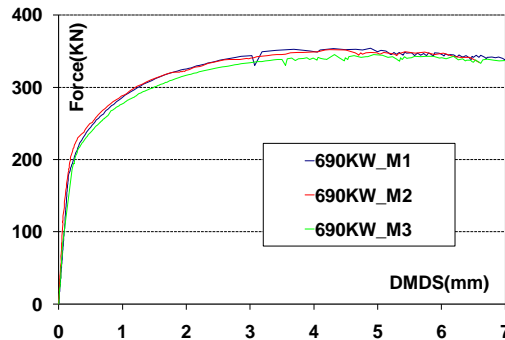


Fig. 5.22 – Load – displacement curves for S690KW\_M1,M2,M3 specimens

Having determined experimentally the *characteristics of welded specimen loaded monotone quasi-static*, it was moved on to a new step in the experimental program, tests on welded specimens *cyclic quasi-static loaded*.

The trial protocol was established in this manner:

- 1 cycle in Force control up to  $F_y/4$
- 1 cycle in Force control up to  $F_y/2$
- 1 cycle in Force control up to  $3F_y/4$
- 3 cycle in Displacement control up to  $D_y$
- 3 cycle in Displacement control up to  $6D_y$
- 3 cycle in Displacement control up to  $2D_y$
- 3 cycle in Displacement control up to  $18D_y$
- 3 cycle in Displacement control up to  $24D_y$
- 3 cycle in Displacement control up to  $30D_y$
- 3 cycle in Displacement control up to  $36D_y$
- 3 cycle in Displacement control up to  $42D_y$
- 3 cycle in Displacement control up to  $48D_y$
- 3 cycle in Displacement control up to  $54D_y$
- 3 cycle in Displacement control up to  $60D_y$
- 3 cycle in Displacement control up to  $66D_y$

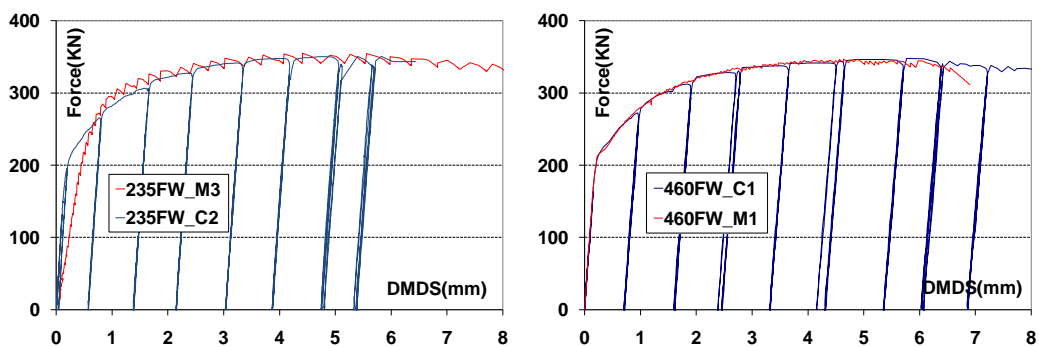


Fig. 5.23 – Load – displacement curves for S235 and S460 specimens(FW Monoton/Cyclic)

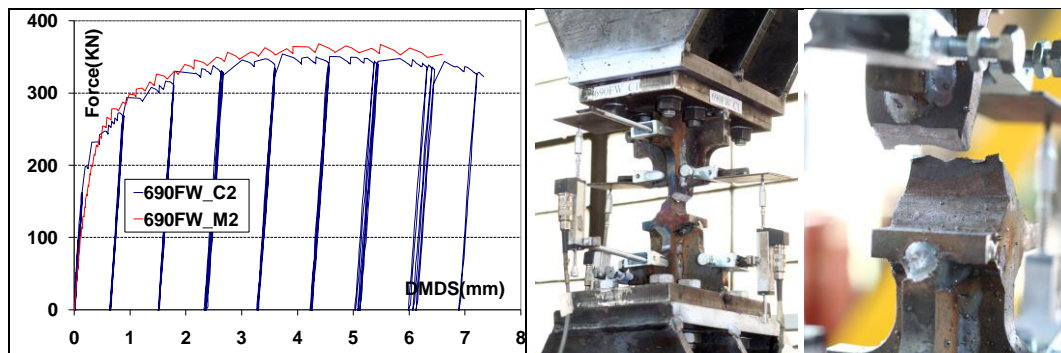
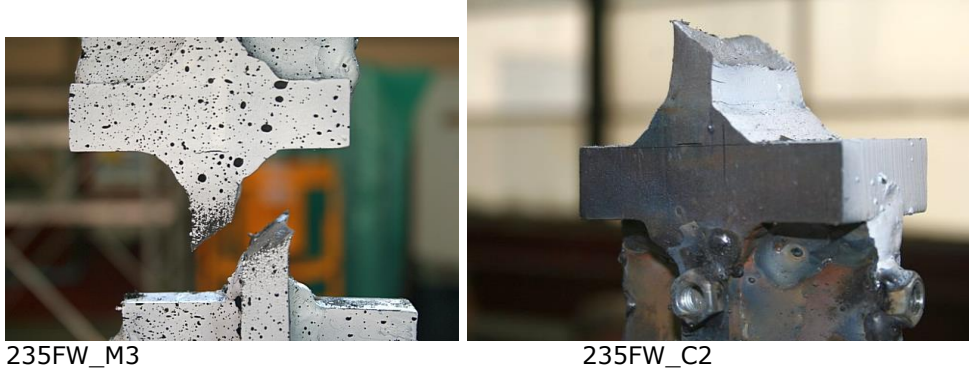


Fig. 5.24 – Load – displacement curves for S690 specimens(FW Monotone/Cyclic)

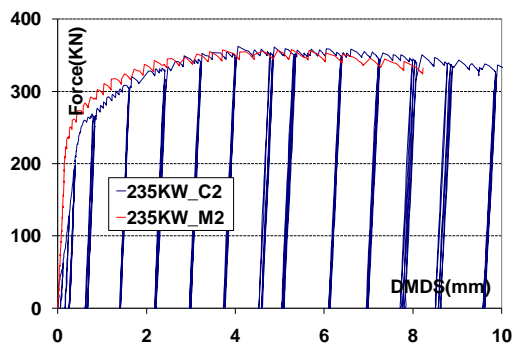
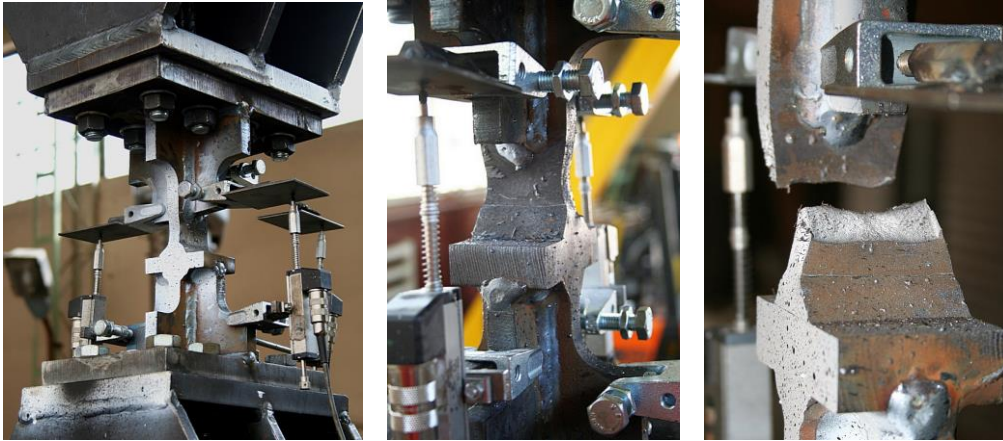


Fig. 5.25 – Load – displacement curves for S235 specimens(KW Monotone/Cyclic)



235KW\_M2

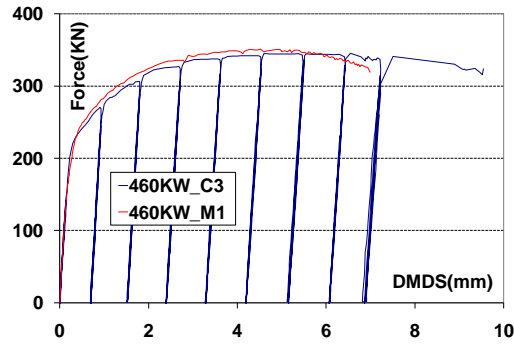


Fig. 5.26 – Load – displacement curves for S460 specimens(KW Monotone/Cyclic)

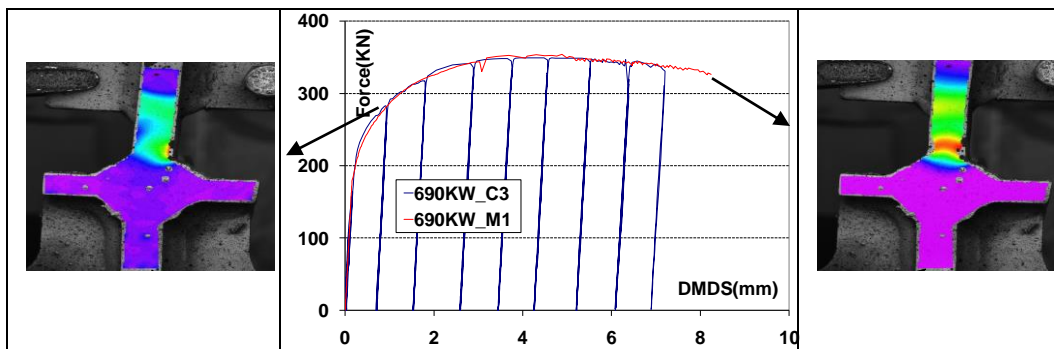


Fig. 5.27 – State of strain in welded specimens at yield and failure using digital image correlation technique

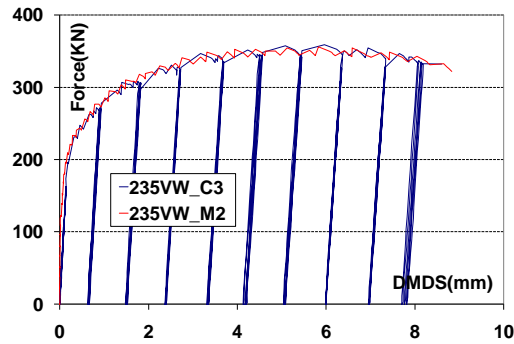


Fig. 5.28 – Load – displacement curves for S235 specimens(VW Monotone/Cyclic)

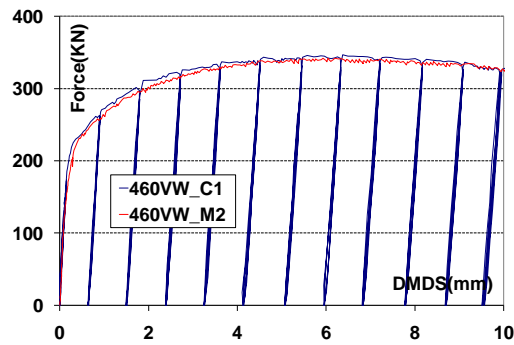


Fig. 5.29 – Load – displacement curves for S460 specimens(VW Monotone/Cyclic)

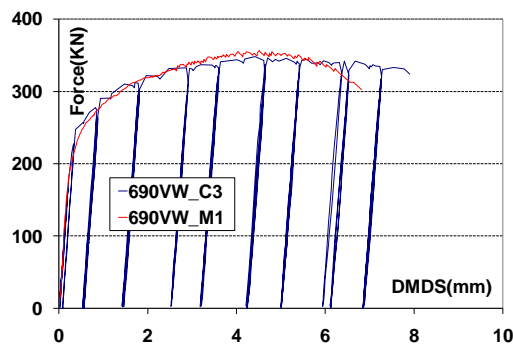


Fig. 5.30 – Load – displacement curves for S690 specimens(VW Monotone/Cyclic)



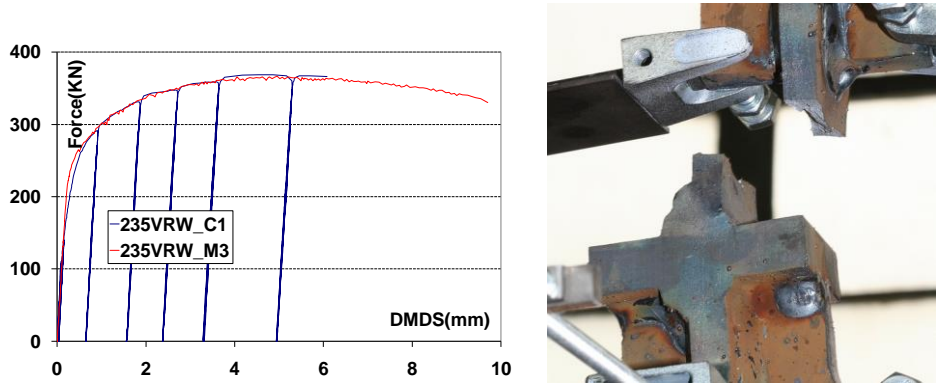


Fig. 5.31 – Load – displacement curves for S235 specimens(VRW Monotone/Cyclic)

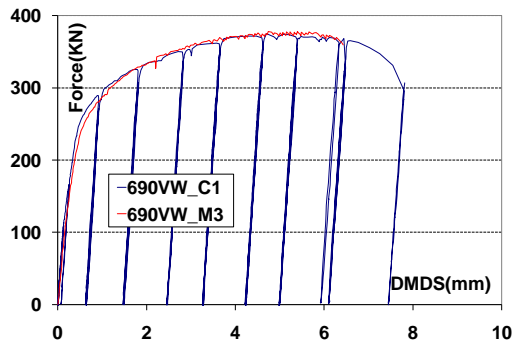


Fig. 5.32 – Load – displacement curves for S690 specimens(VRW Monotone/Cyclic)

Fractography proves a ductile failure mode for all specimens, even if in some cases intergranular brittle micro-failures were observed(see )

ductile failure	ductile failure	mixed brittle-ductile failure
500x magn.	500x magn.	1000x magn.

Fig. 5.33 - Welding details fractography

**5.4.3.3. Conclusions**

Tests on weld details were performed in order to assess the performance of welds connecting different steel grades and to validate the welding technology. Weld

preparation and the technology for  $\frac{1}{2}$  V bevel weld, for instance, is shown in Fig. 5.15. Weld experimental force-displacement are shown in Fig. 5.18 - Fig. 5.26, while Fig. 5.27 shows the state of strain in the area of the weld and the Heat Affected Zone (HAZ). In fact, since the weaker material was S235 in the "web", there are no significant differences in terms of steel grades of "end-plate".

It has to be noticed that all the welds proved a very good behaviour with failure at the end of HAZ or in vicinity, as expected. So, both the choice of welding materials and technology were confirmed. Pulsating cyclic loading did not affect much the response in comparison with monotonic loading.

#### 5.4.4 Tests on T-stub specimens

The **T-stub** corresponds to two T-shaped elements connected through the flanges by means of one or more bolt rows. The T-stub model has been extensively applied to model the tension zone of bolted joints that constitutes the most relevant source of deformability of this type of joints[49]. Within the framework of the so-called component method [81] this zone includes the following basic elemental parts: column flange, end plate or angles in bending, along with the bolts in tension [83][68][82][58].

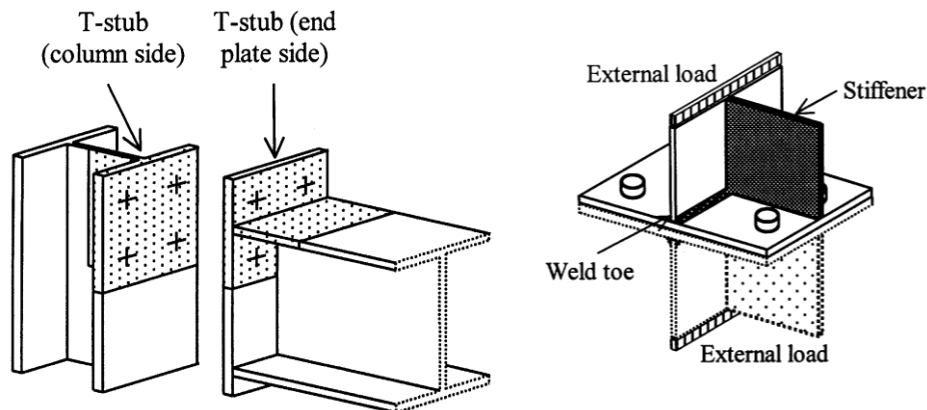


Fig. 5.34 - Different types of bolted T-stub connection assemblies[49]

Fig. 5.34 identifies the T-stub which accounts for the deformation of the column flange and the end plate in bending in the particular case of an extended end plate bolted connection. In this specific case, because the column flange is unstiffened, the T-stub on the column side is orientated at right angles to the end plate T-stub[82].

The models for the column and the end plate sides are different. The T-stub elements on the column flange side are generally hot rolled profiles, whilst on the end plate side such elements comprise two welded plates, the end plate and the beam flange, and a further additional stiffener that corresponds to the beam web (see Fig. 5.34 right). The first model has been extensively studied over the past years and it was the aim of several research programmes that are reported in the literature [83][82][58][13][32][42][76][69]. Rules for the prediction of the connection response have been included in modern design codes as the Eurocode 3[32]. This code approximates the force-deformation ( $F-\Delta$ ) behaviour of this

component by means of an elasto-plastic response, characterized by a full plastic strength,  $F_{Rd}$  and initial stiffness,  $k_{e,0}$ . The post-limit stiffness,  $k_{pl,0}$  is taken as zero, which means that strain hardening and geometric nonlinear effects are neglected. Regarding the component ductility, Eurocode 3[32] presents some qualitative principles based on the main contributions of the T-stub deformation: if the bending deformation of the flanges governs the plastic mechanism, then the ductility is infinite; should the bolt determine collapse, the ductility is limited. These rules are, however, insufficient to ensure adequate ductility in partial strength joints [74]. To fill in this code gap, several authors have proposed analytical or numerical procedures for assessment of the deformation capacity of a T-stub made up of beam rolled profiles [77][70][45].

The current approach to account for the behaviour of T-stubs made up of welded plates consists in a mere extrapolation of the existing rules for the other assembly type. The authors have shown that this assumption is erroneous and can lead to unsafe estimations of the characteristic properties [47][46]. And since the assemblage end plate-fasteners (welds and bolts) is often the weakest joint part, the characterization of its behaviour is very important.

T-stubs are basic components of the design method used in EN 1993-1.8 for evaluation of strength and stiffness of bolted end-plate beam to column joints. This part of the thesis focuses on the experimental research of the quasi-static monotonic and cyclic deformation response of T-stub connections made of different grades of steel (S235,S460,S690). All types of T-stubs are part of beam to column connections with extended end plate. The end plates could be stiffened or unstiffened.

Function the geometry of the beam to column connection there can be identified 3 types of T-stub component:

**Type A** – T-stub full stiffened (Fig. 5.35). For this type of T-stub, the end plate is full strengthened by stiffeners. One stiffener is the web of the beam meanwhile the second stiffener is the stiffener disposed at the end plate extension.

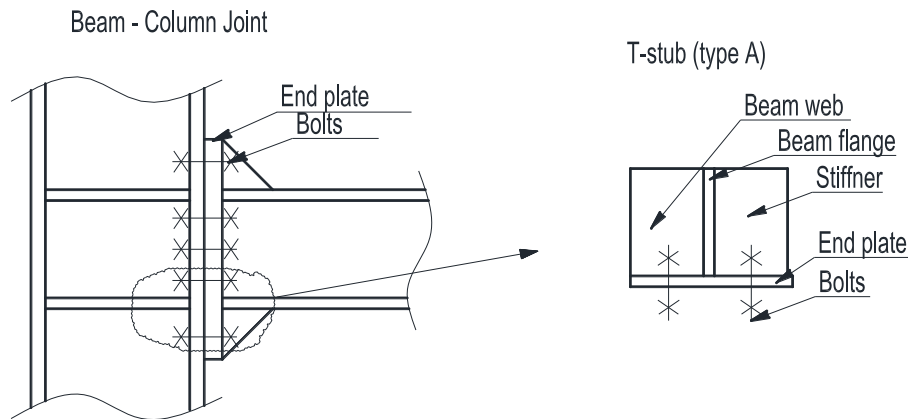


Fig. 5.35 – T-stub Type A

**Type B** - T-stub half stiffened. In this case we can speak about a beam to column connection having an extended end plate without being stiffened. The only stiffener present in this T-stub it is the beam web (Fig. 5.36).

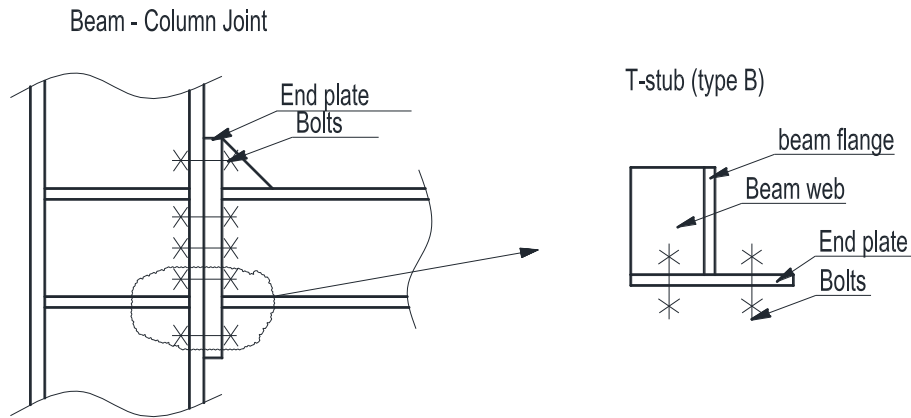


Fig. 5.36 – T-stub Type B

**Type C** – T-stub unstiffened, this type of T-stub correspond to T-stubs formed by intermediate bolt rows (Fig. 5.37).

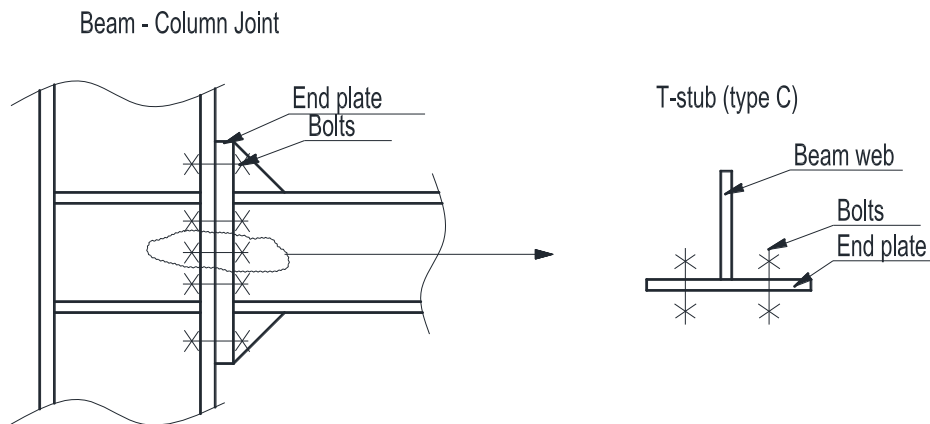


Fig. 5.37 – T-stub Type C

In Eurocode 3, part 1-8 are described 3 possible failure mechanisms (collapse mechanisms) of a T-stub element. The parameter dictating the failure mode is  $\beta_{Rd}$ , parameter defined as the ratio between bending resistance of the flanges(or end plate) an the tension resistance of the bolts.

$$\beta_{Rd} = \frac{4M_{f,Rd}}{2B_{Rd}m} \quad (5.1)$$

Where:

- $M_{f,Rd}$  it is design flexural resistance,
- $B_{Rd}$  it is design axial resistance of a single bolt
- $m$  it is the distance the bolt axis and the section corresponding to flange to web where a plastic hinge can occur.

$$m = d - 0.8r \quad (5.2)$$

Where:

- $d$  is the distance between bolt axis and the web.
- $r$  is the radius of the flange(end plate) to web connection.

**Type 1** mechanism is characterised by four plastic hinges. Two hinges are located at the bolt axes, due to the bending moment caused by the prying forces. The other two hinges are located at the flange (end plate) to web connection. Design resistance formula, according to Eurocode 3 part 1-8 is:

$$F_{1,Rd} = \frac{4M_{f,Rd}}{m} \quad (5.3)$$

In mechanism **Type 2** two plastic hinges occur, located at the section corresponding to the flange (end plate) to web connection. Prying forces  $Q$  arise leading to bolt failure before plastic hinges take place in the end plate at the section corresponding to bolt axis. Design resistance formula, according to Eurocode 3 part 1-8 is:

$$F_{2,Rd} = \frac{2M_{f,Rd} + 2B_{Rd}n}{m + n} \quad (5.4)$$

Where:

- $n$  is the distance between force  $Q$  and the axis of bolt.

**Type 3** mechanism is characterized by the bolt failure only. Bolts collapse before any plastic hinge take place in flange (end plate). Design resistance formula, according to Eurocode 3 part 1-8 is:

$$F_{3,Rd} = 2B_{Rd} \quad (5.5)$$

Design resistance of the T-stub is:

$$F_{T-stub,Rd} = \min(F_{1,Rd}; F_{2,Rd}; F_{3,Rd}) \quad (5.6)$$

Tested specimen are formed by 2 T elements connected through the flanges by mean of 4 high strength bolts M20 class 8.8 (see Fig. 5.38). All T-stubs specimens are obtained from welded plates.

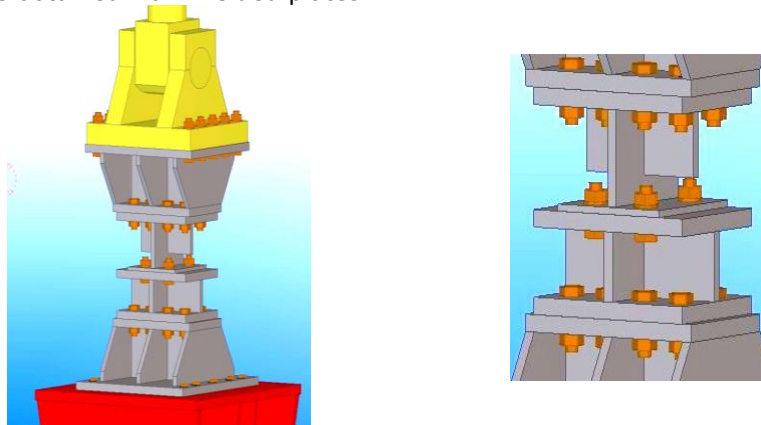


Fig. 5.38 – T-stub specimen

As can be seen in Fig. 5.39, only T element positioned above it is the specimen that was tested. The other T element, the one from below, is a oversized T-stub(type A) designed to resist way above all specimens.

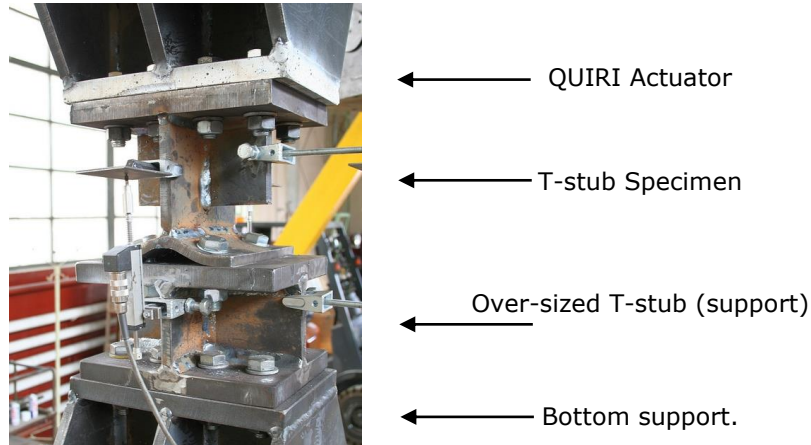


Fig. 5.39 – T-stub test set up.

Labelling of the specimens has been done upon below rules(see Table 5.17).

Element	End plate thickness	T-stub Type	End plate Grade	Type of loading	No. of specimen
<b>TST_16A_S460_C1</b>					
T-stub( <b>TST</b> )	<b>16</b> mm	<b>A</b> (see Fig. 5.35)	<b>S460</b>	<b>Cyclic</b> (quasi-static)	<b>1</b> by 3

Table 5.17 – T-stub specimen legend

If in the case of welded specimens it has been used a number of 4 different types of welding to connect the beam of the web through the end plate. Even though for the T-stub specimens it has been used only one type of welding, K bevel weld. This decision it has been taken due to the fact that history shoes that these type of tests, specially cyclic ones which simulates seismic action are significant sensible to type of welding. Using K bevel weld for T-stub specimens will prevent collapse of the specimen by weld failure.

As mentioned on previous descriptions there are 3 types of T-stubs regarding the way of stiffening, there are also 3 types of materials used for end plate (flange) – meaning S235, S460, S690, there are 2 types of end plate thickness for each type of steel grade depending on the desired collapse mechanism, and there are 2 types of T-stubs regarding the way they are loaded during tests (monotone vs. Cyclic – quasi-static).

For each possible combination it has been tested a number of 3 specimens. Due to the large amount of variables the experimental program has required testing of 108 specimens.

Using component method from Eurocode 3, part 1-8, it has been computed desired T-stub characteristics (plates dimensions, bolts dimensions, distance between bolts) corresponding to Type 1 and Type 2 of collapse mechanism. The



TST	Loading Monotone Cyclic	t	d1	d2	d3	d4	d5	d6	d7	d8
TST_8A_S690	_M1	8	87	88	81	81	80	92	80	82
	_M2	8	93.5	82	82	82	90	87.5	81	82
	_M3	8	88	85	81.5	83	85	91	83	80
TST_8B_S690	_M1	8	85	90	78.5	85			84	82
	_M2	8	84	89	79	85.2			83	81.8
	_M3	8	85.2	89.8	78.5	85			84	82
TST_8C_S690	_M1	8.1			86.2	78.5			81.3	83.5
	_M2	8			82.3	82.9			82.9	81.6
	_M3	8.1			83	81.7			81.3	82.1
TST_12A_S690	_M1	12	93	85	84	82	86	92	85	81
	_M2	12	90	88	82	85	87	91	83	85
	_M3	12.1	88	89	82	86	85	93	81	85
TST_12B_S690	_M1	12.1	85	98	84	85			83	85
	_M2	12	81	95	85	84			79	89
	_M3	12.1	88.6	85.6	84.9	80.4			84.9	81.5
TST_12C_S690	_M1	12			86	81			81	86
	_M2	12			84.3	79.1			82.4	82.5
	_M3	12.1			85.2	79.8			72.5	90.8
TST_10A_S460	_M1	10.2	86	89	85	78	89	87	80	82
	_M2	10.3	86	85	85	78	87	84	81	79
	_M3	10.1	79	93	81	81	87	88	78	85
TST_10B_S460	_M1	10	87	86	82	80			79	82
	_M2	10.1	87	87	82	81			80	81
	_M3	10.2	87	89	81	78			74	83
TST_10C_S460	_M1	10.2			82	80			83	81
	_M2	10.4			81	79			82	78
	_M3	10.3			79	83			81	82
TST_16A_S460	_M1	16.4	88	86	81	82	88	87	83	82
	_M2	16.5	83	87	82	82	88	85	82	81
	_M3	16.3	88	86.3	83.6	83.7	86.9	89.4	84.1	81.6
TST_16B_S460	_M1	16.5	85	88	81	82			75	85
	_M2	16.3	87	90	87	78			83	82
	_M3	16.3	93	84	84	82			80	83
TST_16C_S460	_M1	16			84.5	82.3			78.3	86.5
	_M2	16			82.4	83			84.4	80.4
	_M3	16.1			80.8	81.5			84.5	80
TST_12A_S235	_M1	12	88	85.5	81.3	81.5	83.9	89	82	82
	_M2	12	86.5	88.5	80.5	81	88.3	86.7	79	83.5
	_M3	12.2	88.8	86.1	81.4	81.2	88.2	89.2	80	83.4
TST_12B_S235	_M1	12	90	85	84	82			83	81
	_M2	12	83	96.5	84.5	84.5			81	87
	_M3	12	84.8	90.3	85.0	82.2			82.0	85.3
TST_12C_S235	_M1	12			86	83			79	85
	_M2	12			82	83			83	83



	_M3	12			84	86			87	78
TST_20A_S235	_M1	20.2	89	91	84	83	89	90	84	83
	_M2	20.1	87.5	87.5	82.8	82.6	89	88	81	81.5
	_M3	20.1	86.2	87.2	80.5	82.5	88.5	86.5	84.5	88.5
TST_20B_S235	_M1	20.1	88	86.7	82	84.1			81	84.2
	_M2	20.1	88.2	90.5	83	79.8			81	84.3
	_M3	20.1	89	86	82.8	81			81	82.8
TST_20C_S235	_M1	20			83.0	83.6			82.5	83.6
	_M2	20.1			82.9	81.2			81.0	82.9
	_M3	20.1			81.7	81.8			82.8	85.7

Table 5.19 – Measured properties T-stub specimen (Monotone Loading)

TST	Loading Monotone Cyclic	t	d1	d2	d3	d4	d5	d6	d7	d8
TST_8A_S690	_C1	83	81.5	81	89.3	84.5	83.5	81	85.8	89.7
	_C2	80	83	85	92	83	83	84	82	92
	_C3	78	92	83	84	84	86	88	85	84
TST_8B_S690	_C1	80	92	83	82	82			84	84
	_C2	80	94	84	86	80			82	83
	_C3	80	89	84	83	81			79	82
TST_8C_S690	_C1	8.1			83	81.5			81.3	82.1
	_C2	8.1			86	78.5			81.3	83.5
	_C3	8			82.3	82.9			82.9	81.7
TST_12A_S690	_C1	12	83	93	83	82	85	93	82	82
	_C2	12	83	93	84	82	84	94	83	85
	_C3	12.1	82	94	83	82	84	93	82	83
TST_12B_S690	_C1	12.1	91	89	84	83			90	88
	_C2	12	88	89	85	82			83	84
	_C3	12	90	87	92	93			79	87
TST_12C_S690	_C1	12			88	79			78	89
	_C2	12			86	90			82	85
	_C3	12.1			79.7	85			86.4	79.4
TST_10A_S460	_C1	10.3	87	87	82	81	87	87	82	79
	_C2	10.1	85	91	82	82	87	88	80	82
	_C3	10.5	82	92	77	86	87	85	79	83
TST_10B_S460	_C1	10	87.1	89.5	85.9	88.3			80.1	83.3
	_C2	10	87.8	87.2	83.9	79.3			82.1	79.4
	_C3	10	86.5	90.5	82.9	80.6			78	82
TST_10C_S460	_C1	10.1			82.6	82.3			82.5	82.3
	_C2	10.1			79.6	84.5			83	79
	_C3	10.1			82.1	82.4			82.6	81.4
TST_16A_S460	_C1	16.1	88.7	83.4	82.2	84.4	81.8	92.1	82	84.5
	_C2	16.2	91.5	84.8	82.4	82.7	82	94	82.8	82.5
	_C3	16.2	89.4	91.5	81.6	82.8	83.9	91.1	81.5	82.9
TST_16B_S460	_C1	16.2	88	85	81	81			80	82
	_C2	16.3	93	80	82	80			82	81

	_C3	16.3	87	87	84	80			79	83
TST_16C_S460	_C1	16.3			82.5	84.7			85.5	81.6
	_C2	16.4			84	84.3			87.2	78.7
	_C3	16.2			85.5	80.8			81.8	84
TST_12A_S235	_C1	12	88	85.5	81.3	81.5	83.9	89	82	82
	_C2	11.9	91.8	86.4	82.8	84	86.1	92	83	82.5
	_C3	12	89	85	82	83	84	90	82	83
TST_12B_S235	_C1	12	89.0	87.0	84.5	82.0			83.0	82.5
	_C2	12.1	86.5	91.8	88.3	88.8			80.0	87.0
	_C3	12	88	89	85.2	83.4			81.4	83.8
TST_12C_S235	_C1	12			81	83			83	83
	_C2	12.1			82	82			84	84
	_C3	12			82	81			84	83
TST_20A_S235	_C1	20.1	88	87	83	81.5	90	85.2	84.5	79.2
	_C2	20.1	93.8	85	80.8	82.5	82.5	84	81.7	81.9
	_C3	20.1	89	86	82	82	84	84	82	80.7
TST_20B_S235	_C1	20.1	88.1	88.6	82.5	82.0			81	84.3
	_C2	20.1	88.6	88.3	82.9	80.4			81	83.6
	_C3	20.1	88.5	86.4	82.4	82.6			81	83.5
TST_20C_S235	_C1	20.1			82.2	82.1			82.1	82.2
	_C2	20			82.0	81.8			81.7	82.1
	_C3	20.1			82.2	82.1			81.4	82.6

Table 5.20 - Measured properties T-stub specimen (Cyclic Loading)

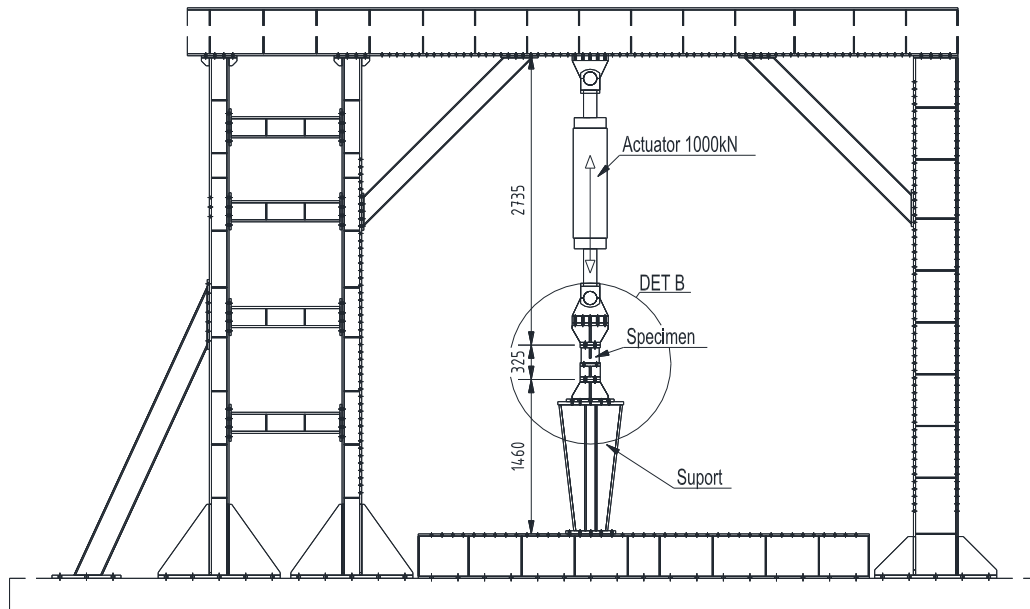
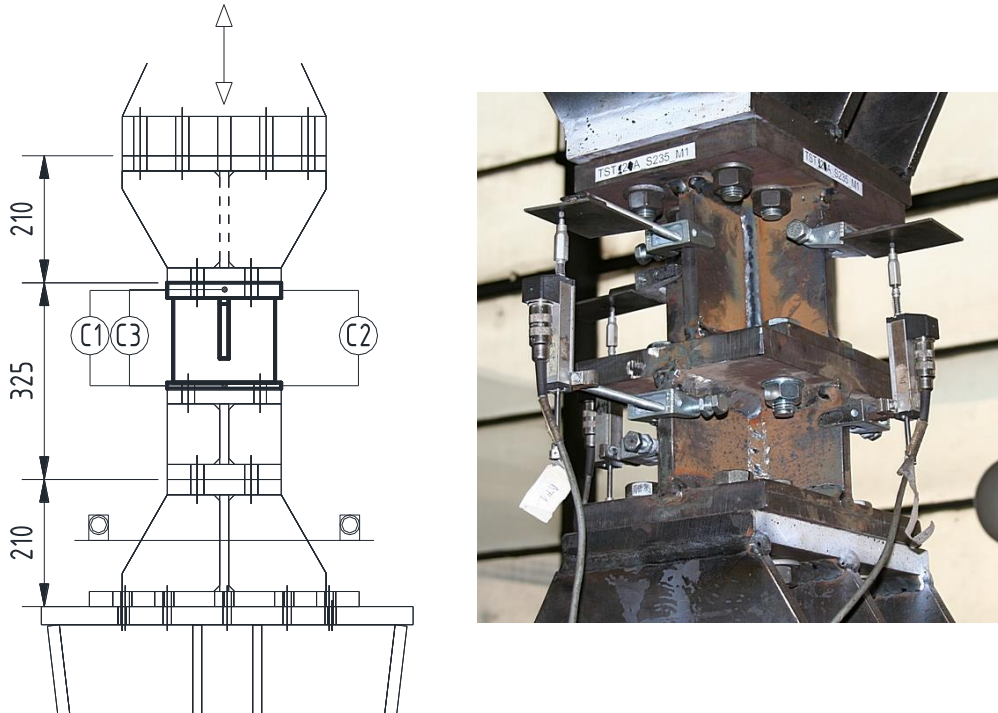





Fig. 5.41 – T-stub specimen – Experimental stand

The specimens were subjected to monotonic tensile force, which was applied under displacement control with a speed of 0.01mm/s up to the collapse. The gap between



Where:  
 Actuator moving direction  
 Displacement transducers  
 Limes Vic-3D – optic measurement device

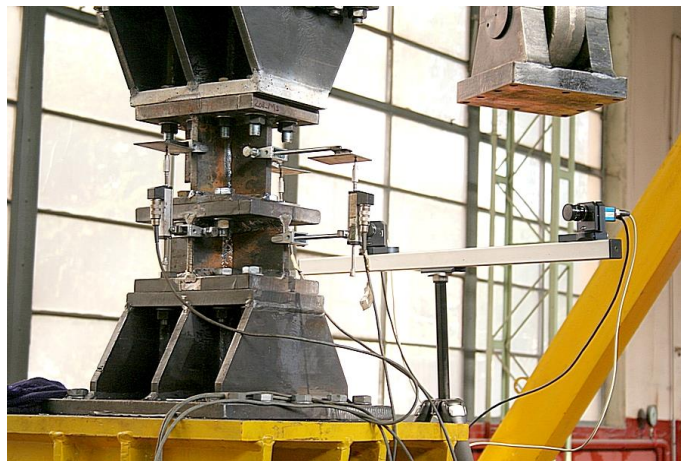


Fig. 5.42 – Displacement transducers and Vic3D on T-stub specimen

the flanges was measured at 3 sides of specimen in the centreline of the webs by 3 displacement transducers. On the fourth side the measurement was performed using optical measurement device unit LIMESS Vic3D (see Fig. 5.42).

Before installation of the specimen into experimental stand, the dimensions of the plate have been recorded and the bolts, M20, grade 8.8 have been hand-tightened. , and finally using a torque wrench it was applied a torque moment of 25daNm, and a angle of rotation of 75°.

#### 5.4.4.1. T-stub specimen – Monotonic tensile test results.

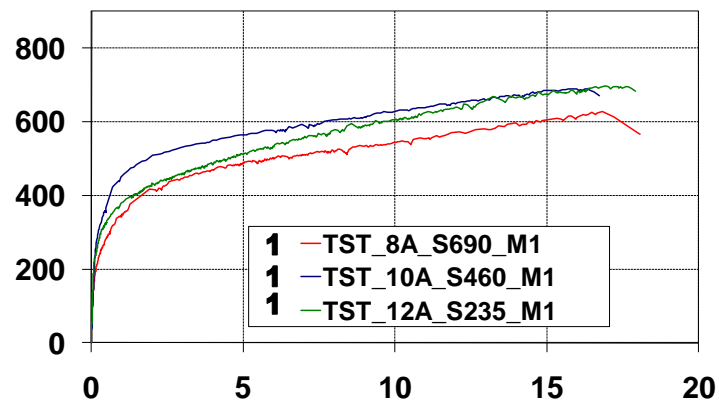


Fig. 5.43 – Force-displacement TST type A -thin End Plate

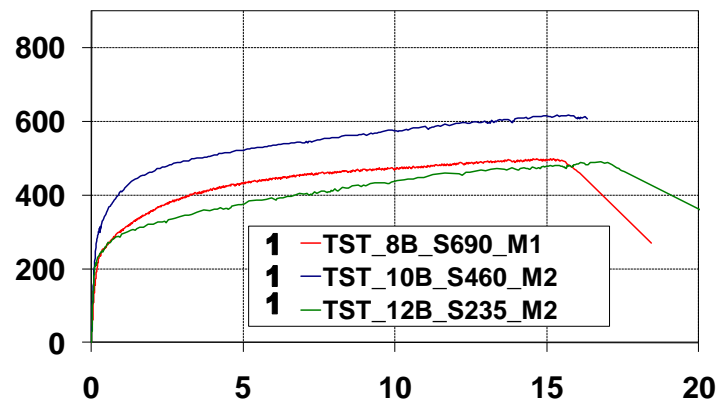


Fig. 5.44 – Force-displacement TST type B -thin End Plate

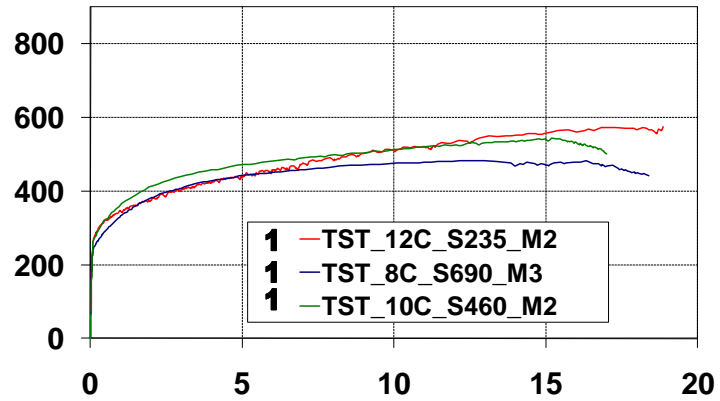


Fig. 5.45 – Force-displacement TST type C –thin End Plate

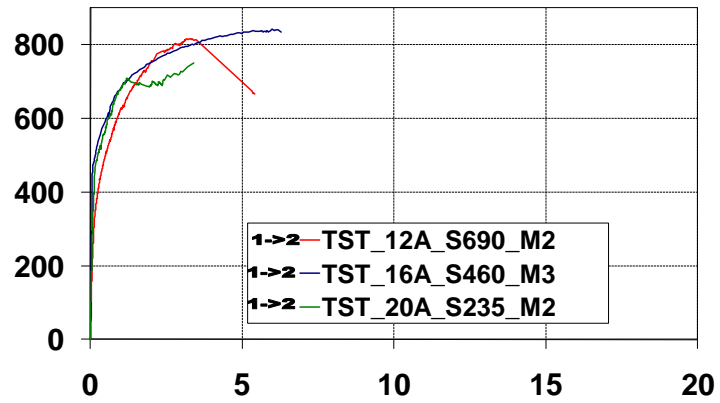


Fig. 5.46 – Force-displacement TST type A –thick End Plate

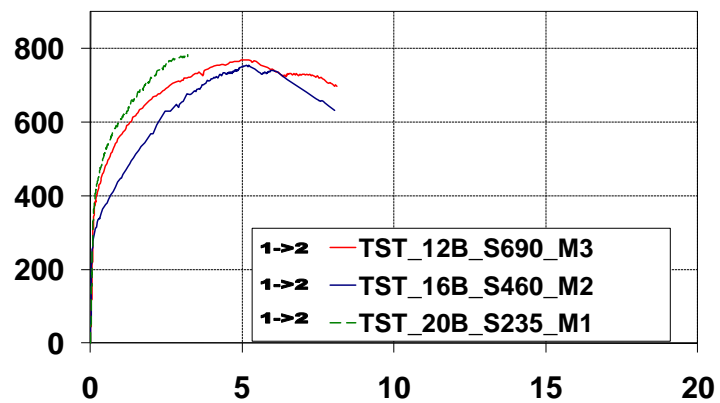


Fig. 5.47 – Force-displacement TST type B –thick End Plate

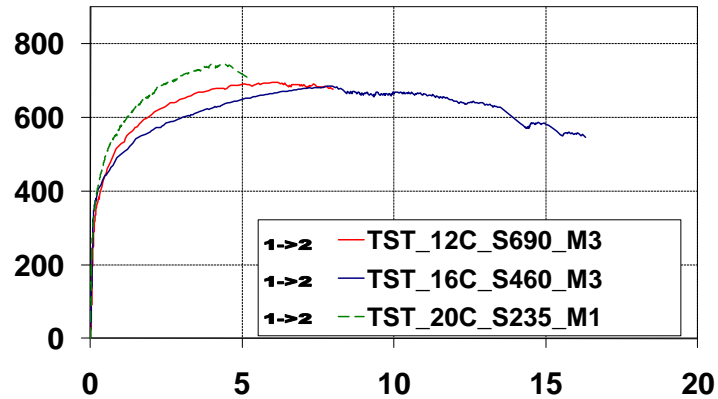


Fig. 5.48 – Force-displacement TST type C –thick End Plate

The following parameters were determined for each experimental test: initial stiffness  $K_{ini}$ , maximum force  $F_{max}$ , yield force  $F_y$ , and ultimate deformation,  $D_y$ . The initial stiffness was obtained by fitting a linear polynomial to the force-displacement data between 0 and 25% of the maximum force. The yield force was determined at the intersection of the initial stiffness and tangent stiffness lines, where the tangent stiffness was obtained by fitting a linear polynomial to force-displacement data between 75% and 100% of the maximum force. The ultimate deformation was determined as the displacement corresponding to a 10% drop of the maximum force (Fig. 5.49 and Fig. 5.50).

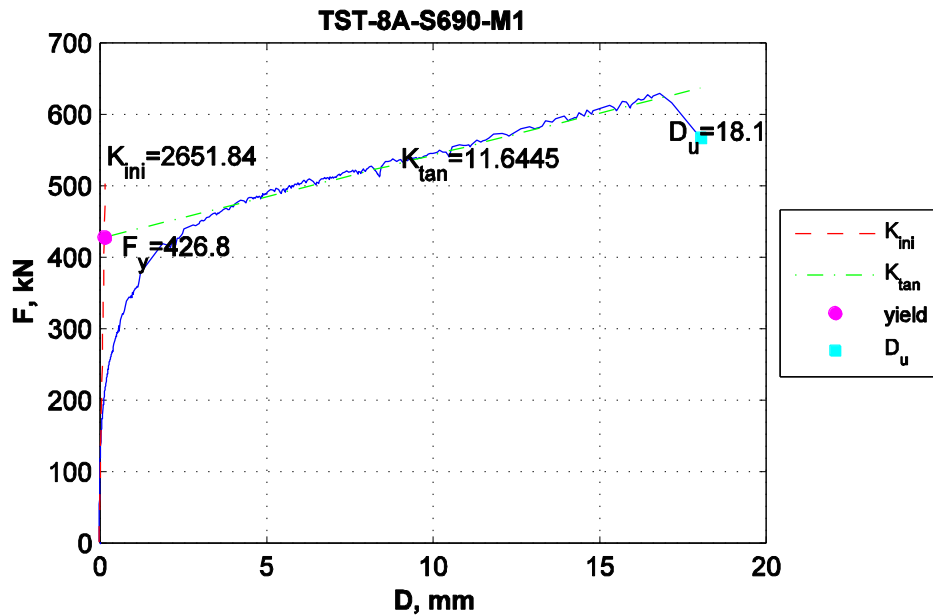
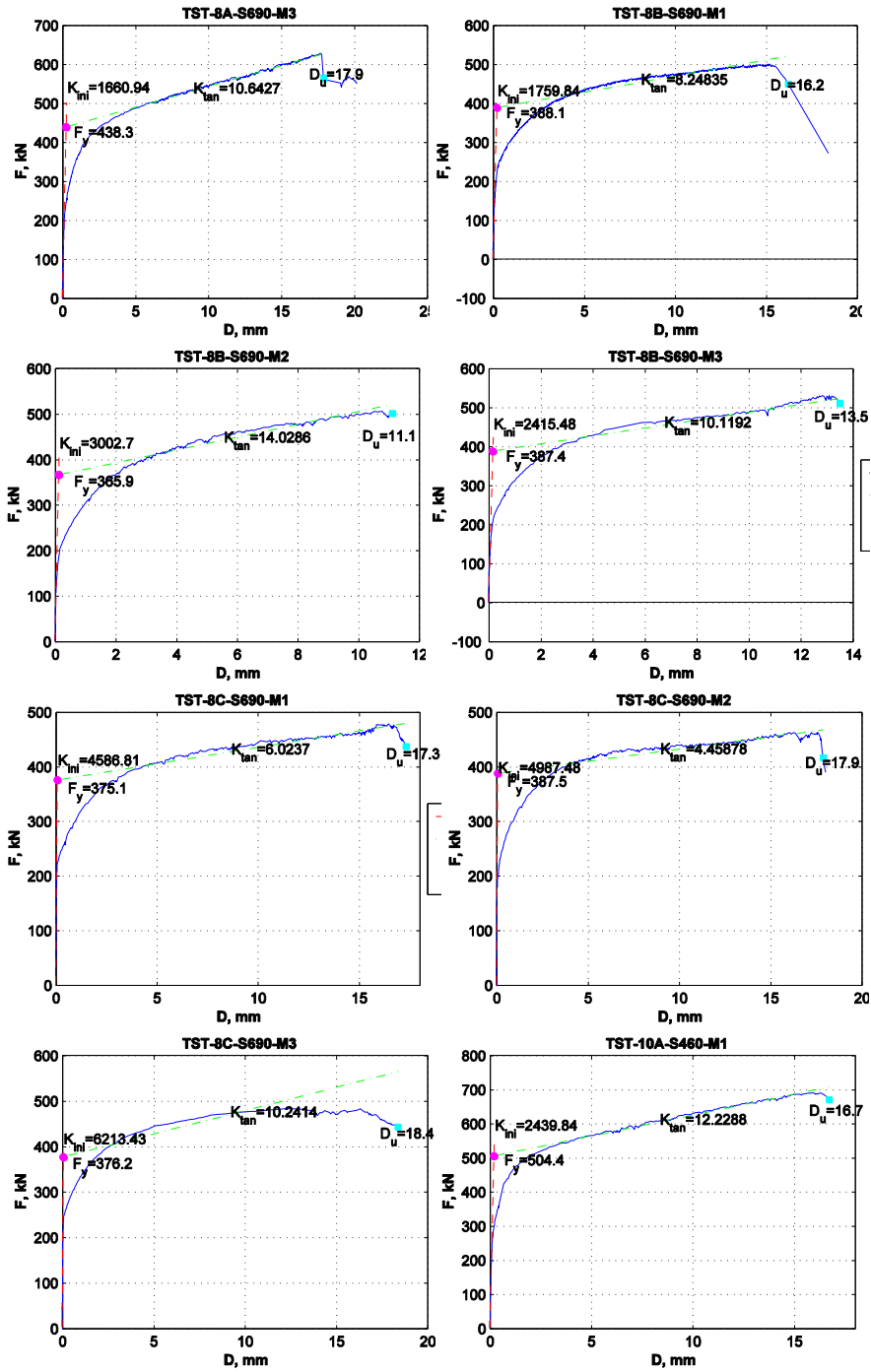
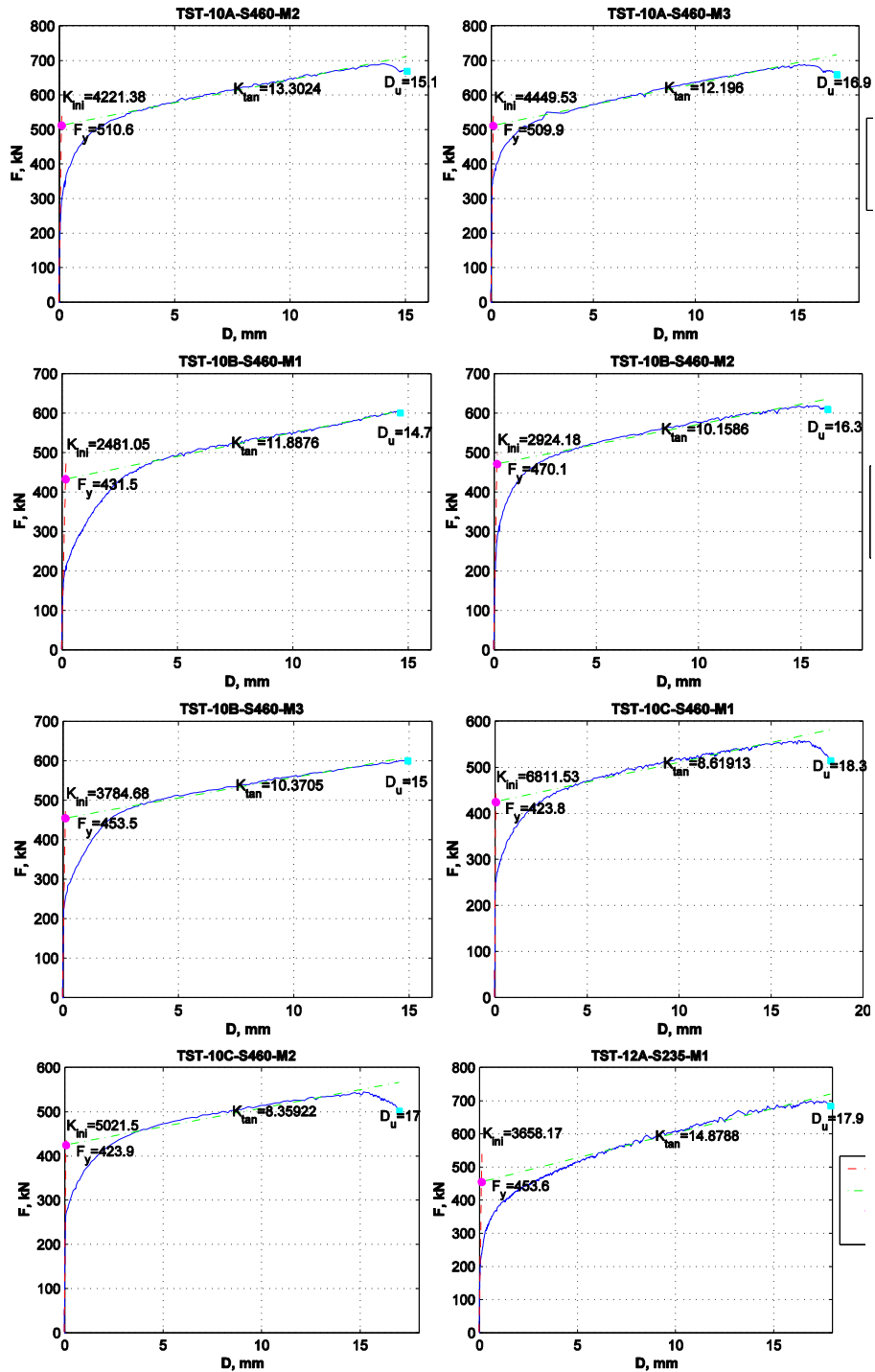
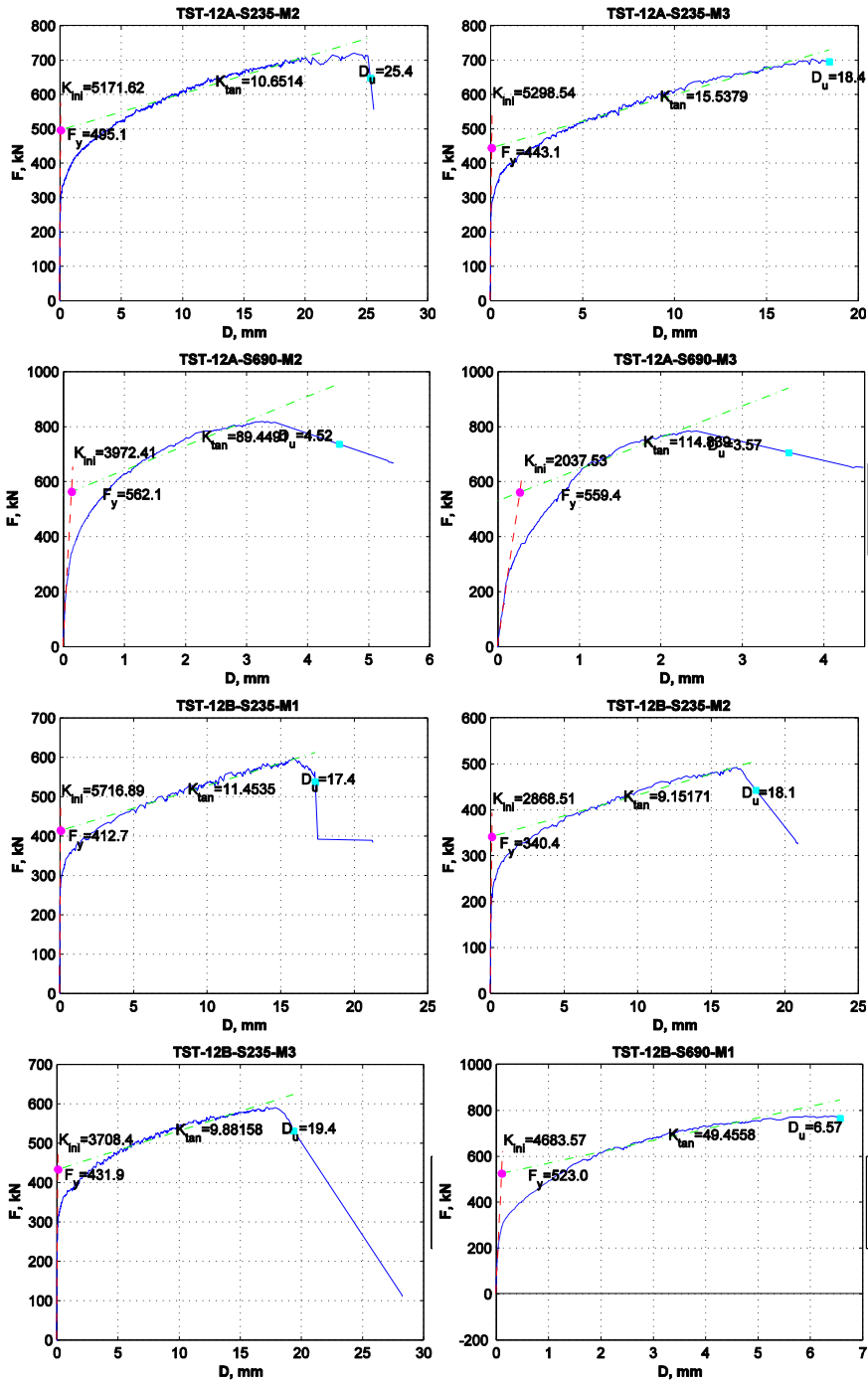


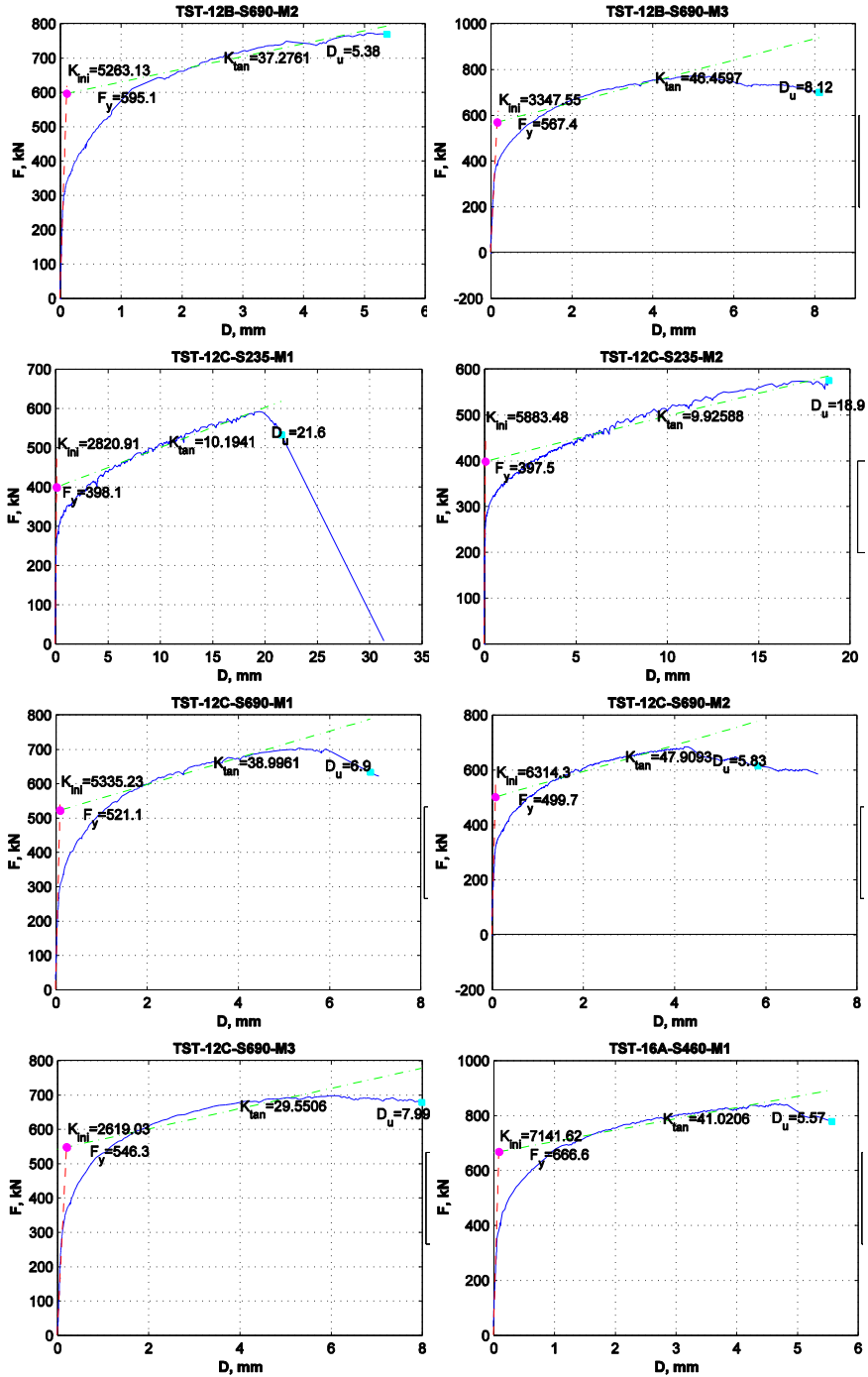
Fig. 5.49 – Experimental characteristics of TST-8A-S690-M1 T-stub specimen

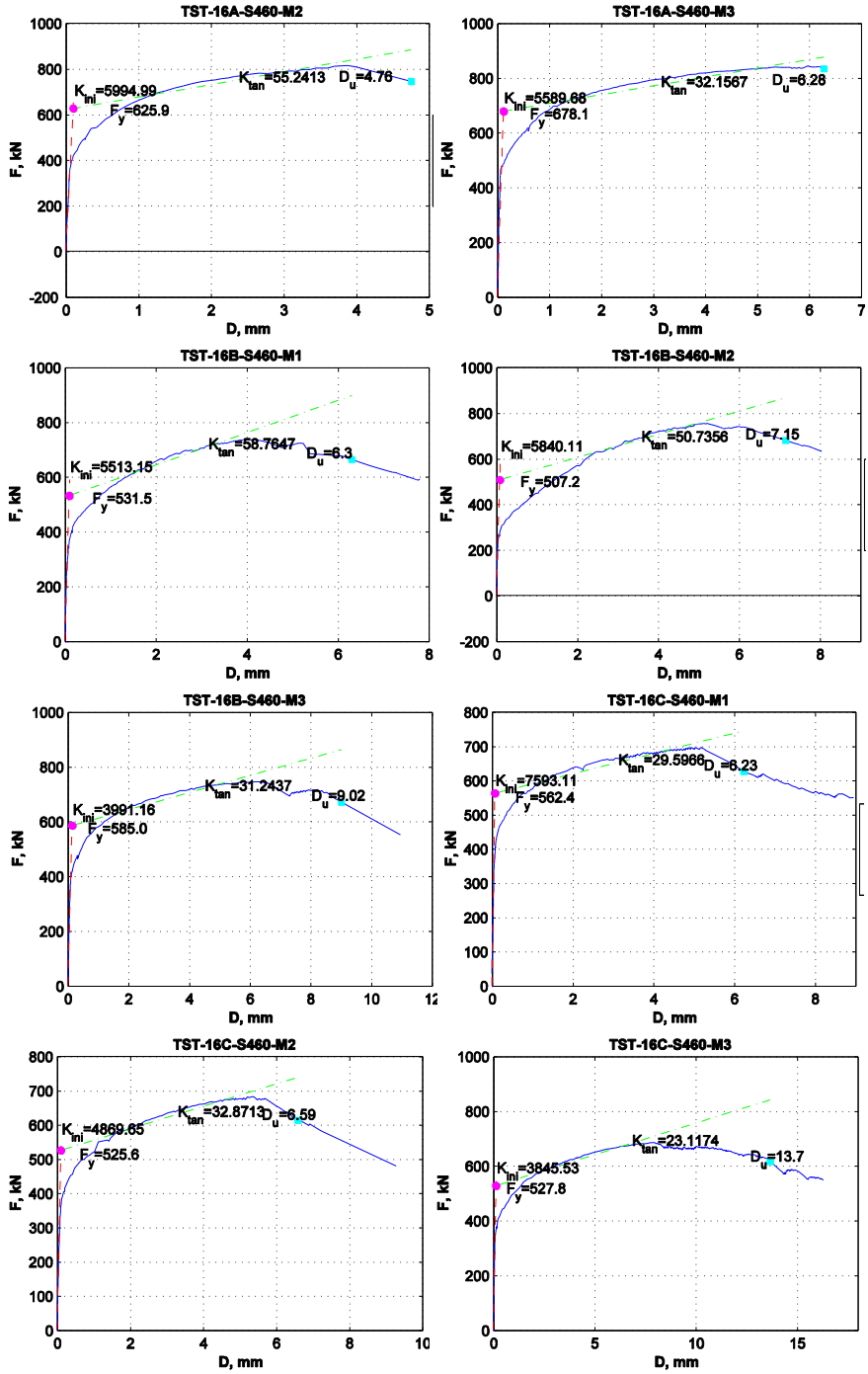












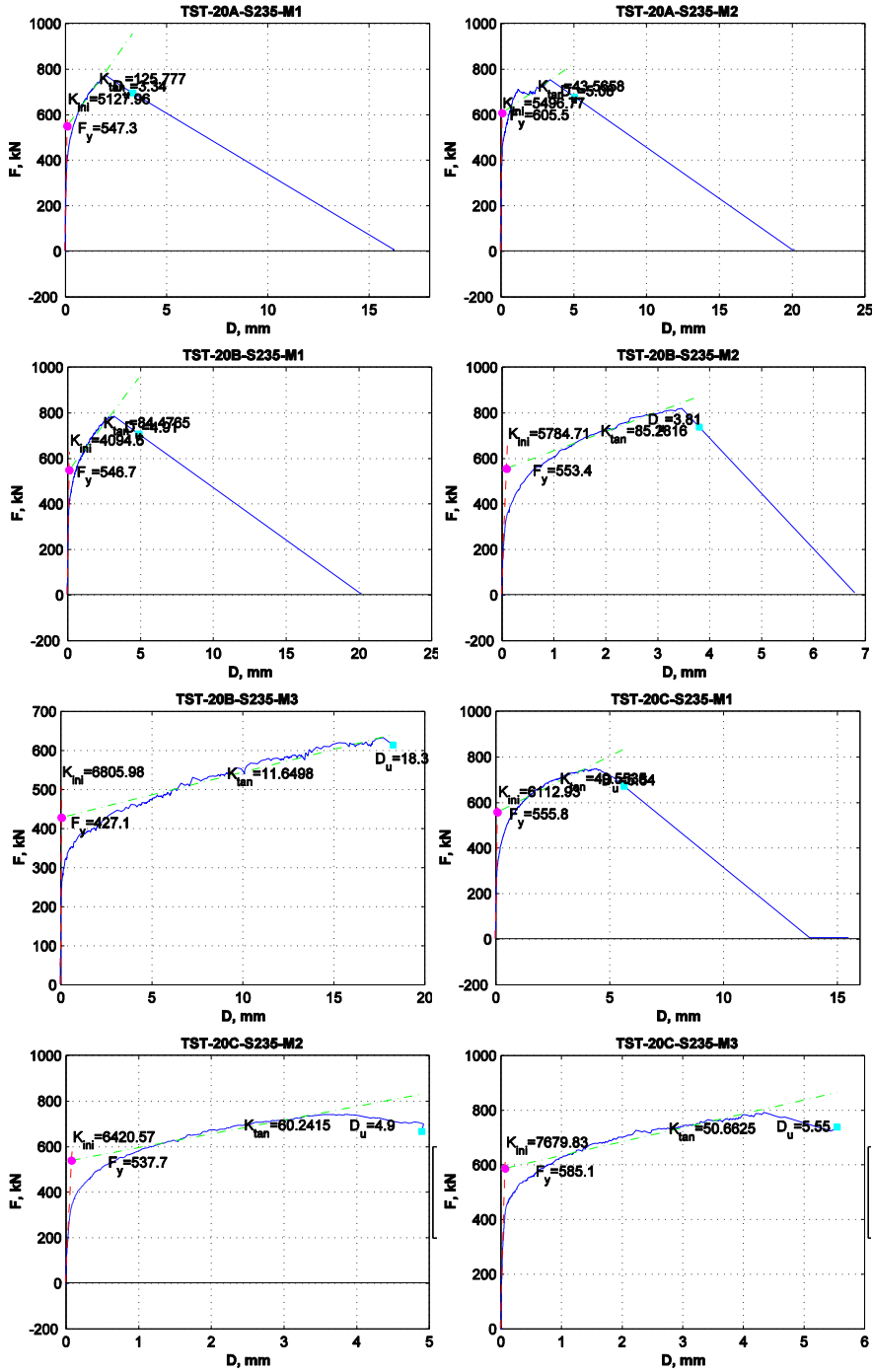


Fig. 5.50 - Experimental characteristics of T-stub specimens

Experimental characteristics of T-stub specimen loaded monotone quasi-static being determined it could proceed in carrying out the cyclic quasi-static loaded tests.

Test protocol set for specimens with thicker end-plate it is described in following lines:

- 1 cycle in Force control up to  $F_y/4$
- 1 cycle in Force control up to  $F_y/2$
- 1 cycle in Force control up to  $3F_y/4$
- 3 cycles in Displacement control up to  $D_y$
- 3 cycles in Displacement control up to  $3D_y$
- 3 cycles in Displacement control up to  $6D_y$
- 3 cycles in Displacement control up to  $9D_y$
- 3 cycles in Displacement control up to  $12D_y$
- 3 cycles in Displacement control up to  $15D_y$
- 3 cycles in Displacement control up to  $18D_y$
- 3 cycles in Displacement control up to  $21D_y$
- 3 cycles in Displacement control up to  $24D_y$
- 3 cycles in Displacement control up to  $27D_y$
- 3 cycles in Displacement control up to  $30D_y$

Test protocol set for specimens with thinner end-plate it is described in following lines:

- 1 cycle in Force control up to  $F_y/4$
- 1 cycle in Force control up to  $F_y/2$
- 1 cycle in Force control up to  $3F_y/4$
- 3 cycles in Displacement control up to  $D_y$
- 3 cycles in Displacement control up to  $6D_y$
- 3 cycles in Displacement control up to  $12D_y$
- 3 cycles in Displacement control up to  $18D_y$
- 3 cycles in Displacement control up to  $24D_y$
- 3 cycles in Displacement control up to  $30D_y$
- 3 cycles in Displacement control up to  $36D_y$
- 3 cycles in Displacement control up to  $42D_y$
- 3 cycles in Displacement control up to  $48D_y$
- 3 cycles in Displacement control up to  $54D_y$
- 3 cycles in Displacement control up to  $60D_y$
- 3 cycles in Displacement control up to  $66D_y$
- 3 cycles in Displacement control up to  $72D_y$
- 3 cycles in Displacement control up to  $78D_y$
- 3 cycles in Displacement control up to  $84D_y$
- 3 cycles in Displacement control up to  $90D_y$

A very important objective of T-stub tests was to confirm the authors' assumption that the A-type T-stub (Table 5.18), corresponding to stiffened extended end-plate, which contains the first bolt row, can be calculated considering the contribution of stiffener as the one of "beam-web", and use the EN1993-1-8 formula for second bolt row (Figure 1).

Loading was applied in displacement control under tension and force control under compression. Compressive force was chosen so as to prevent buckling of the specimen. For specimens of types B and C, it was not possible to have full reversible cycles due to the buckling. A good ductility was observed, in general; however, thicker end-plate specimens, even of S235, do not show the best ductility. It seems that the choice of thickness associated with steel grade is important in the

conception of a proper connection, in order to obtain a good balance between strength, stiffness and ductility of components. Fig. 5.53 and Fig. 5.54 shows examples with all 3 types of observed failure modes, together with the corresponding force-displacement relationships of T-stub specimens. There were no significant differences in force values between failure modes of monotonic and cyclic specimens, both generally agreeing with analytical predictions by EN 1993-1.8.

The ductility of the T-stub specimens was quantified through the ultimate displacement  $D_u$ . Under monotonic loading, ultimate displacement was smaller for specimens with thicker end-plates that failed in modes 2 and 3 involving bolt failure (see Fig. 5.51). Cyclic loading reduced significantly ultimate displacement of specimens with thinner end-plates that failed in mode 1. This behaviour is attributed to low-cycle fatigue that generated cracks in the HAZ near the welds, along yield lines. On the other hand, cyclic loading did not affect much ultimate displacement for specimens with thicker end-plates that failed in modes 2 and 3, governed by bolt response. It is interesting to note that specimens realized from high-strength end plates (S460 and S690, with lower elongation at rupture), had a ductility comparable with the one of specimens realized from mild carbon steel (S235). The parameters governing the ductility of T-stubs were type of loading (monotonic / cyclic) and failure mode (end-plate or bolts).

A comparison between experimental and analytical results was made (Table 5.21 and Fig. 5.52). Theoretical characteristics were evaluated by component method from EN1993-1.8. It may be remarked that, with some exceptions, the procedure from EN1993-1.8, including specimens of type A is confirmed; the exceptions can be covered by safety coefficients

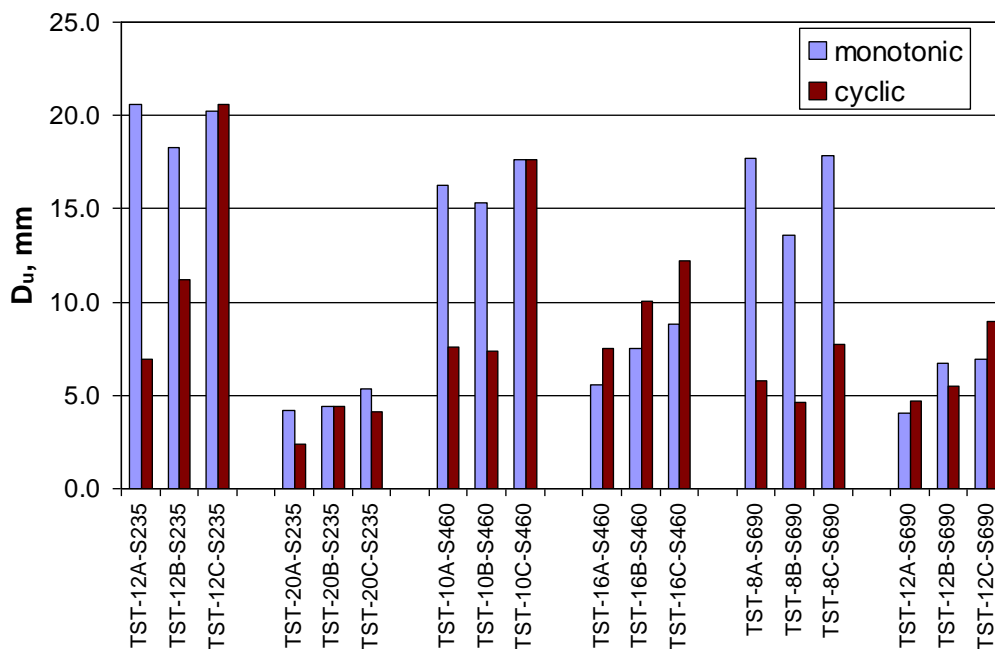


Fig. 5.51 - Ultimate displacement of T-stub specimens: monotonic vs. cyclic loading

Specimen	$F_{y,exp,average}$ [kN]	$F_{y,EC3-1.8}$ [kN]	$F_{y,EC3}/F_{y,exp}$	$F_{max,exp}$ [kN]	$D_{u,exp}$ [mm]	$K_{ini,exp}$ [kN/mm <sup>2</sup> ]
TST-12A-S235	463.9	449.0	0.97	705.6	20.6	4709.4
TST-12B-S235	395.0	369.6	0.94	559.0	18.3	4097.9
TST-12C-S235	397.8	290.3	0.73	582.6	20.2	4352.2
TST-20A-S235	576.4	669.2	1.16	760.8	4.2	5312.4
TST-20B-S235	509.0	616.2	1.21	744.2	4.4	5561.8
TST-20C-S235	559.5	563.2	1.01	758.3	5.4	6737.8
TST-10A-S460	508.3	473.5	0.93	688.7	16.2	3703.6
TST-10B-S460	451.7	410.6	0.91	606.4	15.3	3063.3
TST-10C-S460	423.8	347.7	0.82	550.2	17.6	5916.5
TST-16A-S460	656.8	705.0	1.07	832.8	5.5	6242.1
TST-16B-S460	541.2	641.4	1.19	745.9	7.5	5114.8
TST-16C-S460	538.6	577.9	1.07	687.5	8.8	5436.1
TST-8A-S690	432.0	497.3	1.15	618.4	17.7	2756.1
TST-8B-S690	380.5	450.4	1.18	511.3	13.6	2392.7
TST-8C-S690	379.6	403.5	1.06	474.2	17.9	5262.6
TST-12A-S690	560.7	712.6	1.27	799.5	4.0	3005.0
TST-12B-S690	561.8	646.8	1.15	771.0	6.7	4431.4
TST-12C-S690	522.4	581.0	1.11	693.5	6.9	4756.2

Table 5.21 - Experimental (monotonic) and analytical T-stub characteristics

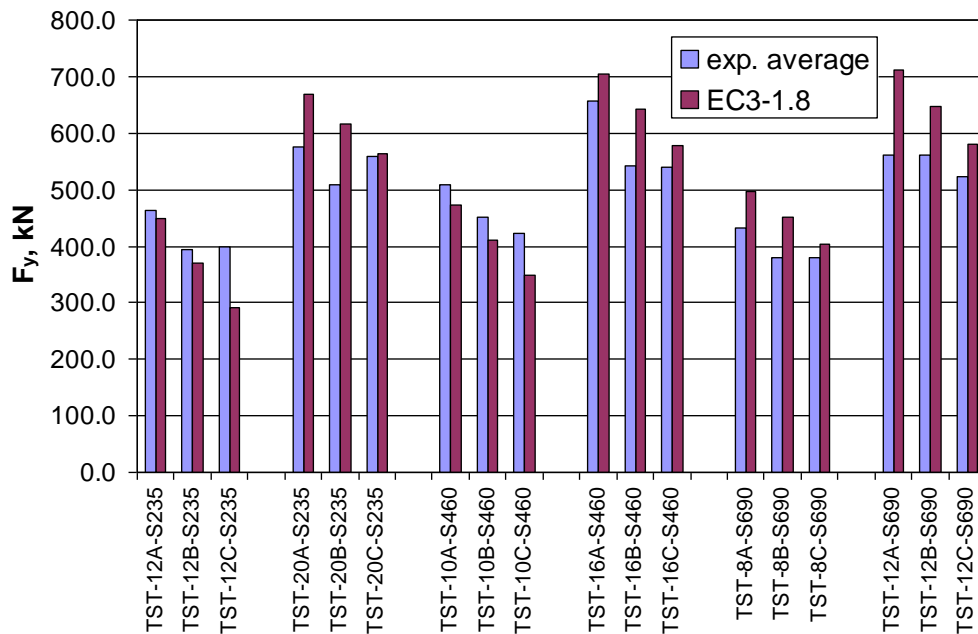
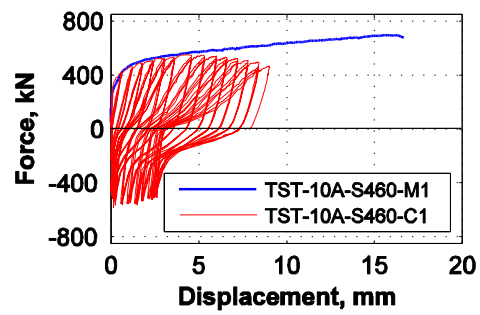
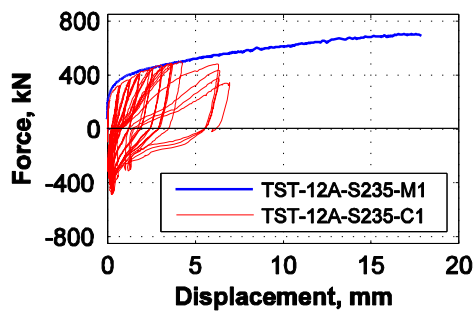
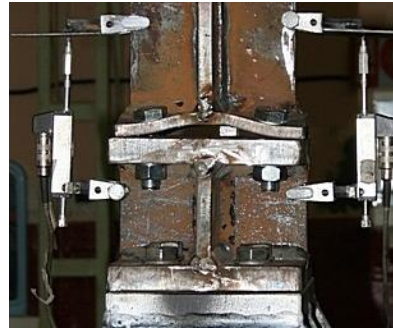
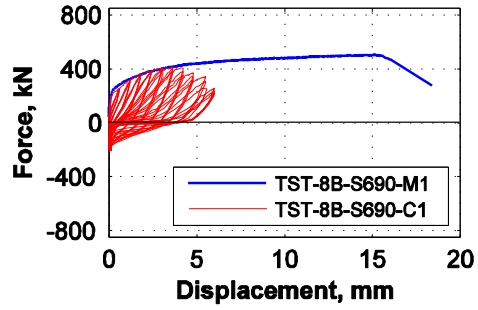
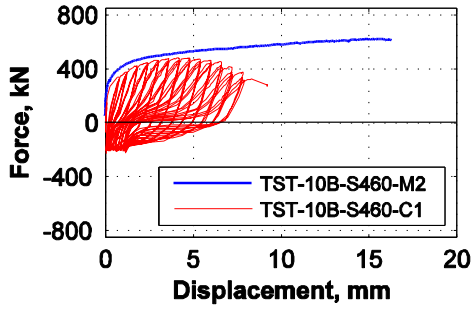
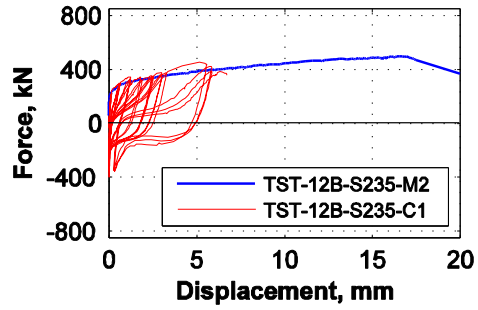
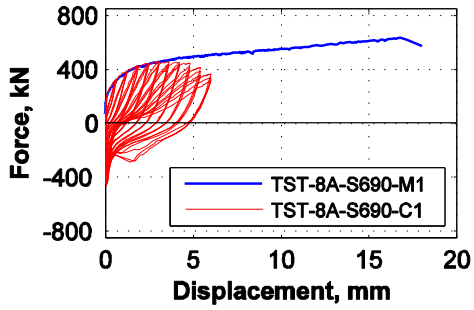


Fig. 5.52 - Yield Force - experimental (monotonic) vs. analytical values

An overview of force-displacement relationships of T-stub specimens is presented in Fig. 5.53 and Fig. 5.54 together with examples. There were no significant differences between failure modes of monotonic and cyclic specimens, both generally agreeing with analytical predictions by EN 1993-1.8







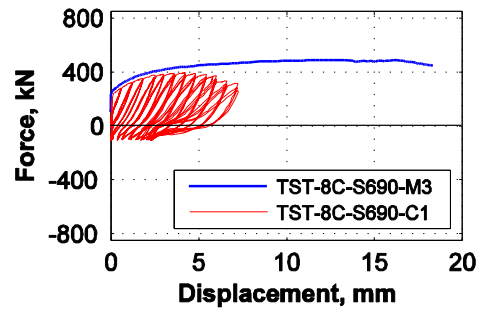
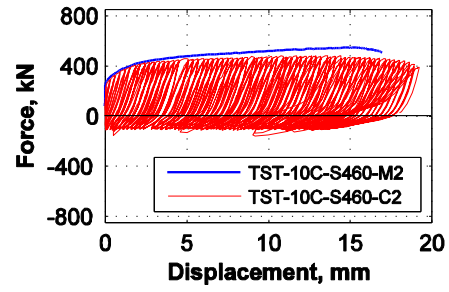
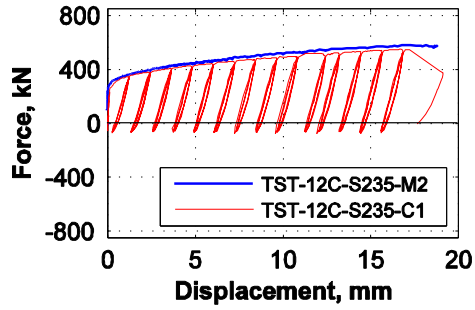
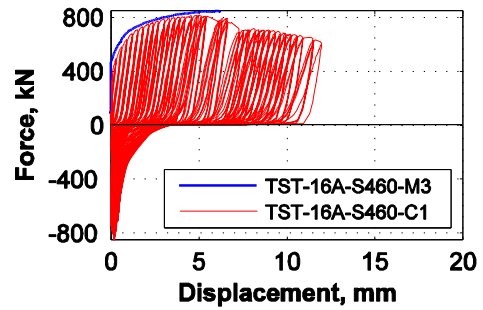
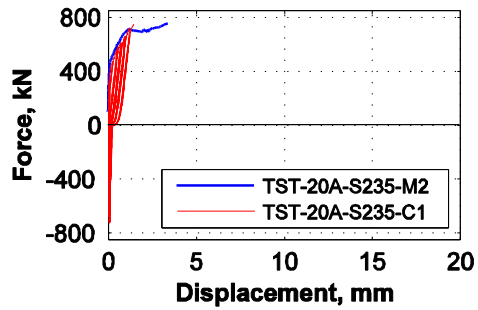
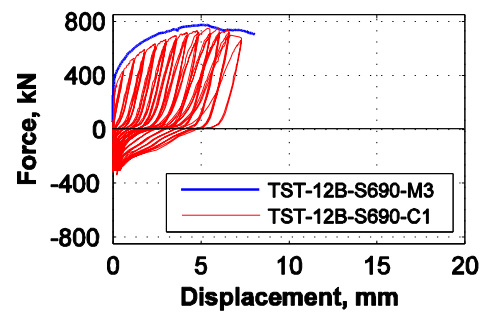
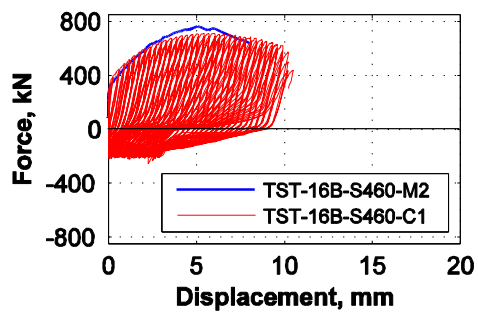
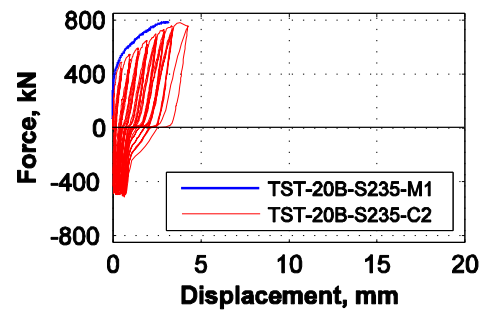
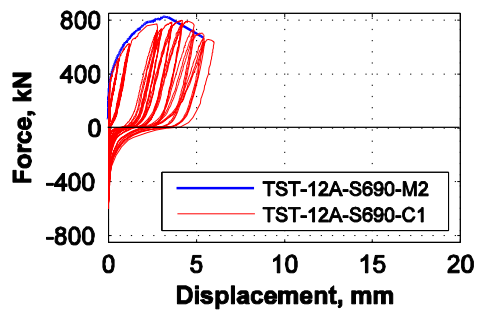
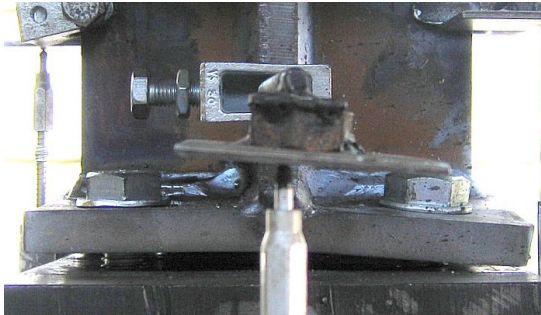


Fig. 5.53 – Force –Displacement relationship for T-stubs with “thin” end plate





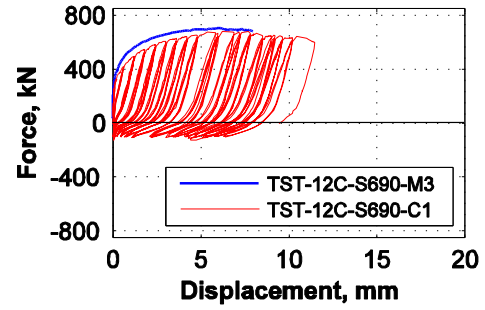
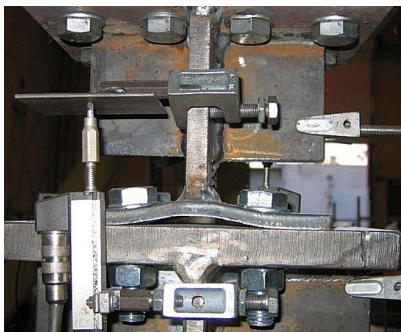
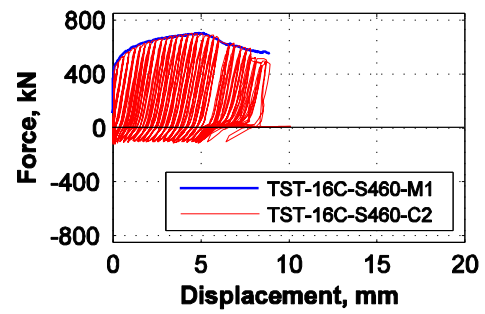
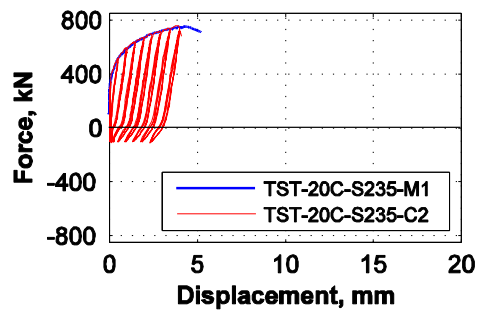


Fig. 5.54 - Force -Displacement relationship for T-stubs with "thick" end plate



**5.4.4.2. RE-EVALUATION OF EXPERIMENTAL RESULTS**

In this section, the test results on DS T-stubs are re-elaborated based on the S-N line approach, considering that the cyclic loading generates a low-cycle fatigue strength problem [14].

The fatigue failure prediction function, used by S-N curve approach, can be expressed by the following equation:

$$N \cdot S^m = K \tag{5.7}$$

where N is the number of cycles to failure at the constant stress (strain) range S. The non-dimensional constant m and the dimensional parameter K depend on both the typology and the mechanical properties of the considered steel component.

Converted in terms of energy, Equation ( 5.7) becomes:

$$N \left( \frac{\Delta E}{E_y} \sigma(F_y) \right)^m = K \tag{5.8}$$

where:  $E_y$  is the energy corresponding to the elastic limit,  $\Delta E$  is the energy dissipated in a cycle, and  $\sigma(F_y)$  is the stress corresponding to the elastic limit. In order to obtain the cumulated energy  $\Delta E_c$ , characterizing the "detail category", the value of  $\Delta E$  should be evaluated to a number  $N=2 \cdot 10^6$  cycles and for  $m=3$ :

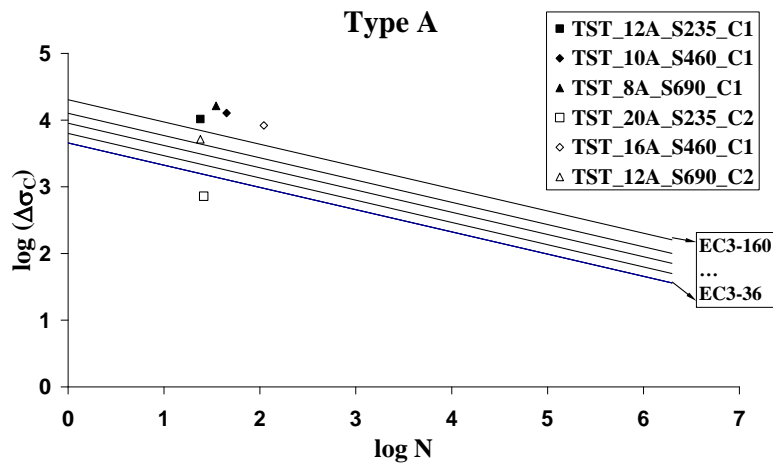
$$\log \Delta E_c = \frac{1}{m} (\log K - \log N) \tag{5.9}$$

Once this value obtained, it is possible to determine the corresponding value of direct stress range  $\Delta \sigma_c$ , as "measure" of detail category (EN 1993-1.9 2005):

$$\Delta \sigma_c = \frac{\Delta E_c}{E_y} \sigma(F_y) \tag{5.10}$$

Figures Fig. 5.55, Fig. 5.56 and Table 5.22 present the re-elaborated test results in terms of low-cycle fatigue approach.

Also, in Table 4, the ductility  $\mu_E$ , calculated in terms of cumulated energy at failure  $E_u$  and elastic limit  $E_y$  is shown.



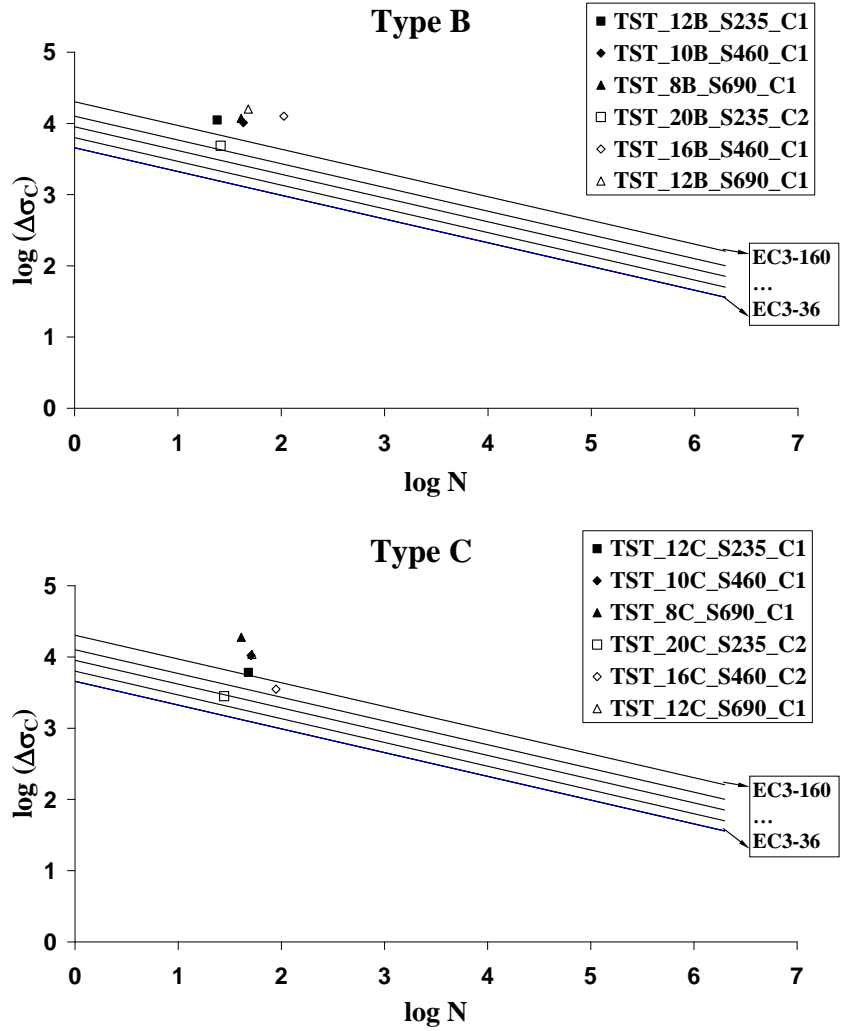
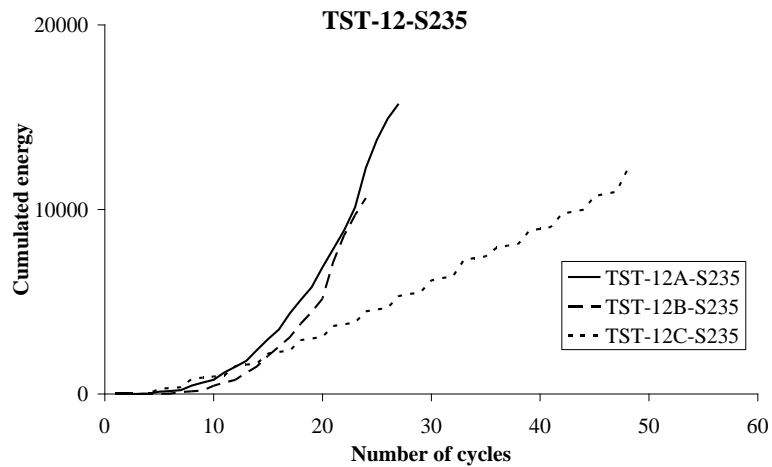


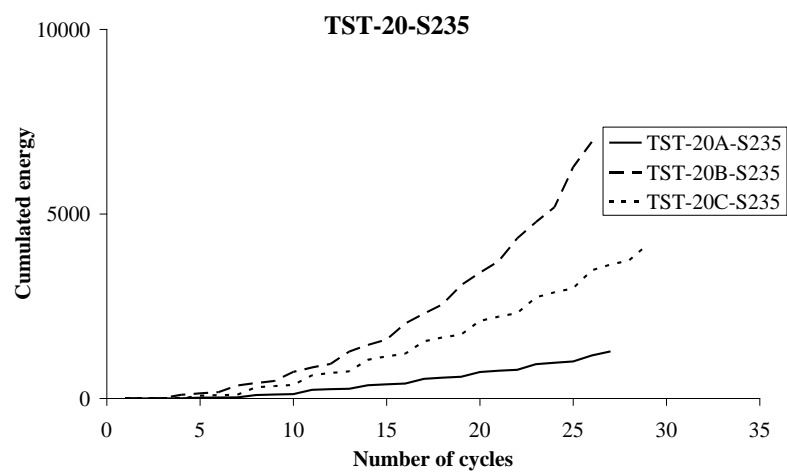
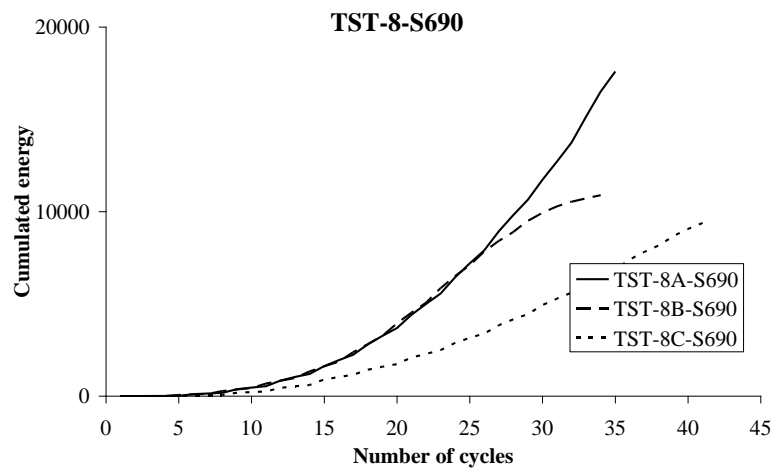
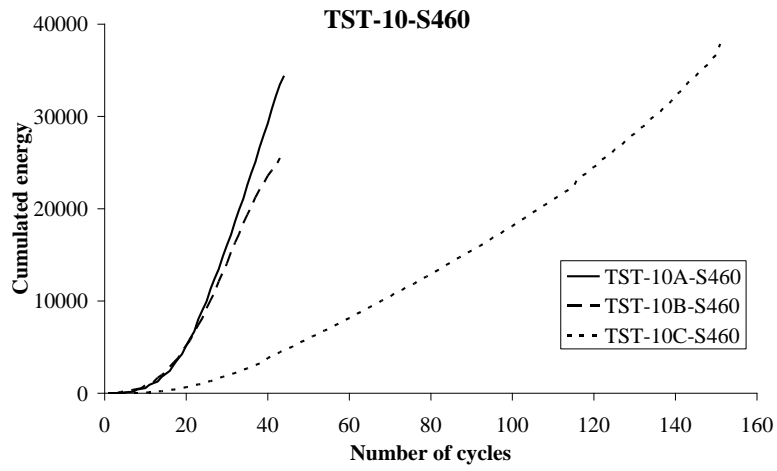
Fig. 5.55 - Fatigue strength curves for normal stress ranges

Specimen	Nr. of cycles	$\Delta\sigma$ [N/mm <sup>2</sup> ]	$\Delta\sigma_c$ [N/mm <sup>2</sup> ]	$\mu_E = \frac{E_u - E_v}{E_v}$	Failure mode
TST-12A-S235	27	10367	247	670	1
TST-12B-S235	24	11146	255	523	1
TST-12C-S235	48	6060	175	583	1
TST-20A-S235	26	720	17	40	3
TST-20B-S235	26	4846	114	279	2→3
TST-20C-S235	28	2810	69	178	2
TST-10A-S460	45	12749	357	920	1
TST-10B-S460	43	10232	285	744	1
TST-10C-S460	151	10438	441	2435	1
TST-16A-S460	110	8296	315	1567	2
TST-16B-S460	106	12614	478	2439	2
TST-16C-S460	89	3530	126	491	2
TST-8A-S690	35	16306	423	456	1
TST-8B-S690	34	11782	303	340	1
TST-8C-S690	41	18867	516	673	1
TST-12A-S690	21	5141	113	70	3
TST-12B-S690	38	15912	425	481	2
TST-12C-S690	52	10832	321	469	2

Table 5.22 - Interpretation of cyclic tests in term of energy

So, the fact of welding plates of different steel grades, one being of HSS and the specimens subjected to cyclic loading, does not affect their safety in fatigue. However, it is important to underline the quality of weld details, also experimentally con-firmed [27].







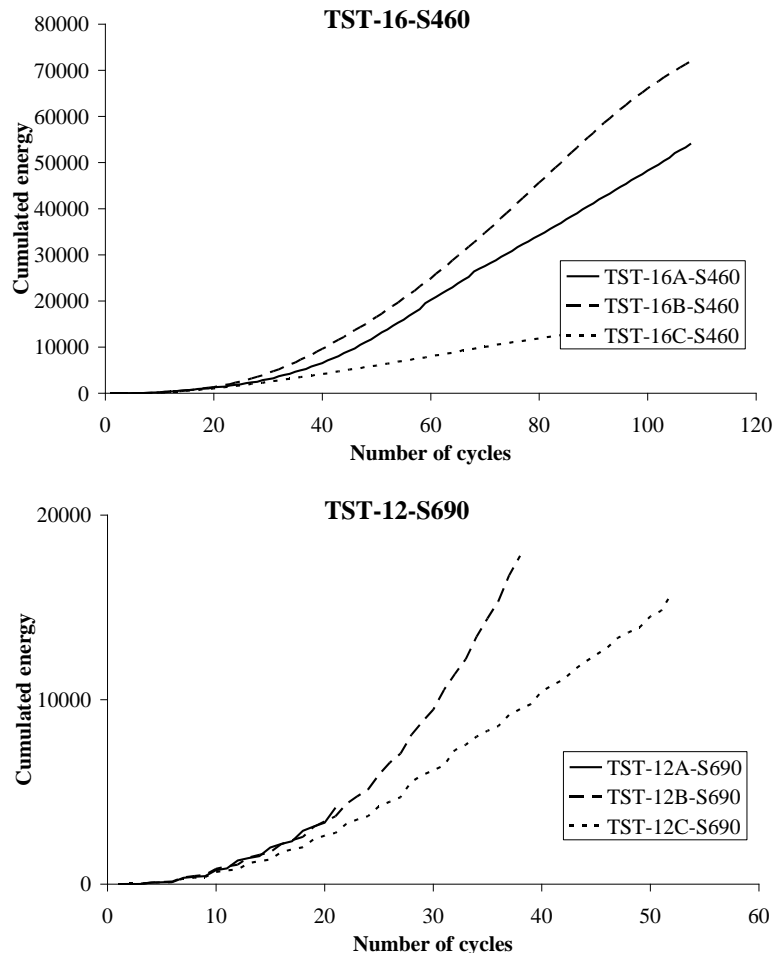


Fig. 5.56 - Cumulated energy

#### 5.4.4.3. Concluding remarks

The objective of the experimental study on welded details and T-stubs described in this chapter was to investigate performance of components in beam to column joints realized from mild and high strength steel grades.

The most important factor affecting the ductility of T-stub components under monotonic loading was the failure mode. Most ductile response was observed for components failing by end-plate bending (mode 1), while failure modes involving bolts (mode 2 and 3) were less ductile. The degree in which cyclic loading affected the ductility of T-stubs was, again, very much dependent on the failure mode. Specimens failing by end-plate bending (mode 1) were characterized by an important decrease of ductility with respect to monotonic loading, due to low-cycle fatigue. On the other hand, ductility of specimens involving bolt failure (modes 2 and 3) was not much affected by cyclic loading. Stiffening of Y-stubs increased their strength, but reduced slightly the ductility.

T-stubs with end-plates realized from high strength steel showed comparable strength with those realized from mild carbon steel. However, one remarks that thinner end plates realized from high strength steel, at the same strength, are provide equal or even larger ductility (due to failure in mode 1 or 2) than thicker mild carbon steel, even if elongation at rupture of high strength steel was lower than the one of mild carbon steel.

The EN1993-1-8 calculation procedure for T-stub components was, in general confirmed by test results, even if the definition of experimental values for yield force still remains a matter of study. Moreover, the use for T-stub of type A, corresponding to the stiffened end-plate, of the same approach as for second bolt row was confirmed, consequently, it can be used to predict the strength and stiffness of bolted beam-to-column joints of stiffened extended end-plates. This confirmation is an important achievement of this research, because the connection of this type has been used for joint specimens ([28]).

Low cycle fatigue interpretation of T-stub tests indicated that welds (double bevel) between components of different steel grades performed safely under cyclic loading, in the sense that detail category values are generally higher than EN 1993-1.9, (see Table 8.5 values).

The elaboration of cyclic test results show the energetic ductility (e.g. dissipation capacity) of T-stubs is given by the following factors:

- T-stub typology: type A – corresponding to stiffened extended-end-plate is in general better than type B (unstiffened extended-end-plate), and almost always than C (the theoretical reference type); the explanation could be a lower sensitivity to low cycle fatigue effects;
- T-stub failure mode: even if the “champion” is TST 16B-S460, which failed in mode 2, statistically, mode 1 is confirmed, as being the “ductile mode” (see EN 1993-1.8 for classification). However, it has to be mentioned that in case of mode 1, the decrease of cyclic ductility compared to monotonic one, mostly for stiffened thin end-plates is significantly larger than in case of failure mode 2 or 3, involving bolt failures (see also [27]);
- Steel grade / plate thickness: the DS solution which combines S460 end-plate with S235 beam is largely better than other combinations. In fact, the worst cyclic behaviour was observed in case of thick S235 end plates; also the thin S690 plates proved a lower ductility. In both cases non-ductile failure modes (mostly 3) and lower strength in fatigue caused an early failure.

## 5.4.5 Beam-to-Column Joints Experimental Program

### 5.4.5.1. Introduction

In the last ten years there is a bigger and bigger demand from steel contractors on the use of high performance steel in members and components connections for steel structures. High performance steel (HPS) is the designation given to steels that offer higher performance in tensile stress, toughness, weldability, cold forming and corrosion compared to mild steel grades [56].

The advantages and disadvantages in use of HPS are highlighted by Galambos [41]. The overall weight of structures can be significantly reduced, resulting in savings in fabrication, erection, transportation to the site and smaller foundations. The reduction of the structural sections means less consumption of steel in construction, as well, which brings benefits, particularly from an environmental point of view. From a mechanical point of view, HPS structures have larger elastic strengths. However, there is no corresponding increase in the Young modulus as the yield stress increases, which may bring some problems of serviceability of structures. Additionally, the ductility of HPS can be limited when compared to mild steels. This can be disadvantageous when the elements are subjected to high-demand deformation conditions, such as seismic events.

Since there is not enough experience in designing steel structures with HPS, and since Eurocode 3 gives rules for the member design up to S460, further research on this subject is needed.

Seismic resistant building frames designed as dissipative structures must allow for plastic deformations in specific members, whose behaviour has to be predicted by proper design. In dual frames (i.e. moment-resisting frames in combination with concentrically braced frames or eccentrically braced frames) members designed to remain predominantly elastic during earthquakes, such as columns for instance, are characterized by high strength demands. Dual steel structural systems, optimized according to a Performance Based Design Philosophy, in which high strength steel is used in "elastic" members and connection components, while mild carbon steel in dissipative members, can be very reliable and cost effective. To get a rational design of a seismic resistant structure – i.e. both safe and economic – the dissipative elements have to approach the plastic capacity under design forces, in order to reduce the demand on non-dissipative members. The best way to accomplish this is not by changing size of sections in dissipative and non-dissipative members because it also changes their stiffness, but to realize them of MCS and HSS, correspondingly. This principle applies both for members and connection components.[27].

The objectives of the beam-to-column joint tests are :

- Evaluation of beam-to-column joint rotation capacity when joint configuration include HSS components.
- Evaluation of the column web shear capacity when joint configuration include HSS components.
- Validation on beam-to-column tests of the assumption that the component of the T-stub corresponding to the outer part of the end-plate can be assimilated in design as a beam web.

A parametric study on two dual-steel building frames has been performed in Chapter 3 of this thesis in order to assess seismic structural performance. Non linear

dynamic analyses were performed. The results of numerical simulations are summarized in Table 5.23. When referring to plastic rotation demands in beams, it has to be considered that the values refer in fact to the beam-column joints as well, if no specific constructional detailing are applied (e.g. dog-bone, beam haunch, etc). It is important to observe the contribution of HSS members in reducing the ductility demand, both for members and joints. However, for beam-to-column joints, at CPLS, this demand still remains significant, particularly for CBF. This fact justifies the interest for experimental study of dual-steel beam-to-column joints (e.g. of both HSS and MCS components).

		EBF	EBF-R46	CBF	CBF-S46	BRB	BRB-S46
		Beams or joints					
ULS	Average	0.014	0.004	0.014	0.003	0.010	0.002
	Maxim	0.016	0.007	0.043	0.016	0.012	0.008
CPLS	Average	0.022	0.014	0.016	0.015	0.012	0.004
	Maxim	0.034	0.021	0.051	0.027	0.020	0.014
		Columns					
ULS	Average	0.007	0.002	0.005	-	0.001	-
	Maxim	0.009	0.004	0.026	0.0001	0.004	-
CPLS	Average	0.0014	0.008	0.007	0.001	0.0011	0.001
	Maxim	0.024	0.017	0.050	0.0022	0.006	0.005

Table 5.23 - Plastic rotation demands (in rad) at ULS and CPLS for the eccentrically and concentrically braced frames, average and maximum of all records

#### 5.4.5.2. Description of testing program

Two types of beam-to-column joints have been tested (Fig. 5.57, Fig. 5.58) resulting a total number of 16 specimens.

- Welded beam-to-column joints;
  - Bolted extended end-plate beam-to-column joints.
- Both monotonic and cyclic loading was applied.

Beams were made of mild carbon steel S235, while columns from both MCS and HSS – S355 and S460. There were 3 types of steel grade used for the end-plates: S235, S460, S690. The thickness of the end-plates have been computed corresponding to no. 2 collapse mechanism. The nominal characteristics of joint specimens are described in Table 5.24.

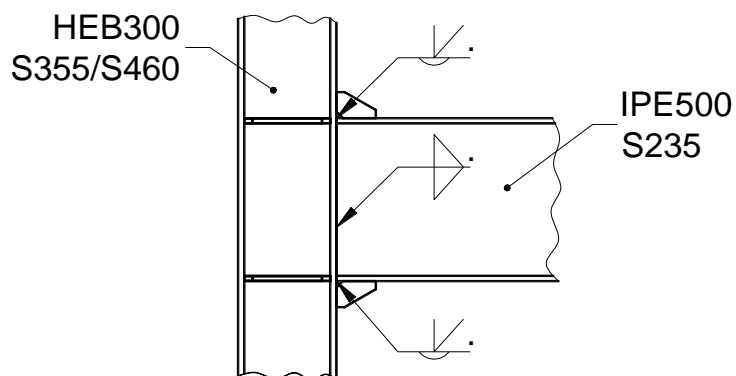


Fig. 5.57 – Welded beam-to-column joint.

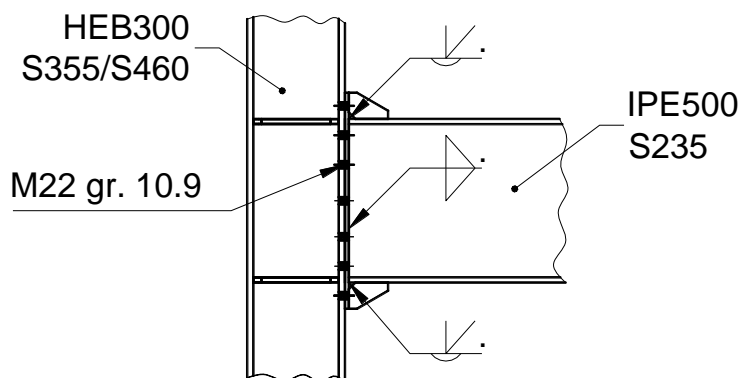


Fig. 5.58 – Bolted extended end-plate beam-to-column joint.

MAG welding was used, with G3Si1 (EN 440) electrodes for welds between MCS components, and ER 100S-G/AWS A5.28 (LNM Moniva) for welds between MCS and HSS components.

Joint type	Label	Column	Beam	End plate
Welded	C355WC	HEB300 (S355)	IPE500 (S235)	-
	C460WC	HEB300 (S460)	IPE500 (S235)	-
Bolted	C355EP12	HEB300 (S355)	IPE500 (S235)	t = 12 mm (S690)
	C460EP12	HEB300 (S460)	IPE500 (S235)	t = 12 mm (S690)
	C355EP16	HEB300 (S355)	IPE500 (S235)	t = 16 mm (S460)
	C460EP16	HEB300 (S460)	IPE500 (S235)	t = 16 mm (S460)
	C355EP20	HEB300 (S355)	IPE500 (S235)	t = 20 mm (S235)
	C460EP20	HEB300 (S460)	IPE500 (S235)	t = 20 mm (S235)

Table 5.24 - Nominal characteristics of joint specimens

The experimental assembling used for beam-to-column specimens can be observed in Appendix B. In the laboratory tests for this type of specimens 3 types of gauges were used:

- 14 displacement transducers (Fig. 5.61)
- force transducers

- optical system Vic3D that measures displacements as well as deformations (Fig. 5.4);

The labelling of the beam-to-column specimens corresponds to the description from Table 5.25 Table 5.5.

Column steel grade	End Plate thickness	Loading type specimen no.
<b>C355EP16_M1</b>		
Column - <b>C</b> <b>S355</b>	End plate - <b>EP</b> <b>12 mm – S690</b> <b>16 mm – S460</b> <b>20 mm – S355</b>	<b>Monotone quasi-static</b> specimen no. <b>1</b>

Table 5.25 – Beam-to-Column legend

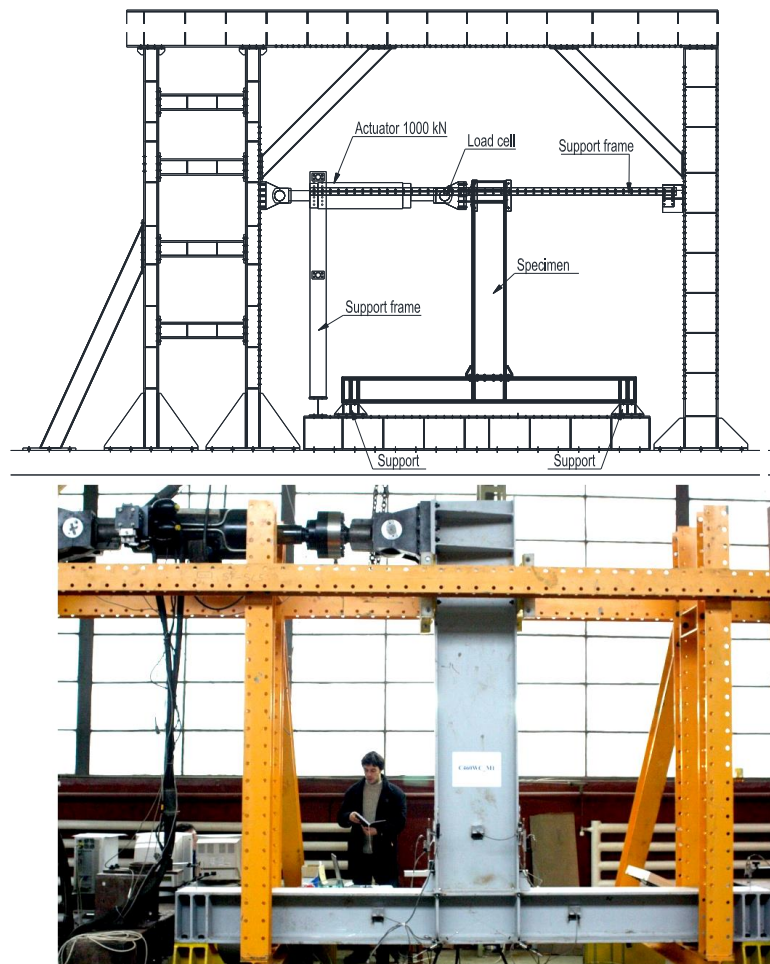


Fig. 5.59 – Beam-to-column joint specimen – test setup

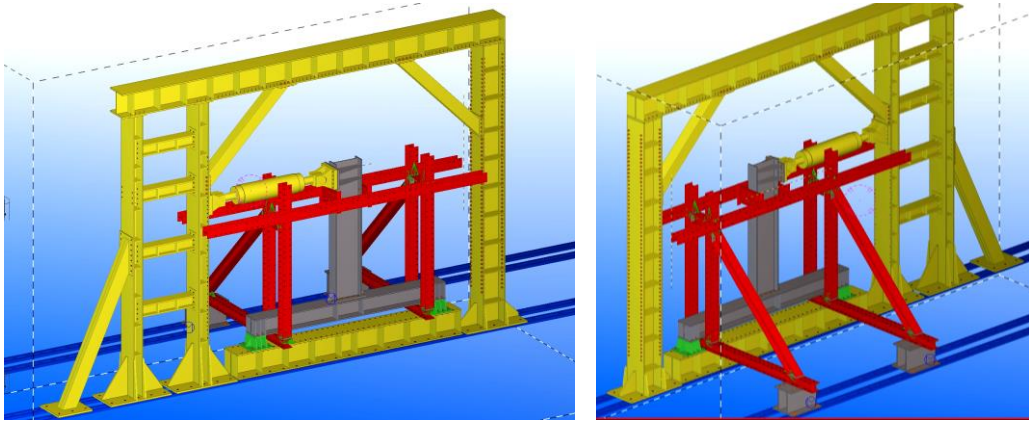


Fig. 5.60 – Beam-to-column joint specimen 3D Model

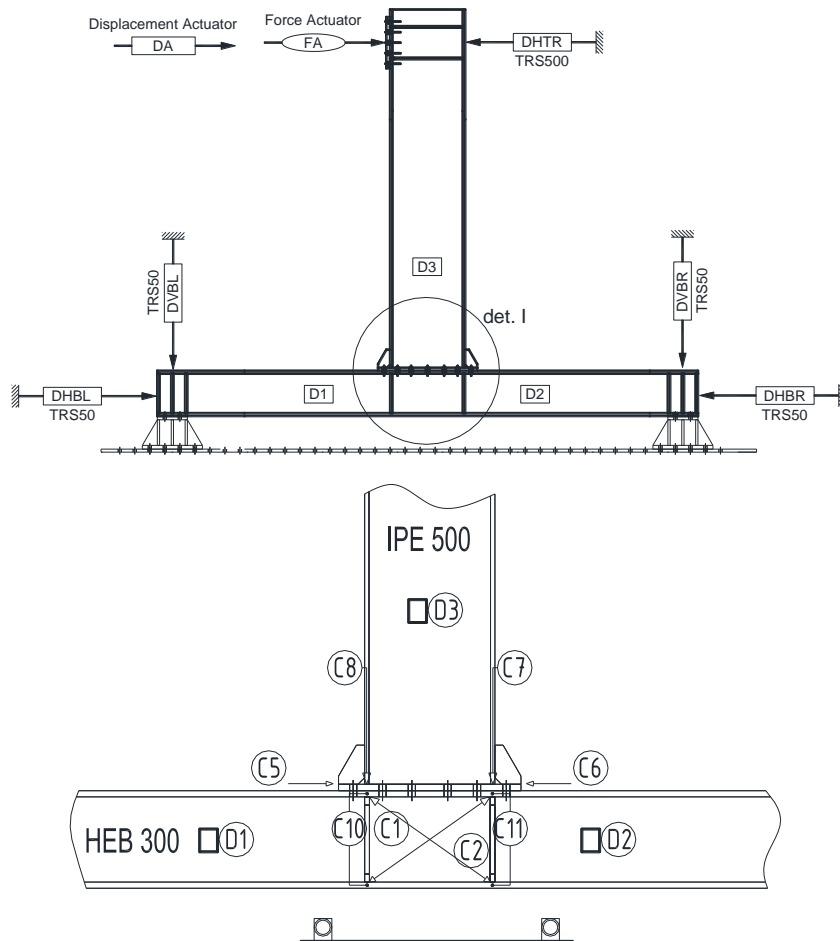
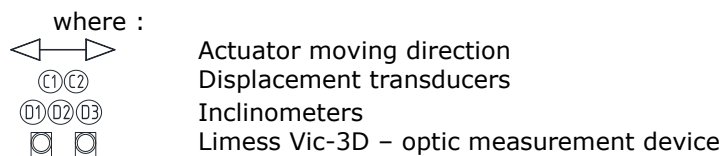


Fig. 5.61 – Measurements devices on beam-to-column joint specimen



Torque wrench tightened partial treated M22 bolts in 24mm diameter holes were used in all test specimens. It was used the same method described at T-stub specimens setup. All bolts were of 10.9 class.

The main features of the test set-up are illustrated in Fig. 5.59, Fig. 5.60, Fig. 5.61. The column was hinged connected to a fixed beam. The load was applied by a 1000KN hydraulic actuator, with maximum piston stroke of  $\pm 200$ mm, through a device that it was welded to the beam free end (Fig. 5.59). Lateral bracing of the entire test setup was provided with a secondary structure as can be seen in Fig. 5.60. The length of the beam 2400mm was chosen to ensure a realistic stress pattern developed at the connection and to be able to obtain ultimate load for joint components with available actuator.

The primary requirements of the instrumentation were the measurement of the applied load, the relevant displacements of the connection (vertical and horizontal displacement of the components and of entire setup regarding to a fixed point from laboratory, angular displacements of beam web and of column web). All measurements have been recorded automatically with intervals of maximum 1 second. It was used the same arrangement of the measuring devices for all test specimens.

EN 1998-1 requires for dissipative moment resistant frames a minimum plastic rotation of beam-to-column joints of 0.035 rad, the contribution of column web being limited to 30%. The reason of this limitation is to prevent premature fracture due to low cycle fatigue in the heat affected zones (HAZ) in the welded connections (e.g. beam-to column, beam-to-end-plate). However, test results currently proved larger contribution of column web [22] and there are authors who recommended extending this contribution to 50% of total inelastic rotation [65]. When HSS columns are used, it can be expected to have a larger elastic component of total rotation capacity of the joint. Also, in case of HSS end-plates, one expects to have a larger capacity to follow in elastic range the distortion of column web in shear and, consequently, a larger margin of safety in regard with low fatigue fracture in HAZ. Having in mind these facts (see also [53]), the joint specimens were designed with strong beams (even the SCWB principle was altered) so that the weakest components would be column web and end-plate.

### 5.4.5.3. Test Results

Materials were supplied by ARCELOR-MITTAL and UnionOcel, Czech Republic. Table 5.26 and Table 5.27 show the measured average values of yield stress  $f_y$ , tensile strength  $f_u$  and elongation at rupture A. Bolts were tested in tension as well (Fig. 5.62), showing an average ultimate strength of 1182.8 N/mm<sup>2</sup>. It can be observed that there is an important difference between nominal and measured material characteristics. On the other hand, an unexpected ductility of S460 is remarked. With these values, the joint properties have been calculated according to EN 1993-1.8 and are presented comparatively with the designed ones in Table 5.28. Due to the fact in EN 1993-1.8 there are no specific provisions for the T-stub component corresponding to the outer part of the end plate (1st bolt row), which was stiffened according to the provisions of AISC (AISC, 2005), a similar procedure



as the one for 2nd bolt row was applied. In fact, the outer "stiffener" was assimilated with beam web. This procedure was confirmed experimentally in the previous paragraph, tests on T-stub specimens.

Nominal steel grade			$f_y$ , N/mm <sup>2</sup>	$f_u$ , N/mm <sup>2</sup>	$A$ , %	Actual steel grade
S235			266	414	38	S235
S460			458	545	25	S460
S690			831	859	13	S690

Table 5.26 - Material properties – flat steel (end-plates, stiffeners) – UnionOcel

Nominal steel (ordered)	Element	Supplier specifications			Tests			Actual steel grade (supplied)
		$f_y$ , N/mm <sup>2</sup>	$f_u$ , N/mm <sup>2</sup>	$A$ , %	$f_y$ , N/mm <sup>2</sup>	$f_u$ , N/mm <sup>2</sup>	$A$ , %	
S235 JR + M (EN 10025-2/2004)	Flange	342	434	31.46	375	470	38	S355
	Web				418	525	25	
S355 JO + M (EN 10025-2/2004)	Flange	453	540	24.86	448	560	32	S460M or ML
	Web				465	603	29	
S460 M (EN 10204/2004/3.1)	Flange	478	598	23.97	464	550	33	S460M or ML
	Web				451	600	30	

Table 5.27 - Material properties – sections, ARCELOR-MITTAL

Specimen	Joint properties		Weakest component			
	$M_{j,Rd}$ [kNm]	$S_{j,ini}$ [kNm/rad]	Bolt row 1 [kN]	Bolt row 2 [kN]	Bolt row 3 [kN]	Bolt row 4 [kN]
C355W	455.8 / 584.1	183184 / 183184	CWPS 941.7 / CWPS 1206.9			
C460W	545.6 / 584.1	183184 / 183184	BFWC 1127.3 / CWPS 1206.9			
C355EP12	447.7 / 563.3	92768 / 92768	EPB 430.5 / EPB 512.8	EPB 430.5 / EPB 512.8	CWPS 80.7 / CWPS 181.2	--- / ---
C460EP12	532.5 / 563.3	92768 / 92768	EPB 430.5 / EPB 512.8	EPB 430.5 / EPB 512.8	EPB 257.1 / CWPS 181.2	BFWC 93.9 / ---
C355EP16	456.4 / 562.2	106830 / 106830	EPB 462.6 / EPB 508.7	EPB 462.6 / EPB 508.7	CWPS 16.6 / CWPS 189.4	--- / ---
C460EP16	549.4 / 562.2	106830 / 106830	EPB 462.6 / EPB 508.7	EPB 462.6 / EPB 508.7	EPB 267.3 / CWPS 189.4	CWPS 19.8 / ---
C355EP20	445.2 / 557.1	112209 / 112209	EPB 421.2 / EPB 489.8	EPB 421.2 / EPB 489.8	CWPS 99.4 / CWPS 227.2	--- / ---
C460EP20	525.0 / 557.1	112209 / 112209	EPB 421.2 / EPB 489.8	EPB 421.2 / EPB 489.8	EPB 229.3 / CWPS 227.2	CWPS 140.6 / ---
Beam plastic resistance $M_{pl,b} = 515.6 / 822.8$ kNm S355 column plastic resistance $M_{pl,c} = 663.5 / 852.3$ kNm S460 column plastic resistance $M_{pl,c} = 859.7 / 852.3$ kNm			$M_{j,Rd}$ - Moment resistance; $S_{j,ini}$ - Initial stiffness; EPB - end plate in bending; CWPS - column web panel in shear; Beam flange and web in compression - BFWC			

Table 5.28 - Properties of joints: nominal / actual material characteristics

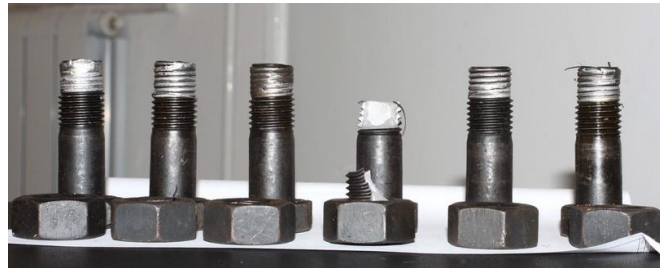
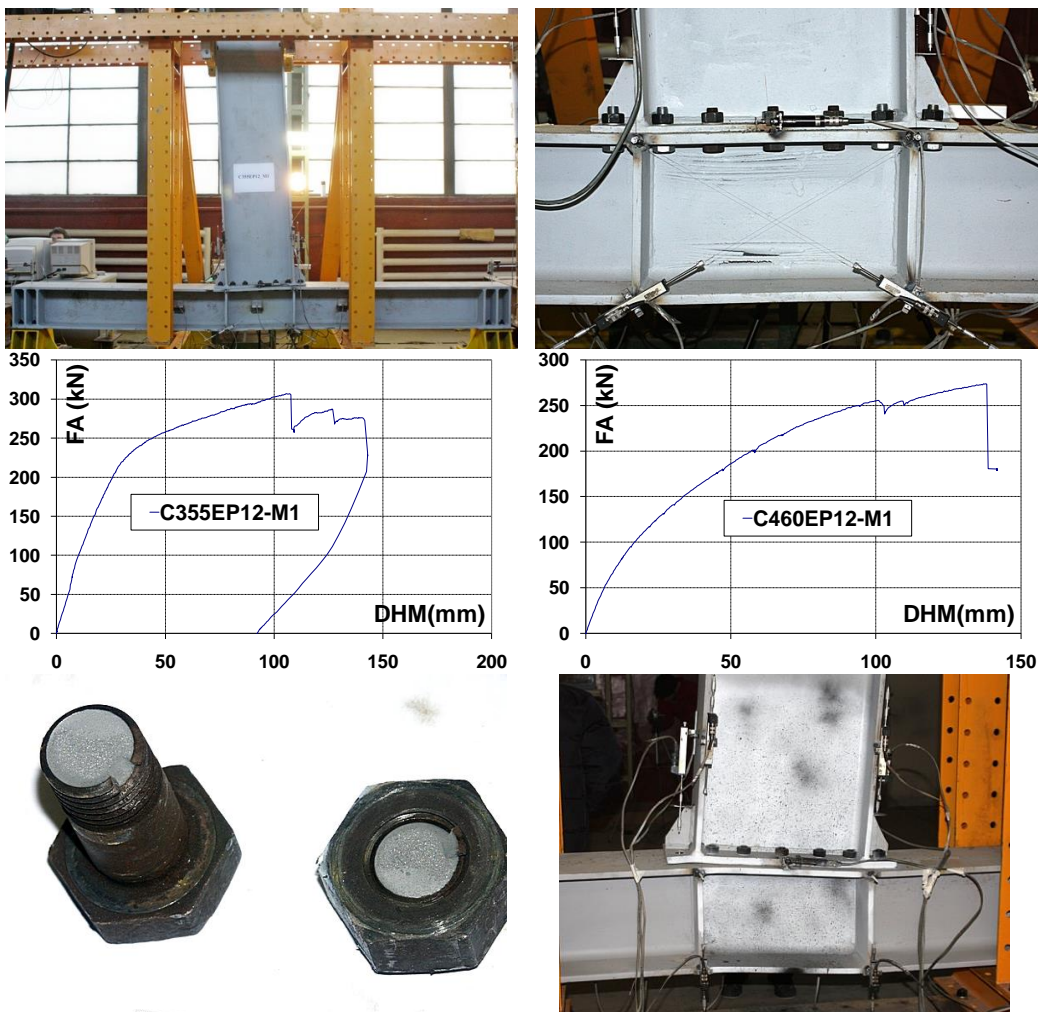


Fig. 5.62 - Bolts collapse mechanism



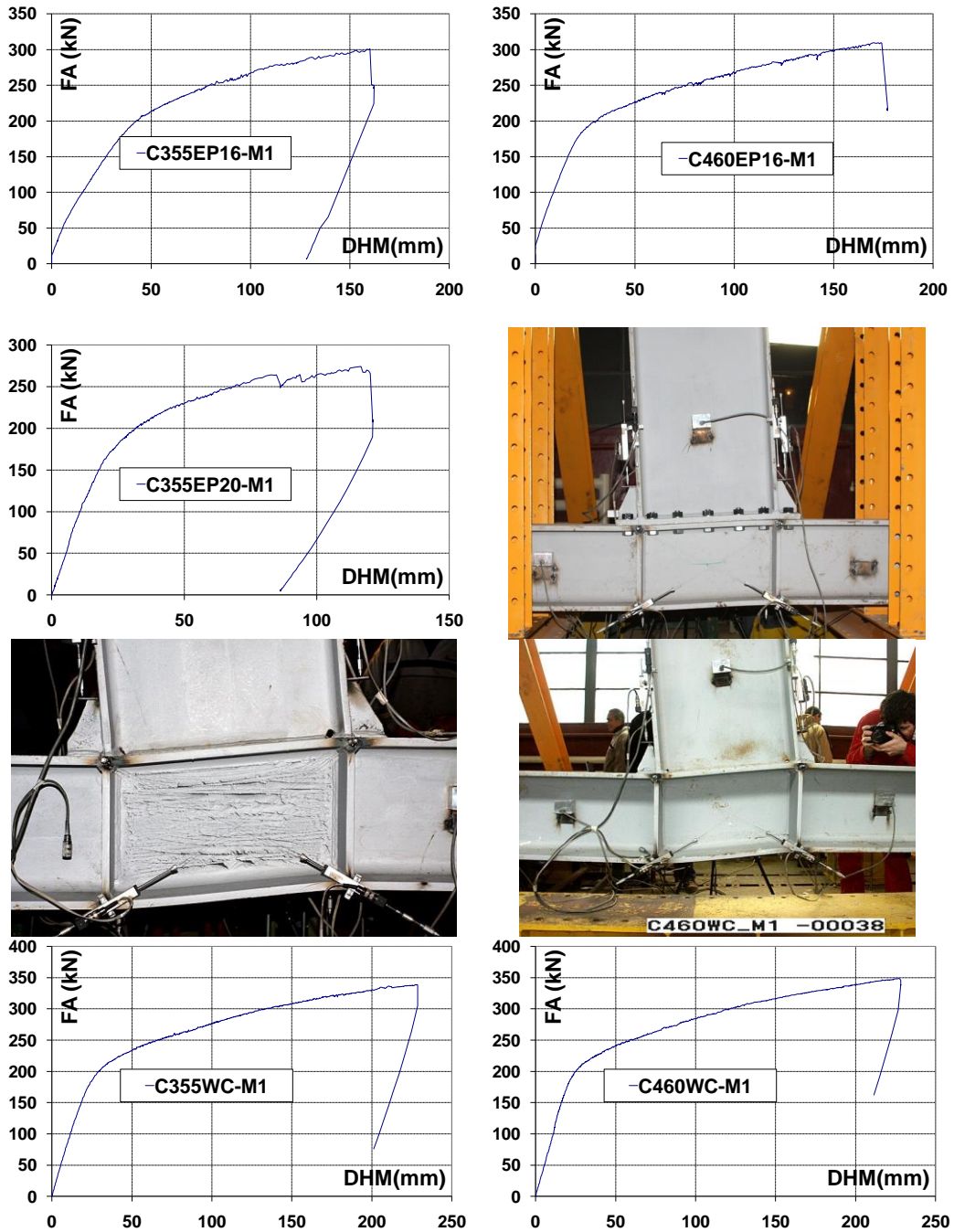


Fig. 5.63 - Force -Displacement relationship for Beam-To-Column specimens loaded Monotonic

The following parameters were determined for each experimental test: initial stiffness  $K_{ini}$ , maximum force  $F_{max}$ , yield force  $F_y$ , and ultimate deformation,  $D_y$ . The initial stiffness was obtained by fitting a linear polynomial to the force-displacement

data between 0 and 25% of the maximum force. The yield force was determined at the intersection of the initial stiffness and tangent stiffness lines, where the tangent stiffness was obtained by fitting a linear polynomial to force-displacement data between 75% and 100% of the maximum force. The ultimate deformation was determined as the displacement corresponding to a 10% drop of the maximum force (Fig. 5.49).

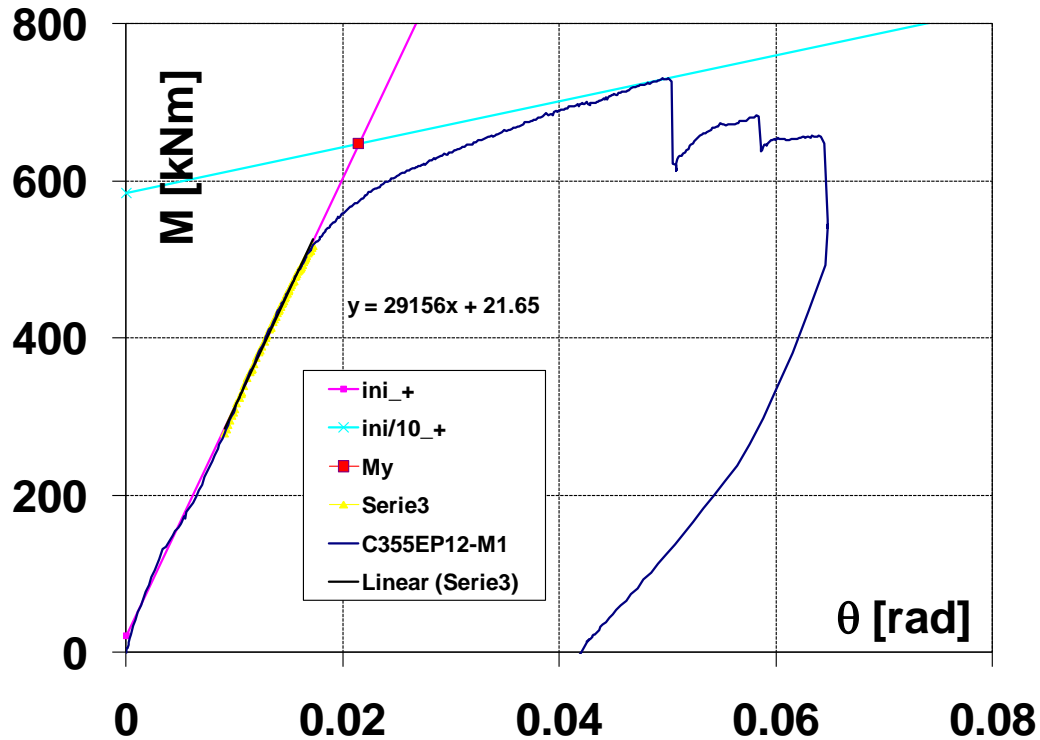


Fig. 5.64 – Experimental characteristics of C355EP12\_M1 specimen

Table 5.29-Table 5.36 shows synthetically the behaviour of tested joints. Associated to that table, there are Table 5.37 and Table 5.38 with the characteristics of the moment – rotation ( $M-\theta$ ) relationship for monotonic and cyclic loading, respectively. It can be observed that column web panel has a major contribution to joint plastic rotation, both under monotonic and cyclic loading. The remainder of plastic rotations was due to end-plate deformations. Analytical predictions by EN 1993-1-8 of the yield moment computed using measured material characteristics were generally conservative with respect to experimental values for monotonic loading. In the case of cyclic loading, experimental values of the yield moment were slightly larger than analytical ones, which is attributed to the procedure used to determine experimental yielding (following procedure from ECCS, 1986).

Monotonic		Cyclic		
$\theta_u$	Failure Mode	Joint Type	Failure Mode	$\theta_u$
0.097	Web column buckling then weld failure	C355WC 	Web column buckling then weld failure	0.060

Table 5.29 – C355WC Test results

Monotonic		Cyclic		
$\theta_u$	Failure Mode	Joint Type	Failure Mode	$\theta_u$
0.098	Web column buckling then weld failure	C460WC 	Web column buckling then weld failure	0.076

Table 5.30 – C460WC Test results

Monotonic		Cyclic		
$\theta_u$	Failure Mode	Joint Type	Failure Mode	$\theta_u$
0.061		C355EP12 		0.039

Table 5.31 – C355EP12 Test results

Monotonic		Cyclic		
$\theta_u$	Failure Mode	Joint Type	Failure Mode	$\theta_u$
0.064		C460EP12 		0.038

Table 5.32 – C460EP12 Test results

Monotonic		Cyclic		
$\theta_u$	Failure Mode	Joint Type	Failure Mode	$\theta_u$
0.068		<b>C355EP16</b> 		0.051

Table 5.33 – C355EP16 Test results

Monotonic		Cyclic		
$\theta_u$	Failure Mode	Joint Type	Failure Mode	$\theta_u$
0.075		<b>C460EP16</b> 		0.039

Table 5.34 – C460EP16 Test results

Monotonic		Cyclic		
$\theta_u$	Failure Mode	Joint Type	Failure Mode	$\theta_u$
0.052		C355EP20 IPE500 S235 EP20mm S235 HEB300 S355		0.018

Table 5.35 – C355EP20 Test results

Cyclic1		Cyclic2		
$\theta_u$	Failure Mode	Joint Type	Failure Mode	$\theta_u$
0.032		C460EP20 IPE500 S235 EP20mm S235 HEB300 S460		0.050

Table 5.36 – C460EP20 Test results



Specimen	$\theta_y$ , rad	$\theta_u$ , rad	$\theta_{panel}^{web}$ , rad	$M_y$ , kNm	$M_{max}$ , kNm
C355WC-M1	0.011	0.097	0.097(100%)	519	787.8
C460WC-M1	0.011	0.098	0.098(100%)	521	830.1
C355EP12-M1	0.013	0.061	0.037(61%)	598.7	729.2
C460EP12-M1	0.016	0.064	0.046(72%)	524.9	650.3
C355EP16-M1	0.015	0.068	0.061(90%)	556.9	716.2
C460EP16-M1	0.011	0.075	0.075(100%)	516.3	736.1
C355EP20-M1	0.012	0.052	0.042(81%)	527	652.3
C460EP20-M1	-	-	-	-	-

Table 5.37 - Characteristics of joints under monotonic loading

Specimen	$\theta_y$ , rad	$\theta_u^+$ , rad	$\theta_u^-$ , rad	$\theta_{panel}^{web}$ , rad	$M_y$ , kNm	$M_{max}^+$ , kNm	$M_{max}^-$ , kNm
C355WC-C1	0.009	0.060	0.059	0.059(100%)	543.1	748.8	756.2
C460WC-C1	0.010	0.076	0.059	0.076(100%)	658.4	959.3	916.3
C355EP12-C1	0.013	0.039	0.039	0.030(77%)	567.3	670.8	661.2
C460EP12-C1	0.015	0.038	0.038	0.027(71%)	664.9	733.8	741.8
C355EP16-C1	0.012	0.051	0.049	0.036(70%)	564.3	706.8	679.6
C460EP16-C1	0.014	0.039	0.045	0.026(58%)	620	737.6	761.8
C355EP20-C1	0.012	0.018	0.035	0.035(100)	617.6	635.2	685.2
C460EP20-C1*	0.015	0.031	0.032	0.022(69%)	600	659.6	651.7
C460EP20-C2	0.014	0.050	0.048	0.033(66%)	616	731.3	683.9

\* Displacement amplitude of cycles, after attainment of yield displacement  $d_y$ , of  $\pm 2d_y$ ,  $\pm 4d_y$ , ..., according to ECCS Recommendation (ECCS, 1986). All other specimens have been tested with cycles of  $d_y$ ,  $\pm 2d_y$ ,  $\pm 3d_y$ ,  $\pm 4d_y$  ...

Table 5.38 - Characteristics of joints under cyclic loading

In Fig. 5.65 is shown the state of strain in the column web panel of bolted specimens under monotonic loading, obtained using the digital image correlation technique. It can be observed that the web panel has a major contribution to plastic deformations of the joints, conclusions that can be also observed from Table 5.37.

In Table 5.39, a brief description of failure modes of joints is presented and in Fig. 5.66, a selection of photos during testing of specimens. It is also useful to remark the fact that residual rotation was in the range of 0.04 – 0.06 rad for bolted joints and around 0.08 rad for welded ones.

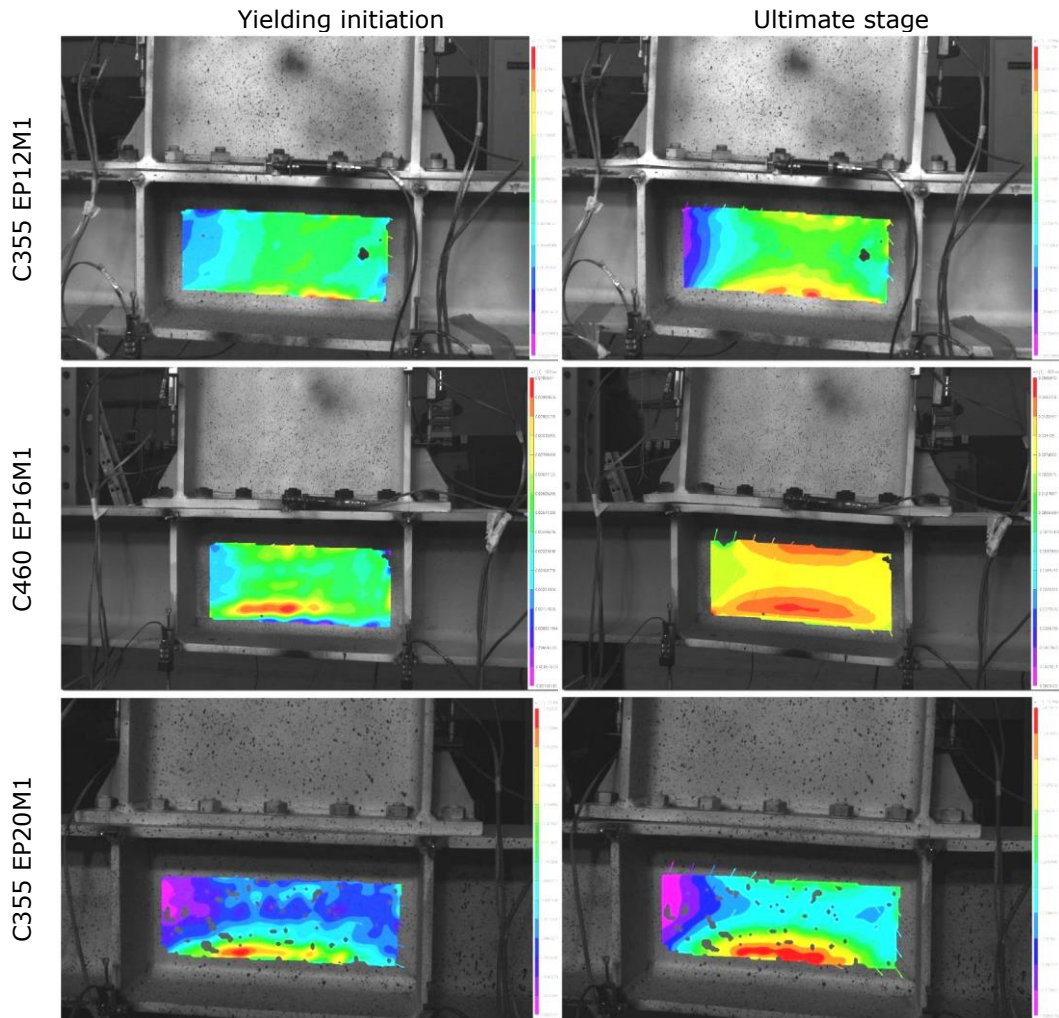
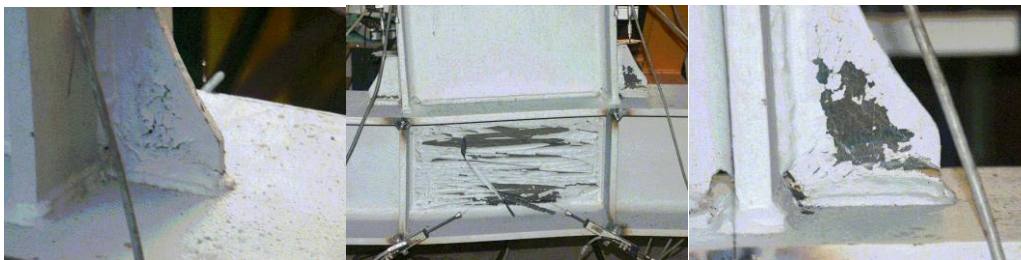


Fig. 5.65 - State of strain in the column web at yield and failure using digital image correlation technique



**C355WC-C1**



**C460WC-M1**



**C460EP12-M1**



**C355EP12-M1**



**C355EP12-C1**



**C460EP16-M1**





Fig. 5.66 - Joint tested specimens

C355WC-M1	Buckling of compressed stiffener between column and beam flanges; shearing of panel zone; buckling of beam flange; weld cracks initiated at stiffener in tension (max displacement 200mm)
C355WC-C1	$2e_y$ – shearing of panel zone; 4(6) $e_y$ – weld cracks initiated at stiffener in tension
C460WC-M1	Buckling of compressed stiffener between column and beam flanges; shearing of panel zone; buckling of beam flange; weld cracks initiated at stiffener in tension (max force 3490kN)
C460WC-C1	$2e_y$ – shearing of panel zone; 4(6) $e_y$ – weld cracks initiated at stiffener in tension
C355EP12-M1	End plate visible deformations in tension zone; shearing of panel zone; T-stub in mode 2 and bolt failure
C355EP12-C1	$3e_y$ – end plate visible deformations on both directions; $4e_y$ – small weld cracks at stiffeners; shearing of panel zone; T-stub in mode 2 and bolt failure
C460EP12-M1	End plate visible deformations in tension zone; shearing of panel zone; T-stub in mode 2 and bolt failure
C460EP12-C1	$3e_y$ – end plate visible deformations on both directions; $4e_y$ – small

	weld cracks at stiffeners; shearing of panel zone; T-stub in mode 2 and bolt failure
C355EP16-M1	Small end plate visible deformations in tension zone; shearing of panel zone; bolt failure in mode 3
C355EP16-C1	3e <sub>y</sub> – end plate visible deformations on both directions; 4e <sub>y</sub> – small weld cracks at stiffeners; shearing of panel zone; T-stub in mode 2 and bolt failure
C460EP16-M1	End plate visible deformations in tension zone; shearing of panel zone; T-stub in mode 2 and bolt failure
C460EP16-C1	Important end plate visible deformation in tension zone; shearing of panel zone; T-stub in mode 2 and bolt failure
C355EP20-M1	Small end plate visible deformation in tension zone; shearing of panel zone; bolt failure in mode 3
C355EP20-C1	Small end plate visible deformation in tension zone; shearing of panel zone; bolt failure in mode 3
C460EP20-C1	3(4) e <sub>y</sub> – small end plate visible deformation in tension zone; shearing of panel zone; bolt failure in mode 3
C460EP20-C2	3(4) e <sub>y</sub> – small end plate visible deformation in tension zone; shearing of panel zone; 4e <sub>y</sub> – bolt failure in mode 3; 5e <sub>y</sub> – weld cracks initiated at stiffeners

Table 5.39 - Brief description of failure modes of joint specimens

#### 5.4.5.4. CONCLUDING REMARKS

It is clear that due to the significant difference between design and actual values of materials that tested specimens are practically other than initially planned. However, the intention to test and evaluate performance of joint specimens of S460 columns has been realized. By increase of beam strength, its contribution to the joint deformability was practically inhibited, but the end-plates have performed as planned. Following conclusions can be announced:

- A very good ductility of HSS component was observed;
- Excepting one case, all cyclic specimens demonstrated their rotation capacity, at least equal to the limit of 0.035 rad specified in EN 1998-1;
- The contribution of web panel larger than 30% does not affect the robustness of joints
- Thick end-plates, even of MCS, reduce the ductility of joints without significant increase of moment capacity.
- No significant degradation of capacity was observed from monotonic to cyclic results.
- The analytical prediction of joint moment resistance based on component method of EN 1993-1.8 seems to be good enough in this case, and the procedure used for the outer bolt row is confirmed.
- The control of upper limit of yield strength is of real importance and fabricators must find a way to introduce that on the material specification, additionally to the lower limit, otherwise the real response of the structure can be very different from the one predicted through design.

Based on experimental results on beam-to-column joints specimens obtained in research program of the base of present thesis, but also on previous results tests obtained in CEMSIG laboratory or in PhD thesis realised by researchers of PUT Timisoara in INSA RENNES (see Appendix A) the ratio between monotone

plastic rotation capacity of a joint and cyclic one is in average 0.50-0.60 . This ratio can be observed in terms of displacement capacity also on T-stubs according to tests presented in this thesis.

Data presented in Appendix A examines this problem using relevant interpretation of the experimental research results obtained by the research team at the "Politehnica" University of Timisoara, INSA of Rennes and collected from the literature.

## 6 NUMERICAL MODELLING PROGRAM

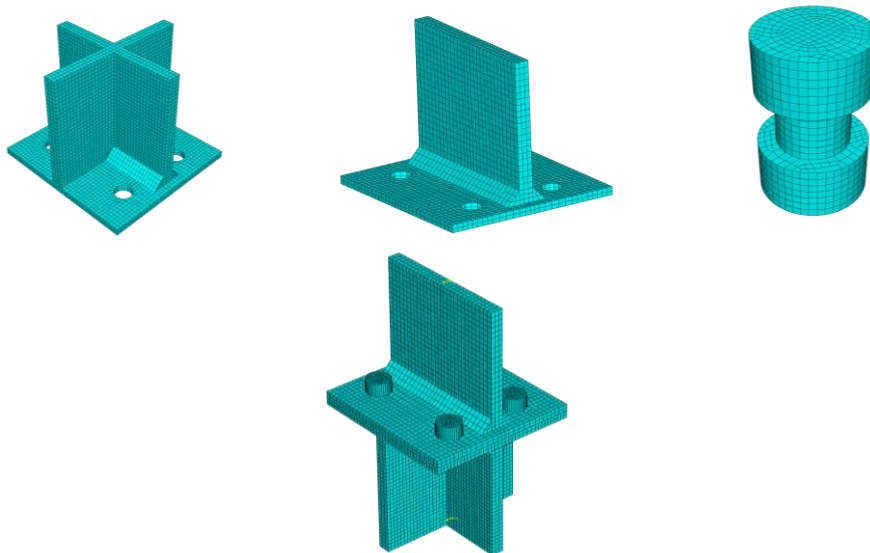
### 6.1 Introduction

The objectives of numerical program was to extend the results obtained by testing on T-stubs and Joints specimens. On this purpose a parametric study was developed on similar typologies of T-stub specimens but with different size, steel grade, arrangements as well on beam-to column specimens. The main idea was to see how the global performance of the joint namely moment capacity and ductility can be controlled by the T-stub macro component.

The finite element environment ABAQUS v6.5 to v6.7 (SIMULIA, 2007) was used to simulate numerical models program. Three different numerical model types were built.

- T-stub models (corresponding to a real joint configuration)
- Beam-to-Column models (corresponding to a real joint configuration)
- Beam-to-Column models (exactly numerical equivalence of joints presented and tested in Chapter 5-Experimental program)

All models were three-dimensional. Deformable bodies were meshed by solid continuum finite elements. The geometry of a model was defined by parts, positioned relative to one another in an assembly. All models consisted of at least two parts: bolts and steel plate(s) . Different interactions were prescribed between parts. The full Newton solution method with nonlinear effect of large deformations and displacement was used to trace nonlinear load-displacement curve.



Tabel 6.1 –T-stub FEM specimens

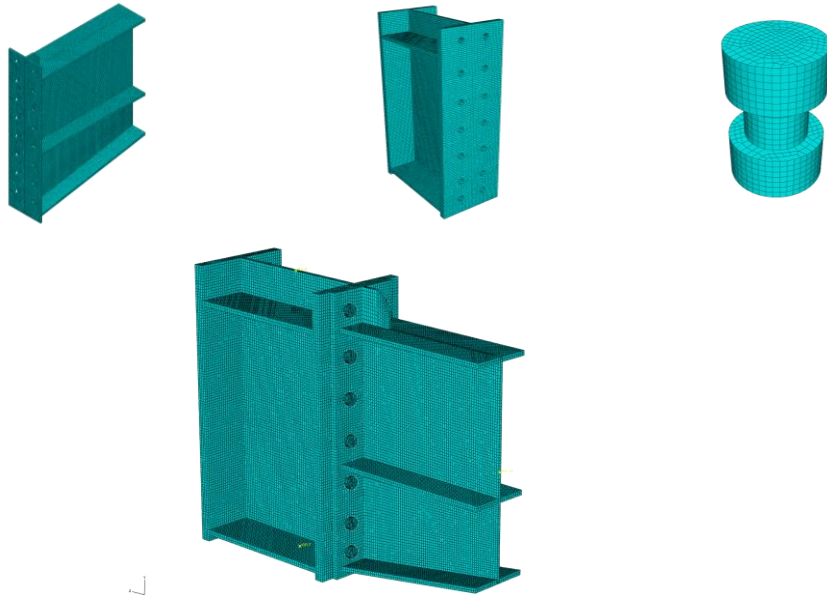


Table 6.2 –Beam-to-Column FEM specimens (BUC & BV)

The used Finite Element type it was the same for all specimens, continuum solid element (brick element) C3D8R (reduced integration with hourglass control) of stress/ displacement type. For material it was used an elastic perfectly plastic model. Between the end plate – column flange and bolts a normal “hard contact” law was defined, with the surfaces separation possibility.

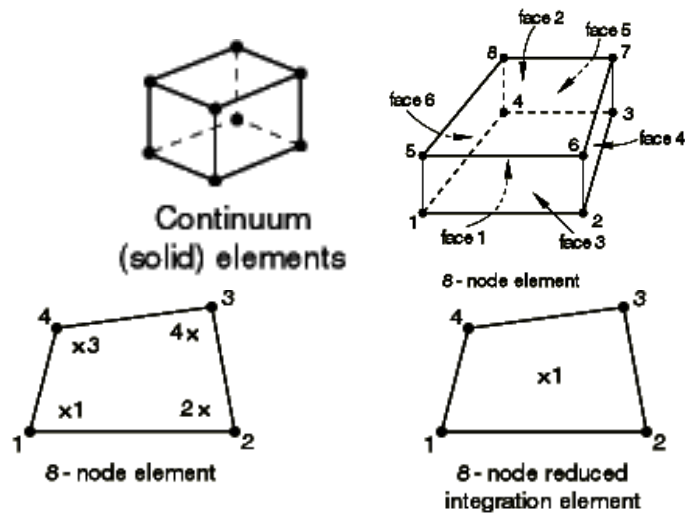


Fig. 6.1 - Continuum solid element – 8 node element

Washers were not considered in numerical model.

To each element it was assigned a defined type of material elastic perfectly plastic model( Fig. 6.2).



The finite element mesh was generated automatically on the basis of approximate element size for a specified cell. Cells were constructed from each part in the model. The largest finite element edge size was equal to plate thickness, if the thickness was smaller than 10 mm. At plate thickness equal to or larger than 10 mm, the edge size was 7,5 mm. There were at least two elements in thickness direction. The mesh was generally denser in the zone of boltholes (end-plates and flanges)

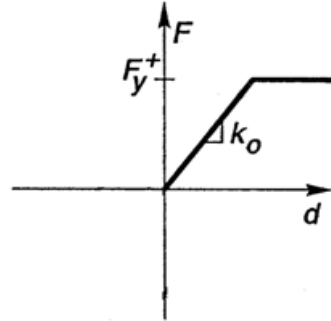


Fig. 6.2 - Elastic perfectly plastic steel material curve.

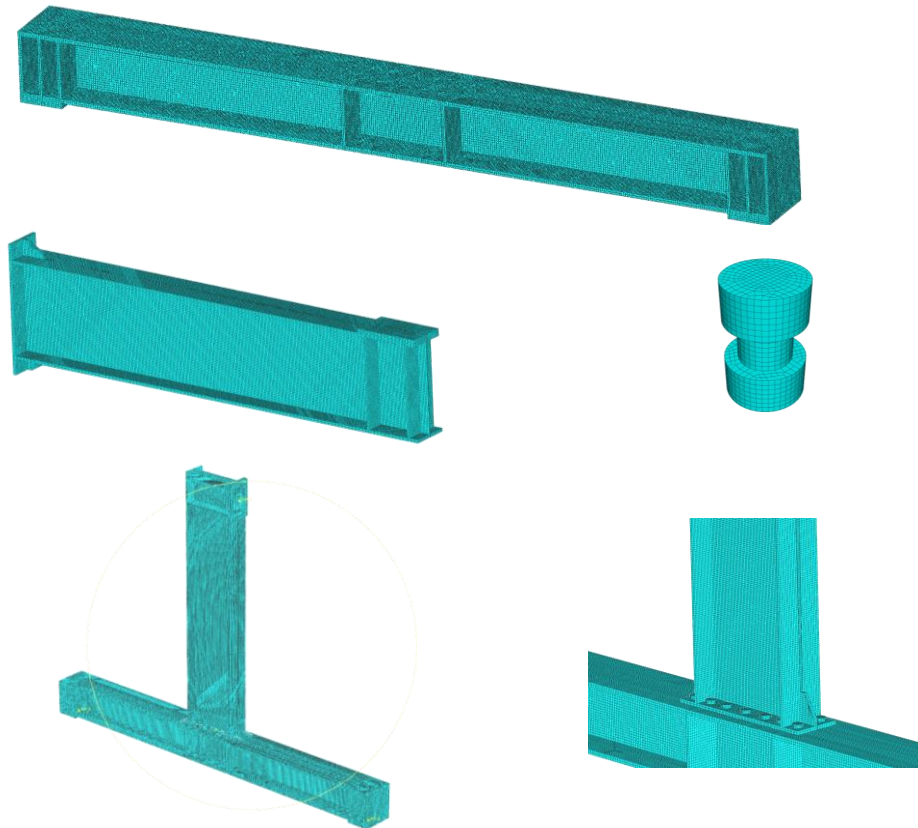


Table 6.3 –Beam-to-Column FEM specimens

According to seismic design provisions [34] Moment Resisting Frames (MRF) comprise full strength/rigid joints, which are demanding a minimum plastic rotation capacity  $\phi_{pl}=0.035\text{rad}$ , and the overstrength of moment capacity of the joint of, at

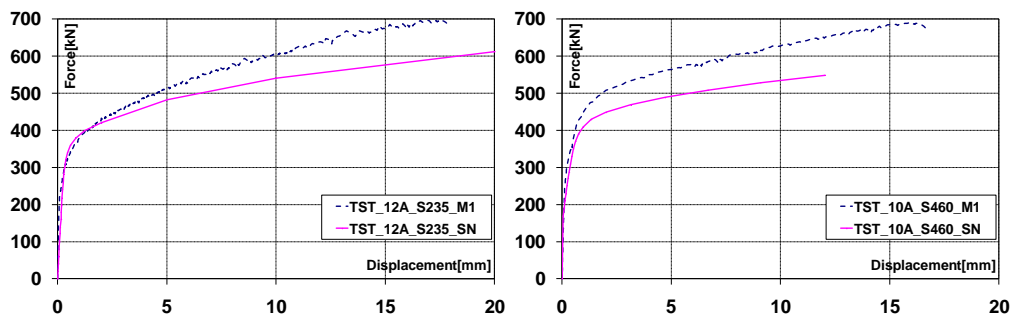
least 1.375 times the plastic bending moment of the beam; for partial resistant/semi-rigid joints the plastic rotation capacity  $\phi_{pl} > \phi_{pl, necessary}$ .

It is well-known that T-stub macro-component is falling down by 3 types of failure mode, named 1, 2 and 3 Table 6.4. After developing the experimental program and starting from previous considerations it was clear that failure mode 2 would be preferable in order to answer both criteria full strength and rotation capacity. Starting from experimental results presented in previous chapter and from a real joint configurations were developed some numerical studies in order to establish the borders for T-stub macro-component failure mode 2→1 and 2→3, and to verify their classification and behaviour in between; after that we are returning to the joints to verify also their classification and behaviour as failure mode in connection with the T-stub.

From the experimental program, a FEM model was settled for T-stub macro-component. The idea it was to start from some real rigid full-resistant joints, to settle the dimensions and steel grade of end plate in order to obtain the borders of type 2 failure mechanism, to make a numerical analysis on extracted T-stubs and compare the results with the theoretical ones and finally to come back to the joints and verify their behaviour and failure mode.

## 6.2 NUMERICAL ANALYSIS

The numerical analysis was started with T-stub simulation. To calibrate the numerical model developed in ABAQUS an analysis was made between Force-Displacement curves obtained by numerical simulation and by experimental tests. The results are presented in Fig. 6.3. It can be observed that the curves are similar in both cases and the numerical simulation failure mode corresponds to experimental failure mode. Due to the large number of specimens and due to god results there were simulated only T-stub corresponding to "thin" end plate.



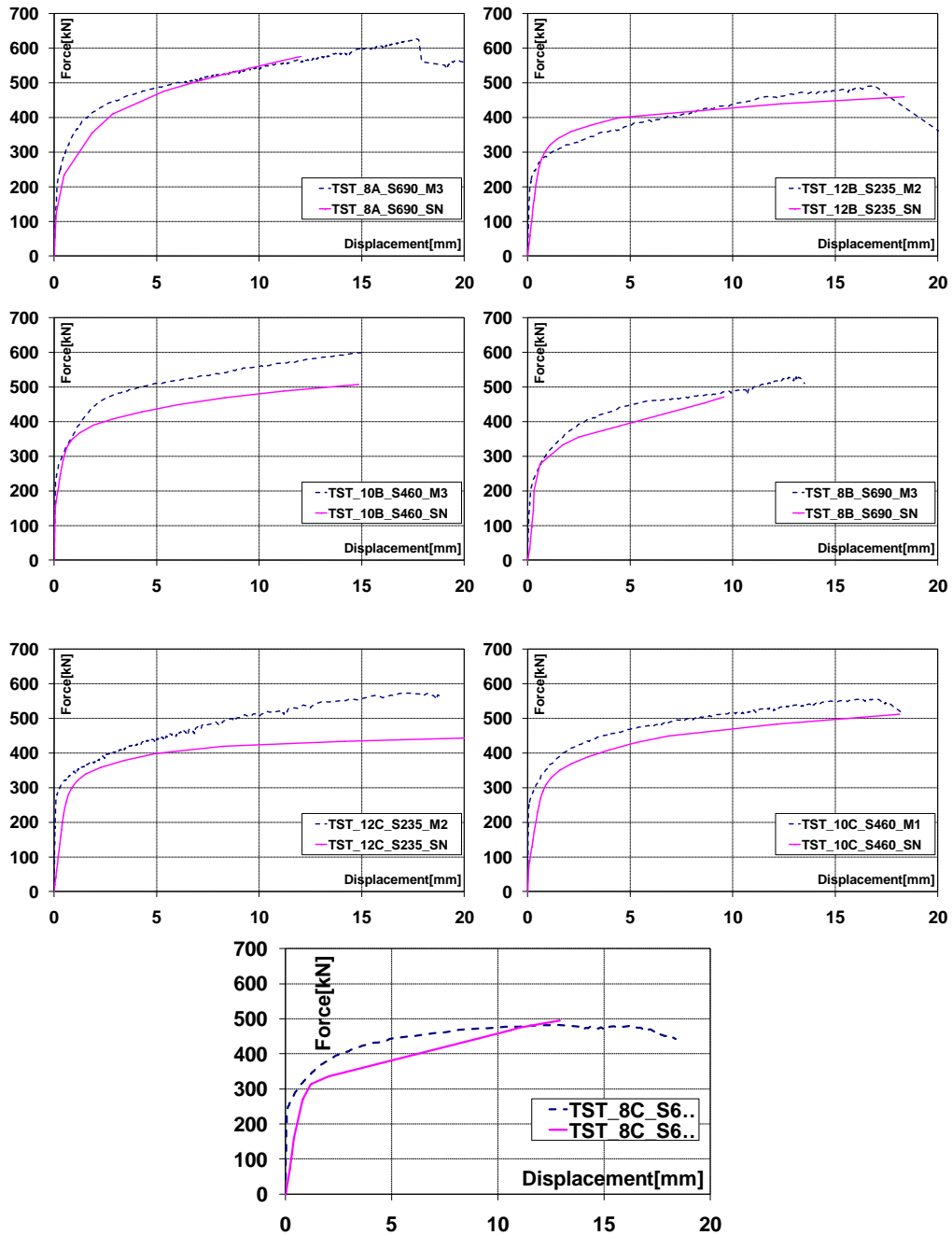


Fig. 6.3 – T-stubs numerical vs. Experimental results

To calibrate the numerical models developed in ABAQUS, a series of analysis were conducted in order to compare the Force-Displacement curves, numerical vs.

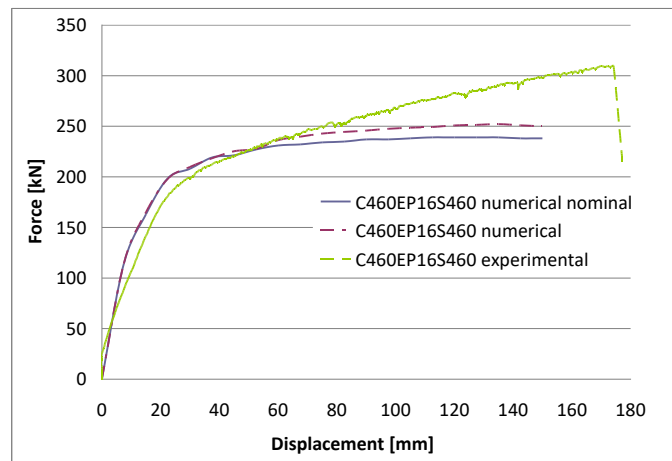
Experimental for a given joint specimen. Considering the nominal and real characteristics of steel.



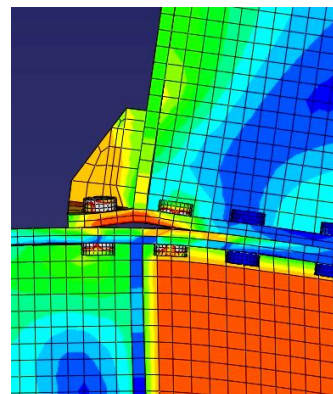
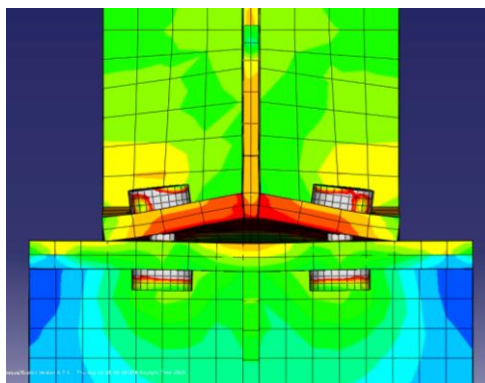
a) Joint configuration



b) Experimental T-stub failure (2→1)



c) C460 EP16 S460



d) Numerical T-stub failure (2→1)

Fig. 6.4 – C460EP16S460 Numerical versus experimental results

The results are presented in Fig. 6.4c for different joints, where C460EP16S460, for instance means column of S460 steel grade and end-plate of the beam with 16mm thickness and made by S460 (Fig. 6.4a). In the second case it differs only the end-plate being with a thickness of 12mm and by steel S690 (Fig. 6.5). It can be also observed that the numerical simulation failure mode (2→1) (Fig. 6.4d, Fig. 6.5c) is the same with the experimental one ( Fig. 6.4c, Fig. 6.5b). It can be observed that the curves obtained numerically fit well with the experimental one in all cases.

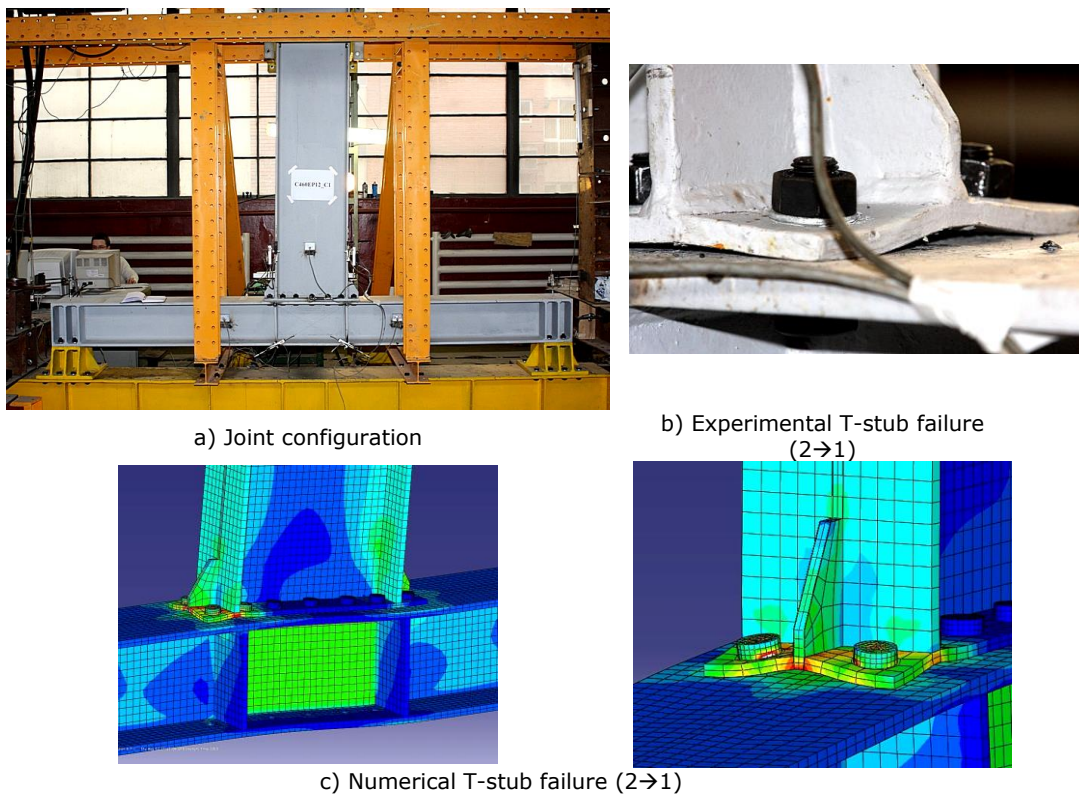


Fig. 6.5 – C460EP12S690 Numerical versus experimental results

During the experimental research, it was used for the end plate of T-stub macro-component, different steel grades as S355, S460 and S690. It is well known that the failure mode of a T-stub macro-component could be type 1, 2 or 3, which means ductile, semi-ductile and fragile (Table 6.4).

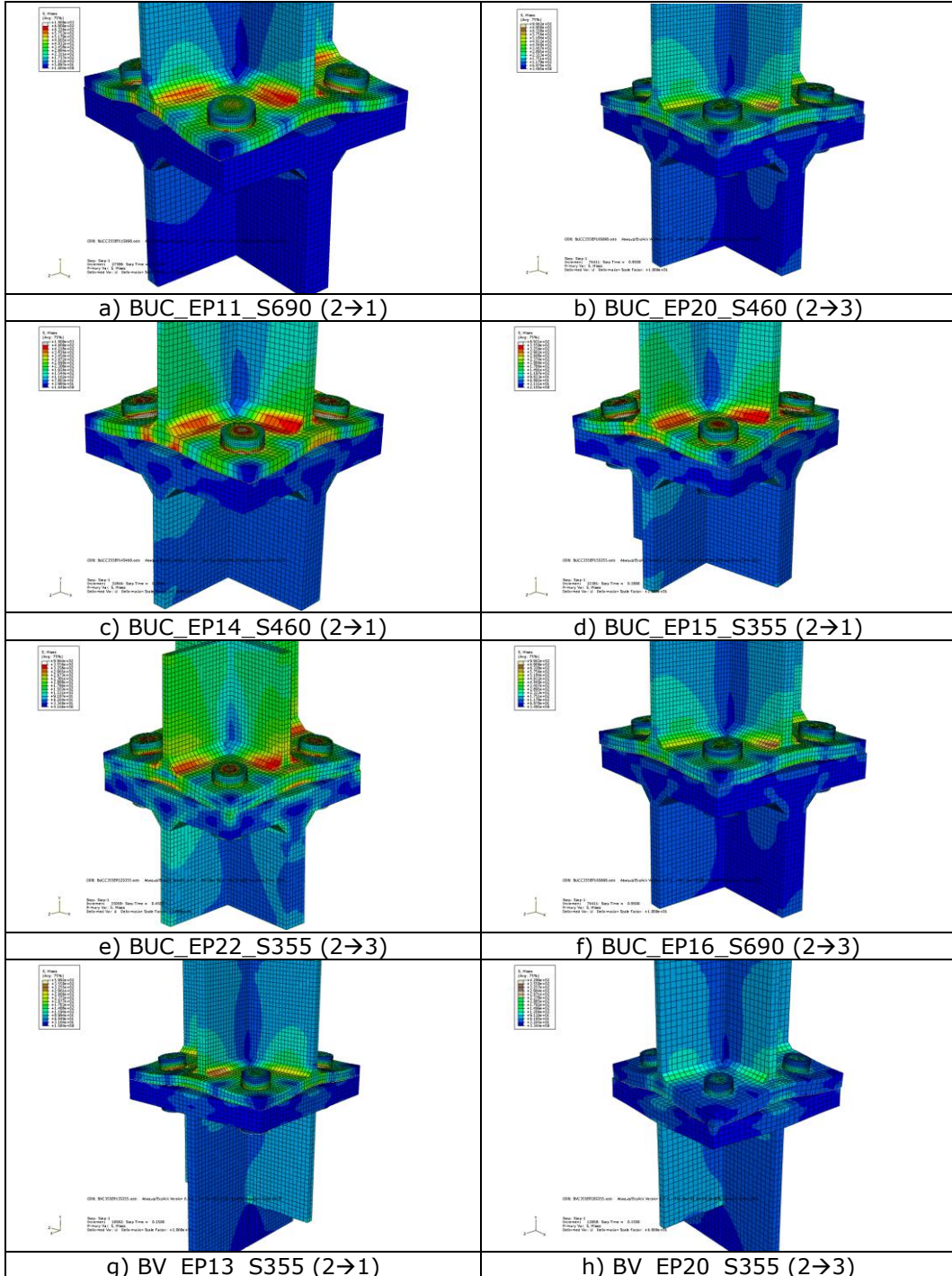
Failure mode	Ductility	Classification
Mode 1	Ductile	Partial-strength / Semi-rigid
Mode 2	Semi-ductile	Full strength / Rigid
Mode 3	Fragile	Full strength / Rigid

Table 6.4 - Classification of joints according to T-stub failure mode

In order to observe the stiffness of the numerical model and to evaluate the influence of the T-stub component in the behaviour of the joint and the rotation capacity, the numerical analysis continued [66] with two types of real rigid full-







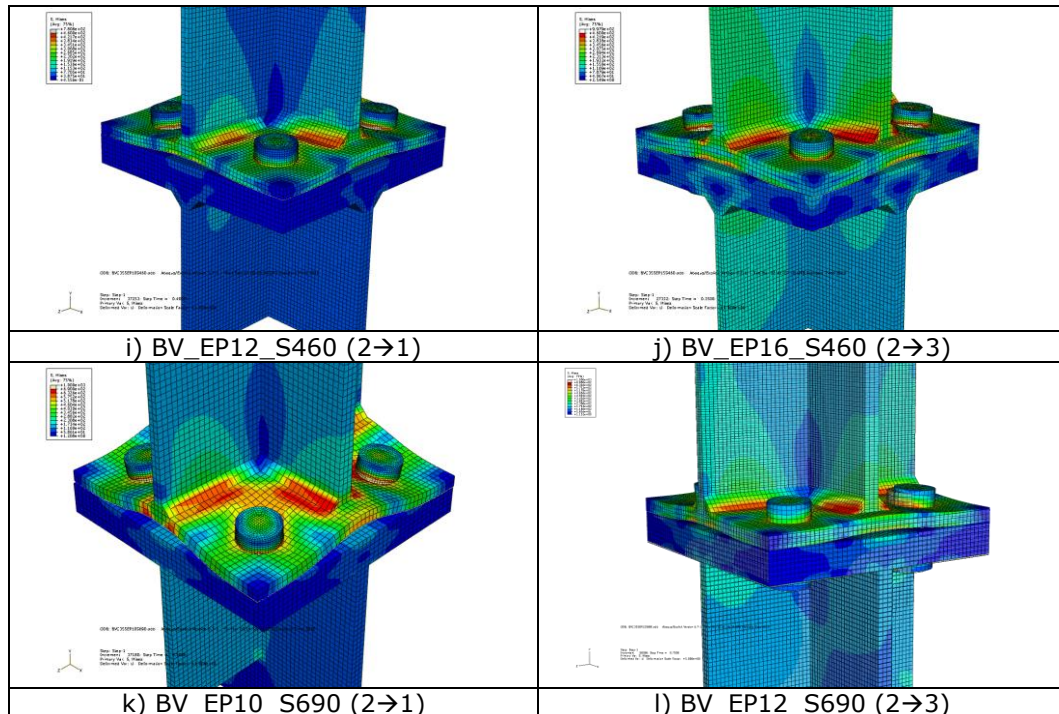


Fig. 6.8 - T-stub behavior and failure mode according to numerical analysis

In failure mode (2), at the end, almost always, the bolt failure (3) might occur. In case of T-stubs designed for failure mode (2→1) (Table 6.5a), which are more ductile, first occurs the plasticization near the end-plate – beam flange junction, and starts the plasticization near the 1st and 2nd bolt rows, prior bolt fractures; in case of specimens of (2→3) failure mode (Table 6.5b), the second plasticization, usually does not occur, and bolt failure (3) arrives earlier. In order to check the behaviour of T-stubs in the MR joints, the response of two specimens of Table 6.6 has been simulated with ABAQUS, for monotonic loading only. The results, with a zoom of T-stub deformation mode are displayed in Fig. 6.11.

Going back from the T-stub to the joints, we analyzed numerically also with ABAQUS, two types of joints from the same family, e.g. Bucharest, but with T-stub configuration from the 2 borders of failure mode (2→1) and (2→3). In Fig. 6.11 there is evident that both are confirming the way that they were designed.



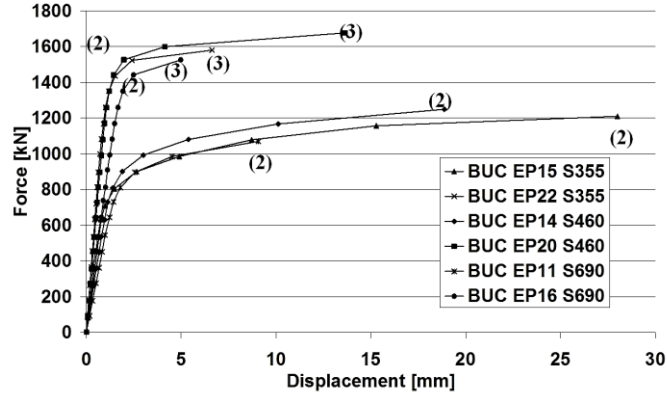


Fig. 6.9 - -Bucharest T-stub behaviour according to numerical analysis

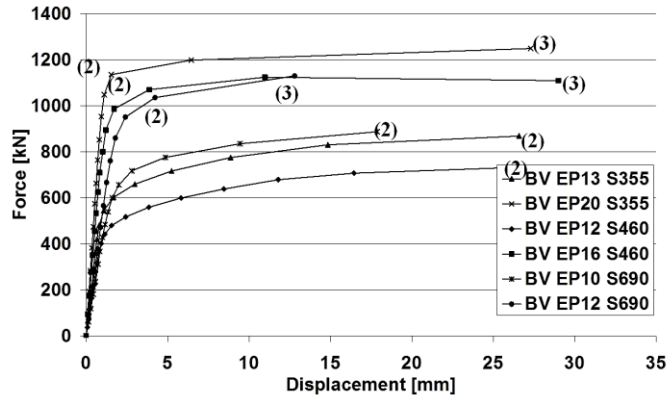


Fig. 6.10 – Brasov T-stub behaviour according to numerical analysis

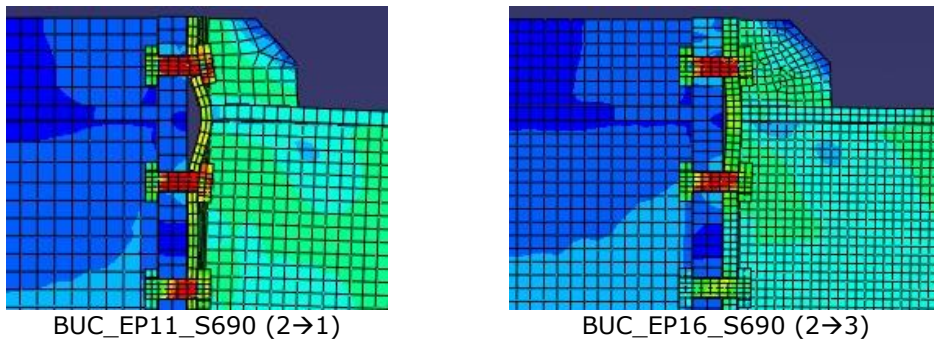


Fig. 6.11 – Bucharest Joint behaviour

In such a joint, where the web panel distortion is limited the rotation capacity supply could be concentrated mainly in the T-stub macro-component which practically controls the ductility of joint.

It was demonstrated by numerical simulation of beam-to-column joints designed for a real building frame, that in case where the column web plastic de-

formation is inhibited, the rotation capacity of the joint can be calculated by end-plate, normally (see Fig. 6.12).

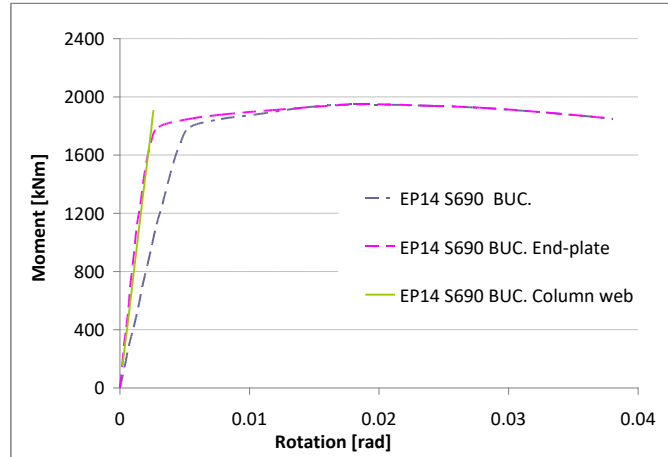
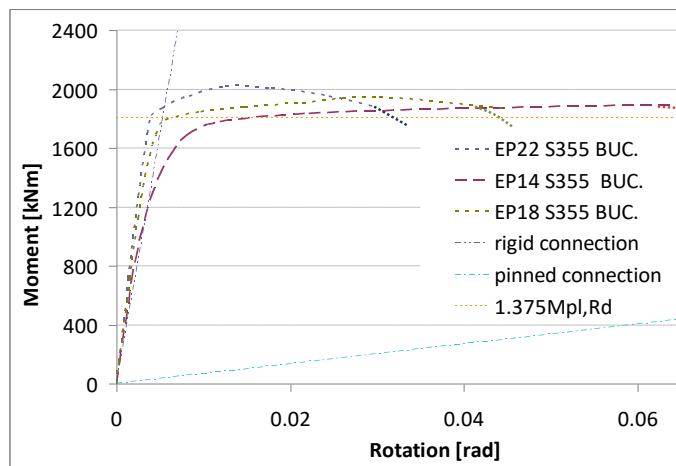


Fig. 6.12 - Joint rotation capacity with components (web panel and end-plate)

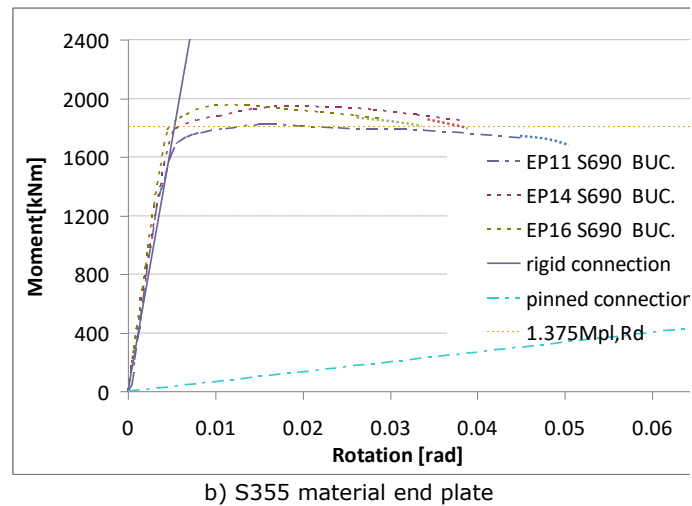
A parametrical study was developed in order to verify previous assumption, so for the real joint of Bucharest structures different configurations were designed in order to have failure mode 2→1, 2→3 and 2. Results of numerical analysis are shown in Fig. 6.13 and the rotation capacity of the joints in Tabel 6.7.

End plate steel grade	Failure mode 2→1	Failure mode 2	Failure mode 2→3
S355	0.080	0.055	0.035
S460	0.080	0.055	0.035
S690	0.055	0.045	0.035

Tabel 6.7 - Joint rotation capacity under numerical analysis



a) S690 material end plate



b) S355 material end plate  
Fig. 6.13 - Joint rotation capacity under numerical analysis

The joint, through the T-stub macro-component is able to develop enough rotation capacity if necessary, if the failure mode of the T-stub is between the borders (2→1) and (2→3), while the column web remains predominantly elastic. The failure mode can be modified by design playing with steel grade and thickness of the end-plate.

The ultimate plastic rotation is usually established at 20% drop of moment compared to maximum value. In previous research, the authors have shown that rotation capacity under cyclic loading could be around 50-60% of the rotation capacity of the joint under monotonic loading.

An example could be in Table 6.8, where, the values of the rotation of the joints from experimental program, under monotonic and cyclic loading can be verified.

Joint configuration	Monotonic $\theta_{pl,m}$	Cyclic $\theta_{pl,c}$	Ratio $\theta_{pl,c} / \theta_{pl,m}$
C355 EP12 S690	0.050	0.030	0.60
C355 EP16 S460	0.050	0.030	0.60
C355 EP20 S355	0.040	0.025	0.625
C460 EP12 S690	0.050	0.030	0.60
C460 EP16 S460	0.060	0.030	0.50
C460 EP20 S355	--	0.040	--

Table 6.8 - Experimental plastic rotation capacity of joints

So, it can be seen from Tabel 6.7 and Fig. 6.13 that, for failure mode (2→1), both for steel grades S355 and S460, the cyclic plastic rotation could reach around 40 mrad, while for S690 around 25-30 mrad. Even these values are lower compared with those presented for HD in EN1998-1, they cover the demand for MR joints in dual frames (e.g. MRF+CBF or EBF). In [31], it was shown that for dual steel frames with 8 or 15 storeys, the plastic deformation demands in MRF joints (plastic rotation demand at the beam ends) should be less than 15-20 mrad for ULS and less than 30-35 mrad for CPLS.

### 6.3 Conclusions

Seismic provisions [33] impose both minimum over-strength ( $1.373 M_{j,Rd}$ ) and ductility (35 mrad) for beam-to-column joints. Since the column web panel contribution is limited by design, in case of bolted extended and stiffened end-plate, the main source of ductility is the end-plate, providing that its plastic failure mechanism is governed by mode 2.

Present chapter demonstrates the end-plate can be sized by design (thickness & steel grade) to supply the ductility requested by code provisions.

Also that starting from real design cases, the beam-to-column joint detailing and its performance on term of ductility vs. moment capacity can be designed to be controlled mainly by the T-stub component. This result, particularly interesting for Dual-Steel / Dual-Frame configuration simplifies the predesign of such a type of structure.

## **7 SUMMARY, CONCLUSIONS AND PERSONAL CONTRIBUTIONS**

### **7.1 Summary**

Seismic resistant building frames designed as dissipative structures must allow for plastic deformations to develop in specific members, whose behaviour has to be predicted by proper design. Members designed to remain predominantly elastic during earthquake, such as columns, are responsible for robustness of the structure and prevention the collapse, being characterized by high strength demands. Consequently a framing solution obtained by combining High Strength Steel - HSS in non-dissipative members (e.g. columns) provided with adequate overstrength, and Mild Carbon Steel - MCS in dissipative members, working as fuses (e.g. beams, links or braces) seems to be logical. The robustness of structures to severe seismic action is ensured by their global performance, in terms of ductility, stiffness and strength, e.g. the "plastic" members of MCS - (S235 to S355) will dissipate the seismic energy, while the "elastic" members (HSS - S460 to S690) by higher resistance of material and appropriate size of sections, will have the capacity to carry the supplementary stresses, following the redistribution of forces, after appearance of plastic hinges. Such a structure is termed Dual-Steels Structure - DS. DS concept is extended to connections, too, on the same philosophy related to ductile and brittle components, in order to achieve both ductility and robustness criteria. In fact, when connecting MCS beams to HSS columns it will result a DS beam-to-column joint.

Starting from the above considerations, a large experimental research program was carried out at the "Politehnica" University of Timisoara, CEMSIG Research Centre (<http://cemsig.ct.upt.ro>) in order to study the performance of dual-steel configuration for beam-to-column joints under monotonic and cyclic loading. Joint specimens, T- stub and weld detail specimens have been tested.

After the introduction in the First Chapter, where the objective of the thesis was defined and a summary state-of-art of the research in the field, based on the literature review was presented Chapter 2 presents a description of structural steels used in constructions and requirements and criteria for choosing steel in structural applications. Also in this chapter it is shortly presented the background experience achieved in beam-to-column joint experiments achieved by team of researchers from CEMSIG, "POLITEHNICA" University of Timisoara.

Chapter 3 presents the opportunities of using HSS in constructions and a parametric study on DS frames who's design target was to obtain a dissipative structure, composed by "plastic" and "elastic" members, able to form a full global plastic mechanism at the failure, in which the history of occurrence of plastic hinges in ductile members can be reliable controlled by design procedures.

Chapter 4 presents building solutions and performance criteria for beam to column joints of multi-storey structures placed in seismic zones.

In Chapter 5 a large experimental research program was designed and carried out in order to study the performance of dual-steel configuration for beam-to-column joints under monotonic and cyclic loading. When HSS is used in members designed to remain predominantly elastic, as columns, for instance, or in end-plates

of bolted joints, T-stub components made of two steel grades are obtained. The aim of the testing program was to investigate experimentally the performance of welded connections and bolted T-stub components realized from two different steel grades.

Chapter 6 is an extension of the testing program by Numerical Simulation on T-stubs and Joints specimens. Using the numerically calibrated beam-to-column joints it was studied the possibility to design efficient beam-to-column connections both from the point of view of capacity and ductility.

## 7.2 Concluding remarks

The conclusions of the most relevant chapters are summarized below:

### Chapter 3

Plastic deformations in dissipative members indicate a moderate damage to all types of structure (MRF+CBR, MRF+EBF, MRF+CBF(BRB), MRF+SW) at SLS.

All structures satisfy the criteria for ULS. Plastic deformations demands in beams are more severe for EBF and SW compared to CBF and BRB. Shear wall frames show a very good ductility comparable with EBF but also provides a higher stiffness. For eight storey buildings plastic hinges appeared at the base of the columns, while for the sixteen not. This shows that in case of higher buildings, when the contribution of gravity loads is lower, the  $\Omega$  factor is more effective in design of non dissipative members.

Structures performed well till the attainment of target displacement at CPLS. In case of EBF plastic rotation demands in links exceed the rotation capacity. However experimental tests on such elements have shown that in case of very short links, plastic rotation capacity may reach 0.17-0.20 rad.

### Chapter 5.

#### Tests on **welded specimens**

It has to be noticed that all the welds proved a very good behaviour with failure at the end of HAZ or in vicinity, as expected. So, both the choice of welding materials and technology were confirmed. Pulsating cyclic loading did not affect much the response in comparison with monotonic loading

#### Tests on **T-stubs specimens**

The EN1993-1-8 calculation procedure for T-stub components was, in general confirmed by test results, even if the definition of experimental values for yield force still remains a matter of study. Moreover, the use for T-stub of type A, corresponding to the stiffened end-plate, of the same approach as for second bolt row was confirmed, consequently, it can be used to predict the strength and stiffness of bolted beam-to-column joints of stiffened extended end-plates. This confirmation is an important achievement of this research, because the connection of this type has been used for joint specimens ([28]).

Low cycle fatigue interpretation of T-stub tests indicated that welds (double bevel) between components of different steel grades performed safely under cyclic loading, in the sense that detail category values are generally higher than those specified in EN 1993-1.9.

#### Tests on **Beam-to-Column Joints**

A very good ductility of HSS component was observed;

The analytical prediction of joint moment resistance based on component method of EN 1993-1.8 seems to be good enough in this case, and the procedure used for the outer bolt row is confirmed.

The control of upper limit of yield strength is of real importance and fabricators must find a way to introduce that on the material specification, additionally to the lower limit, otherwise the real response of the structure can be very different from the one predicted through design.

### Chapter 6

Seismic provisions [33] impose both minimum over-strength ( $1.373 M_{j,Rd}$ ) and ductility (35 mrad) for beam-to-column joints. Since the column web panel contribution is limited by design, in case of bolted extended and stiffened end-plate, the main source of ductility is the end-plate, providing that its plastic failure mechanism is governed by mode 2.

Present chapter demonstrates the end-plate can be sized by design (thickness & steel grade) to supply the ductility requested by code provisions.

Also that starting from real design cases, the beam-to-column joint detailing and its performance on term of ductility vs. moment capacity can be designed to be controlled mainly by the T-stub component. This result, particularly interesting for Dual-Steel / Dual-Frame configuration simplifies the predesign of such a type of structure.

## 7.3 Personal contributions

The main contributions of the thesis based on the demonstration of opportunity of using High Strength Steel in seismic resistant building frames carried out in chapter 2 is the Experimental Program.

The author has designed and realised a complex and complete experimental program on Materials, Welded Specimens, Joint Components and full scale Joints.

Stiffened T-stub specimens have been first time tested on both monotonic and cyclic loading conditions. There are no records on others such tests realised until now in Europe, except monotonic tests only.

Also, tests on stiffened extended end-plate beam-to-column joints designed according to AISC 2005 specifications and adapted to fulfil EN 1998 provisions have been first time tested in Europe.

A subsequent contribution at this point is the reinterpretation of the results on T-stubs in terms of low cycle fatigue parameters.

Another significant contribution of this thesis is the extension of the testing program by Numerical Simulation program on the T-stubs and Joints specimens.

Using the numerically calibrated beam-to-column joints it was demonstrated the possibility to design efficient beam-to-column connections both from the point of view of capacity and ductility of which plasticisation capacity can be controlled namely by the T-stub component.

During the research period, the contributions in the thesis have been published and disseminated by means of scientific articles and within research project as follows:

Dubina, D, **Muntean, N**, Stratan A, Grecea, D, Zaharia R Performance of moment resisting joints of high strength steel components – Cluj Mai 2008

Dubina, D, Stratan, A, **Muntean, N**, Grecea, D, "Dual-steel T-stub behaviour under monotonic and cyclic loading", ECCS/AISC Workshop: Connections in Steel Structures VI, Chicago, Illinois, USA, 23-55, 2008a.

Dubina, D, Stratan, A, **Muntean, N**, Dinu, F, "Experimental program for evaluation of Moment Beam-to-Column Joints of High Strength Steel Components", ECCS/AISC Workshop: Connections in Steel Structures VI, Chicago, Illinois, USA, June 23-55, 2008b.

Dubina, D, **Muntean, N**, Stratan, A, Grecea, D, Zaharia, R, "Testing program to evaluate behaviour of dual steel connections under monotonic and cyclic loading", Proc. of 5th European Conference on Steel and Composite Structures - Eurosteel 2008, 3-5 September, Graz, Austria, 609-614, 2008c.

**Muntean, N**, Stratan, A, Dubina, D, "Experimental evaluation of strength and ductility performance of welded and t-stub connections between high strength and mild carbon steel components", Buletin Stiintific al Universitatii "Politehnica" din Timisoara, 2008.

Dubina, D, Grecea, D, Stratan, A, **Muntean, N.**, " Performance of dual-steel connections of high strength components under monotonic and cyclic loading", STESSA 2009, Behaviour of Steel Structures in Seismic Areas, Taylor & Francis Group, London, 16-20 Aug. 2009, Philadelphia, USA, 437-442, 2009.

**Muntean, N**, Stratan, A, Dubina, D "Strength and ductility performance of welded connections between high strength and mild carbon steel components - experimental evaluation" WSEAS 2009 International conference on sustainability in science engineering Academic Days – Timisoara – Romania 27-29 may 2009

**Muntean, N**, Grecea, D, Dogariu, A, Dubina, D, "Strength and ductility of bolted T-Stub macro-components under mono-tonic and cyclic loading", Proceedings of SDSS'Rio 2010 International Colloquium Stability and Ductility of Steel Structures, 8-10 Sept, Rio de Janeiro, Brazil, 223-230, 2010.

Grecea, D, **Muntean, N.**, Dubina, D, "Control of bolted beam-to-column connections in moment joints by T-stub properties" STESA 2011

### **ACKNOWLEDGMENT**

This research was supported by the contract no. 29/2005 "STOPRISC", funded by Romanian Ministry of Education and Research, within the frame of "Excellence Research" Program, CEEX – Matnantech.



## BIBLIOGRAPHY

- [1] Girao Coelho, A.M., Bijlaard, F.S.K., Gresnigt, N. and Simoes da Silva, L. (2004), "Experimental assessment of the behaviour of bolted T-stub connections made up of welded plates", *Journal of Constructional Steel Research* 60, (pp. 269-311).
- [2] Aalberg, A., Larsen, P. K. 2001. Bearing strength of bolted connections in high strength steel. In: P. Mäkeläinen, J. Kesti, A. Jutila, O. Kaitila, (eds.). *Nordic Steel Construction Conference 2001 - NSCC 2001:proceedings*. Helsinki, NSCC: 859-866.
- [3] Aalberg, A., Larsen, P. K. 2002. The effect of steel strength and ductility on bearing failure of bolted connections. In: A. Lamas, L. S. d. Silva, (eds.). *The Third European Conference on Steel Structures: Proceedings of the 3rd European conference on steel structures*. Coimbra, Universidade de Coimbra: 869-878.
- [4] AISC 341-05, 2005. *Seismic provisions for structural steel buildings*. American Institute for Steel Construction, 2005
- [5] AISC 358-05, 2005. *Prequalified Connections for Special and Intermediate Steel Moment Frames for Seismic Applications*. American Institute for Steel Construction, 2005
- [6] AISC 360 -05, *Specification for Structural Steel Buildings 2005*, American Institute for Steel Construction, 2005.
- [7] AJ Marshall, *COR-TEN Weather and Corrosion Resistant Steel*
- [8] Arcelor sections catalogue
- [9] Beg, D., Hladnik, L. 1996. Slenderness Limit of Class 3 I Cross-sections Made of High Strength Steel. *Journal of Constructional Steel Research*, 38, 3: 201-218.
- [10] Bjorhovde, R. 2004. Development and use of high performance steel. *Journal of Constructional Steel Research*, 60, 3-5: 393-400.
- [11] Bordea, S., Stratan, A. and Dubina, D., "Performance based evaluation of a RC frame strengthened with BRB steel braces", *PROHITECH '09 International Conference*, 21-24 June, 2009, Rome, Italy, 2009.
- [12] Bucak, Ö. 2000. Zum Ermüdungsverhalten von hoch- und höchstfesten Stählen. *Stahlbau*, 69, 4: 311-316.
- [13] Bursi OS, Jaspart JP. Benchmarks for finite element modelling of bolted steel connections. *J Construct Steel Res* 1997;43(1):17-42.
- [14] Calado, L. 2000. Re-elaboration of experimental results. In F. M. Mazzolani (ed.), *Moment Resistant Connections of Steel Frames in Seismic Areas*. E&FN SPON, London, 2000, 341-368.
- [15] Chan, W.T., Badu, S.K., (2005). "Use of high-strength structural steel in Hong-Kong". *Proc. of the 4th Int. Conf. of Advances in Steel Structures*, Shanghai, June 13-15, 2005, Late Papers Volume: 25-36
- [16] Collin, P., Möller, M. 1998. Structural application for high strength steel. In: *Nordic Steel Construction Conference 98: proceedings*. Bergen, Norway, Oslo, Norsk Stålforbund: 67-77.
- [17] Collin, P., Johansson, B. 2005. Design of welds in high strength steel. In: B. Hoffmeister, (ed.). *Eurosteel 2005:4th European Conference on Steel and Composite Structures*. Maastricht, Druck und Verlagshaus Mainz.

- [18] de Freitas, S. T., de Vries, P., Bijlaard, F. S. K. 2005. Experimental research on single bolt connections for high strength steel S690. ECCS\_TC10-05-579, In. ECCS\_TC10-05-579, ECCS TC10.
- [19] Dieter, G. E. 1987. Tension test. In: S. Rao, (ed.). Mechanical Metallurgy. New York [ect.], McGraw-Hill Book Company.
- [20] Dinu, F., Dubina, D. and Neagu, C., "A comparative analysis of performances of high strength steel dual frames of buckling restrained braces vs. dissipative shear walls". Proc. of International Conference STESSA 2009: Behaviour of Steel Structures in Seismic Areas, Philadelphia, 16-20 august 2009, CRC Press 2009, Ed. F.M. Mazzolani, J.M. Ricles, R. Sause, ISBN: 978-0-415-56326-0, 2009.
- [21] Dowling, N. E. 1993. Mechanical testing: Tension test and other basic tests. In. Mechanical behaviour of materials: Engineering methods for deformation, fracture and fatigue. New Jersey, Prentice-Hall International I
- [22] Dubina, D., Stratan, A., Ciutina, A., 2005, Components and Macro-Components of Rotation Capacity of Moment Connections, Proc. of 20th CTA Congress Advances in Steel Constructions, ACS ACAI, Milano.
- [23] Dubina, D., Dinu, F., Stratan and Ciutina, A., "Analysis and design considerations regarding the project of Bucharest Tower International Steel Structure". Proc. of ICMS 2006 Steel a new and traditional material for building, Brasov, Romania, 2006, Taylor&Francis/Balkema, Leiden, The Nederland's, ISBN 10: 0 415 40817 2, Ed. D., Dubina, V. Ungureanu, 2006.
- [24] Dubină, D., Dinu, F., Zaharia, R., Ungureanu, V. and D. Grecea, D., "Opportunity and Effectiveness of using High Strength Steel in Seismic Resistant Building Frames". Proc. of ICMS 2006 Internat. Conf. "Steel, a new and traditional material for building", Poiana Brasov, Romania, September 20-22, 2006, Taylor&Francis/Balkema, Leiden, The Nederland's, ISBN 10: 0 415 40817 2, Ed. D., Dubina, V. Ungureanu, 2006.
- [25] Dubina, D. and Dinu, F. (2007), "High strength steel for seismic resistant building frames", 6th Int. Conf. Steel and Aluminium Structures – ICSAS'07 (Ed. R. G. Beale), Oxford Brooks Univ. (pp. 133-140).
- [26] Dubina, D., Stratan, A. Dinu, F. (in print). "Dual high-strength steel eccentrically braced frames with removable links". Earthquake Engineering & Structural Dynamics, Published Online: 10 Jul 2008.
- [27] Dubina, D., Stratan, A. Muntean, N. and Grecea, D. (2008a), "Dual-steel T-stub behaviour under monotonic and cyclic loading", ECCS/AISC Workshop: Connections in Steel Structures VI, Chicago, Illinois, USA, June 23-55, 2008
- [28] Dubina, D., Stratan, A. Muntean, N. and Dinu, F. (2008b), "Experimental program for evaluation of Moment Beam-to-Column Joints of High Strength Steel Components", ECCS/AISC Workshop: Connections in Steel Structures VI, Chicago, Illinois, USA, June 23-55, 2008.
- [29] Dubina, D, Muntean, N, Stratan, A, Grecea, D, Zaharia, R, "Testing program to evaluate behaviour of dual steel connections under monotonic and cyclic loading", Proc. of 5th European Conference on Steel and Composite Structures - Eurosteel 2008, 3-5 September, Graz, Austria, 609-614, 2008c.
- [30] Dubina, D, Grecea, D, Stratan, A, Muntean, A., " Performance of dual-steel connections of high strength components under monotonic and cyclic loading", STESSA 2009, Behaviour of Steel Structures in Seismic Areas, Taylor & Francis Group, London, 16-20 Aug. 2009, Philadelphia, USA, 437-442, 2009.
- [31] Dubina, D, "Dual-steel frames for multi-storey buildings in seismic areas", Keynote lecture, Proceedings of SDSS'Rio 2010 International Colloquium

- Stability and Ductility of Steel Structures, 8-10 September, Rio de Janeiro, Brazil, 59-80, 2010.
- [32] European Committee for Standardization (CEN). Eurocode 3. prEN 1993-1-8:20xx, Part 1.8: Design of joints, Eurocode 3: Design of steel structures, Final draft (corrected), February 2002, Brussels; 2002.
- [33] EN 1993-1.8. 2003. Eurocode 3. Design of steel structures. Part 1-8: Design of joints, European standard.
- [34] EN 1998-1. 2004. Eurocode 8. Design of structures for earthquake resistance. General rules, seismic actions and rules for buildings, European standard
- [35] Faella C, Piluso V, Rizzano G. Experimental analysis of bolted connections: snug versus preloaded bolts. *J Struct Eng ASCE* 1998;124(7):765–74.
- [36] Fajfar, Gašperšič, 2000, The N2 method for the seismic damage analysis of buildings
- [37] Feldmann M, Eichler B, Schafer D, Hoffmeister B, Kuck J, Vayas I., Karlos V, Sedlacek G. 2011 Choice of steel material for the plastic design of steel frames including seismic resistant structures
- [38] FEMA-350, 2000, Recommended Seismic Design Criteria for New Steel Moment-Frame Buildings, prepared by the SAC Joint Venture for the Federal Emergency Management Agency, Washington, DC.
- [39] FEMA 356,. Prestandard and commentary for the seismic rehabilitation of buildings. Federal Emergency Management Agency and American Society of Civil Engineers, Washington DC, USA, 2000.
- [40] Fukumoto, Y., (1996). "New constructional steels and structural stability". *Engineering Structures*, Vol. 18, No. 10: 786-791.
- [41] Galambos, T.V., Hajjar, J.F., Earls, C.J. & Gross, J.L. 1997. Required properties of high-performance steels. Report NISTIR 6004, Building and Fire Research Laboratory, National Institute of Standards and Technology.
- [42] Gebbeken N, Wanzek T. Benchmark experiments for numerical simulations of T-stubs. In: Viridi KS, editor. Numerical simulation of semi-rigid connections by the finite element method. COST C1, Report of working group 6—Numerical simulation, Brussels; 1999. p. 61–70.
- [43] Gerhard Sedlacek, Christian Müller The use of very high strength steels in metallic construction
- [44] Gioncu V, Mazzolani F, 2002, Ductility of seismic resistant steel structures 2002.
- [45] Girão Coelho AM, Simões da Silva L. Numerical evaluation of the ductility of a bolted T-stub connection. In: Chan SL, Teng JG, Chung KF, editors. *Advances in steel structures. Proc. of 3rd International Conference (ICASS'02)*, Hong Kong. 2002, p. 277–84.
- [46] Girão Coelho AM, Bijlaard F, Simões da Silva L. On the deformation capacity of beam-to-column bolted connections. European Convention for Constructional Steelwork—Technical Committee 10, Structural Connections (ECCS-TC10), Document ECCS-TWG 10.2-02-003; 2002.
- [47] Girão Coelho AM, Bijlaard F, Simões da Silva L. On the deformation capacity of beam-to-column bolted connections. European Convention for Constructional Steelwork—Technical Committee 10, Structural Connections (ECCS-TC10), Document ECCS-TWG 10.2-02-003; 2002.
- [48] Girão Coelho, A. M. 2004. Characterization of the ductility of bolted end plate beam-to-column steel connections. Doctoral dissertation, Coimbra, Universidade de Coimbra.

- [49] Girão Coelho, A. M., Bijlaard, F. S. K., Gresnigt, N., Simoes da Silva, L. 2004a. Experimental assessment of the behaviour of bolted T-stub connections made up of welded plates. *Journal of Constructional Steel Research*, 60, 2: 269-311.
- [50] Girão Coelho, A. M., Bijlaard, F. S. K., Simoes da Silva, L. 2004b. Experimental assessment of the ductility of extended end plate connections. *Engineering Structures*, 26, 9: 1185-1206.
- [51] Girão Coelho, A. M., da Silva, L. S., Bijlaard, F. S. K. 2006a. Ductility analysis of bolted extended end plate beam-to-column connections in the framework of the component method. *Steel and Composite Structures*, 6, 1: 33-53.
- [52] Girão Coelho, A. M., da Silva, L. S., Bijlaard, F. S. K. 2006b. Finite-element modelling of the nonlinear behaviour of bolted T-stub connections. *Journal of Structural Engineering-Asce*, 132, 6: 918-928.
- [53] Girão Coelho, A.M., Bijlaard, F.S.K., 2007, Ductility of High performance Steel Moment Connections, *Advanced Steel Construction*, Vol.3, No.4.
- [54] Greco, N., Earls, C. J. 2003. Structural ductility in hybrid high performance steel beams. *Journal of Structural Engineering-Asce*, 129, 12: 1584-1595.
- [55] Gresnigt, A. M., Steenhuis, C. M. 1997. High strength steels. *Progress in Structural Engineering and Materials*, 1, 1: 31-41.
- [56] Günther, H.-P., Raoul, J., Kuhlmann, U., Lwin, M., Mistry, V.C., Driver, R.G., Grondin, G.Y., Macdougall, C, Miki, C., Kawabata, F., Suegana, K., Watanabe, Y., Takemura, M., Tominaga, T., Samuelsson, A., Schröter, F., Sedlacek, G., Müller, C., Nussabaumer, A., Johansson, B., Höglund, T., Collin, P., Miazzon, A. . 2005. Use and Application of High-Performance Steels for Steel Structures. In: H.-P. Günther, (ed.). *Structural engineering documents 8*. Zürich, IABSE, International Association for Bridge and Structural Engineering.
- [57] IABSE, 2005. Use and application of high performance steels for steel structures. Chapter 5: High Performance steels in EUROPE. IABSE Structural Documents, No,8, International Association for Bridge and structural Engineering, Zurich, Switzerland 2005.
- [58] Jaspert JP. Etude de la semi-rigidite des noeuds poutre-colonne et son influence sur la resistance et la stabilite des ossatures en acier. Ph.D. Thesis. University of Lie`ge, Lie`ge; 1991 [in French].
- [59] Johansson, B. 2004. Design of fillet welds with under- or overmatching electrodes. CEN/TC250/SC3/WG S690, In. CEN/TC250/SC3/WG S690, CEN.
- [60] Johansson, B., Collin, P., (1999). "High-strength steel - the construction material of the future". ECCS TC10 report WG5-129.
- [61] Kim, H. J., Yura, J. A. 1999. The effect of ultimate-to-yield ratio on the bearing strength of bolted connections. *Journal of Constructional Steel Research*, 49, 3: 255-270.
- [62] Kouhi, J., Kortessmaa, M. 1990. Strength tests on bolted connections using high-strength steels (HSS steels) as a base material. Research notes 1185, In. 1185. Espoo, Technical Research Centre of Finland.
- [63] Kuhlmann, U., Bergmann, J. 2005. Effective use of high strength steels in welded structures under fatigue loading. 4th European Conference on Steel and Composite Structures, Eurosteel 2005, B. Hoffmeister,(ed.), Druck und Verlagshaus Mainz, Maastricht.
- [64] Ling, T. W., Zhao, X. L., Al-Mahaidi, R., Packer, J. A. 2007. Investigation of block shear tear-out failure in gusset-plate welded connections in structural

- steel hollow sections and very high strength tubes. *Engineering Structures*, 29, 4: 469-482.
- [65] Lu, L.W. et al., 2000, Critical issues in achieving ductile behaviour of welded moment connections, *Journal of Constructional Steel Research*: 55.
- [66] Muntean, N, Grecea, D, Dogariu, A, Dubina, D, "Strength and ductility of bolted T-Stub macro-components under mono-tonic and cyclic loading", *Proceedings of SDSS'Rio 2010 International Colloquium Stability and Ductility of Steel Structures*, 8-10 Sept, Rio de Janeiro, Brazil, 223-230, 2010.
- [67] Nassar A, Krawinkler H, (1991. Seismic demands for SDOF and MDOF systems), Report no.95. The John A Blume Earthquake Engrg. Centre Stanford University.
- [68] Packer JA, Morris LJ. A limit state design method for the tension region of bolted beam-to-column connections. *Struct Eng* 1977;55(10):446-58.
- [69] Piluso, V. and Rizzano, G. (2007), "Experimental analysis and modelling of bolted T-stubs under cyclic loads", *Journal of Constructional Steel Research*, doi:10.1016/j.jcsr.2007.12.009
- [70] Piluso V, Faella C, Rizzano G. Ultimate behavior of bolted T-stubs. II: Model validation. *J Struct Eng ASCE* 2001;127(6):694-704.
- [71] Puthli, R., Fleischer, O. 2001. Investigations on bolted connections for high strength steel members. *Journal of Constructional Steel Research*, 57, 3: 313-326.
- [72] Rasmussen, K. J. R., Hancock, G. J. 1995. Tests of High-Strength Steel Columns. *Journal of Constructional Steel Research*, 34, 1: 27-52. Rex, C. O., Easterling, W. S. 2003. Behavior and modelling of a bolt bearing on a single plate. *Journal of Structural Engineering-Asce*, 129, 6: 792-800.
- [73] Samuelsson, A.; Schröter, F.: High performance steels in Europe - Production processes, mechanical and chemical properties, fabrication properties. IABSE-Structural Engineering Document No. 8 - Use and application of high performance steels (HPS) for steel structures, 2005.
- [74] Simoes da Silva L, Santiago A, Vila Real P. Post-limit stiffness and ductility of end-plate beam-to-column steel joints. *Compute Struct* 2002;80:515-31.
- [75] Stratan, A. and Dubina, D., "Bolted links for eccentrically braced steel frames", *Proc. of the Fifth Int. Workshop "Connections in Steel Structures V. Behaviour, Strength & Design"*, June 3-5, 2004. Ed. F.S.K. Bijlaard, A.M. Gresnigt, G.J. van der Vegte. Delft University of Technology, Netherlands, 2004.
- [76] Swanson JA, Leon RT. Bolted steel connections: tests on T-stub components. *J Struct Eng ASCE* 2000;126(1):50-6.
- [77] Swanson JA, Leon RT. Stiffness of bolted T-stub connection components. *J Struct Eng ASCE* 2001;127(5):498-505.
- [78] Vamvatsikos, C. A. Cornell (2002) Incremental dynamic analysis, 491-514. In *Earthquake Engineering & Structural Dynamics* 31 (3).
- [79] Veljkovic, M., Johansson, B. 2004. Design of hybrid steel girders. *Journal of Constructional Steel Research*, 60, 3-5: 535-547.
- [80] Takanashi, K., Aburakawa, M., Hamaguchi H., (2005). "Utilization of high performance steels in urban structures". *Advances in Steel Structures ICASS'05*, Vol. 2, 1827-1835, Elsevier, London.
- [81] Weynand K, Jaspart JP, Steenhuis M. The stiffness model of revised Annex J of Eurocode 3. In: Bjorhovde R, Colson A, Zandonini R, editors. *Connections in Steel Structures III. Proc. of the 3rd Intern. Workshop on Connections*, Trento. 1995, p. 441-52.

- [82] Yee YL, Melchers RE. Moment-rotation curves for bolted connections. J Struct Eng ASCE 1986;112(3):615-35.
- [83] Zoetemeijer P. A design method for the tension side of statically loaded bolted beam-to-column connections. Heron 1974;20(1):1-59.
- [84] ABAQUS Inc. "ABAQUS analysis user manual", version 6.6, 2006.

## APPENDIX A

The well designed seismic resistant structure should be provided with balanced stiffness, strength and ductility between its members, connections and foundations. In order to be robust, and make possible a reliable control and prediction of their response, seismic resistant structures are always redundant as the redundancy is the inherent condition of reliability in a structural system. Structural redundancy is dependent on both overstrength and ductility of the active components of structural systems. Moment-resisting (MR) steel frames in seismic areas are traditionally designed on the base of Weak Beam – Strong Column (WBSC) philosophy and their performance is highly dependent on the properties of beam-to-column joints. The plastic rotation capacity of joints is essential for the safe response of MR steel frames, particularly when they are partial strength.

Some simple definitions should be stated in order to better understand the difference between joint and connection (according to Eurocode 3, part 1-8): (i) a joint represents "an assembly of basic components that enables members to be connected together in such a way that the relevant internal forces and moments can be transferred between them"; a connection represents "the location at which two members are interconnected, and the means of interconnection". In this way, A beam-to-column joint consists of a web panel and either one connection (single sided joint configuration) or two connections (double sided joint configuration).

Modern seismic design codes impose in case of MR steel frames lower bound values for the available plastic rotation capacity of beam-to-column joints. However, they do not provide calculation procedures to evaluate the rotation capacity for practical design when using specific joint detailing, but the design should be based on pre-qualification tests. Therefore, a simple method for determination of the joint rotation capacity, to be used in everyday design practice would be of real interest.

The research team already possesses a rich experience in national and international level research in the field. An example is the COPERNICUS "RECOS" ERB IC15-CT96-0201 "Reliability of Moment Resistant Connections of Steel Building Frames in Seismic Areas", project accomplished between 1997 and 1999. Within this project, the Timisoara team (UPT, ACAD-CCFTA, INCERC) performed a large experimental program on beam to column joints (see Fig. 0.1), as well as numerical simulations on homogeneous and dual moment-resisting frames, with rigid and semi-rigid frames.

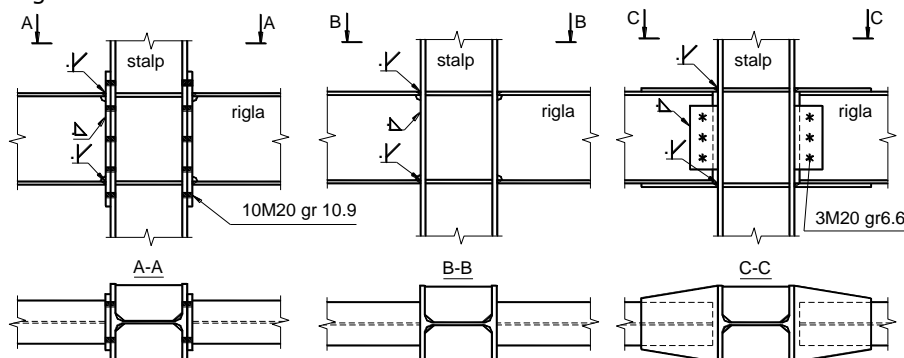




Fig. 0.1 - Joint configurations tested within the COPERNICUS "RECOS" project.

**ROTATION CAPACITY STUDIED BY TESTS**

Four series of tests will be summarized in Table A1 and examined hereafter, i.e.:

- Series CPP, tested at INSA-Rennes [A1]: double-sided welded joints, unstiffened web panel, monotonically and cyclically loaded.
- Series BX, tested at "Politehnica" University of Timisoara – PUT [A2]): double sided bolted extended end-plate with web continuity stiffeners (WCS) joints, X shaped columns (the web panel behaviour in this case can be estimated with that of a double T section with web doubler plates). The specimens have been loaded monotonically and cyclically, both symmetrically and anti-symmetrically.
- Series X, tested at PUT [A3]: three different typologies of double-sided joints, loaded monotonically and cyclically, both symmetrically and anti-symmetrically. The three typologies are: EP – bolted extended end plate with continuity plates; W – welded with WCS, and CWP – welded with WCS and welded beam flange cleats.
- Series G3, tested at INSA-Rennes, [A4]: Single-sided bolted joints with extended end-plate of similar member sections, but with three different end-plate thickness (S15 – 15mm, S20 – 20mm, S25 – 25mm), cyclically loaded.

All these specimens have been tested according to ECCS Recommendations No. 45. The values of total rotation capacity reported in Table A1 have been obtained for a 20% degradation of maximum bending moment, as requested in EN 1998-1.

First of all one observes a significant reduction of rotation capacity between monotonic and cyclic loading, from 80% to 30%. The strong reduction corresponds to double-sided joints loaded symmetrically when the panel zone does not have any contribution to the rotation.

In case of double-sided joints, loaded anti-symmetrically, when the panel zone is working in shear, the rotation capacity increases at least two times, compared with symmetrical case (unfortunately accompanied by a corresponding decrease in strength and stiffness).

Too flexible panel zone induced low cycle fatigue fracture in column flange to beam flange fragile connection (XU-W1), while too strong beam flange and beam flange to column flange connection induced first the low cycle fatigue failure in panel zone, followed soon by welded connection fracture (XU-CWP1). For the bolted joints with sheared panel zone and reasonably flexible end plate, a good rotation capacity can be obtained without difficulty by the combined contribution of both components (XU-EP1).

A detailed description of tests presented in Table A1 can be found in the references.

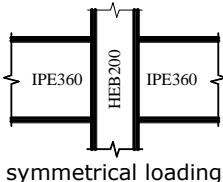
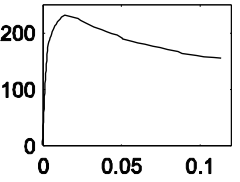
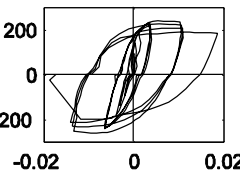
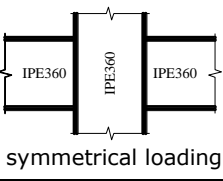
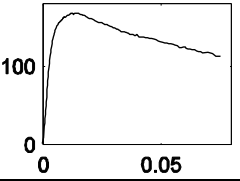
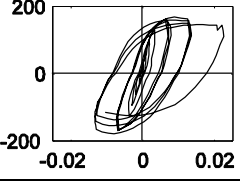
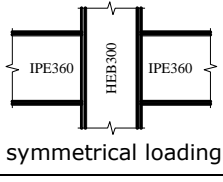
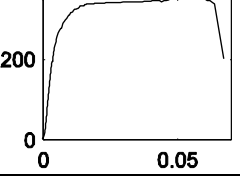
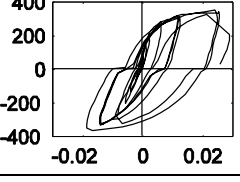
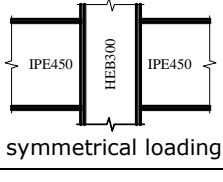
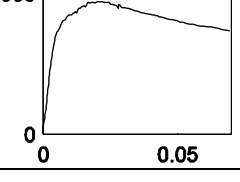
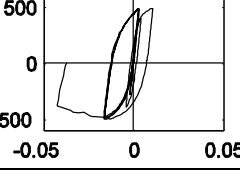
Therefore, to conclude this section, on the basis of observations on 6 different joint typologies, including single and double-sided specimens, loaded symmetrically and anti-symmetrically, the following factors influencing the cyclic rotation capacity can be emphasised:

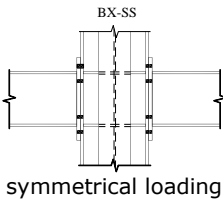
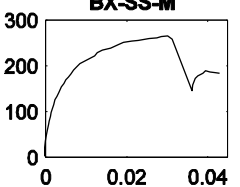
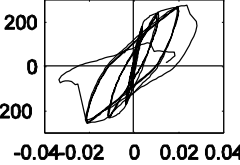
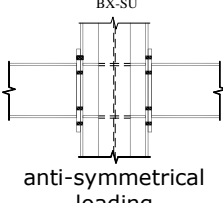
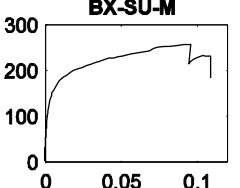
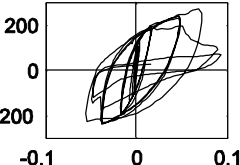
- Joint typology, and for a given typology, the quality of detailing and material properties.
- Loading type, symmetrical or anti-symmetrical, involving the contribution of the panel zone.
- The balance of strength and ductility between active ductile components.

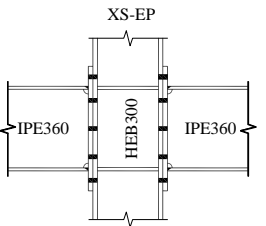
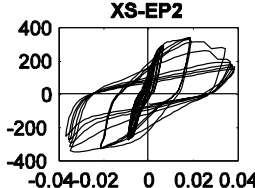
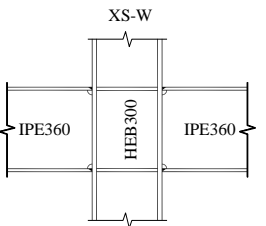
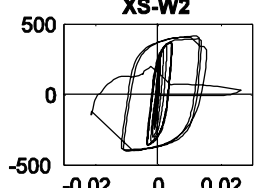


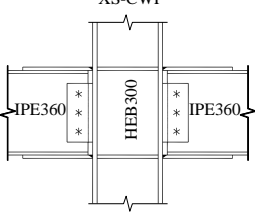
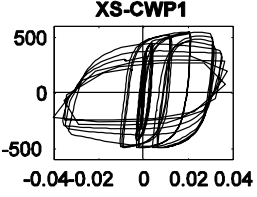
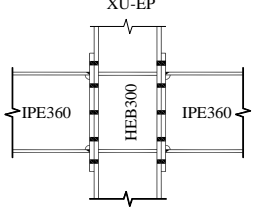
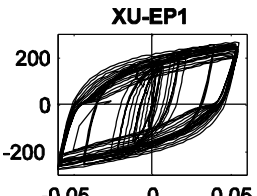
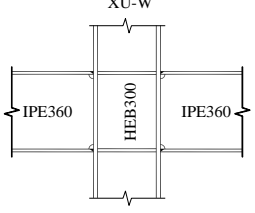
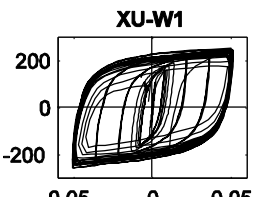
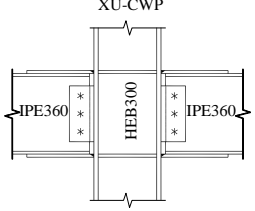
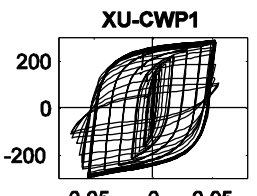
- Overstrength of the fragile component: in case of direct welded beam flange-to-column flange connection there is no possibility to obtain a weld of higher strength than the beam flange without a RBS solution (dog-bone) or reinforcing cleats (but not too strong cleats!). The situation is similar when thick end plates are used in bolted joints, when the bolts, the fragile component, are in danger of early failure.

Based on test results Grecea et al [A5], suggested, for a rough estimation of cyclic rotation capacity to take half of monotonic values. If such a ration between cyclic and monotonic is accepted, the approach proposed by Beg et al [A6] to adopt the component method for evaluation of monotonic rotation capacity, or other similar, could be used as the first step in estimation of the cyclic rotation capacity. However, in order to prevent the premature failure of some fragile or too weak component, a set of pre-qualification criteria for specific joint typologies would be necessary. At the moment, in what concerns the possibility of analytical evaluation of joint rotation, even for monotonic loading, we are in the phase of tests.

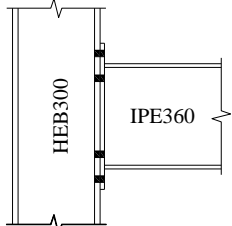
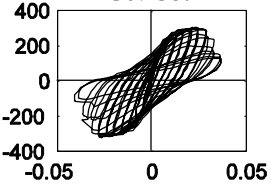
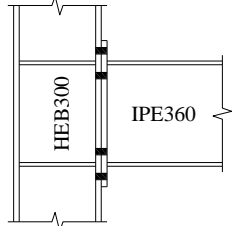
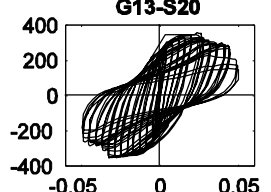
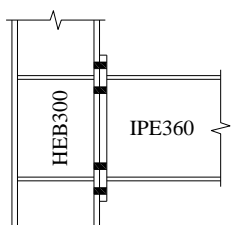
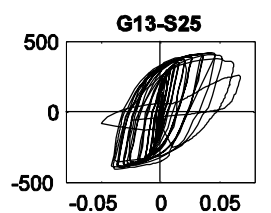
Joint type	Test results					
	Monotonic			Cyclic		
	M- $\theta$ curve	Failure mode	$\theta_u$	M- $\theta$ curve	Failure mode	$\theta_u$
INSA-Rennes series CPP						
CPP11, CPP12  symmetrical loading	 <b>CPP11</b>	Buckling of column web	0.058	 <b>CPP12</b>	Buckling of column web with fracture of column flange and web	0.011
CPP13, CPP14  symmetrical loading	 <b>CPP13</b>	Buckling of column web	0.048	 <b>CPP14</b>	Buckling of column web	0.013
CPP15, CPP16  symmetrical loading	 <b>CPP15</b>	Buckling of column web	0.066	 <b>CPP16</b>	Buckling of column web	0.027
CPP17, CPP18  symmetrical loading	 <b>CPP17</b>	Buckling of column web	0.065	 <b>CPP18</b>	Buckling of column web with fracture of column flange and web	0.039

UPT series BX					
 <p>BX-SS symmetrical loading</p>	 <p><b>BX-SS-M</b> 300 200 100 0 0 0.02 0.04</p>	<p>end-plate and column flange bending</p>	<p>0.034</p>  <p><b>BX-SS-C1</b> 200 0 -200 -0.04 0.02 0 0.02 0.04</p>	<p>fracture of the beam flange to end-plate weld</p>	<p>0.022</p>
 <p>BX-SU anti-symmetrical loading</p>	 <p><b>BX-SU-M</b> 300 200 100 0 0 0.05 0.1</p>	<p>panel zone shearing, end-plate and column flange bending</p>	<p>0.109</p>  <p><b>BX-SU-C1</b> 200 0 -200 -0.1 0 0.1</p>	<p>panel zone shearing, end-plate and column flange bending, with fracture of the beam flange to end-plate weld</p>	<p>0.073</p>

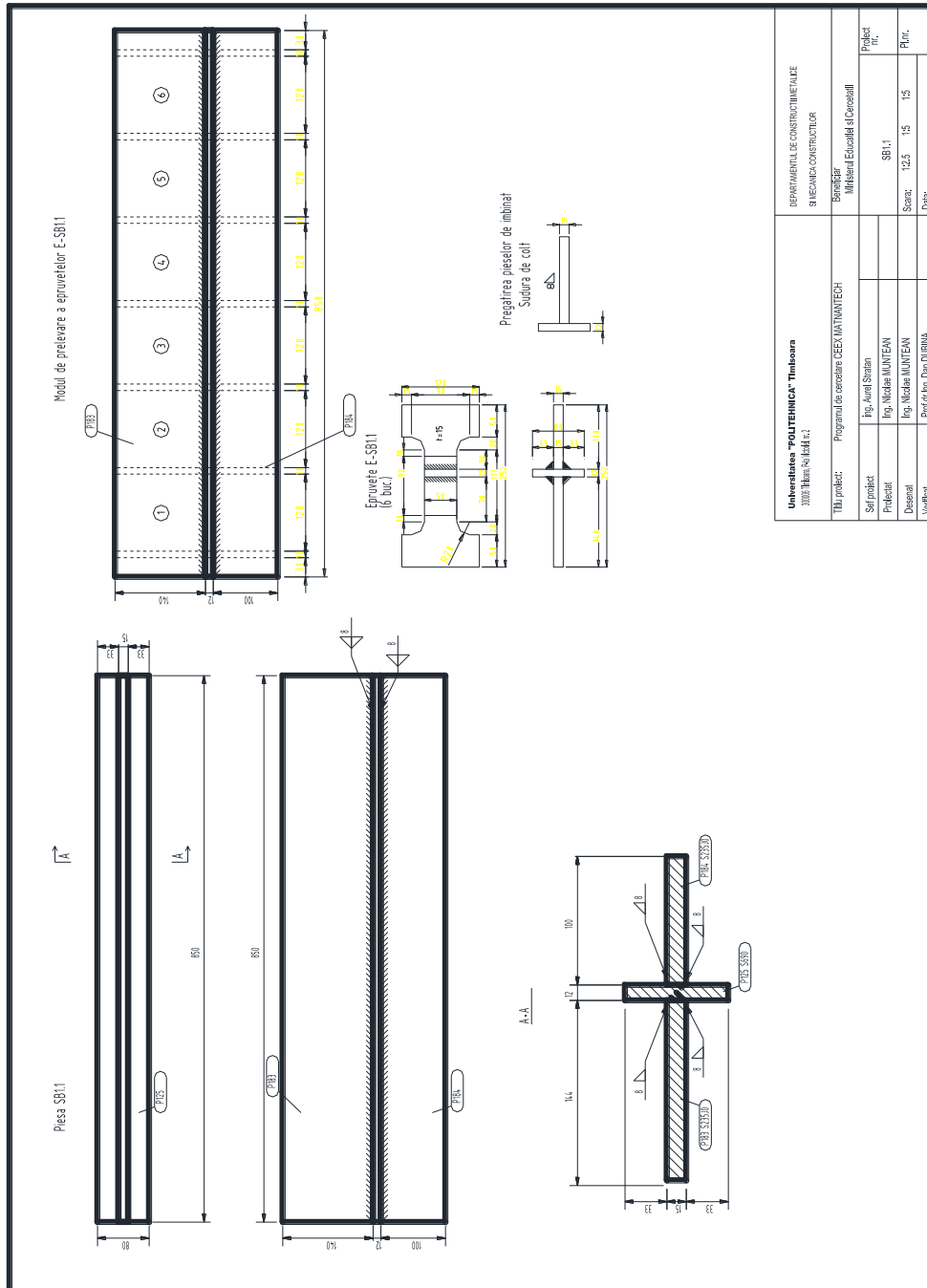
UPT series X			
 <p>XS-EP IPE360 HEB300 IPE360 symmetrical loading</p>	 <p><b>XS-EP2</b> 400 200 0 -200 -400 -0.04 0.02 0 0.02 0.04</p>	<p>end-plate bending, with fracture of the beam flange to end-plate weld</p>	<p>0.034</p>
 <p>XS-W IPE360 HEB300 IPE360 symmetrical loading</p>	 <p><b>XS-W2</b> 500 0 -500 -0.02 0 0.02</p>	<p>buckling of beam flange, fracture of the beam flange to column flange weld</p>	<p>0.015</p>

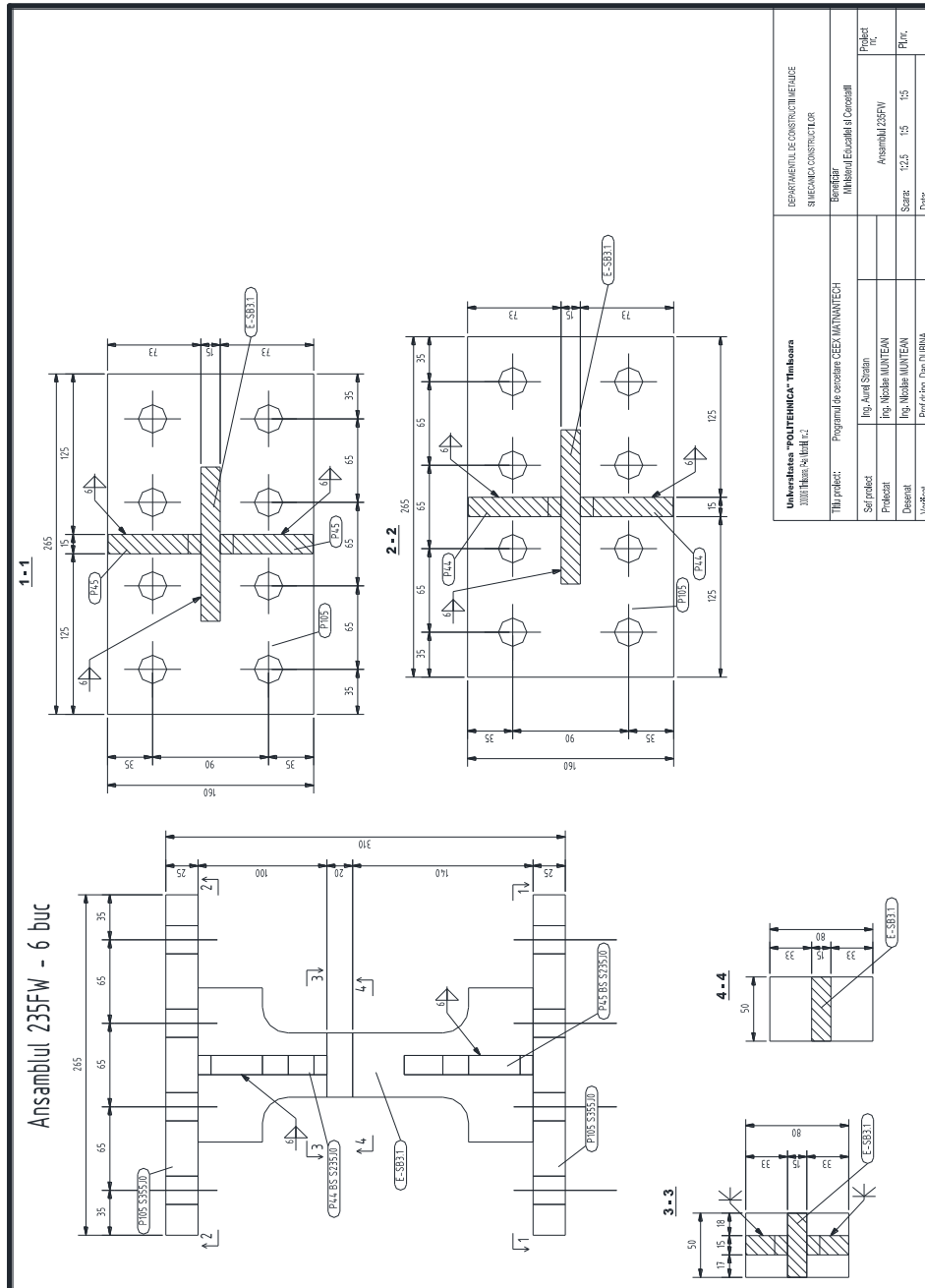
 <p>XS-CWP</p> <p>symmetrical loading</p>	 <p>XS-CWP1</p>	<p>buckling of beam flange and web</p>	<p>0.027</p>
 <p>XU-EP</p> <p>anti-symmetrical loading</p>	 <p>XU-EP1</p>	<p>end-plate bending and panel zone shearing</p>	<p>0.060</p>
 <p>XU-W</p> <p>anti-symmetrical loading</p>	 <p>XU-W1</p>	<p>panel zone shearing and fracture of beam flange weld</p>	<p>0.052</p>
 <p>XU-CWP</p> <p>anti-symmetrical loading</p>	 <p>XU-CWP1</p>	<p>panel zone shearing and fracture of flange cleats weld</p>	<p>0.054</p>

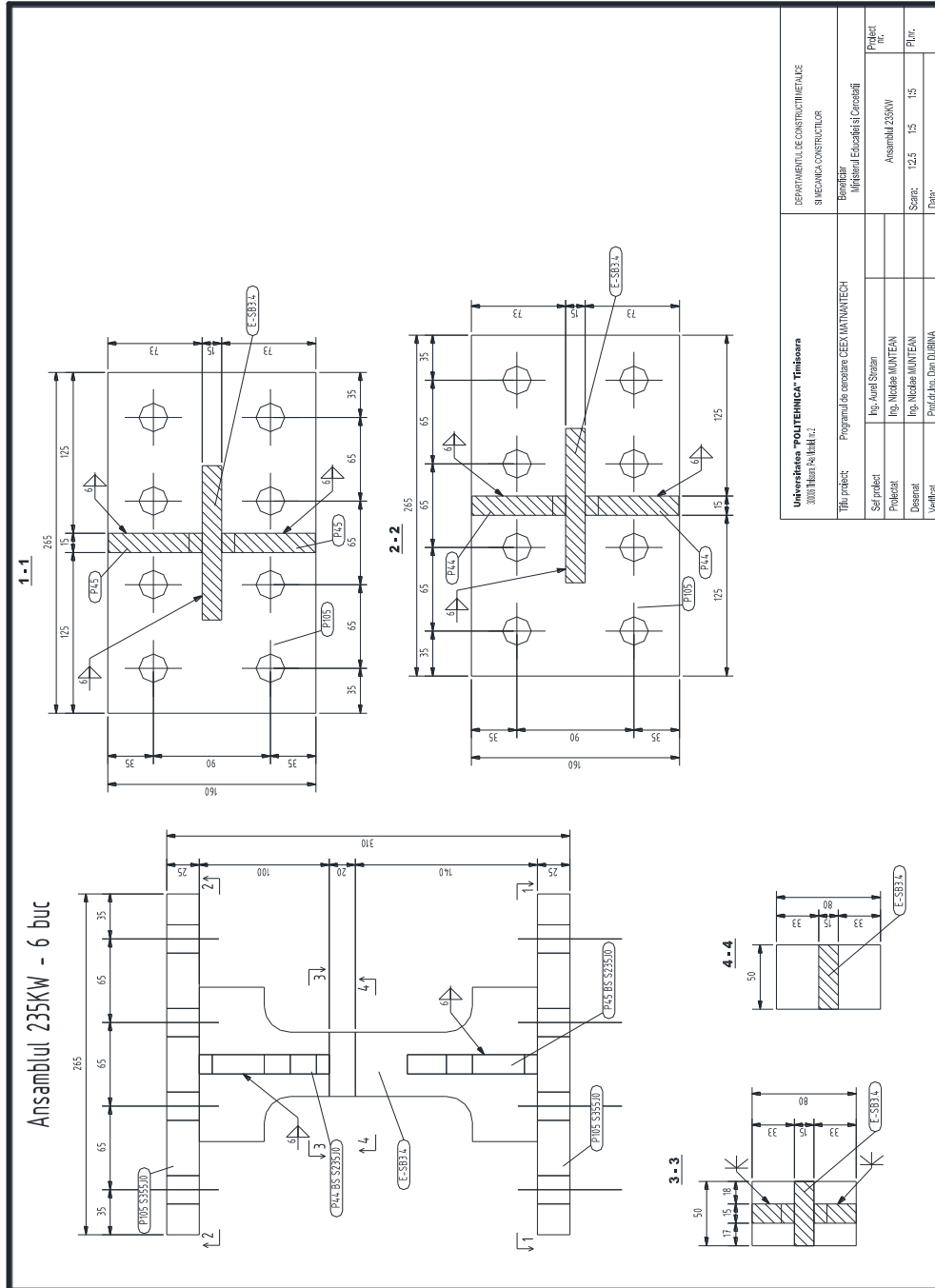
Joint type	Test results		
	Cyclic		
	M-θ curve	Failure mode	$\theta_u$
INSA-Rennes series G13			

<p>G13-S15</p> 	<p><b>G13-S15</b></p> 	<p>end-plate bending, with fracture of the beam flange to end- plate weld</p>	<p>0.031</p>
<p>G13-S20</p> 	<p><b>G13-S20</b></p> 	<p>end-plate bending and flange bending, fracture of the beam flange to end-plate weld</p>	<p>0.042</p>
<p>G13-S25</p> 	<p><b>G13-S25</b></p> 	<p>buckling of beam flange, fracture of the beam flange to end- plate weld</p>	<p>0.041</p>

## **APPENDIX B**

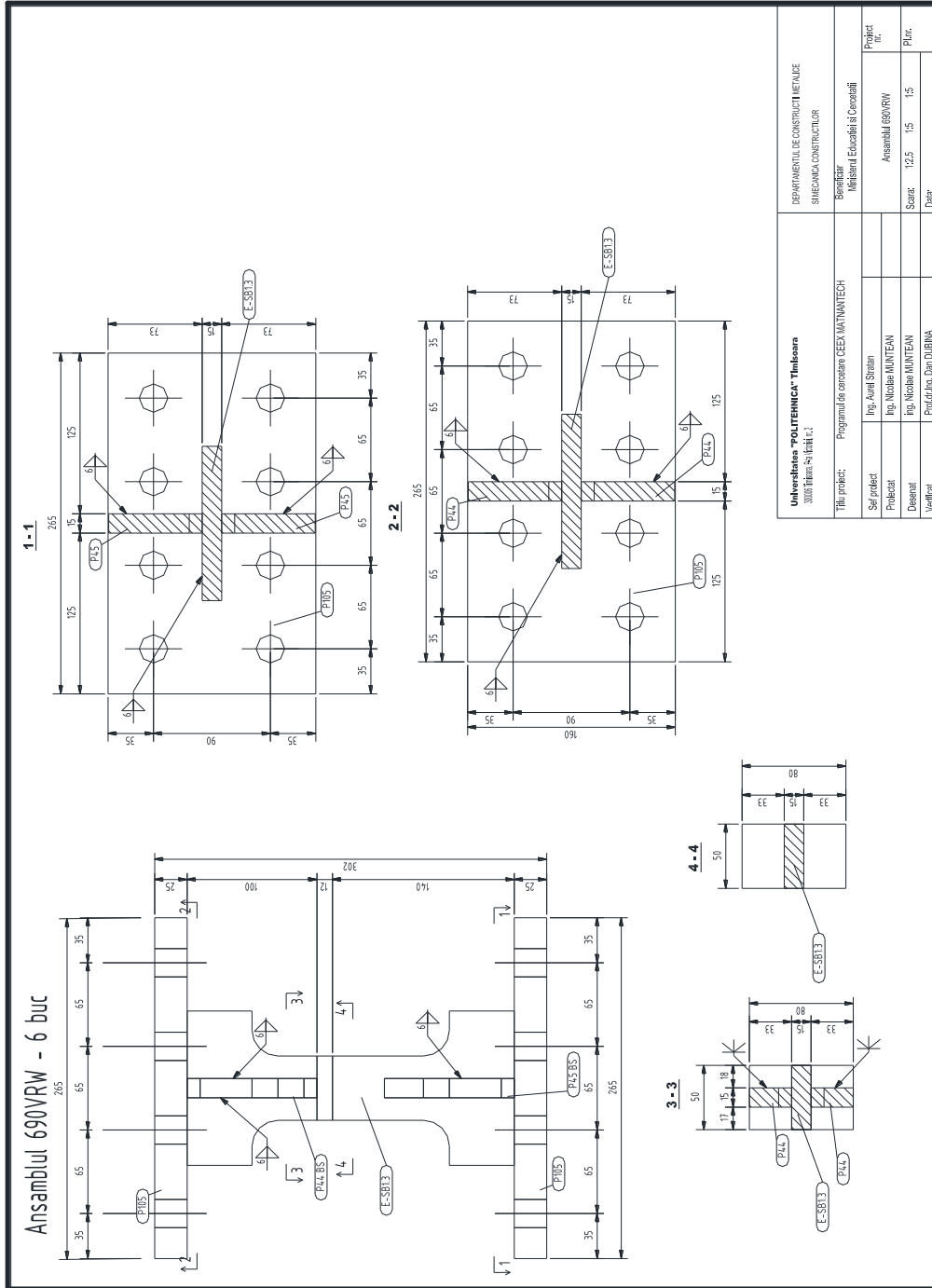


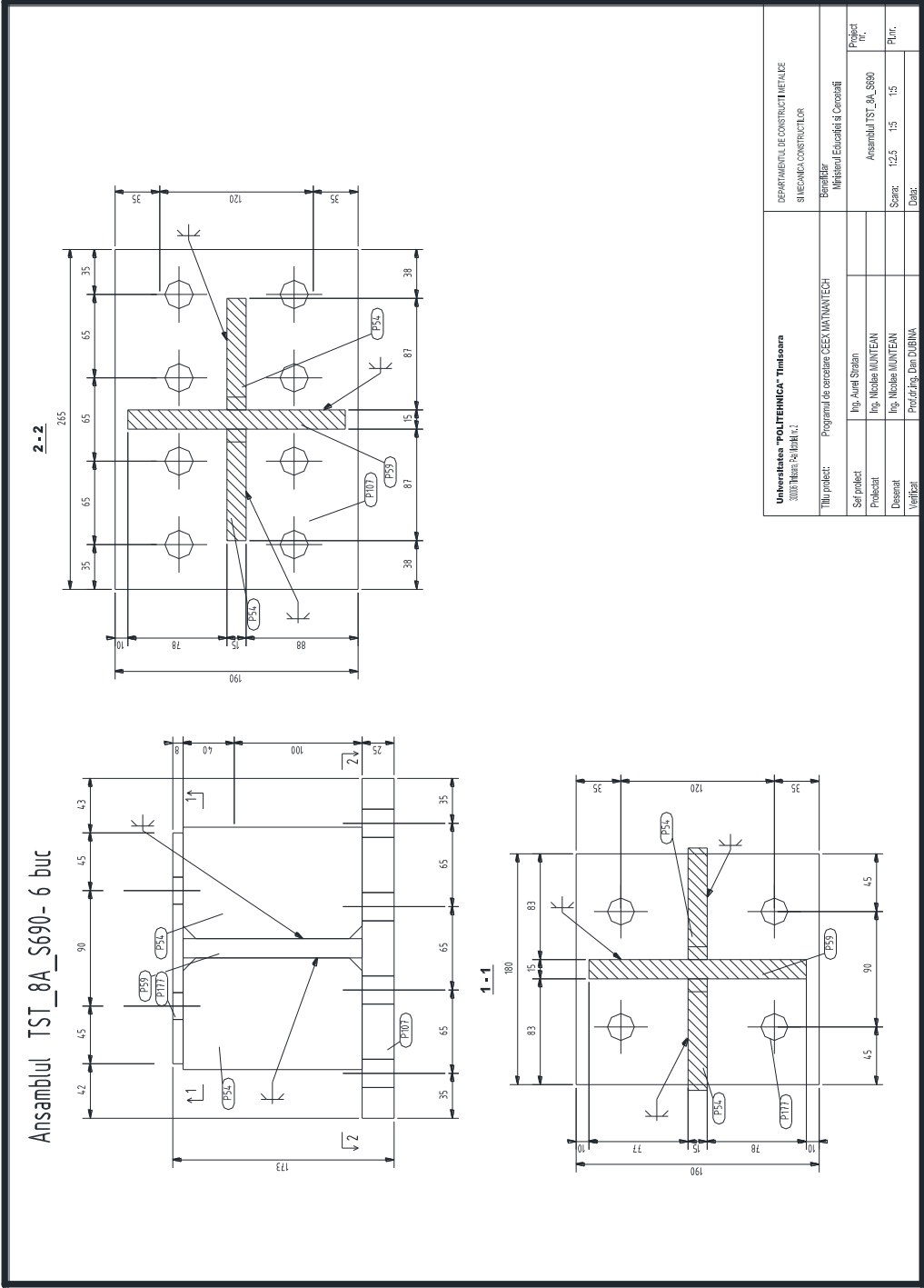


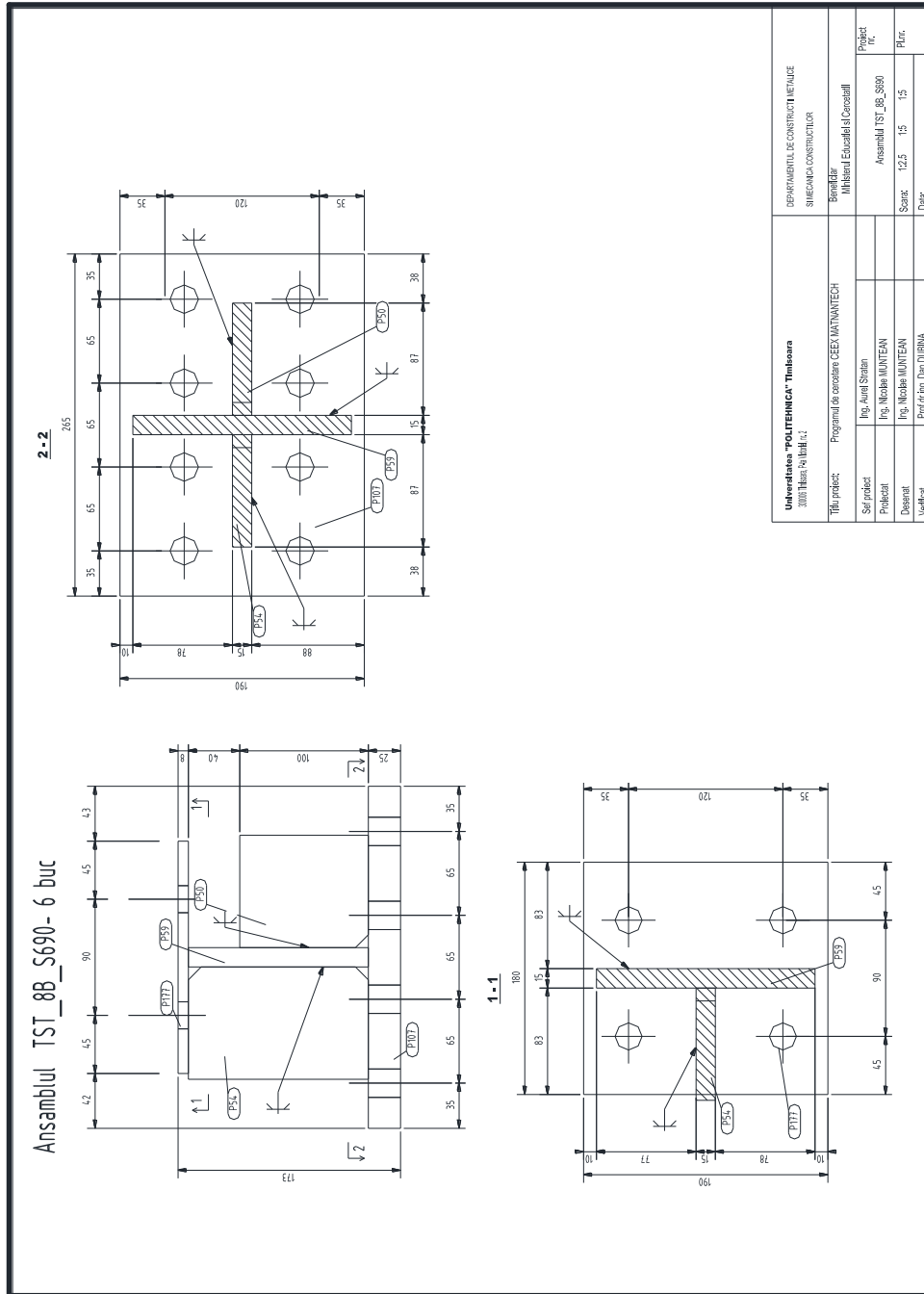




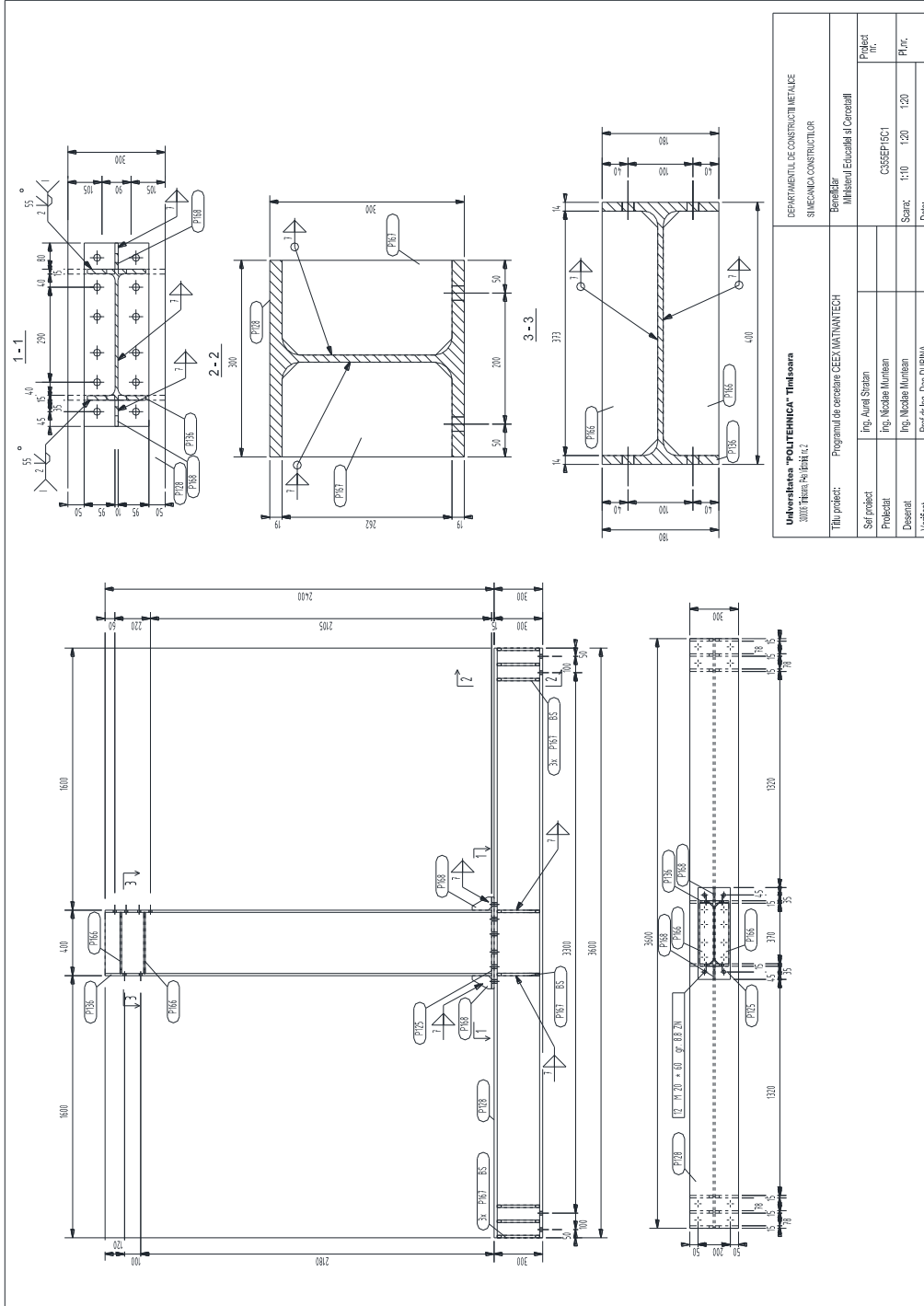












<b>Universitatea "POLITEHNICA" Timisoara</b>		DEPARTAMENTUL DE CONSTRUCTII METALICE	
30017 Titaniu P.01.01.17.02		SIMECANIA CONSTRUCTORILOR	
Titlu proiect: Programul de cercetare CEEEX WATMANTECH		Beneficiar: Institutul Educativ al Cercetarii	
Sef proiect	Fig. Aurel Stapan	Proiect	Fig. Nicodan Murisian
Desenat	Fig. Nicodan Murisian	Scara:	1:10 1:20 1:20
Verificat	Prof. Dr. Ing. Dan DUBINA	Fl. nr.	